Fluides vitreux, sutures craniofaciales, diffusion réactive : quelques contributions à l'étude de ces systèmes multi-échelles ou singuliers

Julien Olivier

THÈSE

Pour obtenir le grade de

DOCTEUR DE L'UNIVERSITÉ DE GRENOBLE

Spécialité : **Mathématiques appliquées**

Arrêté ministériel : 7 août 2006

Présentée par

Julien OLIVIER

Thèse dirigée par **Didier BRESCH**
et codirigée par **Stéphane DESCOMBES**

préparée au sein **du Lama**
et de **l'École doctorale MSTII**

Fluides vitreux, sutures craniofaciales, diffusion réactive : quelques contributions à l'étude de ces systèmes multi-échelles ou singuliers

Thèse soutenue publiquement le **12 juillet 2011**,
devant le jury composé de :

M. Pierre Degond
Directeur de Recherche, CNRS, Rapporteur
M. Benoit Perthame
Professeur, UPMC Paris 6, Rapporteur
M. Athanasios Tzavaras
Professor, University of Crete, Rapporteur
M. Éric Bonnetier
Professeur, Université Joseph-Fourier, Examinateur
M. François Castella
Professeur, Université de Rennes 1, Examinateur
M. Jean-Claude Saut
Professeur, Université Paris-Sud 11, Examinateur
M. Didier Bresch
Directeur de Recherche, CNRS, Directeur de thèse
M. Stéphane Descombes
Professeur, Université de Nice, Co-Directeur de thèse

À tous ceux qui m'ont vu naître,
d'une manière ou d'une autre.

Remerciements

Entreprendre de dresser la liste des gens sans qui cette thèse n'aurait pas aboutie, est presque impossible tant elle est longue. Que ceux que je ne citerais pas nommément me pardonnent : vous et moi savons le rôle que vous avez pu jouer.

Tâchons de remonter le temps. Je remercie donc d'abord tous les membres du jury : Éric Bonnetier, François Castella et Jean-Claude Saut pour avoir supporté mon long discours, Pierre Degond, Benoit Perthame et Athanasios Tzavaras pour avoir rapporté en profondeur mon manuscrit malgré sa longueur et ma propension aux phrases sans fin.

Je remercie la chance de m'avoir fait rencontrer Didier Bresch et Stéphane Descombes il y a déjà six ans de cela. Pour m'avoir permis de rentrer dans le monde de la recherche et ainsi m'avoir offert les années les plus passionnantes et intenses de ma vie, je ne vous remercierai jamais assez. Je dois aussi à Cédric Villani le goût de l'analyse et à Bruno Coucheney le goût des mathématiques.

Je voudrais remercier tous les gens avec qui j'ai pu travailler directement, Michael Renardy, Vincent Calvez, Paul Vigneaux, Hossein Khonsari, Yann Bouret.

Pour enrichissantes qu'elles furent, ces trois années de thèse ne m'aurait pas été supportables sans les amitiés de Matthieu, Mehmet, Dahi et Timack. Je pense aussi à tous ceux que j'ai rencontré ou côtoyé pendant mes années dans les montagnes. Sans ordre particulier : Annette, Florian, Matthieu (l'autre), Xiangdi, Boris, Marguerite, Céline, Catherine, Édouard, Stéphane (l'autre) et d'une manière générale, tous les membres du Lama.

En remontant un peu plus loin, je remercie mes amis lyonnais : Amélie, Delphine, Séverine, Caroline, Maryline, Thomas, Bruno, Nicky, Jérémy, Lionel et bien d'autres.

Enfin on en arrive à ma vie parisienne. Je remercie d'abord mes amis de toujours, Alice, Bénédicte, Laure, Benoît, Fabien, Nicolas et Yann.

Et je remercie mon père, ma mère et ma sœur : vous faites partie de cette thèse tout autant que vous faites partie de ma vie.

Table des matières

Introduction

De la modélisation par les mathématiques

C'est une évidence : une réalité qu'une science cherche à étudier est bien trop complexe pour être approchée dans tous ses détails simultanément. Pour contourner cette difficulté, les scientifiques ont recours à la modélisation que l'on pourrait décrire comme suit : la modélisation consiste, d'une part, à définir un certain nombre de principes liés à l'objet étudié et, d'autre part, à sélectionner certaines quantités, grandeurs et variables supposées pertinentes et finalement à étudier comment les quantités sélectionnées s'articulent avec les principes choisis. La modélisation est par conséquent un compromis entre la complexité de la réalité et la capacité de nos outils à en rendre compte, qui est en général bien plus faible – que ces outils soient conceptuels, expérimentaux, mathématiques ou informatiques.

Le résultat de ce processus de modélisation est un modèle qui, bien souvent, se présentera sous la forme de grandeurs mathématiques reliées entre elles par des équations plus ou moins abstraites, les mathématiques ayant jusqu'à présent montré leur «déraisonnable efficacité dans les sciences naturelles» selon le mot célèbre du physicien E. Wigner[1]. En tout état de cause, ce sont uniquement les modèles mathématiques qui vont nous intéresser dans la suite et uniquement dans le domaine de la physique, la biologie ou la chimie.

L'obtention d'un modèle n'a rien de systématique, c'est donc un travail en soi qui est par nature interdisciplinaire. Les difficultés se situent souvent dans cette traduction des principes qui sont en général *qualitatifs* en leur effet sur les grandeurs qui est donc de l'ordre du *quantitatif*. Un exemple qui nous occupera dans la suite est par exemple le *principe d'objectivité* qui énonce qu'une loi constitutive d'un matériau ne doit pas dépendre du référentiel dans lequel cette loi s'exprime. Nous verrons que nous pouvons traduire

[1] «The miracle of the appropriateness of the language of mathematics for the formulation of the laws of physics is a wonderful gift which we neither understand nor deserve» in The Unreasonable Effectiveness of Mathematics in the Natural Sciences *Communications in Pure and Applied Mathematics*, (1960).

quantitativement ce principe en exprimant l'invariance d'une grandeur (en l'occurrence la contrainte) sous l'action d'un changement de référentiel c'est-à-dire sous l'action d'un groupe. L'écriture de la loi constitutive devra alors prendre en compte cette invariance pour respecter le principe d'objectivité.

Une fois le modèle obtenu, le travail du mathématicien ne s'arrête pas car, d'une certaine façon, les qualités mathématiques d'un modèle sont une mesure de la «qualité» d'un modèle. Prenons l'exemple du *caractère bien posé* d'un modèle. Rappelons rapidement qu'un modèle bien posé au sens d'Hadamard est un modèle qui a une unique solution et dont la solution est «continue» (dans un sens qui peut être compliqué) par rapport aux données externes. L'idée est qu'un modèle bien posé est un modèle qui rend service : il fournit une unique solution à comparer à la réalité expérimentale et assure que, si on fait des petites erreurs de mesure sur les données externes, la solution fournie ne sera pas trop éloignée de celle qu'on voudrait. Le caractère bien posé d'un modèle devrait donc être un pré-requis incontournable à l'utilisation d'un modèle. Il arrive pourtant d'entendre des remarques comme «l'existence et l'unicité de la solution sont évidentes, puisque dans la réalité, l'eau s'écoule»[2] (ou bien, dans un autre contexte, «la pression est positive puisque c'est une pression»[3]).

En fait, les propriétés mathématiques des modèles permettent de discriminer les modèles : un modèle qui assure que la pression calculée est effectivement positive sera préféré à un modèle qui ne permet pas de l'affirmer. Il faut toutefois se garder du manichéisme : il est rare que les modèles soient parfaits – c'est dans leur nature. Qu'on ne sache pas si les solutions de Navier-Stokes incompressible développent des singularités qui montrent qu'on finit par violer l'hypothèse d'incompressibilité, n'empêche pas que ce modèle soit très largement utilisé, et à raison.

Enfin un bon modèle c'est avant tout un modèle qui reproduit fidèlement les données expérimentales du phénomène étudié. Pour cela il convient d'extraire du modèle des simulations reproduisant les situations expérimentales envisagées afin de les comparer. L'idéal est un modèle qui reproduit les données expérimentales aux erreurs près mais parfois on doit se contenter d'un modèle qui reproduit le phénomène observé globalement ou en ordre de grandeur, les valeurs exactes n'étant pas correctement approchées. Ce genre de modèle est néanmoins très utile car il apporte des preuves que les principes envisagés peuvent en grande partie expliquer le phénomène étudié. Dans la réalité, de nombreux mécanismes peuvent s'ajouter mais ils ne rendront

[2] rapporté d'une conférence à l'auteur.

[3] réponse envisagée comme acceptable à une épreuve de mathématique du concours physique de l'ENS.

compte que d'effets correctifs.

Les simulations numériques peuvent être très naturelles si le modèle est initialement conçu pour être un modèle discret. C'est le cas par exemple des modèles fondés sur les automates cellulaires. Mais, dans la plupart des cas qui nous intéresseront dans la suite, les modèles seront des modèles dit continus car s'appuyant sur des objets non discrets (typiquement des fonctions sur l'espace réel). Préparer des simulations numériques cohérentes avec le modèle continu est alors en soi un travail mathématique – et parfois informatique – complet. Il s'agit de calculer des approximations d'objets continus à l'aide d'objets discrets mais surtout il s'agit de vérifier que ces objets discrets respectent des propriétés issues du modèle continu. Par exemple, les concentrations chimiques approchées doivent être positives. Ce travail de discrétisation n'est souvent pas indépendant du travail de modélisation et en bénéficie souvent. On sait par expérience qu'un schéma fondé sur le *splitting* a très peu de chance de donner de bons résultats si ce *splitting* ne respecte pas «la physique du problème» (une condition nécessaire mais pas toujours suffisante).

Nous espérons présenter dans cette thèse des exemples pertinents et des résultats intéressants liés à chacune des problématiques précédentes (modélisation, analyse théorique et simulations numériques). Nous allons tirer ces exemples de deux domaines différents : le premier est la modélisation des matériaux dits vitreux mous ou amorphes (qui constitue la partie principale de ce mémoire de thèse) et le second de domaines comme la biomécanique ou la chimie. Dans le domaine de la modélisation : nous aborderons les questions de la transition vitreuse, l'objectivité pour les lois rhéologiques (chapitre 4), la diffusion d'espèces chimiques à réactions infiniment rapides dans un milieu hétérogène (chapitre 5), la biomécanique hétérogène comme explication du phénomène d'interdigitation dans les sutures crâniennes (chapitre 6). Pour ce qui est de l'analyse théorique, les sujets abordés seront les fonctions implicites et leur comportement au voisinage de singularités (chapitre 1), la pénalisation des équations différentielles avec approche «à la Kato» (chapitre 2), ou par estimation d'erreur (chapitre 3), les équations elliptiques à données peu régulières (chapitre 4). Enfin nous présenterons un schéma de volumes finis relaxé (chapitre 5) ainsi qu'un code d'éléments finis pour l'interdigitation (chapitre 6).

Apports principaux de la thèse

Matériaux vitreux

Commençons par présenter nos travaux en lien avec les matériaux vitreux. À la suite des travaux de Bouchaud, Comtet et Monthus [11], Sollich, Lequeux, Hébraud et Cates [68] ont proposé un premier modèle pour la rhéologie des matériaux vitreux mous (*Soft Glassy Rheology*) à l'aide d'une description de champ moyen (c'est-à-dire que l'état du matériau est représenté globalement (ou macroscopiquement) par une distribution statistique des états locaux (ou états mésoscopiques), ceux-ci étant caractérisés par leur énergie interne et leur déformation élastique. Le modèle suivait ensuite les principes du modèle de piège de Bouchaud *et al.*. Ce modèle donnait de bons résultats mais souffrait d'un défaut (déjà présent dans [11]) : le modèle faisait entrer de façon *ad hoc* la température de transition vitreuse. Hébraud et Lequeux ont alors proposé [37] un modèle de champ moyen fondé sur les mêmes idées (distribution d'état et réorganisation locale des états lors d'un saut) qui propose une formulation auto-consistante de la réorganisation. Nous renvoyons à l'annexe A et aux références qui s'y trouvent pour plus de détails.

Une catégorie classique de matériaux vitreux mous est formée par l'ensemble des *dispersions* : il y a dispersion lorsqu'un matériau solide, liquide ou gazeux est dispersé en bulles qui ne coalescent pas, dans un autre liquide ou gaz. On obtient alors, selon les cas, des suspensions (certaines argiles comme la bentonite), des émulsions (comme la mayonnaise) ou des mousses (mousses de bains).

Notons que les modèles comme le modèle SGR de Sollich *et al.* ou le modèle d'Hébraud-Lequeux visent à décrire un matériau amorphe générique selon des principes généraux : on peut les voir comme des matériaux amorphes idéaux. Il existe néanmoins beaucoup de modèles plus spécifiques à certains matériaux amorphes : citons par exemple le modèle macroscopique multidimensionnel spécifique aux mousses de Bénito, Bruneau, Colin, Gay et Molino [6].

Décrivons rapidement ce modèle. L'état macroscopique du matériau est donné par une distribution $p(t, \sigma)$ sur l'espace des contraintes locales σ qui sont distribuées dans $\mathbf{R}$. Au cours du temps, lorsqu'il est soumis au taux de déformation $\dot{\gamma}(t)$, les contraintes locales peuvent évoluer sous l'action de trois phénomènes :

1. d'abord la contrainte évolue élastiquement, ce qui se traduit par un gain local de $-G_0\dot{\gamma}(t)\partial_\sigma p$;

2. ensuite, lorsque la contrainte locale dépasse un certain seuil, la contrainte relaxe vers 0 avec un temps de relaxation caractéristique T_0 ce qui donne un terme de perte $-1/T_0 \mathbf{1}_{\mathbf{R}\setminus[-\sigma_c,\sigma_c]} p + \Gamma(t)\delta_0(\sigma)$ où l'on a noté $\mathbf{1}_X$ la fonction indicatrice de X, δ_0 la masse de Dirac en 0 et $\Gamma(t)$ le taux de saut appelé *fluidité*

$$\Gamma(t) = \frac{1}{T_0} \int_{|\sigma|>\sigma_c} p(t,\sigma) \mathrm{d}\sigma; \tag{1}$$

3. enfin chaque contrainte locale est soumise à un bruit résultant des réarrangements qui s'opèrent au voisinage des événements de relaxations. Ce bruit est supposé brownien et d'intensité proportionnelle au taux d'événements de relaxation c'est-à-dire proportionnel à la fluidité. On note α cette constante de proportionnalité qui peut s'interpréter comme une fragilité mécanique : plus α est grand et plus le matériau se brise facilement et peut donc s'écouler.

On obtient alors le modèle d'Hébraud-Lequeux en cherchant p qui vérifie :

$$\partial_t p = -G_0 \dot{\gamma}(t) \partial_\sigma p - \frac{1}{T_0} \mathbf{1}_{\mathbf{R}\setminus[-\sigma_c,\sigma_c]} p + \Gamma(t)\delta_0(\sigma) + \alpha\Gamma(t)\partial_{\sigma\sigma} p, \tag{2}$$

$$p \geq 0, \tag{3}$$

$$\int_{\sigma\in\mathbf{R}} p(t,\sigma)\mathrm{d}\sigma = 1, \tag{4}$$

$$p(0,\sigma) = p_0(\sigma). \tag{5}$$

Dans ce modèle la contrainte macroscopique τ du matériau est définie à partir de p par la formule

$$\tau(t) = \int_{\sigma\in\mathbf{R}} \sigma p(t,\sigma)\mathrm{d}\sigma. \tag{6}$$

Le modèle d'Hébraud-Lequeux peut donc être classé dans la famille des modèles *cinétiques* fondée sur une équation de type *Fokker-Planck* : une équation du deuxième ordre portant sur la densité de probabilité $p(v_1,\ldots,v_n)$ de trouver une particule au voisinage du point $(v_1,\ldots,v_n)$ de l'espace des phases, lorqu'elle suit un mouvement stochastique,

$$\partial_t p = -\sum_i \partial_{v_i}(pV^i(v_1,\ldots,v_n)) + \sum_{i,j} \partial^2_{v_i v_j}(pD^{ij}(v_1,\ldots,v_n)),$$

où V est la tendance (le *drift* en anglais) et D est le tenseur de diffusion. Le problème peut-être le plus emblématique de l'utilisation de ce type d'équation est la dynamique des gaz parfaits homogènes pour lesquels

$$D = Id \qquad \text{et} \qquad V(v) = -v.$$

L'espace des phases est alors l'espace des vitesses de particules. Notons immédiatement que, dans ce cas, on peut réécrire le second membre de la façon suivante (voir Desvillettes et Villani [26] ou Degond, Lemou et Picasso [24] avec des développements spécialement liés aux fluides viscoélastiques) :

$$\operatorname{div}(pv) + \Delta p = \operatorname{div}\left(M(v)\nabla\left(\frac{p}{M(v)}\right)\right),$$

où M est traditionnellement appelée *maxwellienne*, $M(v) = \dfrac{1}{(2\pi)^{n/2}} e^{-|v|^2/2}$. Dans ce cas il est facile de voir que l'unique solution de l'équation stationnaire sous contrainte $\displaystyle\int p = 1$ est $p = M$.

Dans le cas du modèle d'Hébraud-Lequeux, on peut considérer que l'on a affaire à une équation de Fokker-Planck dans laquelle l'espace des phases est l'espace des contraintes de cisaillement. L'équation (2) d'Hébraud-Lequeux présente toutefois des caractéristiques très différentes :

- l'équation est non-linéaire car le coefficient de diffusion $\alpha\Gamma(t)$ dépend lui-même de la solution *via* (1) ;
- l'équation est non-conservative : en effet, à cause du terme de saut $-1/T_0 \mathbf{1}_{\mathbf{R}\setminus[-\sigma_c,\sigma_c]} p + \Gamma(t)\delta_0(\sigma)$, nous ne pouvons pas mettre l'équation sous une forme où la dérivée temporelle de p $\partial_t p$ serait égale à la dérivée par rapport à σ d'une certaine expression. Il en résulte notamment une multiplicité des états stationnaires.

Enfin, pour achever cette mise en contexte du modèle d'Hébraud-Lequeux, nous pouvons évoquer d'autres modèles rhéologiques s'appuyant sur une description cinétique en particulier le fameux modèle des haltères (en anglais *dumbell*) pour les solutions de polymères diluées qui existe sous diverses formes plus ou moins complexes (voir par exemple Le Bris [46]). Dans ce modèle, une très longue molécule de polymères est réduite au vecteur X formant ses deux extrémités. On décrit ensuite la distribution statistique du vecteur X à l'aide d'une équation de Fokker-Planck (ou plutôt de sa version inhomogène l'équation de Vlasov-Fokker-Planck) :

$$\partial_t p + u \cdot \nabla_x p = -\operatorname{div}_X\left(\left(\nabla_x u X - \frac{1}{2We}\nabla\Pi(X)\right)p\right) + \frac{1}{2WeM}\Delta_X p, \quad (7)$$

où $\Pi(X)$ décrit le potentiel de la force de rappel qui s'exerce sur l'haltère du fait des contraintes entropiques (un vecteur très long cache une molécule très dépliée qui a donc moins de marge de manœuvre pour se déformer). Suivant la complexité du potentiel on obtient des modèles plus ou moins réalistes, les plus connus étant :

– le cas des haltères linéaires,

$$\Pi(X) = \frac{1}{2}|X|^2.$$

– le cas des haltères à extension finie (FENE),

$$\Pi(X) = -\frac{bM}{2}\log\left(1 - \frac{|X|^2}{bM}\right).$$

Bien qu'autorisant une extension infinie des polymères (ce qui n'est pas réaliste) le modèle des haltères linéaires a une très grande importance en rhéologie, car il est équivalent à un modèle purement macroscopique très utilisé : le modèle de Maxwell surconvecté (voir l'annexe A pour plus d'information sur ce modèle). C'est l'un des rares cas en rhéologie où l'on a une justification microscopique d'un modèle macroscopique. Pour une revue des résultats concernant ces modèles nous renvoyons vers Le Bris et Lelièvre [47]. Notons que l'un des premiers résultats mathématiques d'existence de solution pour les modèles de fluides basés sur des descriptions cinétiques a été donné par Renardy [63].

Dans les chapitres 1, 2 et 3 nous nous intéressons à la version stationnaire de (2)–(5), c'est-à-dire au problème suivant :

$$0 = -G_0\dot{\gamma}\partial_\sigma p - \frac{1}{T_0}\mathbf{1}_{\mathbf{R}\setminus[-\sigma_c,\sigma_c]}p + \Gamma\delta_0(\sigma) + \alpha\Gamma\partial_{\sigma\sigma}p, \tag{8}$$

$$p \geq 0, \tag{9}$$

$$\int_{\sigma\in\mathbf{R}} p(\sigma)\mathrm{d}\sigma = 1. \tag{10}$$

et plus particulièrement à la composée des applications : $\dot{\gamma} \mapsto p$ la solution de (8)–(10) et de l'application $p \mapsto \tau$ où τ est calculé *via* (6). Autrement dit, on veut étudier les courbes de flot associées au modèle d'Hébraud-Lequeux stationnaire. Évidemment puisqu'on parle de LA solution de (8)–(10) il faut s'assurer que cette solution existe et est unique dans un cadre fonctionnel approprié, ce qui est exact dès lors que $\dot{\gamma} \neq 0$ d'après un théorème de Cancès, Catto et Gati [16] dont nous redonnons la démonstration au cours

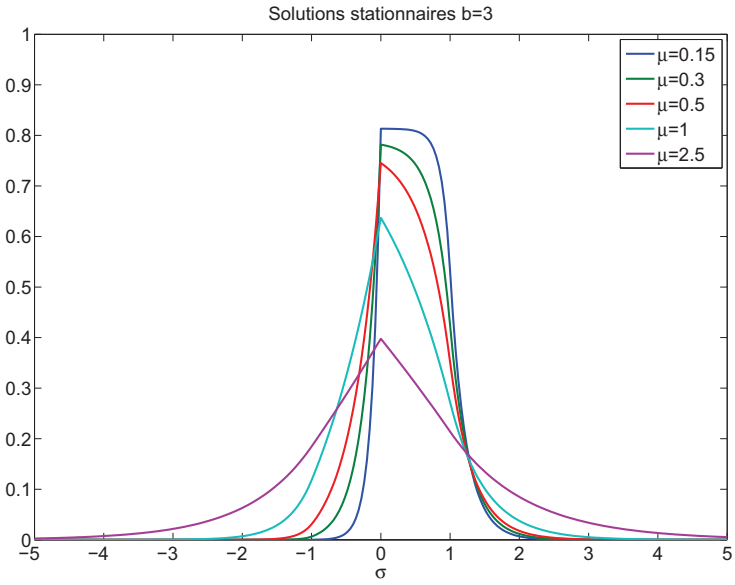

FIG. 1: Exemples de solution du système (8)–(10)

du chapitre 1. On peut voir quelques exemples de telles solutions dans la figure 1.

L'intérêt principal de ce chapitre est la démonstration de l'énoncé suivant :

Théorème 1. *Notons $\eta_c = G_0 T_0$. Soit $p(\dot\gamma, \sigma)$ l'unique solution du problème (8)–(10) lorsque le taux de cisaillement est non nul c'est-à-dire $\dot\gamma \neq 0$. Alors les comportements possibles pour $\tau(\dot\gamma) = \int_{\sigma\in\mathbf{R}} \sigma p(\dot\gamma,\sigma)\mathrm{d}\sigma$ lorsque $\dot\gamma \to 0$ sont les suivants :*

si $\alpha > \sigma_c^2/2$ *Le fluide se comporte comme un fluide newtonien de viscosité apparente $\eta(\alpha/\sigma_c^2)$. Si l'on définit $\eta^*(\mu)$ par la formule*

$$\eta^*(\mu) = 1 + \frac{3\mu - 1 + 1/2(4\mu-1)^{3/2}}{24\mu(\mu-1/2)^2},$$

alors nous avons

$$\tau(\dot\gamma) \sim \eta(\alpha/\sigma_c^2)\dot\gamma$$

où la viscosité apparente η est donnée par $\eta(\alpha/\sigma_c^2) = \eta^*(\alpha/\sigma_c^2)\eta_c$;

si $\alpha < \sigma_c^2/2$ *Le fluide présente un seuil dynamique τ_0. Plus précisément : on*

définit d'abord $c(\mu)$ *comme la seule racine positive de l'équation*

$$\frac{c(\mu)(\cosh(1/c(\mu)) - 1)}{\sinh(1/c(\mu))} = \mu$$

et $\tau^*(\mu)$ *par la formule*

$$\tau^*(\mu) = \left(\frac{1}{2\mu} - 1\right) c(\mu),$$

alors nous avons

$$\tau(\dot\gamma) \to \tau_0(\alpha/\sigma_c^2)$$

où τ_0 *est donné* $\tau_0(\alpha/\sigma_c^2) = \tau^*(\alpha/\sigma_c^2)\sigma_c$ *;*

si $\alpha = \sigma_c^2/2$ *le fluide suit une loi de puissance d'exposant* $1/5$ *ce qui signifie qu'on a*

$$\tau(\dot\gamma) \sim \frac{24^{2/5}}{12}\sigma_c^{4/5}\eta_c^{1/5}\dot\gamma^{1/5}.$$

Ce théorème précise donc le comportement de la courbe $(\dot\gamma, \tau(\dot\gamma))$ en fonction du paramètre μ. Cette courbe est vraiment l'un des outils fondamentaux en rhéologie : ce sont les courbes expérimentales que l'on obtient dans la plupart des dispositifs expérimentaux tels que les cellules de Couette, ou les rhéomètres cône-plan (pour plus de détail sur l'expérimentation en rhéologie, nous renvoyons à Oswald [57], Hébraud [36] ou Goyon [33]). On trouvera des exemples de telles courbes dans l'annexe A pour quelques modèles classiques tels que celui de Bingham (figure A.4 p. 242) ou d'Herschel-Bulkley (figure A.5 p. 243).

L'énoncé en lui-même signifie que le modèle d'Hébraud-Lequeux rend compte du phénomène de la *transition vitreuse* dans le matériau : le fluide change de type rhéologique en fonction d'une «température» de transition jouée ici par la fragilité α : on passe brusquement d'un comportement newtonien lorsque la température est suffisamment élevée à un comportement à seuil lorsque la température est en dessous d'une température de transition à laquelle le fluide a un comportement intermédiaire de loi de puissance. On trouve une illustration de cette transition vitreuse dans la figure 1.2 p. 42.

Cette propriété avait été remarquée par Hébraud et Lequeux mais à notre connaissance n'avait pas été démontrée auparavant. La démonstration s'appuie sur une expression analytique de la solution de (8)–(10) : celle-ci est obtenue par intégration de l'équation différentielle et couplée avec une équation transcendante de type $f(\dot\gamma, \Gamma) = 0$ que l'on résout grâce au théorème des fonctions implicites. L'analyse de l'asymptotique $\dot\gamma \to 0$ passe par une étude relativement compliquée du comportement de la solution implicite $\Gamma(\dot\gamma)$ car

la fonction f est violemment singulière au voisinage du point d'intérêt $(0,0)$ (voir par exemple son expression p. 43 dans des variables adimensionnées, x étant proportionnel à Γ et y proportionnel à $\dot{\gamma}$). Il faut donc désinguliariser le problème par un changement de variables appropriées (certains changements de variables pouvant paraître naturels mais n'étant pas efficaces au final). Il faut ensuite calculer la contrainte associée au paramètre $\dot{\gamma}$ et montrer que le comportement asymptotique de $\Gamma(\dot{\gamma})$ permet de trouver le comportement de τ. Ceci nécessite de nouveau une analyse assez minutieuse même si les outils théoriques sont assez basiques. En effet, la différence entre la valeur exacte (à $\dot{\gamma}$ fixé) et son asymptotique supposée est contrôlée par un produit de termes dont certains sont singuliers dans la limite $\dot{\gamma} \to 0$.

Le chapitre 1 a fait l'objet d'une publication dans la revue *Zeitschrifft für Angewandte Mathematik und Physik*, [53].

Alors que nous travaillions à la démonstration du premier chapitre, nous cherchions parallèlement à généraliser le modèle d'Hébraud-Lequeux à des types d'écoulement qui ne se limitaient pas au seul cas du cisaillement simple. En effet il est bien connu que pour un matériau même simple, un seul type d'écoulement n'est pas suffisant pour connaître toutes les propriétés d'un fluide. On peut tout simplement penser au cas des fluides newtoniens compressibles qui ont deux viscosités, et le cisaillement simple ne permet d'avoir accès qu'à une seule information (une combinaison linéaire de ces deux viscosités). Bien entendu, il fallait que le modèle généralisé garde les bonnes propriétés du modèle original. Pour décrire le modèle nous avons besoin de quelques notations. Ce modèle est de nouveau une modélisation de type Fokker-Planck et cette fois la densité de probabilité est définie sur l'espace des matrices symétriques de dimension 6 en 3d et de dimension 3 en 2d. Le point générique de cet espace est $\Sigma = (\Sigma_{ij})_{i\leq j}$ et p est donc une fonction des coordonnées Σ_{11}, Σ_{22}, Σ_{33}, Σ_{12}, Σ_{13}, Σ_{23}. On le munit du produit scalaire

$$\Sigma : \Sigma' = \sum_i \Sigma_{ii}\Sigma'_{ii} + 2\sum_{i\leq j} \Sigma_{ij}\Sigma'_{ij}, \tag{11}$$

et on note $|\cdot|$ la norme associée. On définit les opérateurs

$$\Delta_\Sigma p = \sum_i \partial_{\Sigma_{ii}\Sigma_{ii}} p + \frac{1}{2}\sum_{i\leq j} \partial_{\Sigma_{ij}\Sigma_{ij}} p, \tag{12}$$

et

$$\nabla_\Sigma p = (\partial_{\Sigma_{ij}} p)_{i,j}. \tag{13}$$

Enfin on généralise la fluidité en,

$$\Gamma(p) = \int_{|\Sigma|>1} p(\Sigma) \prod_{i\leq j} \mathrm{d}\Sigma_{ij}. \tag{14}$$

On notera dorénavant $\mathrm{d}\Sigma = \prod_{i\leq j} \mathrm{d}\Sigma_{ij}$.

Pour le champ de vitesse u on utilise les notations classiques $W(\nabla u)$ et $D(\nabla u)$ pour les parties respectivement antisymétrique et symétrique de ∇u. Il nous reste à définir pour a appartenant à $[-1, 1]$,

$$g_a(\Sigma, \nabla u) = \Sigma W(\nabla u) - W(\nabla u)\Sigma - a(D(\nabla u)\Sigma + \Sigma D(\nabla u)). \tag{15}$$

Le modèle prend alors la forme suivante,

$$\begin{aligned}\partial_t p(t,x,\Sigma) + u\cdot\nabla_x p - g_a(\Sigma,\nabla u) : \nabla_\Sigma p = \\ -2G_0 D(\nabla u) : \nabla_\Sigma p(t,x,\Sigma) \\ - \frac{\mathbf{1}_{|\Sigma|>\sigma_c}(\Sigma)}{T_0} p(t,x,\Sigma) + \Gamma(p)(t,x)\rho(\Sigma) \\ + \alpha\Gamma(p)(t,x)\Delta_\Sigma p(t,x,\Sigma)\end{aligned} \tag{16}$$

complété avec la condition

$$\int_{\mathbf{R}^6} p(t,x,\Sigma)\mathrm{d}\Sigma = 1. \tag{17}$$

Dans l'équation (16), on a séparé le second membre en la somme de trois termes, chacun correspondant aux effets 1–3 référencés p. 4. Il est à noter que ρ joue le rôle qui était dévolu à la masse de Dirac en 0 : ce doit être une mesure à support contenu dans la boule unité, invariante dans un sens qui sera précisé dans le chapitre 4. Enfin on récupère le tenseur des contraintes macroscopiques par intégration :

$$T_{ij}(t,x) = \int_{\mathbf{R}^6} p(t,x,\Sigma)\Sigma_{ij}\mathrm{d}\Sigma. \tag{18}$$

Pour la conception de ce modèle la question la plus importante a été celle de l'objectivité. Le principe est qu'une loi physique ne doit pas dépendre de l'observateur. En mécanique, ce principe se traduit par une indépendance des équations par changement de référentiel. Cette question est occultée lorsqu'on se restreint à des situations de cisaillement simple. Mais c'est un problème en rhéologie lorsqu'on passe d'un modèle en cisaillement simple à un modèle général. L'exemple peut-être le plus simple est la généralisation du modèle de Maxwell. En cisaillement simple ce modèle prend la forme suivante :

$$\partial_t \tau + \frac{1}{T_0}\tau = G_0\dot{\gamma}. \tag{19}$$

Si on essaie de généraliser naïvement cette équation en

$$\partial_t T + \frac{1}{T_0} T = G_0 D(\nabla u),$$

on tombe sur une équation qui n'est pas invariante par changement de référentiel. Il est connu (voir l'annexe A et les références qui s'y trouvent) que, pour obtenir une équation qui soit de nouveau invariante par changement de référentiel, *on peut* ajouter des termes qui sont précisément $g_a(T, \nabla u)$. Il existe ici un trou entre condition nécessaire et suffisante car on sait que l'on doit changer les équations et on sait comment on peut les changer mais on ne sait pas s'il existe d'autres façons de le faire et pourquoi on doit utiliser $g_a(T, \nabla u)$. En conséquence, le sens de ce paramètre a n'est pas clair. Comme nous l'avons mentionné, il existe une justification dans le cas des polymères dilués de la valeur $a = 1$ mais certaines expériences sur d'autres matériaux conduisent à prendre a proche de -1 pour un meilleur accord avec les données expérimentales. Enfin citons le résultat de Lions et Masmoudi dans [48] qui montre le caractère bien posé, global en temps, des solutions faibles d'un modèle proche du modèle de Maxwell (le modèle d'Oldroyd) dans le cas $a = 0$. Pour les résultats mathématiques dans le cas $a \neq 0$, il n'existe essentiellement que des résultats d'existence locale en temps de solution forte (voir par exemple Renardy [62]). Pour une revue des résultats mathématiques associés à ce type de modèle, nous renvoyons à Saut [67].

Nous retrouvons cette problématique pour le modèle d'Hébraud-Lequeux : considérons l'équation (2) et $\sigma_c = 0$. Dans ce cas nous avons $\Gamma(t) = 1$ et l'équation se réécrit :

$$\partial_t p = -G_0 \dot{\gamma} \partial_\sigma p - \frac{1}{T_0} p + \delta_0 + \alpha \partial^2_{\sigma\sigma} p.$$

Nous pouvons multiplier cette équation par σ et intégrer sur $\mathbf{R}$. En utilisant (6) on obtient alors :

$$\partial_t \tau = G_0 \dot{\gamma} - \frac{1}{T_0} \tau,$$

c'est-à-dire l'équation de Maxwell (19) ; ce qui explique l'apparition du terme $g_a(\Sigma, \nabla u) : \nabla_\Sigma p$ dans (16).

Il reste à savoir si ce modèle rend bel et bien compte d'un phénomène de type transition vitreuse et, si oui, de quelle façon la généralisation à des situations multidimensionnelles a modifié cette transition. Plus précisément, la question que nous nous posons est la suivante : si nous nous plaçons dans un cadre stationnaire et homogène (plus de dépendance en temps et en espace) avec un flot prescrit et petit (c'est-à-dire en supposant la relation $\nabla u = \varepsilon M$ où M est une matrice donnée) alors que peut-on dire de la limite de T lorsqu'ε

tend vers 0 ? Il apparaît très rapidement que la stratégie utilisée pour mener la même étude dans le cas 1d n'a aucune chance de fonctionner dans le cas multidimensionnel, faute de forme analytique simple pour les solutions des équations de transport-diffusion stationnaires. Avant de pouvoir répondre à la question, il a donc fallu chercher une nouvelle démonstration du théorème 1, suffisamment souple et générale pour avoir une chance de s'adapter au cas multidimensionnel.

La démonstration donnée dans le chapitre 1 fait tout pour court-circuiter la solution p en lui cherchant une forme analytique que l'on sait intégrer pour ne raisonner que sur $\dot{\gamma}$, Γ et τ. Nous allons présenter maintenant une nouvelle approche, développée au chapitre 2, qui prend le parti inverse de développer asymptotiquement la solution p de (8)-(10) pour $\dot{\gamma}$ petit, et de ne raisonner que sur elle afin d'en déduire par simple intégration le développement de τ.

Cette nouvelle méthode nous l'avons trouvée par analogie avec un problème *a priori* sans rapport, celui de la pénalisation d'obstacle. Imaginons un fluide de Stokes s'écoulant dans un domaine Ω et supposons que ce domaine contienne un obstacle ω. Les équations sur la vitesse du fluide sont alors :

$$\begin{cases} -\nu\Delta u + \nabla\pi = f, & \text{dans } \Omega \setminus \omega \\ \operatorname{div} u = 0, & \text{dans } \Omega \setminus \omega \\ u = 0, & \text{sur } \partial\omega \end{cases} \tag{20}$$

complétées avec des conditions aux bords de Ω. Pour des raisons de commodité, on peut vouloir préférer travailler dans le domaine Ω lui-même et non $\Omega \setminus \omega$ (par exemple si Ω est un canal rectiligne, on peut vouloir tirer parti de ses symétries). Dans ce cas on peut modifier les équations précédentes en ajoutant un terme de *pénalisation* :

$$\begin{cases} -\nu\Delta u^\varepsilon + \nabla\pi^\varepsilon + \dfrac{1}{\varepsilon}\mathbf{1}_\omega u^\varepsilon = f, & \text{dans } \Omega \\ \operatorname{div} u^\varepsilon = 0. & \text{dans } \Omega \end{cases} \tag{21}$$

L'heuristique est que, lorsque ε est très petit, on doit avoir $\mathbf{1}_\omega u^\varepsilon \approx 0$ pour éviter l'explosion du système, ce qui revient à dire que u^ε est nul dans ω et donc sur son bord. On retrouve ainsi, à la limite, le système initial.

Cette heuristique a été justifiée dans le cas des équations de Navier-Stokes incompressible par Angot, Bruneau and Fabrie, [2], pour la convergence L^2 et Carbou and Fabrie [20] pour la convergence H^1. Remarquons immédiatement que l'étude de la convergence H^1 nécessite de prendre en compte le comportement de u^ε au voisinage de l'obstacle car il faut tenir compte de la *couche limite* (numérique) et de son énergie. Cette approche a aussi été justifiée pour des problèmes d'ondes par Fornet et Guès [30] et Fornet[28, 29].

L'analogie avec le problème qui nous occupe est la suivante : à la suite du chapitre 1 nous savions que dans la limite $\dot{\gamma} \to 0$ de (8)–(10) dans le cas $\alpha < \sigma_c^2/2$, Γ était équivalent à $c\dot{\gamma}$. Si nous remplaçons dans (8)–(10) Γ par son équivalent et que nous divisons par $\dot{\gamma}$ nous obtenons l'équation suivante :

$$-\alpha c \partial^2_{\sigma\sigma} p + G_0 d_\sigma p + \frac{1}{T_0 \dot{\gamma}} \mathbf{1}_{\mathbf{R}\setminus[-\sigma_c,\sigma_c]} p = c\delta_0.$$

Cette équation est formellement la même que (21) où l'obstacle serait le complémentaire du segment $[-\sigma_c, \sigma_c]$. Nous avons donc cherché des développements asymptotiques qui prenaient en compte ce phénomène de couche limite déjà mentionné.

La mise en œuvre n'est toutefois pas immédiate : par exemple, on ne trouve pas le problème vérifié par la solution fondamentale (c'est-à-dire le terme de plus bas ordre ou la limite potentielle) simplement en remplaçant $\dot{\gamma}$ par 0 dans (8). La forme du développement n'est pas non plus évidente *a priori*. Le meilleur point de vue est ici de postuler une forme très générale de développement asymptotique et ensuite de raisonner pour en expliciter la forme nécessaire : cette méthode a pu servir de base pour une analyse similaire sur le modèle multidimensionnel. Les chapitres 2 et 4 sont d'ailleurs très similaires en termes de structure. Néanmoins, les deux chapitres ont leur intérêt propre : le chapitre 2 introduit la méthode et nous nous servons du contexte unidimensionnel pour mener une analyse complète, jusqu'à démontrer un théorème de convergence analytique inspiré des méthodes de perturbation analytique «à la Kato» [43] ; le chapitre 4 admet une analyse moins poussée de la convergence mais les calculs qui y sont menés sont beaucoup plus difficiles et il est aussi nécessaire de faire appel à des arguments d'analyse des équations aux dérivées partielles plus fins.

Nous devons notamment étudier des équations elliptiques dans des cadres L^β où β peut être strictement plus petit que 2, à données peu régulières (mesures). D'autre part, l'opérateur de «transport» (dans l'espace des contraintes) se réduit en 1d à ∂_σ mais dans notre modèle multidimensionnel, nous obtenons un opérateur de transport à coefficients affine en contrainte qui dépend du type d'écoulement imposé au matériau. Pour la bonne marche de la démonstration nous avons besoin de propriétés sur les caractéristiques de cet opérateur (caractéristiques transverses sur la sphère unité) que nous devons vérifier pour les flots qui nous intéressent. Enfin, pour le cas de la transition, nous devons évaluer certaines intégrales (pour en déterminer la nullité). En 1d nous pouvons le faire par la résolution explicite des équations de profils mais dans notre modèle, nous devons étudier les symétries des équations afin d'en déduire les symétries des solutions et utiliser des fonctions tests judicieuses inspirées par la théorie des harmoniques sphériques.

Dans la suite, les résultats sont formulés sur le modèle *adimensionné* qui prend la forme suivante :

$$-\phi\partial_{\sigma\sigma}p + y\partial_\sigma p + \mathbf{1}_{\mathbf{R}\setminus[-1,1]}p = \frac{\phi}{\mu}\delta_0(\sigma), \tag{22}$$

$$p \geq 0, \tag{23}$$

$$\int_{\sigma\in\mathbf{R}} p(\sigma)\mathrm{d}\sigma = 1. \tag{24}$$

Dans cette écriture y joue le rôle de $\dot\gamma$, μ joue le rôle de α et ϕ/μ joue le rôle de Γ (ϕ est donc le coefficient de diffusion mécanique). Notons que nous avons bien la relation d'autoconsistance

$$\Gamma = \frac{\phi}{\mu} = \int_{|\sigma|>1} p(\sigma)\mathrm{d}\sigma, \tag{25}$$

et que la contrainte adimensionnée se calcule toujours à l'aide de la formule

$$\tau = \int_{\mathbf{R}} \sigma p(\sigma)\mathrm{d}\sigma. \tag{26}$$

Pour présenter les résultats du chapitre 2, le modèle (22)–(24) doit être reformulé en distinguant la solution à l'intérieur et à l'extérieur du segment $[-1,1]$, et nous nommons $q = p_{|[-1,1]}$ et $r = p_{|\mathbf{R}\setminus[-1,1]}$. Le système se réécrit alors :

$$-\phi\partial_\sigma^2 q + y\partial_\sigma q = \frac{\phi}{\mu}\delta_0 \qquad \text{dans }]-1,1[, \tag{27a}$$

$$-\phi\partial_\sigma^2 r + y\partial_\sigma r + r = 0 \qquad \text{dans } \mathbf{R}\setminus[-1,1], \tag{27b}$$

$$r(\pm\infty) = 0, \tag{27c}$$

$$q \geq 0, \tag{27d}$$

$$r \geq 0, \tag{27e}$$

$$r(\pm1) = q(\pm1), \tag{27f}$$

$$\partial_\sigma r(\pm1) = \partial_\sigma q(\pm1), \tag{27g}$$

$$\int_{|\sigma|>1} r(\sigma)\mathrm{d}\sigma + \int_{-1}^{1} q(\sigma)\mathrm{d}\sigma = 1, \tag{27h}$$

sans oublier la définition de la fluidité,

$$\frac{\phi}{\mu} = \int_{|\sigma|>1} r(\sigma)\mathrm{d}\sigma. \tag{28}$$

Le développement asymptotique pouvant faire apparaître des termes de type «couche limite» pour r, nous introduisons la fonction distance au bord $\{-1,1\}$, $\theta_e(\sigma) = |\sigma| - 1$. Nous faisons alors les *ansätze* suivants :

$$q(\sigma) = \sum_{k=0}^{+\infty} y^{k/s} \overline{Q}^k(\sigma), \tag{29a}$$

$$r(\sigma) = \sum_{k=0}^{+\infty} y^{k/s} \overline{R}^k(\sigma) + y^{k/s} R^k\left(\operatorname{sign}(\sigma), \frac{\theta_e(\sigma)}{y^{l/s}}\right), \tag{29b}$$

ce qui implique, en utilisant (28), que ϕ/μ se développe de la façon suivante :

$$\frac{\phi(y)}{\mu} = \sum_{k=0}^{+\infty} \tilde{c}_k y^{k/s}. \tag{29c}$$

Ici l et s sont des entiers *inconnus*. Nous devons commencer par les déterminer ce qui se fait au moyen de la proposition suivante :

Proposition 1 (**Forme nécessaire des *ansätze***). *Les paramètres des* ansätze *sont les suivants :*

si $\mu > 1/2$ **:** *alors* $s = 1$ *et il n'y a pas de terme de couche limite (*l *n'est pas défini et les* R^k *sont nuls) ;*

si $\mu < 1/2$ **:** *alors* $s = 2$ *et* $l = 1$*, ce qui veut dire que la couche limite a pour taille* $y^{1/2}$ *et le développement se fait en puissance de* $y^{1/2}$*. À l'extérieur, les termes* $\overline{R}^k$ *sont nuls ;*

si $\mu = 1/2$ **:** *alors* $s = 5$ *et* $l = 2$*, ce qui veut dire que la couche limite a pour taille* $y^{2/5}$ *et le développement se fait en puissance de* $y^{1/5}$*. À l'extérieur, les termes* $\overline{R}^k$ *sont nuls.*

Cette proposition, bien que formelle (on ne donne à ce stade aucune information sur la validité de ces ansätze), est le cœur du chapitre car la démonstration de cette proposition fournit une méthode qui pourra être appliquée au cadre multidimensionnel. On voit d'autre part ressortir la transition vitreuse par le fait que l'on doit utiliser des développement différents suivant la valeur du paramètre μ (n'oublions pas toutefois que le modèle est continu par rapport à $\mu > 0$).

Nous n'avons pas rencontré souvent ce type de comportement sur les développements asymptotiques. On peut toutefois noter dans un article de Gérard-Varet sur les couches limites d'origine physique [32], une transition similaire sur la couche limite d'Ekmann dans le cadre des fluides rapidement tournants. Elle change de taille selon qu'on se trouve près de l'équateur

ou non : loin de l'équateur la couche limite est de taille $\varepsilon^{1/2}$, contre $\varepsilon^{4/5}$ lorsque l'on est à l'équateur.

Pour démontrer cette proposition, on introduit les ansätze (29a)–(29c) dans les équations (27a)–(27h) et on identifie les puissances de y. On cherche alors à identifier le problème fondamental (c'est-à-dire les équations vérifiées par les termes d'ordre le plus bas), ce qui dépend des choix de s et l. Puis on analyse ce problème et on montre son caractère bien posé ou non : on montre que ce caractère bien posé dépend de μ. Finalement, on identifie l et s en examinant les problèmes d'ordre plus élevé.

Comme nous l'avons dit, on peut tirer parti du caractère $1d$ du modèle pour mener une analyse complète de la convergence, ce qui conduit au théorème suivant :

Théorème 2. *La solution de* (27a)–(27h) *peut être développée en une série* convergente *dont les termes sont décrits de la façon suivante :*

si $\mu > 1/2$, *il n'y a pas de terme de couche limite (*$\overline{Q}$ *et* $\overline{R}$ *sont des fonctions de* σ*) et nous avons*

$$q = \overline{Q}^0 + y\overline{Q}^1 + y^2\overline{Q}^2 + \cdots,$$
$$r = \overline{R}^0 + y\overline{R}^1 + y^2\overline{R}^2 + \cdots,$$

ainsi que

$$\frac{\phi}{\mu} = \overline{c}_0 + \overline{c}_1 y + \overline{c}_2 y^2 + \cdots;$$

si $\mu < 1/2$, *la couche limite est de taille* $y^{1/2}$ *et nous avons*

$$q = \overline{Q}^0 + y^{1/2}\overline{Q}^1 + y\overline{Q}^2 + \cdots,$$
$$r = \sqrt{y}R^1 + yR^2 + \cdots,$$

ainsi que

$$\frac{\phi}{\mu} = c_1 y + c_2 y^{3/2} + \cdots,$$

où R^k *depend de* $(|\sigma| - 1)/y^{1/2}$ *;*

si $\mu = 1/2$, *la couche limite est de taille* $y^{1/5}$ *et nous avons*

$$q = \overline{Q}^0 + y^{1/5}\overline{Q}^1 + y^{2/5}\overline{Q}^2 + \cdots,$$
$$r = y^{2/5}R^2 + y^{3/5}R^3 + \cdots,$$

ainsi que

$$\frac{\phi}{\mu} = c_2 y^{4/5} + c_3 y + \cdots ,$$

où R^k *depend cette fois de* $(|\sigma| - 1)/y^{2/5}$.

Notons que la convergence de la série est démontrée dans un espace de type Sobolev à poids exponentiel de sorte que, dans cet espace, la forme linéaire

$$(q, r) \mapsto \int_{[-1,1]} \sigma q(\sigma) \mathrm{d}\sigma + \int_{\mathbf{R}\setminus[-1,1]} \sigma r(\sigma) \mathrm{d}\sigma, \tag{30}$$

est une forme linéaire continue. Nous avons donc gratuitement le corollaire suivant :

Corollaire 1. *Sur la contrainte, nous avons la discussion suivante :*
si $\mu > 1/2$, *la contrainte se développe en*

$$\tau = \eta_0 y + \eta_1 y^2 + \ldots ,$$

si $\mu < 1/2$, *la contrainte se développe en*

$$\tau = \tau_0 + A_0 \sqrt{y} + \ldots ,$$

si $\mu = 1/2$, *la contrainte se développe en*

$$\tau = B_0 y^{1/5} + B_1 y^{2/5} + \ldots .$$

Notons que dans le corollaire précédent, les constantes η_0, τ_0 et B_0 sont non nulles (et qu'on retrouve alors les valeurs calculées dans le théorème 1 une fois reformulées en constantes adimensionnées).

Le théorème se démontre, entre autres, en utilisant la théorie des perturbations analytiques d'opérateurs dans l'esprit de Kato [43]. L'idée centrale est de considérer le problème (27a)–(27h) comme un problème à deux paramètres y et ϕ. On change ces paramètres (ce qui rappelle la désingularisation utilisée dans le chapitre 1) puis on exprime (q, r) comme la solution d'un opérateur elliptique, dont la dépendance en ses paramètres est analytique. On conclut en utilisant le théorème des fonctions implicites (toujours dans sa version analytique). Cette approche permet de montrer la convergence de la série (par analyticité) alors que généralement pour ces problèmes de type pénalisation, on ne montre que des développements asymptotiques (éventuellement à tout ordre, voir par exemple le chapitre 6 du livre de Boyer et Fabrie [12]).

Le chapitre 2 est tiré d'un article accepté dans *SIAM J. Appl. Math.*, en collaboration avec Michael Renardy.

Pour illustrer la souplesse de la méthode mise au point au chapitre 2, nous l'avons appliquée au problème suivant : quel est le comportement du modèle d'Hébraud-Lequeux lorsque, cette fois, le taux de cisaillement $\dot{\gamma}$ devient très grand. Du point de vue mathématique, il s'agit donc d'étudier la limite du système (22)–(24) lorsque y tend vers l'infini. Du point de vue expérimental, les matériaux vitreux tendent à devenir de plus en plus newtoniens lorsque le cisaillement est grand. Dans [37], Hébraud et Lequeux affirmaient que leur modèle reproduisait ce fait. De plus la viscosité à la limite était indépendante de la température μ. Nous avons cherché à démontrer cette affirmation et obtenu le théorème (on note $y = 1/\varepsilon$) :

Théorème 3. *Lorsque ε tend vers 0, la contrainte τ donnée par (26), où p est solution de (22)–(24), admet l'asymptotique suivante :*

$$\tau \sim \frac{1}{\varepsilon},$$

ou plus précisément

$$\tau = \frac{1}{\varepsilon} + \mathcal{O}(1).$$

En variables dimensionnées, nous obtenons que la contrainte est équivalente à $G_0 T_0 \dot{\gamma}$ ce qui traduit, bel et bien, un comportement newtonien à viscosité indépendante de la température μ.

Pour montrer ce théorème, nous utilisons le même principe que pour l'étude à faible cisaillement : nous développons asymptotiquement la solution de (22)–(24) dans un espace dans lequel la forme linéaire en p (26) est continue. Ce faisant nous en déduisons par simple intégration le développement de la contrainte τ. Ce résultat se traduit dans la proposition suivante :

Proposition 2. *La solution p du problème (22)–(24) peut s'écrire $p = p^{\mathrm{app}} + p^{\mathrm{rem}}$, où p^{app} est définie par*

$$p^{\mathrm{app}} = \begin{cases} \varepsilon \exp\left(\dfrac{\sigma}{\mu\varepsilon}\right) & si\ \sigma \leq 0, \\ \varepsilon & si\ 0 \leq \sigma \leq 1, \\ \varepsilon \exp\left(-\varepsilon(\sigma - 1)\right) & si\ 1 \leq \sigma, \end{cases} \tag{31}$$

et p^{rem} *est un terme de reste vérifiant*

$$\left\| \exp\left(-\frac{\cdot}{2\mu\varepsilon}\right) p^{\mathrm{rem}} \right\|_{\mathrm{L}^2(-\infty,0)} = \mathcal{O}(\varepsilon^{5/2}), \tag{32}$$

$$\|p^{\mathrm{rem}}\|_{\mathrm{L}^2(0,1)} = \mathcal{O}(\varepsilon^{3/2}), \tag{33}$$

$$\left\| \exp\left(\frac{\varepsilon}{2}(\cdot - 1)\right) p^{\mathrm{rem}} \right\|_{\mathrm{L}^2(1,+\infty} = \mathcal{O}(\varepsilon^{3/2}). \tag{34}$$

Une illustration de ce théorème est donné par les figures 2 et 3 où l'on a représenté respectivement la solution stationnaire et son logarithme, pour $\mu = 1$ et différentes valeurs de ε ainsi que le logarithme de la solution.

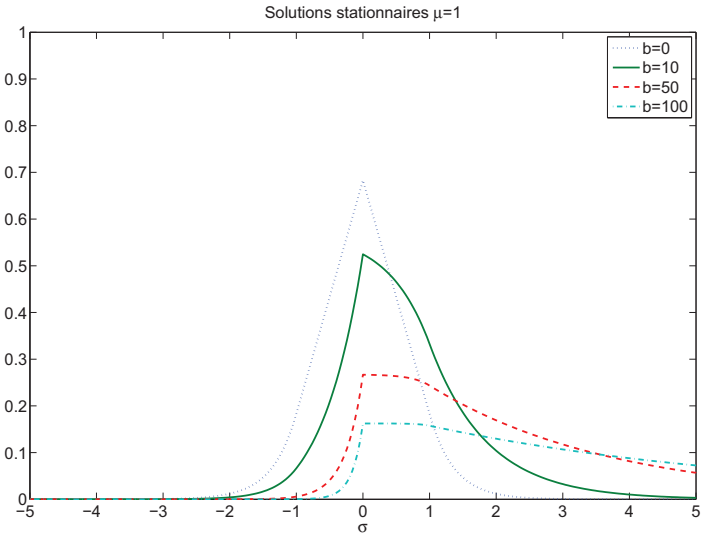

FIG. 2: Solution stationnaire de (26) pour des valeurs de $b = 1/\varepsilon$ de plus en plus grandes

Nous avons opté cette fois pour une approche par développements asymptotiques tronqués (ici à l'ordre 1) contrairement à ce que nous avions fait dans le chapitre 2. En effet, ceci nous a permis d'identifier les difficultés inhérentes à cette démarche et peut servir de marchepied à une analyse similaire sur le modèle multidimensionnel du chapitre 4.

Ces difficultés, quelles sont-elles ? Comme on peut le voir dans l'énoncé de la proposition 2, le développement ne dépend pas de μ. Nous n'avons donc pas à nous soucier d'un changement de comportement comme dans le chapitre 2. La difficulté principale réside dans l'obtention d'un développement

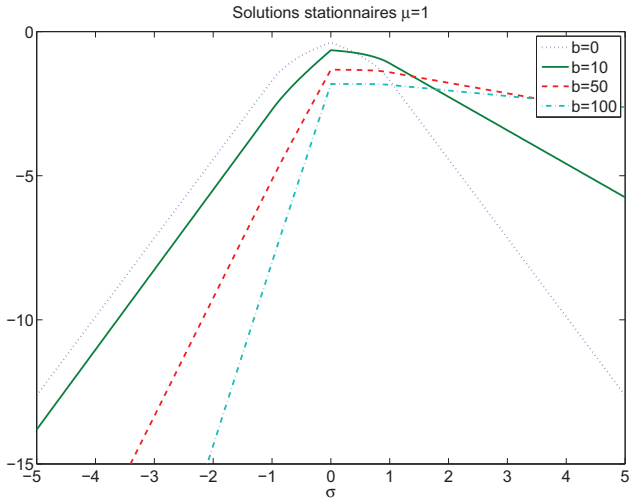

FIG. 3: Logarithme de la solution stationnaire de (26) pour des valeurs de $b = 1/\varepsilon$ de plus en plus grandes

asymptotique de Γ qui n'est défini qu'implicitement par l'équation (24). La réponse à cette question est donnée par le lemme suivant :

Lemme 1. *La fluidité* Γ *admet le développement*

$$\Gamma = 1 + \mathcal{O}(\varepsilon). \tag{35}$$

Ce lemme est utilisé à plusieurs reprises pour démontrer les estimations (32)–(33) qui, elles, mesurent la qualité de l'approximation de la proposition 2. Pourtant sa démonstration nécessite à elle seule un développement asymptotique avec son propre cortège d'estimations de reste !

Il faut noter que ce schéma de preuve n'utilise jamais le théorème des fonctions implicites. D'une certaine façon, le raisonnement par le théorème des fonctions implicites est remplacé par un argument utilisant uniquement le théorème des valeurs intermédiaires. Une telle preuve peut permettre de démontrer un théorème d'existence pour ε petit de (22)–(24) (mais on n'obtient pas l'unicité par cette méthode).

Le chapitre 3 est tiré d'un article soumis pour un numéro spécial de *Science China Mathematics*, dans le cadre de la *French-Chinese Summer School* sur *les effets de tenseur de contraintes sur les fluides.*

Nous sommes maintenant munis d'un certain nombre d'outils pour nous attaquer à la question suivante : le modèle multidimensionnel (16) que nous

avons conçu admet-il des propriétés similaires au modèle initial de Hébraud-Lequeux ? La réponse que nous apportons à cette question dans le chapitre 4 n'est pas encore tout à fait complète, même d'un point de vue formel. Nous pensons cependant avoir apporté des éléments qui laissent à penser que c'est bien le cas.

Rappelons que nous nous situons dans le cas d'un fluide au repos ($u = 0$), stationnaire et homogène (pas de dépendance de p en t et x, et la matrice ∇u est une matrice constante) et enfin à un faible taux de déformation ($\nabla u = \varepsilon M$). La forme de l'équation (16) est agréable d'un point de vue modélisation pour sa concision mais, pour pouvoir l'analyser, nous devons choisir une base de l'espace des matrices symétriques et exprimer l'équation dans cette base. Une fois ceci accompli, nous aboutissons à la formulation suivante :

$$\begin{cases} -\mu\Gamma\Delta p + \varepsilon(A\Sigma + A^0)\cdot\nabla p + h(|\Sigma|)p = \Gamma\rho, \\ \displaystyle\int_{\Sigma\in\mathbf{R}^6} p(\Sigma)\mathrm{d}\Sigma = 2^{3/2}. \end{cases} \tag{36}$$

Dans cette formulation, Σ est le point courant de $\mathbf{R}^6$, Δ est le laplacien usuel, ∇ l'opérateur de gradient usuel, $|\cdot|$ la norme euclidienne sur $\mathbf{R}^6$ et h est $\mathbf{1}_{\mathbf{R}\setminus[-1,1]}$. A est une matrice qui regroupe les informations provenant du terme $g_a(\Sigma, \nabla u) : \nabla_\Sigma p$ dans la formulation (16) alors que A^0 est un vecteur qui provient de $G_0 D(\nabla u) : \nabla_\Sigma p$; A ne dépend donc que de M et a alors que A^0 ne dépend que de M et de G_0.

On le voit, le problème est formellement très ressemblant à (22)–(24), à la différence notable que la vitesse du transport n'est plus constante.

Nous avons travaillé sous l'hypothèse qu'il existait au moins une solution au problème (36) ce qui est loin d'aller de soi. Mais rappelons que notre objectif était uniquement d'expliciter les comportements possibles pour notre modèle à faible cisaillement afin de valider son potentiel : si le modèle s'écroulait dans ce domaine, il fallait le modifier.

Nous allons énoncer quelques résultats qui sont valides dans au moins deux cas qui sont intéressants du point de vue rhéologique :

cisaillement simple : c'est le cas lorsque la matrice M vaut

$$M = \begin{pmatrix} 0 & 1 & 0 \\ 0 & 0 & 0 \\ 0 & 0 & 0 \end{pmatrix}.$$

En effet nous devons retrouver les mêmes résultats que pour le modèle d'Hébraud-Lequeux qui est écrit en cisaillement ;

flot élongationnel : c'est le cas lorsque la matrice M vaut

$$M = \begin{pmatrix} 2 & 0 & 0 \\ 0 & -1 & 0 \\ 0 & 0 & -1 \end{pmatrix} \qquad \text{ou} \qquad M = \begin{pmatrix} 1 & 0 & 0 \\ 0 & -1 & 0 \\ 0 & 0 & 0 \end{pmatrix}.$$

Ce sont des situations classiques dans lesquelles le matériau ne subit aucun cisaillement.

Les résultats peuvent s'étendre à d'autres cas, mais expliciter les hypothèses nécessaires n'éclaircirait pas particulièrement le problème : il vaut mieux parcourir la démonstration et s'assurer que chaque hypothèse intermédiaire est vérifiée pour un flot en particulier.

Pour décrire le résultat nous notons $q = p_{|B}$ et $r = p_{|\mathbf{R}^6 \setminus B}$ où B est la boule unité de $\mathbf{R}^6$. Nous notons encore $\theta_e(\Sigma) = |\Sigma| - 1$ la distance extérieure à la sphère unité.

Théorème 4. *1. Les développements asymptotiques d'une solution de* (36) *ne peuvent avoir que trois formes :*

– *première forme,*

$$\begin{cases} q(\Sigma) = \overline{Q}^0 + \varepsilon \overline{Q}^1 + \varepsilon^2 \overline{Q}^2 + \dots, \\ r(\Sigma) = \overline{R}^0 + \varepsilon \overline{R}^1 + \varepsilon^2 \overline{R}^2 + \dots, \end{cases} \tag{37}$$

où $\overline{Q}^k$ et $\overline{R}^k$ sont des fonctions de Σ,

– *deuxième forme,*

$$\begin{cases} q(\Sigma) = \overline{Q}^0 + \varepsilon^{1/2} \overline{Q}^1 + \varepsilon \overline{Q}^2 + \dots, \\ r(\Sigma) = \varepsilon^{1/2} R^1 + \varepsilon R^2 + \dots, \end{cases} \tag{38}$$

où $\overline{Q}^k$ est une fonction de Σ et R^k une fonction de $(\Sigma/|\Sigma|, \theta_e(\Sigma)/\varepsilon^{1/2})$,

– *troisième forme,*

$$\begin{cases} q(\Sigma) = \overline{Q}^0 + \varepsilon^{1/5} \overline{Q}^1 + \varepsilon^{2/5} \overline{Q}^2 + \dots, \\ r(\Sigma) = \varepsilon^{2/5} R^2 + \varepsilon^{3/5} R^3 + \dots, \end{cases} \tag{39}$$

où $\overline{Q}^k$ est une fonction de Σ et R^k une fonction de $(\Sigma/|\Sigma|, \theta_e(\Sigma)/\varepsilon^{2/5})$.

2. Définissons E la solution de

$$\begin{cases} -\Delta E = \rho \quad \textit{dans } |\Sigma| \leq 1, \\ E = 0 \qquad\quad \textit{sur } |\Sigma| = 1, \end{cases} \tag{40}$$

et notons

$$\mu_c = 2^{-3/2} \int_{|\Sigma| \leq 1} E(\Sigma) \mathrm{d}\Sigma; \tag{41}$$

si $\mu > \mu_c$, *alors la solution ne peut avoir un développement que de type* (37) *ou* (38),

si $\mu = \mu_c$, *alors la solution ne peut avoir un développement que de type* (39) *ou* (38),

si $\mu < \mu_c$, *alors la solution ne peut avoir un développement que de type* (38).

Comme on le voit, ce résultat est plus faible que son analogue $1d$, la proposition 2, car il ne permet pas d'associer à une gamme de μ un seul type de développement asymptotique excepté dans le cas $\mu < \mu_c$. La raison en est la suivante : en $1d$, le problème fondamental de type (38) fait intervenir une équation de type $F(c) = \mu$ (l'inconnue est c) et nous savons calculer l'expression analytique de F : nous savons donc démontrer que cette fonction est croissante de 0 à 1/2. Ce n'est plus le cas pour le modèle multidimensionnel car la monotonie nous échappe : on sait démontrer que le problème fondamental associé au développement de type (38) est bien posé pour μ si, et seulement si, $2^{3/2}\mu$ est une valeur prise par une certaine fonction F. Cette fonction est définie de la façon suivante : notons H_ν la solution du problème suivant :

$$\begin{cases} -\nu\Delta H_\nu + (A\Sigma + A^0)\cdot\nabla H_\nu = \nu\rho & \text{dans } |\Sigma| < 1, \\ H_\nu = 0 & \text{sur } |\Sigma| = 1, \end{cases} \tag{42}$$

alors $F(\nu)$ est simplement l'intégrale de H_ν sur la boule unité. Sous certaines hypothèses, encore une fois vérifiées pour les cas particuliers qui nous intéressent (cisaillement simple et flot élongationnel), nous sommes capables de calculer les limites de cette fonction F :

$$\lim_{\nu\to 0} F(\nu) = 0, \tag{43}$$

$$\lim_{\nu\to+\infty} F(\nu) = 2^{3/2}\mu_c. \tag{44}$$

Les hypothèses en question (celles de la proposition 4.6) précisent en fait la structure de l'opérateur de transport $A\Sigma + A^0$ en imposant que les caractéristiques issues de points de la boule unité croisent obligatoirement la sphère.

Remarquons au passage qu'obtenir ces limites nécessite d'étudier des perturbations, singulière ou régulière, du système (42). Or ici nous ne travaillons pas nécessairement dans un cadre très agréable pour ce faire, car ρ peut être peu régulière (penser à $\rho = \delta_0$ qui serait la généralisation la plus immédiate de l'équation (2)) et seulement dans l'espace de Sobolev $\mathrm{W}^{-1,\beta}$ avec $1 < \beta \leq 2$. Sorti du cadre variationnel classique $\rho \in \mathrm{W}^{-1,2}$, il faut utiliser des résultats

un peu plus fins sur les équations elliptiques (notamment AGMON, DOUGLIS et NIRENBERG [1] ou MEYERS [49]).

La continuité de F étant assurée par les conditions de régularité imposée à ρ, nous savons alors que $F(]0,+\infty[)$ contient au moins l'intervalle $]0,2^{3/2}\mu_c[$. Par conséquent, le problème est bien posé pour μ dans l'intervalle $]0,\mu_c[$. Néanmoins, nous ne savons pas démontrer que la fonction F est monotone, ce qui n'exclut donc pas que le problème fondamental du développement de type (38) soit bien posé pour d'autres valeurs.

Le chapitre 4 est constitué d'une première version d'un article écrit en collaboration avec MICHAEL RENARDY.

Biologie et chimie

Pour conclure, nous allons présenter les travaux que nous avons effectués en dehors du cadre «math/physique» avec deux problèmes issus pour l'un de la biologie (et même de la médecine) et pour l'autre essentiellement de la chimie (même si des considérations physiologiques seront présentes).

Le chapitre 5 est consacré à l'étude de la réaction-diffusion dans l'hypothèse où les réactions sont infiniment rapides par rapport à la diffusion. Le contexte initial était de décrire la balnéothérapie : dans ce mode thérapeutique, les patients sont immergés dans un bain enrichi en CO_2. Ce CO_2 se diffuse ensuite à travers la peau jusqu'aux capillaires sanguins où il est absorbé. L'objectif est d'équilibrer le niveau de CO_2 dans le sang. Cette étude avait été proposée à BEAR et BRESCH avec en vue une optimisation des conditions du bain pour un objectif donné (rapidité de l'absorption ou quantité absorbée, par exemple). Dans un article finalement non publié, ils en avaient tiré un modèle fondé essentiellement sur l'idée suivante : il y a 6 espèces chimiques à considérer (H^+, OH^-, H_2CO_3, $C0_2$, HCO_3^- et CO_3^{2-}) et 5 relations «chimiques» (4 relations d'équilibre chimique et l'éléctroneutralité). Il n'y a donc plus qu'un seul degré de liberté à fixer pour obtenir un problème bien posé. Ce degré de liberté est fixé par une équation de diffusion : on commence par écrire une équation de diffusion sur les 6 espèces et, sous l'hypothèse que toutes ces espèces diffusent à la même vitesse, en utilisant la stœchiométrie du problème, on en déduit que la quantité totale d'espèces carbonatées diffuse sans terme source de réaction.

Une objection à ce raisonnement était : a-t-on le droit de passer par l'étape «système de réaction-diffusion sur toutes les espèces» ? En effet, si ces espèces diffusent, elles n'en sont pas moins contraintes de vérifier certaines relations algébriques. Or on sait que, génériquement, on ne peut pas diffuser sous

contrainte. Supposons en effet qu'un vecteur $X \in \mathbf{R}^M$ suive une équation de réaction diffusion de la forme :

$$\partial_t X - \Delta X = S(X), \tag{45}$$

tout en étant contraint par les relations $\Gamma(X) = 0$ où $\Gamma : \mathbf{R}^M \to \mathbf{R}^{M-1}$. Si on écrit la courbe à laquelle appartient X de façon explicite à l'aide de ϕ et du degré de liberté $\kappa \in \mathbf{R}$, on peut écrire $X(t,x) = \phi(\kappa(t,x))$. L'équation (45) donne alors l'information suivante sur κ :

$$(\partial_t \kappa - \Delta\kappa)\phi'(\kappa) + |\nabla\kappa|^2\phi''(\kappa) = (S \circ \phi)(\kappa). \tag{46}$$

Or, génériquement, $\phi'(\kappa)$ et $\phi''(\kappa)$ sont des vecteurs indépendants de l'espace. Voici donc ce qui peut se passer : d'abord $S \circ \phi$ peut ne pas se développer dans la base $(\phi'(\kappa), \phi''(\kappa))$, auquel cas il n'y a certainement pas de solution ; si $S \circ \phi$ a la bonne écriture, (46) donne en fait *deux* équations sur κ qui est une donnée scalaire et donc le problème est génériquement surcontraint. Le seul remède serait que $\phi'(\kappa)$ et $\phi''(\kappa)$ soient liés, ce qui signifie que la variété des contraintes sur X est une droite, donc essentiellement que ces contraintes sont toutes linéaires. Or ce n'est pas notre cas ici.

L'apport principal de ce chapitre est double. D'abord nous apportons une réponse de modélisation à l'objection mathématique précédente. Cette réponse peut se résumer simplement par : «oui, un tel raisonnement est correct». Il n'en reste pas moins que nous avons dû retourner aux principes de base de la diffusion et de la réaction d'espèces chimiques pour nous en convaincre. Ce qu'il a fallu comprendre c'est que la loi de conservation de la masse et les deux premiers principes de la thermodynamique forcent le système à rester sur la variété d'équilibre implicitement par l'existence d'un terme source *ad hoc*. Ce terme peut être vu comme un multiplicateur de Lagrange associé aux contraintes d'équilibre. Le système prend la forme suivante :

$$\begin{cases} \partial_t \overrightarrow{C} - \operatorname{div}(\mathcal{D}\nabla\overrightarrow{C}) = \nu^T\sigma \\ \Gamma(\overrightarrow{C}) = 0 \end{cases} \tag{47}$$

où $\nu \in \mathcal{M}_{NM}(\mathbf{R})$ est la matrice des coefficients stœchiométriques algébriques (chaque ligne correspond à une réaction et chaque colonne correspond à une espèce) et $\mathcal{D}$ est la matrice diagonale des coefficients de diffusion. Le système $\Gamma(\overrightarrow{C}) = 0$ contient les diverses équations d'équilibre chimique. Nous obtenons ce modèle sous l'hypothèse que la cinétique chimique est infiniment plus rapide que le processus de diffusion physique. Bien entendu s'il existe des réactions lentes, il suffit de rajouter leur cinétique dans le second membre,

de même si d'autres processus physiques lents sont à l'œuvre (présence d'un champ éléctrique agissant sur les ions par exemple).

Il y a plusieurs avantages à évacuer la cinétique rapide de cette manière :

- nous n'avons pas à modéliser cette cinétique ce qui est un problème difficile même pour certaines réactions simples. D'autre part les constantes qui peuvent apparaître dans de tels modèles peuvent être difficiles à déterminer expérimentalement ;
- *a contrario* nous n'utilisons dans Γ que les constantes d'équilibre des réactions qui ne dépendent que de la thermodynamique et sont plus facilement accessibles ;
- nous évitons de calculer des intermédiaires réactionnels qui ne sont présents que lors des régimes transitoires mais qui n'apparaissent pas dans le bilan chimique aux échelles de temps macroscopiques ;
- puisque la chimie préserve la masse et l'éléctroneutralité, c'est encore le cas du système final, pourvu que la physique sous-jacente les préserve elle-aussi. Remarquons tout de même que cette question est délicate dans la réalité pour ce qui concerne l'éléctroneutralité.

De la même façon qu'on peut traiter les équations de mécanique des fluides incompressibles en éliminant la pression à l'aide du projecteur de Leray, on peut éliminer l'inconnue σ ce qui conduit à l'équation sur $\overrightarrow{C}$ suivante :

$$\partial_t \overrightarrow{C} - (Id - \chi(\overrightarrow{C}))\mathrm{div}\,(\mathcal{D}\nabla \overrightarrow{C}) = 0, \tag{48}$$

où $\chi(\overrightarrow{C}) = \nu^T \left(\mathrm{d}\Gamma(\overrightarrow{C})\nu^T\right)^{-1} \mathrm{d}\Gamma(\overrightarrow{C})$ est une matrice locale de projection. On voit que l'on tombe sur une équation non linéaire, mais surtout non conservative. Or nous voulions simuler ce système de réaction-diffusion par une démarche de type volume fini pour tirer parti de leur souplesse sur la variation des coefficients de diffusion en espace (étant donné que la peau est, à un niveau très simplifié, un milieu bicouche, chaque couche ayant sa propre porosité). Nous avons tenu compte de cette difficulté en raisonnant plutôt sur le système (47) : sous cette forme, un schéma volume fini serait tout à fait classique si nous connaissions l'expression de σ en fonction de $\overrightarrow{C}$. Comme cette inconnue n'est définie qu'implicitement, il nous reste à expliquer comment donner des approximations de ses moyennes sur chacun des volumes finis. Nous proposons une approximation fondée sur les idées de la modélisation.

Plusieurs problèmes numériques se sont posés. Le plus important a peut-être été de comprendre ce que signifiait la contrainte $\Gamma(\overrightarrow{C}) = 0$ au niveau numérique. Comment distinguer entre $\Gamma(\overrightarrow{C}) = 10^{-7}$ et $\Gamma(\overrightarrow{C}) = 10^{-14}$ dans un contexte où les concentrations elles-mêmes peuvent avoir des ordres de

grandeurs très différents (dans nos simulations la concentration de H^+ varie entre 10^{-7} et $10^{-6} mol \cdot L^{-1}$, la concentration de OH^- entre 10^{-8} et $10^{-7} mol \cdot L^{-1}$, la concentration de CO_2 et de HCO_3^- entre 0 et $10^{-3} mol \cdot L^{-1}$) ? La contrainte est-elle «mieux» satisfaite dans un cas que dans l'autre ? Notre façon de voir a été de déterminer, si à partir d'une composition chimique $\overrightarrow{C}$, le système avait besoin de «faire beaucoup de chimie».

L'autre problème important que nous avons rencontré est : comment calculer la quantité qui a traversé pour une espèce ? En effet, nous avons remarqué que le système était essentiellement non conservatif et par conséquent la notion de flux n'est plus claire. Le problème central est de distinguer dans une variation locale de quantité de matière ce qui provient de l'extérieur et ce qui résulte de la réaction chimique qui a lieu localement. Cette question est aussi liée au problème des conditions aux bords : quel sens peut avoir la prescription d'un flux *diffusif* ou une composition donnée ?

Nous comparons ensuite dans un cas simple notre modèle à une solution de référence dans le cas où l'on connaît la cinétique : nous regardons l'eau pure (c'est-à-dire uniquement les ions H^+ et OH^-) en supposant qu'un milieu homogène est en contact avec des solutions tamponnées de pH fixés différents du pH initial. Nous obtenons que notre schéma est plus proche de la solution de référence qu'un simple schéma de diffusion/projection comme on peut le voir sur la figure 5.2 p. 203.

Le chapitre 5 présente la version initiale d'un article en collaboration avec Yann Bouret et Stéphane Descombes.

Enfin, le chapitre 6 est issu d'un projet débuté au Cemracs 2009 consacré à la modélisation mathématique en médecine. Ce projet a pour ambition de comprendre la formation des sutures crânofaciales qui présentent deux particularités. La première est que bien que la formation osseuse soit gouvernée par des processus de migrations cellulaires, les sutures sont en pratique extrêmement longues à se refermer chez les sujets sains (de l'ordre de la vingtaine d'années chez l'homme). La seconde est que la suture évolue pour passer d'une géométrie linéaire entre ses berges à une structure complexe, presque fractale. Ce phénomène est connu sous le nom d'*interdigitation*.

La question de la fermeture est importante car une fermeture trop précoce des sutures entraîne des pathologies connues sous le nom de sténose qui se traduisent par des déformations du crâne. Ce genre de pathologie concerne à des degrés divers une personne sur environ deux mille. Pour illustrer l'importance du sujet, la formation des sutures et leur interdigitation un article de 2009 [50] a été publié par Miura, Perlyn, Kinboshi, Ogihara, Kobayashi-Miura, Morriss-Kay et Shiota. Dans leur article, les auteurs modélisent la formation des sutures à l'aide de deux variables u et v,

u représentant l'état du mélange entre os et mésenchyme, et v représentant la concentration d'un facteur chimique régulateur du phénomène. En écrivant des équations de réaction-diffusion sur ces deux variables et en utilisant les travaux de Hagberg et Meron [35] Miura *et al.* en tirent l'apparition de motifs labyrinthiques. La fermeture des sutures est, quant à elle, traitée par une extinction de la partie diffusive exponentielle en temps. Les auteurs classent leur modèle dans la catégorie des «modèles-jouets». Cependant leur modèle a l'avantage d'être suffisament simple pour en permettre une analyse théorique, d'une part, et utilisent des concepts connus des biologistes du développement, d'autre part.

Nous avions une approche différente. On s'est aperçu, [64], que les forces subies par le crâne influençaient la persistence et la complexification des sutures. Le point de départ du projet était donc : peut-on expliquer les phénomènes observés à partir de considérations purement biomécaniques ? Le principal apport du chapitre 6 est de proposer un modèle couplant des équations de biologie du développement classiques avec de la mécanique des milieux continus. Nous avons donc écrit un modèle qui couple mécanique et biologie, essentiellement à travers le concept d'*haptotaxis* : nous postulons que les cellules mesenchymales peuvent se déplacer plus rapidement dans des «tubes» de fibres de collagène, à condition que ces fibres s'alignent collectivement pour former ces tubes. Cette propension à s'aligner et les directions d'alignement collectif sont justement contrôlées par les effets mécaniques locaux ressentis par les fibres. Ceci nous permet de coupler de façon originale des modèles biologiques et mécaniques qui, pris indépendamment, sont des modèles simples et classiques.

Nous réalisons enfin des simulations numériques de ce modèle et voyons effectivement apparaître une instabilité d'interface qui fait nettre des tortuosité ressemblant au développement des sutures réelles.

Le chapitre 6 est une première version d'un article en collaboration avec Hossein Khonsari, Paul Tafforeau, Paul Vigneaux, Didier Bresch et Vincent Calvez.

Première partie

Matériaux vitreux

Chapitre 1

Approche directe de la transition vitreuse dans le modèle d'Hébraud-Lequeux

Résumé du chapitre

Le résultat principal de ce chapitre tient aux deux propositions 1.1 et 1.2 mais, en réalité, plus à leur démonstration qu'à leur énoncé. En effet ces deux résultats traduisent l'existence d'une transition vitreuse pour les matériaux régis par le modèle d'Hébraud-Lequeux, ce qui était déjà annoncé par Hébraud et Lequeux eux-mêmes dans [37]. En revanche il n'existait pas de démonstration mathématique de ce fait. Dans ce chapitre nous adoptons les notations adimensionnées de Cancès, Catto et Gati dans [16] et donc, par rapport au système (8) p. 7, le rôle du taux de cisaillement $\dot{\gamma}$ est joué par le paramètre adimensionné b tandis que le paramètre de fragilité α est adimensionné en un paramètre μ.

Le modèle d'Hébraud-Lequeux (stationnaire) doit être vu comme un modèle à deux inconnues, Γ et p, et deux équations couplées sur ces inconnues : une équation différentielle ordinaire à coefficients non constants (1.1) et une équation «algébrique» (plutôt non différentielle en réalité) (1.2). Ces équations sont contrôlées par deux paramètres qui apparaissent dans les coefficients de l'équation différentielle, b et μ. Enfin la quantité physique d'intérêt dans ce modèle est la contrainte macroscopique τ définie en fonction de p par (1.5). Étudier l'existence d'une transition vitreuse revient à étudier le comportement du système lorsque le paramètre b tend vers 0 et en particulier le comportement de τ en fonction de b.

La philosophie de l'étude de ce premier chapitre pourrait se résumer

à court-circuiter l'équation différentielle. En effet, cette équation est assez simple pour que l'on puisse résoudre p en fonction de Γ de façon analytique. Résoudre exactement le système d'Hébraud-Lequeux revient donc à résoudre l'équation algébrique (1.2) pour obtenir la seule inconnue qui reste, Γ. Ce schéma est en fait le schéma utilisé par Cancès *et al.* pour montrer l'existence et l'unicité de la solution du système. Nous redonnons néanmoins cette démonstration en détail dans l'appendice pour la commodité du lecteur.

Nous cherchons maintenant à étudier la limite $b \to 0$ du système. En suivant le schéma précédent, il nous faut étudier l'équation qui définit Γ et comprendre maintenant sa dépendance en b. L'expression de cette fonction notée f_μ est donnée par (1.8) (où x et y sont des quantités réduites, plus agréables à manipuler, définies en fonction de Γ et b respectivement) et l'existence et l'unicité de Γ ne sont données qu'à travers le théorème des fonctions implicites. Nous ne disposons donc pas d'expression analytique pour Γ vu comme fonction de b. Pire encore, la fonction (1.8) n'est bien régulière qu'en dehors du point $(0,0)$ et nous voulons prouver (à la suite d'Hébraud et Lequeux) que, dans certains cas ($\mu \leq 1/2$), c'est justement vers ce point que va tendre $(\Gamma(b), b)$. Nous devons donc étudier l'asymptotique d'une fonction définie implicitement par f_μ au voisinage du bord du domaine de définition de f_μ et même au voisinage d'une de ses singularités. C'est l'objet de la démonstration de la proposition 1.1, qui repose essentiellement sur des changements de variables adaptés : on obtient ainsi un nouveau problème de fonction implicite mais cette fois régulière au voisinage du point d'intérêt, et auquel on peut donc appliquer le théorème des fonctions implicites.

Une fois cette démonstration achevée, nous sommes munis du comportement de l'inconnu Γ en fonction de b pour b petit. Il nous reste à démontrer le théorème 1.2. Puisque nous avons court-circuité l'inconnue p on peut voir la contrainte τ comme étant donnée en fonction des paramètres (donc b et μ) et de l'inconnue restante Γ : le comportement de la contrainte τ à petit cisaillement est donc le comportement d'une fonction (1.13) de (Γ, b) mais que l'on doit voir en réalité comme une fonction de $(\Gamma(b), b)$. Malheureusement, $\Gamma(b)$ n'est pas connu, ce que l'on connaît c'est son développement asymptotique au voisinage de 0. Il faut donc extraire de l'expression de τ en fonction de (Γ, b) et de l'asymptotique de $\Gamma(b)$ en fonction de b le comportement de $\tau(\Gamma(b), b)$ en fonction de b. Pour ce faire, on s'appuie simplement sur l'inégalité de Taylor-Lagrange de 1.15. Néanmoins, il faut être minutieux dans cette analyse car d'étranges problèmes peuvent survenir lorsqu'on remplace certaines expressions par d'autres alors qu'elles sont égales le long de la courbe $(\Gamma(b), b)$. D'autres part nous devons obtenir des majorations uniformes ce qui nécessite d'analyser relativement finement les singularités de certaines expressions.

Ce chapitre a fait l'objet d'une publication dans la revue *Zeitschrifft für Angewandte Mathematik und Physik*, [53].

1.1 Introduction

In this article we are interested in a rheological model for glassy material in simple shear flow configuration. Glassy materials range from suspensions (like bentonite for example) to emulsions or to foams. Among other features, these materials exhibit a transition as a control parameter goes through a critical value. This control is for instance, in the case of suspensions, related to the density of solid particle in the fluid.

One model available to describe such material is the Hébraud-Lequeux (HL) model. In Section 1.2, we rapidly review the model and the physical quantities it involves. We prove in the following that this model exhibits such a transition.

Let us first give some notations. We note H the Heaviside function $\mathbf{1}_{\mathbf{R}^+}$ and $h(\sigma) = H(|\sigma| - 1)$ (which is then a "switch" with value 1 outside $[-1, 1]$ and 0 inside); we also note by δ_0 the Dirac measure. The real constants De and λ are given below while b is a real parameter given by the experimental setting (it can thus vary but we can consider it a known data of the problem). The real constant μ is what we will call in the following *the control parameter* and, as b, may vary but can always be considered given. Finally let us define $\Gamma(p) = \displaystyle\int_{|\sigma|>1} p(\sigma)\mathrm{d}\sigma$ a quantity sometimes called the *fluidity*. We are then looking for a density of probability p that solves the following equation:

$$-\lambda b\partial_\sigma p - Deh(\sigma)p + De\Gamma(p)\delta_0(\sigma) + \mu De\Gamma(p)\partial_\sigma^2 p = 0. \tag{1.1}$$

This model thus presents a threshold (set to 1 in nondimensional form) and a relaxation to a zero stress state (described by the Dirac δ_0) when the stress σ grows beyond the threshold. The equation is supplemented with the following conditions:

$$p \in \mathrm{H}^1(\mathbf{R}), \quad p \geq 0, \quad \int_{\mathbf{R}} p(\sigma)\mathrm{d}\sigma = 1. \tag{1.2}$$

Indeed p represents the density of probability to find a block of material in stress σ. We treat here b as a given independent variable (actually we shall rather use $y = \lambda b/De$ as an independent variable) and keep it unconstrained. The variable b is the nondimensional version of the *shear rate* $\dot{\gamma}$.

What we are really interested in is the *total stress* in the material given by $\tau = \displaystyle\int \sigma p\mathrm{d}\sigma$ but seen as a function of $\dot{\gamma}$ and especially its behaviour at low shear rate that is to say when the shear rate $\dot{\gamma}$ tends to 0. While this behaviour can be found in the physics literature (and also here in Section 1.3), the main result of this paper is to give a mathematical proof of it in

Section 1.5 and is based on the study of a two variable function alongside a curve.

However, this curve is the graph of a function ϕ_μ only given implicitly by (1.8) and we have first to study the behaviour of this function in a neighbourhood of 0. Section 1.4 is devoted to this analysis.

Finally, the reason for the apparition of an implicit function in this problem comes from the construction of the solution of Eqs (1.1)-(1.2) itself. We give this construction in the appendices for the sake of self-containment even if it is not the main focus of this paper.

1.2 Hébraud-Lequeux Model

In this section we rapidly describe the rheological model that we use afterwards. To study a material at a continuous level we have to give a constitutive equation that links the stress with the deformation rate. For Newtonian fluids this relation is simply expressing a linear relation between the stress and the deformation rate. For non Newtonian (or complex) fluids there exists a wide variety of nonlinear laws. For example we have Bingham fluids or more generally Herschel-Bulkley fluids.

For the Hébraud-Lequeux (HL) model we go down to the mesoscopic scale, a scale where we can still consider the material continuous but where we can describe some heterogeneities in the material. The principle of this model is that a block of material at a mesoscopic level is not in a single stress state anymore but is described by a density of probability p over the stress space. In a way, the block carries all possible stresses with a coefficient described by the density of probability p. The Hébraud-Lequeux equation describes the evolution of this density p over time. In the following equation, G_0 and T_0 are physical constants, $\dot\gamma$ is the shear rate, and σ_c is the relaxation threshold. We note $\Gamma(q) = \dfrac{1}{T_0}\displaystyle\int H(|\sigma|-\sigma_c)q(\sigma)\mathrm{d}\sigma$ and $D = \alpha\Gamma$ for a physical constant α. We then have

$$\begin{cases} \partial_t p = -G_0\dot\gamma\partial_\sigma p + D(p)\partial_\sigma^2 p - \dfrac{1}{T_0}H(|\sigma|-\sigma_c)p + \Gamma(p(t))\delta_0(\sigma), \\ p(0,\sigma) = p_0(\sigma). \end{cases} \tag{1.3}$$

The solution must also verify the following conditions:

$$p \in \mathrm{L}^2_t(\mathrm{H}^1_\sigma(\mathbf{R})) \text{ and } \quad \forall t\, p(t,.) \geq 0, \quad \int_{\mathbf{R}} p(t,\sigma)\mathrm{d}\sigma = 1. \tag{1.4}$$

The quantity of interest for the physicist is the *total stress* or *macroscopic stress* since it is the one that can actually be measured in a rheometer (see e.g Oswald [57] for details). In the case of the HL model, the total stress τ at time t is linked to the density of probability $p(t,.)$ via the formula

$$\tau(p(t)) = \int_{\sigma\in\mathbf{R}} \sigma p(t,\sigma)\mathrm{d}\sigma \tag{1.5}$$

We refer to Hébraud and Lequeux in [37] for details on the physical interpretation of this equation. What is important to note for this paper, is that the control parameter in the system is α and the critical value at which the transition takes place is $\sigma_c^2/2$.

This equation has been studied from a mathematical point of view by Cancès, Catto and Gati in [16]. They have addressed the question of well-posedness of (1.3)-(1.4). For other mathematical studies on the time-dependent HL model we refer to the work of Cancès, Catto, Gati and Le Bris in [17] for the study of a micro-macro coupling of a Hébraud-Lequeux equation with a macroscopic velocity field which aims at describing the flow of a material in a Couette cell. These studies rely upon PDE methods. Another approach is a probabilistic approach via the theory of stochastic processes and martingales for which we refer to the work of Ben Alaya and Jourdain in [5].

Cancès et al. also looked at the stationary solutions of the equation, proving existence by giving the solution and its form (1.7) and stating uniqueness via the growth of a function. Since the uniqueness part was not so clear to us and because we work with different notations (some of the nondimensional constants that appear here where set to 1 in their paper) we give a proof of uniqueness in appendix 1.7. The stationary solution solves an ODE in σ which we obtain by formally removing the term $\partial_t p$ in (1.3). This is the starting point of our study. We shall actually work on the nondimensional version (1.1) which we give again below for convenience.

What we study in the following are the flow curves given by the model, that is to say the relation between a given shear rate $\dot\gamma$ and the corresponding macroscopic stress which is $\tau(p)$ with p the stationary solution corresponding to $\dot\gamma$. The transition we observe is in the behaviour as $\dot\gamma \to 0$ of the flow curve.

Let us now explain how we obtain the nondimensional system (1.1) we use in the rest of this work. We take the same notations as Gati in her PHD thesis [31]. We have to choose a time scale T which is the duration of the physical experimentation (thus the material may not have the same properties if you observe it for a long or a short time); the stress scale is given by σ_c then all of the quantities appearing in (1.3) become:

$$t' = t/T,\ \sigma' = \sigma/\sigma_c,\ b = T\dot{\gamma}$$

and

$$p'(t',\sigma') = \sigma_c p(Tt', \sigma_c\sigma'), \quad \Gamma'(p'(t')) = \int_{|\sigma'|>1} p'(t',\sigma')\mathrm{d}\sigma' = T_0\Gamma(p(Tt')).$$

and the following nondimensional constants appear in the system

$$De = T/T_0 \qquad \mu = \alpha/\sigma_c^2 \qquad \lambda = G_0/\sigma_c \tag{1.6}$$

We find here De the so-called Deborah number. Then the nondimensional stationary Hébraud-Lequeux equation we have obtained is (we have dropped the primes for the sake of clarity):

$$-\lambda b\partial_\sigma p - Deh(\sigma)p + De\Gamma(p)\delta_0(\sigma) + \mu De\Gamma(p)\partial_\sigma^2 p = 0.$$

The conditions on p read the same as in the time-dependent case, namely:

$$p \in \mathrm{H}^1(\mathbf{R}), \quad p \geq 0, \quad \int_{\mathbf{R}} p(\sigma)\mathrm{d}\sigma = 1.$$

A related topic to the study of stationary solutions of the HL model is the question of long-time behaviour of the solution to the time-dependent equation. This has been addressed in some cases by Cancès and Le Bris in [18] by an entropy-decay method.

1.3 Presentation of the Main Results

Firstly we give again the existence and uniqueness theorem (which can partly be found in [16]) we rely upon:

Theorem 1.1. *There exists a unique solution p to equation* (1.1) *with conditions* (1.2) *which is of the form:*

$$p(\sigma, b) = \begin{cases} \alpha_+ \exp(\beta_+(\sigma+1)) & \text{if } \sigma \leq -1 \\ \alpha_+(1-\rho\beta_+ + \rho\beta_+\exp((\sigma+1)/\rho)) & \text{if } -1 < \sigma \leq 0 \\ \alpha_-(1-\rho\beta_- + \rho\beta_-\exp((\sigma-1)/\rho)) & \text{if } 0 < \sigma \leq 1 \\ \alpha_- \exp(\beta_-(\sigma-1)) & \text{if } 1 < \sigma \end{cases} \tag{1.7}$$

where α_+ *and* α_- *and the constants* ρ, β_+, β_- *depend on* b *and a variable* Γ. *The actual solution is the one for which we have the additional relation* $g(\mu\Gamma, \lambda b/De) = \mu$ *between* Γ *and* b *where*

$$g(x,y) = \frac{\frac{2x^2}{y^2}\left(\cosh\left(\frac{y}{x}\right)-1\right) + x\cosh\left(\frac{y}{x}\right) + \left(\frac{3x^2}{y}+xy\right)\sinh\left(\frac{y}{x}\right)}{\sqrt{y^2+4x}\cosh\left(\frac{y}{x}\right) + \left(\frac{2x}{y}+y\right)\sinh\left(\frac{y}{x}\right)} \\ \frac{+\sqrt{y^2+4x}\left(\frac{x^2}{y^2}\left(\cosh\left(\frac{y}{x}\right)-1\right) + \frac{x}{y}\sinh\left(\frac{y}{x}\right) + x\cosh\left(\frac{y}{x}\right)\right)}{\sqrt{y^2+4x}\cosh\left(\frac{y}{x}\right) + \left(\frac{2x}{y}+y\right)\sinh\left(\frac{y}{x}\right)}.$$

fixing Γ *in terms of* b. *Actually we have* $\Gamma = \Gamma(p)$. *Moreover, since* $\partial_x g(x,y) > 0$ *for all* x *and* y *positive then there exists a function* ϕ_μ *defined on* $]0, +\infty[$ *that gives* $\Gamma = \phi_\mu(\lambda b/De)/\mu$.

For the sake of self-containment, this proposition is proved in details in Appendix 1.6 (See also Appendix 1.7 for details on the uniqueness part which requires a special care). Then before we can turn to the main result of this paper we have to prove the following

Proposition 1.1. *Let* ϕ_μ *the function defined in Proposition 1.1. For every* μ *we introduce* $\bar{\phi}_\mu$, *the first non zero term of the expansion of* ϕ_μ *at* $y = 0$ *that is to say we have* $\phi_\mu(y) \sim \bar{\phi}_\mu(y)$. *Then there exists a positive constant* $c(\mu)$ *such that when* y *decreases to 0 we have:*

if $\mu > 1/2$, $\bar{\phi}_\mu(y) = c(\mu)$,

if $\mu < 1/2$, $\bar{\phi}_\mu(y) = c(\mu)y$,

if $\mu = 1/2$, $\bar{\phi}_\mu(y) = c(1/2)y^{4/5}$.

These behaviours can be seen on Figure 1.1. The definition of $c(\mu)$ in each case is given alongside the proof of this corollary in Section 1.4. We can now state (in physical variables) the main result of this paper:

Theorem 1.2. *We note* $\eta_c = G_0 T_0$. *Let* $p(\dot{\gamma}, \sigma)$ *be the unique solution given by Proposition 1.1 at shear rate* $\dot{\gamma}$. *Then we have the following behaviours for the function* $\tau(\dot{\gamma}) = \int_{\sigma\in\mathbf{R}} \sigma p(\dot{\gamma}, \sigma)\mathrm{d}\sigma$ *at* $\dot{\gamma} \to 0$*:*

If $\alpha > \sigma_c^2/2$ *the fluid behaves like a Newtonian fluid with an apparent viscosity* $\eta(\alpha/\sigma_c^2)$. *Let us first define* $\eta^*(\mu)$ *via the formula*

$$\eta^*(\mu) = 1 + \frac{3\mu - 1 + 1/2(4\mu-1)^{3/2}}{24\mu(\mu-1/2)^2}$$

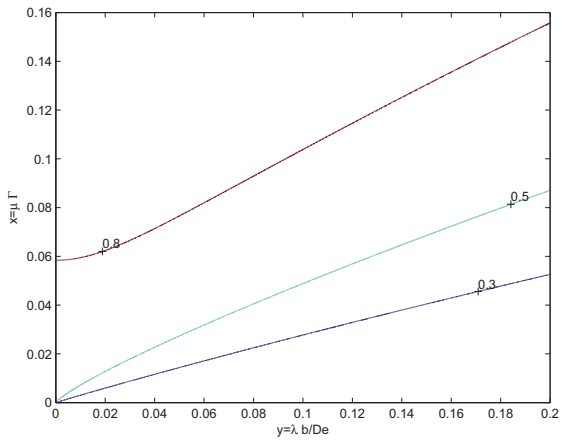

Figure 1.1: Numerical Representation of ϕ_μ for $\mu = 0.3, 0.5$ and 0.8.

We then have

$$\tau(\dot{\gamma}) \sim \eta(\alpha/\sigma_c^2)\dot{\gamma}$$

where the apparent viscosity η *is given by* $\eta(\alpha/\sigma_c^2) = \eta^*(\alpha/\sigma_c^2)\eta_c$.

If $\alpha < \sigma_c^2/2$ *the fluid presents a stress threshold* τ_0. *We first define* c *to be the unique positive root of the following equation*

$$\frac{c(\cosh(1/c) - 1)}{\sinh(1/c)} = \frac{\alpha}{\sigma_c^2}$$

and τ^* *by the formula*

$$\tau^* = \left(\frac{\alpha}{2\sigma_c^2} - 1\right) c.$$

We then have

$$\tau(\dot{\gamma}) \to \tau_0(\alpha/\sigma_c^2)$$

with τ_0 *given by* $\tau_0(\alpha/\sigma_c^2) = \tau^*(\alpha/\sigma_c^2)\sigma_c$.

If $\alpha = \sigma_c^2/2$ *the fluid follows a power law with exponent* $1/5$ *meaning that*

$$\tau(\dot{\gamma}) \sim \frac{24^{2/5}}{12}\sigma_c^{4/5}\eta_c^{1/5}\dot{\gamma}^{1/5}$$

This theorem is important because it describes a transition which is one of the characteristic features of glassy materials. Figure 1.2 shows the different

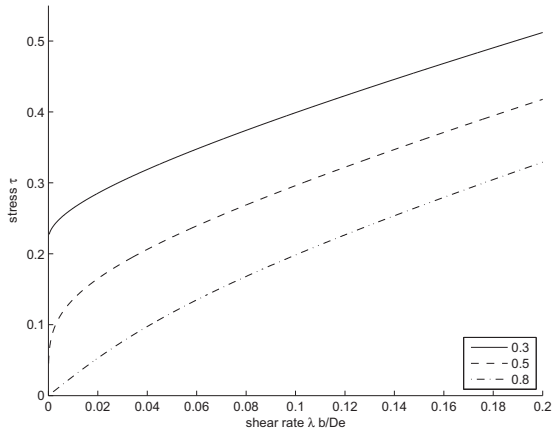

Figure 1.2: Numerical Representation of τ for $\mu = 0.3, 0.5$ and 0.8.

kinds of behaviour one may find. These asymptotic results can be found without proof in Hébraud's PHD thesis and subsequently on several other Physics paper. But this is actually the first time that a mathematical proof of this theorem is given. We were also able to give the numerical constants in the asymptotic for all μ whereas only the cases $\mu \to 1/2$ had been given. The following corollary might be useful too:

Corollary 1.1. *When $\mu = \alpha/\sigma_c^2$ is close to 1/2 we have:*

if $\mu > 1/2$ $\eta^*(\mu) \sim \dfrac{1}{12}(\mu - \dfrac{1}{2})^{-2}$

if $\mu < 1/2$ $\tau^*(\mu) \sim \dfrac{1}{\sqrt{6}}(\dfrac{1}{2} - \mu)^{1/2}$

1.4 Asymptotic Behaviour of $\phi_\mu(y)$ at $y \to 0$

Before we can turn to the main point of this paper, that is to say the behaviour of the macroscopic stress as y decreases to 0, we will need the behaviour of ϕ_μ (the function defined in Proposition 1.1) as y decreases to 0 explicitly. Indeed, it is easier to think of the solution to (1.1) as depending on two parameters x and y and when looking for y dependent behaviour to remember that x and y are linked via $x = \phi_\mu(y)$ (see Appendix 1.6 for instance). Let us recall here that ϕ_μ is defined implicitly by the relation $f_\mu(\phi_\mu(y), y) = 0$ and

$$
\begin{aligned}
f_\mu(x,y) =& \frac{1}{\mu}\left[\frac{2x^2}{y^2}\left(\cosh\left(\frac{y}{x}\right)-1\right)+x\cosh\left(\frac{y}{x}\right)+\left(\frac{3x^2}{y}+xy\right)\sinh\left(\frac{y}{x}\right)\right.\\
&\left.+\sqrt{y^2+4x}\left(\frac{x^2}{y^2}\left(\cosh\left(\frac{y}{x}\right)-1\right)+\frac{x}{y}\sinh\left(\frac{y}{x}\right)+x\cosh\left(\frac{y}{x}\right)\right)\right]\\
&-\sqrt{y^2+4x}\cosh\left(\frac{y}{x}\right)-\left(\frac{2x}{y}+y\right)\sinh\left(\frac{y}{x}\right).
\end{aligned}
\tag{1.8}
$$

The function ϕ_μ has different behaviours with different values of μ which is the first sign of the transition. The rest of this section is devoted to compute these behaviours and to prove them rigorously that is to say to prove Proposition 1.1.

1.4.1 The simplest case $\mu > 1/2$

The function f_μ in (1.8) has a very wild behaviour at the neigbourhood of $(0,0)$. However, it can be continued (with the same formula) with a $\mathcal{C}^\infty$ regularity on the domain $\mathbf{R}_+^* \times \mathbf{R}$. We then have:

$$f_\mu(c,0) = \frac{1+3\sqrt{c}+4c+2c\sqrt{c}}{\mu} - 2\sqrt{c} - 2$$

for any positive c. The function $\zeta : c \mapsto (1+3\sqrt{c}+4c+2c\sqrt{c})/(2\sqrt{c}+2)$, is strictly increasing over $\mathbf{R}_+$ and tends to $1/2$ as $c \to 0$. Consequently, for every $\mu > 1/2$ there exists $c(\mu) > 0$ such that $\zeta(c(\mu)) = \mu$ which amounts to $f_\mu(c(\mu),0) = 0$. As a matter of fact, one can excplicitly compute

$$c(\mu) = \mu - \frac{\sqrt{4\mu-1}}{2}.$$

On the other side, $\partial_x f_\mu(c(\mu),0)$ cannot be zero. We can then apply the implicit function theorem for f_μ at point $(c(\mu),0)$ and with the uniqueness property we have made for $\phi_\mu(y)$ we have that $\forall \mu > 1/2$, $\lim_{y\to 0} \phi_\mu(y) = c(\mu)$. For $\mu > 1/2$ we pose $\bar{\phi}_\mu(y) = c(\mu)$.

As a matter of fact we will need another term in the expansion of ϕ_μ at $y = 0$ which we can obtain in this case by computing the derivatives of ϕ_μ. We find that we have $\phi'_\mu(0) = 0$ and $\phi''_\mu(0) \neq 0$. Thus we have

$$\phi_\mu(y) - \bar{\phi}_\mu(y) \sim c_1(\mu) y^2 \tag{1.9}$$

as y goes to zero.

1.4.2 Preliminary computation for cases $\mu \leq 1/2$

We can note that as μ tends to $1/2$, $c(\mu)$ tends to 0, leading us to believe that as μ tends to $1/2$, $\phi_\mu(y)$ tends to 0 as y tends to 0. We thus need to make a change of variable in order to alleviate the difficulty in the vicinity of (0,0). We then pose $X = x$ and $Y = y/x$. The map $T : (x, y) \mapsto (x, y/x)$ is a $\mathcal{C}^1$-diffeomorphism of $\mathbf{R}_+^* \times \mathbf{R}$ in itself whose inverse map is $T^{-1} : (X, Y) \mapsto (X, YX)$.

We then get a new function:

$$\begin{aligned}
F_\mu(X,Y) =& (f_\mu \circ T^{-1})(X,Y) \\
=& \frac{1}{\mu}\left[\frac{2(\cosh(Y)-1)}{Y^2} + X\cosh(Y) + (3\frac{X}{Y} + X^2Y)\sinh(Y)\right] \\
& - (\frac{2}{Y} + YX)\sinh(Y) \\
& + \sqrt{Y^2X^2 + 4X}\times \\
& \left(\frac{1}{\mu}\left[\frac{\cosh(Y)-1}{Y^2} + \frac{\sinh(Y)}{Y} + X\cosh(Y)\right] - \cosh(Y)\right).
\end{aligned}$$

Let us note that this function does not have a singularity at $Y = 0$. In the $\mu < 1/2$ case we wish to show that $(X, Y) = T(\phi_\mu(y), y)$ tends to $(0, 1/c(\mu))$ with $c(\mu) > 0$ and in the $\mu = 1/2$ case we wish to show that (X, Y) tends to $(0, 0)$. We thus need to study F_μ in a neighborhood of the axis $X = 0$. Indeed, F_μ can be continuously continued at $\{X = 0\}$. However, due to the square root, the derivatives of F_μ tends to $+\infty$ as X tends to 0. It is, thus, not possible to continue F_μ with a $\mathcal{C}^1$ regularity on a neighbourhood of the axis $\{X = 0\}$ and we will not be able to apply the implicit function theorem directly on F_μ as we did on f_μ for $\mu > 1/2$.

We remark that if we note

$$\begin{aligned}
A_\mu(X,Y) =& \frac{1}{\mu}\left[\frac{2(\cosh(Y)-1)}{Y^2} + X\cosh(Y) + (3\frac{X}{Y} + X^2Y)\sinh(Y)\right] \\
& - (\frac{2}{Y} + YX)\sinh(Y) \\
B(X,Y) =& Y^2X^2 + 4X \\
C_\mu(X,Y) =& \frac{1}{\mu}\left[\frac{\cosh(Y)-1}{Y^2} + \frac{\sinh(Y)}{Y} + X\cosh(Y)\right] - \cosh(Y)
\end{aligned}$$

F_μ is in reality of the form

$$F_\mu(X,Y) = A_\mu(X,Y) + \sqrt{B(X,Y)}C_\mu(X,Y).$$

We want to remove the square root to remove the problem of the continuity of the derivative. We thus introduce the function G_μ defined by

$$G_\mu(X,Y) = A_\mu(X,Y)^2 - B(X,Y)C_\mu(X,Y)^2.$$

The relation $F_\mu(X,Y) = 0$ clearly implies $G_\mu(X,Y) = 0$. But we are interested in the reverse implication and pay attention to the signs of the terms in the equation. We have in fact that $F_\mu(X,Y) = 0$ is equivalent to:

$$\begin{cases} B(X,Y) = 0 \\ A_\mu(X,Y) = 0 \end{cases}$$

$$\text{or} \quad \begin{cases} B(X,Y) > 0 \\ A_\mu(X,Y) = 0 \\ C_\mu(X,Y) = 0 \end{cases} \tag{1.10}$$

$$\text{or} \quad \begin{cases} B(X,Y) > 0 \\ A_\mu(X,Y)C_\mu(X,Y) < 0 \\ A_\mu(X,Y)^2 - B(X,Y)C_\mu(X,Y)^2 = 0 \end{cases}$$

We have plotted on Figures 1.3 and 1.4 the curves $\{A_\mu = 0\}$, $\{B = 0\}$ and $\{C_\mu = 0\}$ along with the parts of the (X,Y) plane where we have equivalence between the relations $F_\mu = 0$ and $G_\mu = 0$. Finally, let us note that G_μ is analytic in the whole plane (X,Y).

1.4.3 The case $\mu < 1/2$

In this case, we are interested in the points $(0, 1/c)$, for which B vanishes. Consequently, G_μ vanishes at $(0,1/c)$ if, and only if F_μ vanishes and if, and only if, A_μ vanishes. We have:

$$A_\mu(0,1/c) = \frac{2c^2(\cosh(\frac{1}{c}) - 1)}{\mu} - 2c\sinh\left(\frac{1}{c}\right)$$

The function $\chi : c \mapsto c(\cosh(1/c) - 1)/\sinh(1/c)$ is strictly increasing, tends to 0 when c tends to 0 and tends to $1/2$ when c tends to $+\infty$. Then for all $\mu < 1/2$, there exists a unique $c(\mu) > 0$, such that $A_\mu(0,1/c) = 0$. We remark that we have the following property:

$$\begin{aligned} \partial G_\mu(X,Y) = 2A(X,Y)\partial A(X,Y) - \partial B(X,Y)C(X,Y)^2 \\ - 2B(X,Y)C(X,Y)\partial C(X,Y). \end{aligned}$$

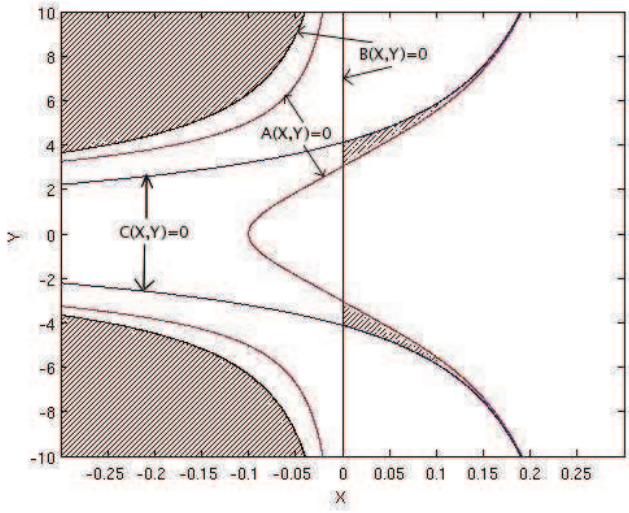

Figure 1.3: Setting of the A,B and C functions in the (X,Y) plane for $\mu = 0.3$. The grey area corresponds to the parts where $F_\mu(X,Y) = 0 \Leftrightarrow G_\mu(X,Y) = 0$. The curves are defined on the whole plane even if only the part $X > 0$ is physically relevant.

where ∂ denotes a derivative with respect to either X or Y

Now $B(X,Y) = Y^2X^2 + 4X$ so we have $\partial_X B(0, 1/c(\mu)) = 4$. Consequently, $\partial_X G(0, 1/c(\mu))$ is equal to $-4C(0, 1/c(\mu))^2$ which is not zero (on the contrary, $\partial_Y G(0, 1/c(\mu))$ is clearly zero) because $C_\mu(0, 1/c(\mu)) = c^2 \sinh(1/c) + c$ which is positive (as c is positive). We then have ψ a smooth function (at least $\mathcal{C}^\infty$) such that $\psi(1/c(\mu)) = 0$ and $G_\mu(\psi(Y), Y) = 0$ for Y in a neighbourhood of $1/c(\mu)$. Moreover we have $\partial_Y \psi(1/c(\mu)) = 0$ because $\partial_Y G(0, 1/c(\mu)) = 0$.

We now have to check if the part $Y \neq 0$ of the curve $Y \mapsto (\psi(Y), Y)$, is really the curve $F_\mu(X,Y) = 0$ so we have to check the signs of $A_\mu(\psi(Y), Y)$, $B(\psi(Y), Y)$ and $C_\mu(\psi(Y), Y)$ and verify if we are in one of the cases of Equivalence (1.10). We show that we are in the third case.

We said that we have $C_\mu(0, 1/c(\mu)) > 0$. Then by continuity, for Y not too far from $1/c(\mu)$, $C_\mu(\psi(Y), Y)$ is positive. We now check the sign of $Y \mapsto B(\psi(Y), Y)$. At $1/c(\mu)$ this function is zero and one can check that its first derivative also vanishes. Its second derivative however is

$$4\psi''(1/c(\mu)) = \partial_Y A_\mu(0, 1/c(\mu))^2 / (2C_\mu(0, 1/c(\mu))^2).$$

On the other hand $Y \mapsto A_\mu(\psi(Y), Y)$ vanishes at $1/c(\mu)$ and its first derivative is $\partial_Y A_\mu(0, 1/c(\mu))$. We are then going to show that $\partial_Y A_\mu(0, 1/c(\mu)) < 0$,

which will allow us to conclude that for $Y > 1/c(\mu)$, $A_\mu(\psi(Y), Y) < 0$, $C_\mu(\psi(Y), Y) > 0$ and $B(\psi(Y), Y) > 0$ and that $F_\mu(\psi(Y), Y) = 0$. We note c instead of $c(\mu)$ for the sake of simplicity. We now compute $\partial_Y A_\mu(0, 1/c(\mu))$:

$$\begin{aligned}\partial_Y A_\mu(0, 1/c)) &= \frac{2}{\mu}(c^2 \sinh(1/c) - 2c^3(\cosh(1/c) - 1)) \\ &\quad - 2(c\cosh(1/c) - c^2 \sinh(1/c)) \\ &= \frac{2c^2}{\mu}\sinh(1/c) - 2c\cosh(1/c) - \frac{2c^3}{\mu}(\cosh(1/c) - 1)\end{aligned}$$

because $(2c^3(\cosh(1/c) - 1))/\mu - 2c^2 \sinh(1/c) = 0$ by definition of $c(\mu)$. Let us now consider the function

$$\alpha : t \mapsto \frac{2t^2 \sinh(1/t)^2}{t(\cosh(1/t) - 1)} - 2t\cosh(1/t)$$

we have that $\alpha(c(\mu)) - \frac{2c^3}{\mu}(\cosh(1/c) - 1) = \partial_Y A_\mu(0, 1/c)$ and that $\alpha(t) = -2t$. We can thus conclude that $\partial_Y A_\mu(0, 1/c) < 0$.

The relation $F_\mu(\psi(Y), Y) = 0$ leads to $f_\mu(\psi(Y), Y\psi(Y)) = 0$ and the uniqueness property we have for ϕ_μ allows us to write $\psi(Y) = \phi_\mu(Y\psi(Y))$, for all $Y > 1/c(\mu)$. By letting Y going to $1/c(\mu)$ we see that we must have $\phi_\mu(y) \to 0$ as $y \to 0$. In the same manner we have $\frac{\phi_\mu(Y\psi(Y))}{Y\psi(Y)} = \frac{1}{Y}$ from which we can conclude that $\phi_\mu(y)/y \to c(\mu)$. We have then shown that $\phi_\mu(y) \sim c(\mu)y$ in a neighbourhood of $y = 0$ for $\mu < 1/2$. In this case we pose $\bar{\phi}_\mu(y) = c(\mu)y$. As in the case $\mu > 1/2$ we look for more information on the expansion of $\phi_\mu(y)$. We use the relation $\phi_\mu(y) = \psi(y/\phi_\mu(y))$ and use that $\psi(Y) = 1/2\psi''(1/c)(Y - 1/c)^2 + o(Y - 1/c)^2$. We can conclude after some computation that

$$|\phi_\mu(y) - \bar{\phi}_\mu(y)| \sim \sqrt{c^5/\psi''(1/c)}y^{3/2} \tag{1.11}$$

as y goes to 0. Interestingly enough, we do not have a second term of the expansion since we do not know the sign of the difference.

1.4.4 The case $\mu = 1/2$

We can treat the case $\mu = 1/2$ in the same way that we did for $\mu < 1/2$ by studying the function $G_{1/2}$. Firstly we notice that $G_{1/2}(0, 0) = 0$. What's more we have $\partial_X G_{1/2}(0, 0) = -16$ which allows us to use the implicit function theorem (only in this case it is simpler since we do not have constants that

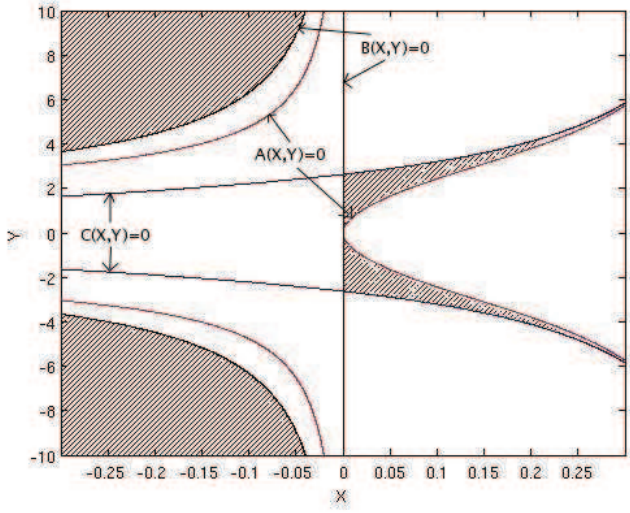

Figure 1.4: Setting of the A,B and C functions in the (X,Y) plane for $\mu = 0.5$. The curve $G_{1/2}(X,Y) = 0$ needs to start at $(0,0)$ and we see that the behaviour of A and C at this point impose a stronger order of annulation for ψ

depend on μ). We still note ψ the function depending on Y such that $\psi(0) = 0$ and we have in the vicinity of $(0,0)$, $G_{1/2}(X,Y) = 0 \Leftrightarrow X = \psi(Y)$. We now check by implicit differentiation that the first three derivative of ψ at 0 vanish and that $\psi^{(4)}(0) = 1/24$. Consequently ψ is positive in a neighbourhood of $Y = 0$. We have $C_{1/2}(0,0) = 2$ which gives us the sign of $C_{1/2}(\psi(Y),Y)$ for small Y and we next have to check the signs of $B(\psi(Y),Y)$ and $A(\psi(Y),Y)$. We check that $Y \mapsto B(\psi(Y),Y)$ has its derivatives at $Y = 0$ equal to zero up to order 3 included and that its fourth derivative is positive at $Y = 0$. Thus $B(\psi(Y),Y)$ is positive for small Y. On the other hand, the first derivative of $Y \mapsto A_{1/2}(\psi(Y),Y)$ vanishes at $Y = 0$ and its second derivative is $-1/3$. We thus have that $A_{1/2}(\psi(Y),Y)$ is negative for small Y. We can now conclude that $F_{1/2}(\psi(Y),Y) = 0$ for Y in a neighbourhood of 0.

We have again that, $\phi_{1/2}(Y\psi(Y)) = \psi(Y)$ for all Y small enough. We conclude in the same manner that $\phi_{1/2}(y)$ tends to 0 at $y = 0$. Moreover, since we have $\psi(Y) \sim c_0 Y^4$ with $c_0 = 1/24^2$, we have that $\phi_{1/2}(y)/y^{4/5}$ tends to $c(1/2) = c_0^{1/5}$ when y decreases to 0. We pose $\bar{\phi}_{1/2}(y) = c(1/2)y^{4/5}$.

We now check that $\psi^{(5)}(0) = 0$ and $\psi^{(6)}(0) \neq 0$ from what we can conclude that

$$\phi_{1/2}(y) - \bar{\phi}_{1/2}(y) \sim c_1 y^{6/5}. \tag{1.12}$$

1.5 Transition on τ the Macroscopic Stress

Now that we have proved the behaviours of the function ϕ_μ as in Proposition 1.1, our aim is to prove the behaviours of τ the total stress. We want to show that it exhibits a transition at $\mu = 1/2$. The path is now straightforward: we first compute the total stress like in (1.5) by integrating p against σ using its form given by (1.7). then we try to find the behaviour of the total stress as a function of y when y decreases to 0 using our previous results. However some care should be taken as to why the behaviour is correct.

1.5.1 The stress τ as a function of x and y

Using the form (1.7) of the solution one can compute the macroscopic stress attached to the shear by the formula

$$\int_{\sigma\in\mathbf{R}} \sigma p(\sigma)\mathrm{d}\sigma = \tau(x,y)$$

where

$$\begin{aligned}\tau(x,y) =& y + \frac{x}{2\mu y} - \frac{x^3}{\mu y^3} \\ &+ \frac{x^2}{y^3\Delta(x,y)}\left(\frac{y^2}{x} - 2(\cosh\left(\frac{y}{x}\right) - 1)\right) \\ &+ \frac{x^3}{y^4\Delta(x,y)}\left(y\left(\left(\frac{y}{x}\right)^2 + \frac{4}{x}\right)^{1/2} + 2\sinh\left(\frac{y}{x}\right)\right)\end{aligned} \tag{1.13}$$

and

$$\begin{aligned}\Delta(x,y) =& \frac{2x}{y^2}\left(\cosh\left(\frac{y}{x}\right) - 1\right) + \cosh\left(\frac{y}{x}\right) + \left(\frac{3x}{y} + y\right)\sinh\left(\frac{y}{x}\right) \\ &+ \left(\left(\frac{y}{x}\right)^2 + \frac{4}{x}\right)^{1/2}\left[\left(\frac{x}{y}\right)^2\left(\cosh\left(\frac{y}{x}\right) - 1\right) + \frac{x}{y}\sinh\left(\frac{y}{x}\right) + x\cosh\left(\frac{y}{x}\right)\right].\end{aligned} \tag{1.14}$$

We refer to Appendix 1.8 for the details of the computation.

1.5.2 Asymptotical behaviour of $\tau(\phi(y), y)$

From the previous paragraph we are now able to compute the macroscopic stress τ attached to a given shear rate y. Theoretically, we just have to compute the corresponding x by $x = \phi_\mu(y)$ and then to compute the value of

$\tau(\phi_\mu(y), y)$ using (1.13). Now what we are really interested in is the behaviour of the one variable function $y \mapsto \tau(\phi_\mu(y), y)$ at $y = 0$. Yet we do not know ϕ_μ since it is only given implicitly by (1.8). However we do know the behaviour of ϕ_μ at $y = 0$ given by the explicit function $\bar{\phi}_\mu$ that we computed in Section 1.4. Our hope is to draw from the behaviour of $\tau(\bar{\phi}_\mu(y), y)$ at $y = 0$, the behaviour of $\tau(\phi_\mu(y), y)$. By behaviour we mean that we want to find the first non zero term of the expansion of $\tau(\phi_\mu(y), y)$.

Theoretical inequality. We first look at the kind of inequality we are going to use. Let us forget for a moment the origin of our problem and say we are given a smooth two variable function $\widetilde{\tau}$ that we want to study alongside a curve given by $(\phi(y), y)$. Assume $\bar{\phi}(y)$ is equivalent to $\phi(y)$. By using Taylor's formula with integral remainder on $\widetilde{\tau}$ we get the following inequality.

$$\begin{aligned}\left|\frac{\widetilde{\tau}(\phi(y), y)}{\widetilde{\tau}(\bar{\phi}(y), y)} - 1\right| &= \left|\frac{\widetilde{\tau}(\phi(y), y) - \widetilde{\tau}(\bar{\phi}(y), y)}{\widetilde{\tau}(\bar{\phi}(y), y)}\right| \\ &\leq \left|\frac{\phi(y) - \bar{\phi}(y)}{\widetilde{\tau}(\bar{\phi}(y), y)}\right| \int_0^1 |\partial_x \widetilde{\tau}(s\phi(y) + (1-s)\bar{\phi}(y), y)| \mathrm{d}s\end{aligned} \tag{1.15}$$

When we see this inequality we see that we need the behaviour of $|\phi(y) - \bar{\phi}(y)|$. Actually we need it for two reasons. Firstly we need the precise behaviour of $|\frac{\phi(y) - \bar{\phi}(y)}{\widetilde{\tau}(\bar{\phi}(y), y)}|$. Secondly if we hope to control the integral we need to have an estimation of the position of the segment $[(\phi(y), y), (\bar{\phi}(y), y)]$ in the (x, y) plane which is given by a second term in the expansion of ϕ.

What we wanted to point out by this little study is that there is absolutely no guarantee that the behaviour of $\widetilde{\tau}(\phi(y), y)$ is given by $\widetilde{\tau}(\bar{\phi}(y), y)$ beforehand. We have to prove that the right hand side of (1.15) tends to 0 which is not obvious at all and can be false even if $\phi(y) \sim \bar{\phi}(y)$.

The problem with τ given by (1.13) and the introduction of $\widetilde{\tau}$. We now want to apply (1.15) to τ given by (1.13). As a matter of fact if we use (1.14) and (1.13) on the curve $(\bar{\phi}_\mu(y), y)$ as we planned, we fail to recover the correct behaviour for $\tau(\phi_\mu(y), y)$ except for $\mu < 1/2$. We can in fact compute that in case $\mu = 1/2$, $\tau(\bar{\phi}_\mu(y), y)$ follows a power law with exponent $1/5$ but with a different constant than the one given by Theorem 1.2 while in the case $\mu > 1/2$, $\tau(\bar{\phi}_\mu(y), y)$ diverges as $1/y$ when it should converge as y (again according to Theorem 1.2 written in (x, y) variables). This leaves us with the question of how to prove the theorem.

Remember that in the end what we are really interested in is the behaviour of $\tau(\phi_\mu(y), y)$ not $\tau(\bar{\phi}_\mu(y), y)$. We now use the implicit definition of ϕ_μ to construct a two variable function $\widetilde{\tau}$ such that $\tau(\phi_\mu(y), y) = \widetilde{\tau}(\phi_\mu(y), y)$ and that $\widetilde{\tau}(\bar{\phi}_\mu(y), y)$ gives the correct behaviour for ϕ_μ that is to say that we can prove that the right hand side of (1.15) tends to 0.

We make the following remark: the equation (1.8) which defines implicitly ϕ_μ can be put in an equivalent form $\Delta(x, y) = \widetilde{\Delta}(\mu, x, y)$ with

$$\widetilde{\Delta}(\mu, x, y) = \mu \left(\sqrt{\frac{y^2}{x^2} + \frac{4}{x}} \cosh\left(\frac{y}{x}\right) + \left(\frac{2}{y} + \frac{y}{x}\right) \sinh\left(\frac{y}{x}\right) \right)$$

and Δ is given by equation (1.14) and is the quantity that appears naturally in the expression of $\tau(x, y)$ given by (1.13) (see Appendix 1.8 as to why). This is in fact how one constructs the function f_μ in the first place (See Appendix 1.6.3). Consequently if we define $\widetilde{\tau}$ by

$$\begin{aligned} \widetilde{\tau}(x, y) =& y + \frac{x}{2\mu y} - \frac{x^3}{\mu y^3} \\ &+ \frac{x^2}{y^3 \widetilde{\Delta}(\mu, x, y)} \left(\frac{y^2}{x} - 2(\cosh\left(\frac{y}{x}\right) - 1) \right) \\ &+ \frac{x^3}{y^4 \widetilde{\Delta}(\mu, x, y)} \left(y \left(\left(\frac{y}{x}\right)^2 + \frac{4}{x} \right)^{1/2} + 2 \sinh\left(\frac{y}{x}\right) \right) \end{aligned} \tag{1.16}$$

we know that we have $\tau(\phi_\mu(y), y) = \widetilde{\tau}(\phi_\mu(y), y)$ and we will show that $\widetilde{\tau}$ is the correct function to consider to study (1.15). Now this raises the question as to why $\widetilde{\tau}$ works and not τ and whether this fact was predictible.

Behaviour of $\left| \frac{\phi(y) - \bar{\phi}(y)}{\widetilde{\tau}(\bar{\phi}(y), y)} \right|$. To control the right hand side of (1.15) we see that we need the behaviour of $\widetilde{\tau}(\bar{\phi}(y), y)$ which we give now:

If $\mu > 1/2$ $\widetilde{\tau}(\phi(y), y) \sim \eta(\mu) y$.

If $\mu < 1/2$ $\widetilde{\tau}(\phi(y), y) \to \tau_0(\mu)$.

If $\mu = 1/2$ $\widetilde{\tau}(\phi(y), y) \sim 24^{2/5}/12 y^{1/5}$.

In the end these behaviours will also be the respective behaviours of $\tau(\phi_\mu(y), y)$. Using this information and the one from $\phi_\mu - \bar{\phi}_\mu$ given by equations (1.9), (1.11) and (1.12) we can say that

Proposition 1.2. *We have the following behaviours :*

If $\mu > 1/2$ $\left|\dfrac{\phi(y)-\bar{\phi}(y)}{\widetilde{\tau}(\bar{\phi}(y),y)}\right|$ *behaves like* y.

If $\mu < 1/2$ $\left|\dfrac{\phi(y)-\bar{\phi}(y)}{\widetilde{\tau}(\bar{\phi}(y),y)}\right|$ *behaves like* $y^{3/2}$.

If $\mu = 1/2$ $\left|\dfrac{\phi(y)-\bar{\phi}(y)}{\widetilde{\tau}(\bar{\phi}(y),y)}\right|$ *also behaves like* y.

where we have dropped the constants for the sake of clarity. All these computations are straightforward since everything is explicit.

End of the proof: study of $\displaystyle\int_0^1 |\partial_x\widetilde{\tau}(s\phi(y)+(1-s)\bar{\phi}(y),y)|\mathrm{d}s$

The case $\mu > 1/2$**.** As usual, let us start with the simplest case $\mu > 1/2$. Using Proposition 1.1 we have that ϕ_μ converges to a constant $c > 0$. The function $\partial_x\widetilde{\tau}$ can be continued by continuity at $(c,0)$ when $c > 0$. It is then bounded in the vicinity of this point. Now we know that for y close enough to 0, $[(\phi_\mu(y),y),(\bar{\phi}_\mu(y),y)]$ is in any closed ball centered at $(c,0)$. By compactness $d_x\widetilde{\tau}$ is bounded and thus the integral is uniformly bounded as y decreases to zero and we then have $\tau(\phi(y),y) \sim \widetilde{\tau}(\bar{\phi}(y),y)$. As a matter of fact if we look at (1.15) what we have really proved is the following expansion:

$$\tau(\phi_\mu(y),y) = \eta(\mu)y + \mathcal{O}(y^2)$$

For the other two cases the difficulty is increased since we have ϕ_μ and $\bar{\phi}_\mu$ closing in to 0. But the dependence in y/x of $\widetilde{\tau}_\mu$ and thus of $\partial_x\widetilde{\tau}$ leave us no hope to ever show continuity at $(0,0)$ and uniform boundedness of the integral. In fact we can see numerically that the function diverges. What we have to prove is that the divergence of the integral is somehow compensated by $|\dfrac{\phi(y)-\bar{\phi}(y)}{\widetilde{\tau}(\bar{\phi}(y),y)}|$.

The case $\mu < 1/2$**.** In the $\mu < 1/2$ case we know by Proposition 1.1 that for y close to 0, the curve $\{(\phi_\mu(y),y)\}$ is tangent to a ray $\{(c(\mu)y,y)\}$. Now we look at the expansion of $\partial_x\widetilde{\tau}(x,y)$ alongside a ray $(y/t,y)$ and we find that its first term is of the form $M(t)/y$ with $M(t)$ bounded if t is in $\mathbf{R}$. This suggests that the divergence of $\partial_x\widetilde{\tau}(x,y)$ is uniformly in $1/y$ close to a ray. Indeed, if we check the function $(t,y) \mapsto y\partial_x\widetilde{\tau}(y/t,y)$ we can see that it can be continuously continued up to $y = 0$ as long as t is positive. This means that as long as (x,y) is in a closed angular sector with its peak at $(0,0)$ and

included in the $x > 0, y > 0$ open quarter plane (which means that none of its edges are axis), $y\partial_x\widetilde{\tau}(x,y)$ is bounded.

Thus, we just have to check that as y decreases to 0, the segment $[(\phi_\mu(y), y), (\bar{\phi}_\mu(y), y)]$ stays in such a closed angular sector, so as to have $\int_0^1 |\partial_x\widetilde{\tau}(s\phi_\mu(y)+(1-s)\bar{\phi}_\mu(y), y)|\mathrm{d}s \leq M/y$ for a given constant M which does not depend on y (but can depend on μ). This is true because of Proposition 1.1 which states that $\phi_\mu(y)/y \to c > 0$.

Since by Proposition 1.2 $\left|\dfrac{\phi_\mu(y)-\bar{\phi}_\mu(y)}{\widetilde{\tau}(\bar{\phi}_\mu(y),y)}\right|$ is in this case of order $y^{3/2}$, what we just show is enough to conclude that $\tau(\phi_\mu(y),y) \sim \widetilde{\tau}(\bar{\phi}_\mu(y),y)$. Again we have proved slightly more than announced since we have the expansion

$$\tau(\phi_\mu(y),y) = \tau_0(\mu) + \mathcal{O}(\sqrt{y})$$

It would actually be interesting to know if $\tau(\phi_\mu(y),y) - \tau_0(\mu) \sim \sqrt{y}$ to know what Herschel-Bulkley fluid law best fits the behaviour of a HL fluid at low shear rate. It seems numerically that it is actually the case.

The case $\mu = 1/2$. What has been said should make us worry over the $\mu = 1/2$ case. Indeed in this case, by looking back at Proposition 1.2, we see that we need a divergence of the integral that is strictly weaker that $1/y$ and it seems that we have shown that the divergence is of order $1/y$ when closing in to $(0,0)$. In reality, one should notice that $M(t)$ tends to 0 as t tends to 0, that is to say when the half-line we are considering becomes close to the (Ox) axis. In the $\mu = 1/2$ case, $\bar{\phi}_{1/2}(y) = 1/24^{2/5}y^{4/5}$ which means that the (Ox) axis is tangent to the curves. The previous divergence rate does not apply here. In fact we have $\partial_x\widetilde{\tau}(ty^{4/5}, y))$ uniformly bounded by $M/y^{3/5}$ as long as t is away from 0 which is the case in the region where $[(\phi(y),y),(\bar{\phi}(y),y)]$ lies.

We will not write the full expression of $\partial_x\widetilde{\tau}(ty^{4/5},y)$ but we will say that it can be written as the sum of 8 terms and all of them are diverging faster than $y^{3/5}$. But all these terms can in fact be taken by pairs so as to alleviate

the strong divergence. For example we have the term $1/y$ and the term:

$$T = -\frac{t^2\left(\frac{y^{6/5}}{t} - 2\cosh\left(\frac{y^{1/5}}{t}\right) + 2\right)}{y^{7/5}\left(\frac{1}{2}\sqrt{\frac{y^{2/5}}{t^2} + \frac{4}{ty^{4/5}}}\cosh\left(\frac{y^{1/5}}{t}\right) + \left(\frac{1}{y} + \frac{y^{1/5}}{2t}\right)\sinh\left(\frac{y^{1/5}}{t}\right)\right)^2} \times$$
$$\left[\frac{1}{4}\frac{\cosh\left(\frac{y^{1/5}}{t}\right)}{\sqrt{\frac{y^{2/5}}{t^2} + \frac{4}{ty^{4/5}}}}\left(-\frac{2}{y^{2/5}t^3} - \frac{4}{t^2y^{8/5}}\right) - \frac{1}{2}\sqrt{\frac{y^{2/5}}{t^2} + \frac{4}{ty^{4/5}}}\frac{\sinh\left(\frac{y^{1/5}}{t}\right)}{y^{3/5}t^2}\right.$$
$$\left. - \frac{1}{2}\frac{\sinh\left(\frac{y^{1/5}}{t}\right)}{y^{3/5}t^2} - \left(\frac{1}{y} + \frac{y^{1/5}}{2t}\right)\frac{\cosh\left(\frac{y^{1/5}}{t}\right)}{y^{3/5}t^2}\right] \quad (1.17)$$

which happens to be equivalent to $-1/y$ as y tends to 0 with t fixed. The sum of these two terms is also equivalent to $1/y^{3/5}$. As in the previous paragraph this is not enough since we want some uniformity in t but it suggests that by adding and then multiplying by $y^{3/5}$ we might get what we are looking for. We first rewrite (1.17) in order to suppress any obvious singularities:

$$T = -\frac{t^2\left(\frac{y^{4/5}}{t} - \frac{2\cosh\left(\frac{y^{1/5}}{t}\right) - 2}{y^{2/5}}\right)}{\left(\frac{1}{2}y^{2/5}\sqrt{\frac{y^{6/5}}{t^2} + \frac{4}{t}}\cosh\left(\frac{y^{1/5}}{t}\right) + \left(\frac{1}{y^{1/5}} + \frac{y}{2t}\right)\sinh\left(\frac{y^{1/5}}{t}\right)\right)^2} \times$$
$$\left[\frac{1}{4}\frac{\cosh\left(\frac{y^{1/5}}{t}\right)}{\sqrt{\frac{y^{6/5}}{t^2} + \frac{4}{t}}}\left(-\frac{2y^{3/5}}{t^3} - \frac{4}{t^2y^{3/5}}\right) - \frac{1}{2}\sqrt{\frac{y^{6/5}}{t^2} + \frac{4}{t}}\frac{\sinh\left(\frac{y^{1/5}}{t}\right)}{y^{2/5}t^2}\right.$$
$$\left. - \frac{1}{2}\frac{\sinh\left(\frac{y^{1/5}}{t}\right)}{t^2} - \left(\frac{1}{y} + \frac{y^{1/5}}{2t}\right)\frac{\cosh\left(\frac{y^{1/5}}{t}\right)}{t^2}\right] \quad (1.18)$$

Now the denominator, which we note by

$$\mathcal{D}(t, y^{1/5}) = \left(\frac{1}{2}y^{2/5}\sqrt{\frac{y^{6/5}}{t^2} + \frac{4}{t}}\cosh\left(\frac{y^{1/5}}{t}\right) + \left(\frac{1}{y^{1/5}} + \frac{y}{2t}\right)\sinh\left(\frac{y^{1/5}}{t}\right)\right)^2 \quad (1.19)$$

is never 0 since $\sinh(u)/u$ is bounded away from 0 and so is t. We now see that the part that is dominant in the numerator of T when taking y to 0 with t fixed is $\cosh(y^{1/5}/t)/y$. We can then rewrite T as

$$T = \frac{S(t, y^{1/5}) + \frac{t^2\left(\frac{y^{4/5}}{t} - \frac{2\cosh\left(\frac{y^{1/5}}{t}\right) - 2}{y^{2/5}}\right)\cosh\left(\frac{y^{1/5}}{t}\right)}{yt^2}}{\mathcal{D}(t, y^{1/5})} \quad (1.20)$$

where S contains all the terms in the numerator of T of lower order (again y tends to 0 and t is fixed). It is easy to check that in fact $u^3S(t, u)$ is a

continuous function of its arguments as long as t is bounded away from 0. In particular we have that in any rectangle $[a,b]\times[0,\varepsilon]$ for which $b>a>0$ $u^3S(t,u)$ is bounded which means that $y^{3/5}S(t,y^{1/5})$ is bounded.

Now for the dominant part we need to reduce to a common denominator. We expand the denominator:

$$\mathcal{D}(t,y^{1/5})=\widehat{\mathcal{D}}(t,y^{1/5})+\left(\frac{\sinh\left(\frac{y^{1/5}}{t}\right)}{y^{1/5}}\right)^2 \tag{1.21}$$

so that in $\widehat{\mathcal{D}}(t,u)$ we have collected all the terms that tend to 0 as u tends to 0. In fact we can even check that $\widehat{\mathcal{D}}(t,u)/u^2$ is a countinuous function. Now we compute $y^{3/5}(1/y+T)$ using (1.20) and (1.21) to see that we have:

$$\begin{aligned}y^{3/5}\left(1/y+T\right)=\frac{y^{3/5}}{\mathcal{D}(t,y^{1/5})}\Bigg[&\frac{\widehat{\mathcal{D}}(t,y^{1/5})}{y}+S\left(t,y^{1/5}\right)\\&+\left(\frac{1}{y}\left(\frac{\sinh\left(\frac{y^{1/5}}{t}\right)}{y^{1/5}}\right)^2-\frac{1}{y}\left(\frac{2\cosh\left(\frac{y^{1/5}}{t}\right)-2}{y^{2/5}}\right)\cosh\left(\frac{y^{1/5}}{t}\right)\right)\Bigg]\end{aligned} \tag{1.22}$$

In this expression we have seen that all the terms have been accounted for except for the last one, which was the most problematic. One can check that in fact this last term can be seen as a continuous function of $y^{1/5}/t$ (it can even be expanded in a power series of $y^{1/5}/t$) and thus is also bounded as long as t stays away from 0. The rest of $y^{3/5}\partial_x\widetilde{\tau}(ty^{4/5},y)$ can be treated in the same way. and can be considered a bounded function uniformly in y and t. Now thanks to the fact that by Proposition 1.1 for $\mu=1/2$ we have $\bar{\phi}_{1/2}(y)=1/24^{2/5}y^{4/5}$ and that by (1.12)$|\phi_{1/2}(y)-\bar{\phi}_{1/2}(y)|/y^{4/5}$ is bounded as y tends to 0, we have that $\displaystyle\int_0^1|\partial_x\widetilde{\tau}(s\phi_{1/2}(y)+(1-s)\bar{\phi}_{1/2}(y),y)|\mathrm{d}s\leq M/y^{3/5}$ and we can conclude in this case too, using again (1.15) and (1.2), that $\tau(\phi_{1/2}(y),y)\sim\widetilde{\tau}(\bar{\phi}_{1/2}(y),y)$ and we even have:

$$\widetilde{\tau}(\phi_{1/2}(y),y)=c(\mu)y^{1/5}+\mathcal{O}(y^{2/5}).$$

Appendix to chapter 1

1.6 Construction of the Solution to Eqs (1.1)-(1.2)

To prove Proposition (1.1) we will in fact, only expand the computations of [16], in our own framework (mainly we have different notations) only for the sake of self-containment. The idea is pretty simple. First of all, the nonlinear differential equation is decoupled as a linear differential equation and a nonlinear consistency equation. If not for the Dirac measure (which is zero almost everywhere anyway) the linear differential equation could be easily solved by means of the characteristic polynomial of the equation. We thus treat here the Dirac as zero and solve the equation on $\mathbf{R}^*$. This will leave us three degree of freedom (but one will be taken care of by the consistency equation) and we fix the other two by imposing the constraint on regularity and integral. Finally we verify that the function we construct is a solution to the initial problem.

We work under the assumption that b is positive. The equation (1.1) is nonlinear because of the coefficient $\Gamma(p)$. To alleviate this difficulty we simply rewrite (1.1) as (1.23)-(1.24)

$$0 = -\lambda b \partial_\sigma p - De h(\sigma) p + De\Gamma\delta_0(\sigma) + \mu De\Gamma\partial_\sigma^2 p \tag{1.23}$$

$$\Gamma = \Gamma(p). \tag{1.24}$$

To proceed further we attack the first equation considering that Γ is a given positive constant and we afterwards fix Γ using the second equation of the above system.

1.6.1 Solving the linear equation in $\mathcal{D}'(\mathbf{R}^*)$

We solve (1.23) first in $\mathcal{D}'(\mathbf{R}^*)$ which amounts to say that we turn the Dirac to 0 namely we are looking at the equation:

$$0 = -\lambda b \partial_\sigma p - De h(\sigma) p + \mu De \Gamma \partial_\sigma^2 p$$

on $\mathbf{R}^*$. It can easily be solved on each open interval $]-\infty,-1[,]-1,0[,]0,1[$ and $]1,\infty[$ and since the equation is of order two on each interval, we have two degrees of freedom to tune the solution on each interval. On the unbounded interval we set one of the constant to 0 in order to suppress an exponential growth that would prevent the solution from being in L^1. Next we fix the constant on the other interval by enforcing $\mathcal{C}^1$ regularity at -1 and 1. Now one could wonder why $\mathcal{C}^1$ while we are looking for solution in $\mathrm{H}^1(\mathbf{R})$ which are merely continuous on the real line. It is because if there were jumps in the derivative of p at -1 or 1, this would induce Dirac measures at these points in the second order derivative and we have nothing in the equation that would compensate these Dirac measures.

Expression of the Solution of (1.23). The functions p which solve (1.23) in the sense of distribution on $\mathbf{R}^*$ and which are in $\mathcal{C}^1(\mathbf{R}^*)$ and verify

$$\int_{\mathbf{R}^*} p^2 + \int_{\mathbf{R}^*} (\partial_\sigma p)^2 < \infty$$

are given by the following formulae:

$$p(\sigma) = \begin{cases} \alpha_+ \exp(\beta_+(\sigma+1)) & \text{if } \sigma \le -1 \\ \alpha_+(1-\rho\beta_+ + \rho\beta_+ \exp(\frac{1}{\rho}(\sigma+1))) & \text{if } -1 < \sigma \le 0 \\ \alpha_-(1-\rho\beta_- + \rho\beta_- \exp(\frac{1}{\rho}(\sigma-1))) & \text{if } 0 < \sigma \le 1 \\ \alpha_- \exp(\beta_-(\sigma-1)) & \text{if } 1 < \sigma \end{cases} \tag{1.25}$$

where β_+, β_- are the roots (respectively positive and non positive) of the equation

$$\mu De \Gamma X^2 - \lambda b X - De = 0 \tag{1.26}$$

and ρ is $\mu De\Gamma/(\lambda b) = 1/(\beta_+ + \beta_-)$. By the definition of $\beta_\pm$ and ρ we remark that we have:

$$1 - \rho\beta\pm = \rho\beta\mp\,. \tag{1.27}$$

The degrees of freedom are now α_+ and α_-.

Determination of the $\alpha_\pm$ used in (1.7). To fix α_+ and α_- we impose continuity at $\sigma = 0$ (because as we said, we are interested in solutions in

$\mathrm{H}^1(\mathbf{R})$ thus continuous) and $\int p = 1$. These two conditions give us the following system on α_+,α_-:

$$\begin{cases} 0 = \left(1 - \rho\beta_+ + \rho\beta_+ e^{1/\rho}\right)\alpha_+ - \left(1 - \rho\beta_- + \rho\beta_- e^{-1/\rho}\right)\alpha_- \\ 1 = \left(\dfrac{1}{\beta_+} + (1 - \rho\beta_+) + \rho^2\beta_+\left(e^{1/\rho} - 1\right)\right)\alpha_+ \\ \qquad + \left(\dfrac{-1}{\beta_-} + (1 - \rho\beta_-) + \rho^2\beta_-\left(1 - e^{-1/\rho}\right)\right)\alpha_- \end{cases} \tag{1.28}$$

Existence of $\alpha_\pm$. Provided that the determinant of this system is not zero we have fixed a unique couple (α_+, α_-). Let us check that this is the case by computing this determinant:

$$\begin{aligned} \Delta =& 2 - \rho^2\beta_+\beta_-\left(\cosh\left(\frac{1}{\rho}\right) - 1\right) + \cosh\left(\frac{1}{\rho}\right) + \left(-\frac{1}{\rho\beta_+\beta_-} + 3\rho\right)\sinh\left(\frac{1}{\rho}\right) \\ &+ (\beta_+ - \beta_-)\left[\rho^2\left(\cosh\left(\frac{1}{\rho}\right) - 1\right) + \rho\sinh\left(\frac{1}{\rho}\right) - \frac{1}{\beta_+\beta_-}\cosh\left(\frac{1}{\rho}\right)\right]. \end{aligned} \tag{1.29}$$

We see that in fact $\Delta > 0$ (remember that $\beta_+ > 0$, $\beta_- < 0$ and since $b > 0$, $1/\rho > 0$).

Positivity of $\alpha_\pm$. At this point let us also check that $\alpha_\pm > 0$. We have by Cramer's rule for linear systems:

$$\Delta\alpha_+ = 1 - \rho\beta_- + \rho\beta_- e^{-1/\rho} \text{ and } \quad \Delta\alpha_- = 1 - \rho\beta_+ + \rho\beta_+ e^{1/\rho}. \tag{1.30}$$

Using Remark (1.27), we have $1-\rho\beta_-+\rho\beta_- e^{-1/\rho}$ equal to $\rho(\beta_+ + \beta_- e^{-1/\rho})$. But since $\beta_- < 0$ and $\rho > 0$ we have $e^{-1/\rho} < 1$ and $\beta_- e^{-1/\rho} > \beta_-$ and thus $\beta_+ + \beta_- e^{-1/\rho} > \beta_+ + \beta_- > 0$. Consequently, $\alpha_+ > 0$ and the same holds true for α_-. Returning to equation (1.7) we see that the positivity of $\alpha_\pm$ gives the positivity of the function p on $]-\infty, -1[$ and $]1, +\infty[$. But since α_+, β_+ and ρ are positive, it turns out that p is increasing on the interval $]-1, 0[$ and since its value at -1 is by construction $\alpha_+ > 0$, p remains positive on $]-1, 0[$. Again the same holds true on $]0, 1[$. Note that from (1.29)-(1.30), $\alpha_\pm$ depend on ρ and $\beta_\pm$ which in turn depend on b and Γ.

1.6.2 Solving the nonlinear problem (1.23)-(1.24)

Fixing Γ *using* (1.24). Let us sum up what we have obtained so far. We have now a function p which lies in $\mathrm{H}^1(\mathbf{R})$ that solve (1.23) in the space

$\mathcal{D}'(\mathbf{R}^*)$ that is to say in the sense of distribution but with test functions identically zero in a neighbourhood of zero. We also have that $p > 0$ and $\int p = 1$, the second constraint being exactly the second equation of system (1.28) and we have so, for every positive Γ. We now adjust Γ, so that (1.24) is satisfied. To do this we integrate p for $|\sigma| > 1$ using (1.7). In terms of $\alpha_\pm$, (1.24) amounts to:

$$\frac{\alpha_+}{\beta_+} - \frac{\alpha_-}{\beta_-} = \Gamma. \tag{1.31}$$

This is a nonlinear implicit equation on Γ because as we mentionned before $\alpha_\pm$ and $\beta_\pm$ depend on Γ. Let us admit for the moment that this equation has a unique solution which means that as long as we give a positive b we can find a unique positive Γ that satisfies (1.31). Let us see now that we have found a solution to (1.1).

Proof that p solves (1.1) *in* $\mathcal{D}'(\mathbf{R})$. We now show that p verifies in fact (1.1) on the whole real line. We note that p is continous on the real line and differentiable except at $\sigma = 0$. Its derivative in $\mathcal{D}'(\mathbf{R})$ is thus its derivative almost everywhere. The derivative $\partial_\sigma p$ being continous except at $\sigma = 0$ and differentiable except at $\sigma \in \{0, -1, 1\}$ its derivative is its derivative almost everywhere plus the jump at 0, $[\partial_\sigma p]_0 \delta_0(\sigma)$. Since p verifies (1.1) almost everywhere, it is only left to show that:

$$\begin{aligned} -\mu De\Gamma[\partial_\sigma p]_0 + De\Gamma &= \mu De\Gamma(\alpha_-\beta_- e^{-1/\rho} - \alpha_+\beta_+ e^{1/\rho}) + De\Gamma \\ &= 0 \end{aligned}$$

which becomes

$$\alpha_+\beta_+ e^{1/\rho} - \alpha_-\beta_- e^{-1/\rho} = 1/\mu. \tag{1.32}$$

We multiply (1.32) by Δ and use (1.30) to obtain:

$$\beta_+ e^{1/\rho}(1 - \rho\beta_- + \rho\beta_- e^{-1/\rho}) - \beta_- e^{-1/\rho}(1 - \rho\beta_+ + \rho\beta_+ e^{1/\rho}) = \Delta/\mu$$

which is equivalent to

$$\beta_+ e^{1/\rho}(1 - \rho\beta_-) - \beta_- e^{-1/\rho}(1 - \rho\beta_+) = \Delta/\mu$$

and then to

$$\rho(\beta_+^2 e^{1/\rho} - \beta_-^2 e^{-1/\rho}) = \Delta/\mu.$$

That's what we want to prove.

We now use (1.31) to obtain:

$$\frac{\alpha_+}{\beta_+} - \frac{\alpha_-}{\beta_-} = \Gamma \;\Leftrightarrow\; \alpha_+\beta_- - \alpha_-\beta_+ = \Gamma\beta_+\beta_-.$$

Recalling that $\beta_\pm$ are roots of equation (1.26), we have $\beta_+\beta_- = -1/\mu\Gamma$ and therefore $\alpha_+\beta_- - \alpha_-\beta_+ = -1/\mu$. We multiply by $-\Delta$ this equality and use (1.30) to obtain:

$$\begin{aligned}\frac{\Delta}{\mu} &= \beta_+(\Delta\alpha_-) - \beta_-(\Delta\alpha_+)\\ &= \beta_+(1-\rho\beta_+ + \rho\beta_+ e^{1/\rho}) - \beta_-(1-\rho\beta_- + \rho\beta_- e^{-1/\rho})\\ &= \beta_+(\rho\beta_- + \rho\beta_+ e^{1/\rho}) - \beta_-(\rho\beta_+ + \rho\beta_- e^{-1/\rho})\\ &= \rho(\beta_+^2 e^{1/\rho} - \beta_-^2 e^{-1/\rho}).\end{aligned}$$

The jump condition is thus verified. We can see in fact that (1.32) is equivalent to (1.31). Thus the only solution in $\mathcal{D}(\mathbf{R})$ of (1.23) are in fact solutions of (1.1). This is not that surprising since if one integrates equation (1.23) over the real line you obtain *a priori* that $\Gamma = \Gamma(p)$.

What is left now is to understand how we can use (1.31) to fix Γ and be sure that, as we claimed, there exists a unique Γ that fits the consistency equation.

1.6.3 Implicit relations that link Γ and b

To obtain an explicit function that gives implicitly Γ we just have to use (1.31) and use the value of $\alpha_\pm$ given by (1.29) and (1.30) . It is easier to use new variables defined by $x = \mu\Gamma$ and $y = \lambda b/De$. Actually x is the nondimensional diffusion coefficient in stress space while $y = \dot\gamma/\dot\gamma_c$ with $\dot\gamma_c = G_0T_0/\sigma_c$ the critical shear rate in the system. Let us begin by rewriting Δ with these variables:

$$\begin{aligned}\Delta(x,y) = \frac{2x}{y^2}\left(\cosh\left(\frac{y}{x}\right)-1\right) + \cosh\left(\frac{y}{x}\right) + \left(\frac{3x}{y}+y\right)\sinh\left(\frac{y}{x}\right)\\ + \left(\left(\frac{y}{x}\right)^2 + \frac{4}{x}\right)^{1/2}\left[\left(\frac{x}{y}\right)^2\left(\cosh\left(\frac{y}{x}\right)-1\right) + \frac{x}{y}\sinh\left(\frac{y}{x}\right) + x\cosh\left(\frac{y}{x}\right)\right].\end{aligned}$$

Now using the consistency equation (1.31) we find that

$$\Delta\Gamma = (2\rho - 1/(\rho\beta_+\beta_-))\sinh(1/\rho) - (\beta_+ - \beta_-)/(\beta_+\beta_-)\cosh(1/\rho)$$

which we write in the (x,y) variables using the actual values of $\beta_\pm$ in terms of the coefficient of (1.26)

$$\frac{1}{\mu}\Delta(x,y)x = x\left(\left(\frac{y}{x}\right)^2 + \frac{4}{x}\right)^{1/2}\cosh\left(\frac{y}{x}\right) + \left(2\frac{x}{y}+y\right)\sinh\left(\frac{y}{x}\right).$$

We now have the desired implicit function linking Γ and b:

$$\begin{aligned} f_\mu(x,y) =& \frac{1}{\mu}\left[\frac{2x^2}{y^2}\left(\cosh\left(\frac{y}{x}\right)-1\right)+x\cosh\left(\frac{y}{x}\right)+\left(\frac{3x^2}{y}+xy\right)\sinh\left(\frac{y}{x}\right)\right. \\ &\left.+\sqrt{y^2+4x}\left(\frac{x^2}{y^2}\left(\cosh\left(\frac{y}{x}\right)-1\right)+\frac{x}{y}\sinh\left(\frac{y}{x}\right)+x\cosh\left(\frac{y}{x}\right)\right)\right] \\ &-\sqrt{y^2+4x}\cosh\left(\frac{y}{x}\right)-\left(\frac{2x}{y}+y\right)\sinh\left(\frac{y}{x}\right). \end{aligned}$$

and we want $f_\mu(x,y)=0$. Interestingly enough, this function depends on the nondimensional control parameter.

On the open quarter plane$\{x>0,\, y>0\}$, $f_\mu(x,y)=0$ is equivalent to $g(x,y)=\mu$ with:

$$g(x,y)=\frac{\frac{2x^2}{y^2}\left(\cosh\left(\frac{y}{x}\right)-1\right)+x\cosh\left(\frac{y}{x}\right)+\left(\frac{3x^2}{y}+xy\right)\sinh\left(\frac{y}{x}\right)}{\sqrt{y^2+4x}\cosh\left(\frac{y}{x}\right)+\left(\frac{2x}{y}+y\right)\sinh\left(\frac{y}{x}\right)} \\ \frac{+\sqrt{y^2+4x}\left(\frac{x^2}{y^2}\left(\cosh\left(\frac{y}{x}\right)-1\right)+\frac{x}{y}\sinh\left(\frac{y}{x}\right)+x\cosh\left(\frac{y}{x}\right)\right)}{\sqrt{y^2+4x}\cosh\left(\frac{y}{x}\right)+\left(\frac{2x}{y}+y\right)\sinh\left(\frac{y}{x}\right)}.$$

It is easy to check that for a given $y>0$ the function $x\mapsto g(x,y)$ tends to 0 as x tends to 0 and tends to infinity as x tends to infinity. Since it is obviously continuous, this guarantees that there exists at least one Γ that solves the consistency equation and we have at least one solution to our problem. In fact we can show that $\partial_x g(x,y)>0$ for all x and y positive. This gives us at the same time the uniqueness we claimed and the regularity of the function giving x in terms of y. We now introduce ϕ_μ the implicit function satisfying

$$\forall y>0\,\forall\mu>0 \quad f_\mu(x,y)=0 \Leftrightarrow \quad g(x,y)=\mu \Leftrightarrow \quad x=\phi_\mu(y).$$

1.7 Proof of Uniqueness in Proposition 1.1

We give in this section some details on the computations for the uniqueness part of Proposition 1.1. Remember that we have:

$$g(x,y)=\frac{\frac{2x^2}{y^2}\left(\cosh\left(\frac{y}{x}\right)-1\right)+x\cosh\left(\frac{y}{x}\right)+\left(\frac{3x^2}{y}+xy\right)\sinh\left(\frac{y}{x}\right)}{\sqrt{y^2+4x}\cosh\left(\frac{y}{x}\right)+\left(\frac{2x}{y}+y\right)\sinh\left(\frac{y}{x}\right)}$$
$$+\frac{+\sqrt{y^2+4x}\left(\frac{x^2}{y^2}\left(\cosh\left(\frac{y}{x}\right)-1\right)+\frac{x}{y}\sinh\left(\frac{y}{x}\right)+x\cosh\left(\frac{y}{x}\right)\right)}{\sqrt{y^2+4x}\cosh\left(\frac{y}{x}\right)+\left(\frac{2x}{y}+y\right)\sinh\left(\frac{y}{x}\right)}$$

and we want to prove that $\partial_x g(x,y)>0$ for any given x and y both positive. We first compute $\partial_x g(x,y)$:

$$\partial_x g(x,y)=\frac{1}{\sqrt{y^2+4x}\cosh\left(\frac{y}{x}\right)+\left(2\frac{x}{y}+y\right)\sinh\left(\frac{y}{x}\right)}\times$$
$$\left[\frac{4x}{y^2}\left(\cosh\left(\frac{y}{x}\right)-1\right)-\frac{2}{y}\sinh\left(\frac{y}{x}\right)+\cosh\left(\frac{y}{x}\right)-\frac{y}{x}\sinh\left(\frac{y}{x}\right)+\left(\frac{6x}{y}+y\right)\sinh\left(\frac{y}{x}\right)\right.$$
$$-\left(3+\frac{y^2}{x}\right)\cosh\left(\frac{y}{x}\right)+\frac{2\left(\frac{x^2}{y^2}\left(\cosh\left(\frac{y}{x}\right)-1\right)+\frac{x}{y}\sinh\left(\frac{y}{x}\right)+x\cosh\left(\frac{y}{x}\right)\right)}{\sqrt{y^2+4x}}$$
$$\left.+\sqrt{y^2+4x}\left(\frac{2x}{y^2}\left(\cosh\left(\frac{y}{x}\right)-1\right)-\frac{\cosh\left(\frac{y}{x}\right)}{x}+\cosh\left(\frac{y}{x}\right)-\frac{y}{x}\sinh\left(\frac{y}{x}\right)\right)\right]$$
$$-\frac{1}{\left(\sqrt{y^2+4x}\cosh\left(\frac{y}{x}\right)+\left(2\frac{x}{y}+y\right)\sinh\left(\frac{y}{x}\right)\right)^2}\times$$
$$\left[\frac{2\cosh\left(\frac{y}{x}\right)}{\sqrt{y^2+4x}}-\frac{y}{x^2}\sqrt{y^2+4x}\sinh\left(\frac{y}{x}\right)+\frac{2}{y}\sinh\left(\frac{y}{x}\right)-\left(\frac{2}{x}+\frac{y^2}{x^2}\right)\cosh\left(\frac{y}{x}\right)\right]\times$$
$$\left[2\frac{x^2}{y^2}\left(\cosh\left(\frac{y}{x}\right)-1\right)+x\cosh\left(\frac{y}{x}\right)+\left(3\frac{x^2}{y}+xy\right)\sinh\left(\frac{y}{x}\right)\right.$$
$$\left.+\sqrt{y^2+4x}\left(\frac{x^2}{y^2}\left(\cosh\left(\frac{y}{x}\right)-1\right)+\frac{x}{y}\sinh\left(\frac{y}{x}\right)+x\cosh\left(\frac{y}{x}\right)\right)\right]$$

To handle such an expression (whose sign is anything but obvious) we reduce to the same denominator and write the numerator and the denominator as polynomials of the variables x, y, $c = \cosh(y/x)$, $s = \sinh(y/x)$, and $r = \sqrt{y^2+4x}$. We obtain:

$$\begin{aligned}\partial_x g(x,y) = {} & \frac{1}{y\left(rcy+2xs+sy^2\right)^2 r}\times \\ & \big(-4xy^3+4x^2y+2y^5c^2-12x^3s-2y^4s-y^5c-y^5r+14x^2c^2ry \\ & +4x^2rcs-4xrcy-8xy^2rs-2xy^3rc-8x^2yrc-y^5+8rxcsy^2+2y^5c^2r \\ & +2y^6cs+2cy^4rs+12xc^2ry^3+34x^2y^2cs+16xy^4cs+12xc^2y^3+16x^2c^2y \\ & -6x^2yr-2xy^4s-8xy^2s-4x^2rs+4xry+12x^3cs-2y^3rc-6xy^3r \\ & -12x^2y^2s-y^4rs-20x^2cy-10xy^3c\big)\end{aligned}$$

As y and x are positive c, s and r are also positive. So the denominator is positive and in the numerator, a monomial is positive if it has a plus and negative if it has a minus. The trick to show that the numerator is positive is to combine monomial and use the fact that $c-1>0$ and $s-y/x>0$. Let us give an example. The numerator contains $16x^2y^2c^2+4x^2y+12x^3cs-8xy^2-12x^3s-20x^2yc$ (expression which in facts contains the negative monomial that were the most difficult to combine to obtain a positive quantity). One can check that in fact this expression can be written under the form $8x^2yc(c-1)+12x^3(c-1)(s-y/x)+8x^2ys(s-y/x)$ which is now clearly positive. As a result we obtain (we write t instead of y/x):

$$\begin{aligned}\partial_x g(x,y) = {} & \frac{1}{y\left(rcy+2xs+sy^2\right)^2 r}\times \\ & \Big[2xy^3rc\left(c-1\right)+12x^3\left(c-1\right)\left(s-t\right)+2xy^3\left(c^2-1\right)+y^5r\left(c^2-1\right) \\ & +y^5c\left(c-1\right)+y^5\left(c^2-1\right)+2xy^2rc\left(s-t\right)+6x^2yrs\left(s-t\right)+2xy^2rs\left(c-1\right) \\ & +8x^2yrc\left(c-1\right)+y^4rs\left(c-1\right)+4x^2r\left(c-1\right)\left(s-t\right)+12x^2y^2s\left(c-1\right) \\ & +2xy^3s\left(s-t\right)+8x^2ys\left(s-t\right)+2x^2y^2c\left(s-t\right)+8x^2yc\left(c-1\right) \\ & +8xy^3c\left(c-1\right)+2xy^4s\left(c-1\right)+6xy^3r\left(c^2-1\right)+4rxcsy^2 \\ & +y^5c^2r+2y^6cs+cy^4rs+4xc^2ry^3+20x^2y^2cs+14xy^4cs\Big]\end{aligned}$$

which is now the sum of positive term, hence the result.

1.8 Computations for the Stress as a Two Variables Function

We first note that if we multiply (1.1) by σ and integrate over the real line we find that, $\displaystyle\int_{|\sigma|>1} \sigma p(\sigma)\mathrm{d}\sigma = \lambda b/De = y$ (this can be checked by direct computation on the form of p given by (1.7) but it is longer). We only have to compute $\displaystyle\int_{|\sigma|\leq 1} \sigma p(\sigma)\mathrm{d}\sigma$ and thanks to (1.7) we find that:

$$\begin{aligned}\tau &= \frac{\lambda b}{De} + \frac{1}{2}\left(-\alpha_+\left(1-\rho\beta_+\right) + \alpha_-\left(1-\rho\beta_-\right)\right)\\ &\quad + \rho^2\alpha_+\beta_+\left(1-\rho(e^{1/\rho}-1)\right) + \rho^2\alpha_-\beta_-\left(1-\rho(1-e^{-1/\rho})\right)\\ &= I_1 + I_2 + I_3 + I_4\end{aligned} \tag{1.33}$$

This formula can be simplified using the definition of ρ, β_+ and β_- and the system (1.28) defining α_+ and α_-:

$$\begin{aligned}2I_2 &= -\alpha_+(1-\rho\beta_+) + \alpha_-(1-\rho\beta_-)\\ &= \rho(-\alpha_+\beta_- + \alpha_-\beta_+) && \text{using (1.27)}\\ &= \rho\beta_+\beta_-\left(\frac{\alpha_-}{\beta_-} - \frac{\alpha_+}{\beta_+}\right)\\ &= \rho\frac{1}{\mu(-\Gamma)}(-\Gamma) && \text{using (1.26) and (1.31)}\\ &= \frac{\rho}{\mu}\end{aligned} \tag{1.34}$$

and

$$\begin{aligned}I_3 + I_4 &= \rho^2\alpha_+\beta_+\left(1-\rho(e^{1/\rho}-1)\right) + \rho^2\alpha_-\beta_-\left(1-\rho(1-e^{-1/\rho})\right)\\ &= \rho^2\left(\alpha_+\beta_+ + \alpha_-\beta_-\right) + \rho^3\left(\alpha_+\beta_+ - \alpha_-\beta_-\right)\\ &\quad - \rho^3\left(\alpha_+\beta_+e^{1/\rho} - \alpha_-\beta_-e^{-1/\rho}\right)\\ &= J_1 + J_2 + J_3\end{aligned} \tag{1.35}$$

Using (1.32) we have $\alpha_+\beta_+e^{1/\rho} - \alpha_-\beta_-e^{-1/\rho} = 1/\mu$ and thus

$$J_3 = -\rho^3/\mu \tag{1.36}$$

For J_1 and J_2 we use the values of α_+ and α_- given by (1.30). We thus

multiply J_1 by Δ (given by (1.29)) to obtain:

$$\begin{aligned}\frac{\Delta J_1}{\rho^2} &= (\Delta\alpha_+)\beta_+ + (\Delta\alpha_-)\beta_- \\ &= (\rho\beta_+ + \rho\beta_- e^{-1/\rho})\beta_+ + (\rho\beta_- + \rho\beta_+ e^{1/\rho})\beta_- \\ &= \rho(\beta_+^2 + \beta_-^2) + \rho\beta_+\beta_-(e^{1/\rho} + e^{-1/\rho}) \\ &= \rho(\beta_+ + \beta_-)^2 - 2\rho\beta_+\beta_- + 2\rho\beta_+\beta_-\cosh(1/\rho) \\ &= \frac{1}{\rho} + 2\rho\beta_+\beta_-(\cosh(1/\rho) - 1)\end{aligned} \tag{1.37}$$

because by defintion of $\beta_\pm$ and ρ, we have $\beta_+ + \beta_- = 1/\rho$. Now we turn to J_2

$$\begin{aligned}\frac{\Delta J_2}{\rho^3} &= (\Delta\alpha_+)\beta_+ - (\Delta\alpha_-)\beta_- \\ &= (\rho\beta_+ + \rho\beta_- e^{-1/\rho})\beta_+ - (\rho\beta_- + \rho\beta_+ e^{1/\rho})\beta_- \\ &= \rho(\beta_+^2 - \beta_-^2) - \rho\beta_+\beta_-(e^{1/\rho} - e^{-1/\rho}) \\ &= \beta_+ - \beta_- - 2\rho\beta_+\beta_-\sinh(1/\rho)\end{aligned} \tag{1.38}$$

Let us emphasize that we use Cramer's rule and equation (1.30). That means that Δ in these expressions is the determinant of system (1.28) and given by equation (1.29). In the end, using (1.33) to (1.38) we have:

$$\begin{aligned}\tau =& \frac{\lambda b}{De} + \frac{\rho}{2\mu} - \frac{\rho^3}{\mu} \\ &+ \frac{\rho^2}{\Delta}\left(\frac{1}{\rho} + 2\rho\beta_+\beta_-(\cosh(1/\rho) - 1)\right) \\ &+ \frac{\rho^3}{\Delta}\left(\beta_+ - \beta_- - 2\rho\beta_+\beta_-\sinh(1/\rho)\right)\end{aligned} \tag{1.39}$$

Recall that we defined in Section 1.6.3 the variables $x = \mu\Gamma =$ and $y = \lambda b/De$ and that by (1.26) we have $\beta_+\beta_- = -1/x$. Also we have $\rho = x/y$. We now rewrite this equality in the (x, y) variables.

$$\begin{aligned}\tau(x,y) =& y + \frac{x}{2\mu y} - \frac{x^3}{\mu y^3} \\ &+ \frac{x^2}{y^3\Delta(x,y)}\left(\frac{y^2}{x} - 2(\cosh\left(\frac{y}{x}\right) - 1)\right) \\ &+ \frac{x^3}{y^4\Delta(x,y)}\left(y\left(\left(\frac{y}{x}\right)^2 + \frac{4}{x}\right)^{1/2} + 2\sinh\left(\frac{y}{x}\right)\right)\end{aligned}$$

Chapitre 2

La transition vitreuse vue à travers les développements asymptotiques

Résumé du chapitre

Dans ce chapitre nous nous posons, comme au chapitre 1, la question de la transition vitreuse dans le modèle d'Hébraud-Lequeux, sous un angle presque inverse. Rappelons d'abord que le modèle d'Hébraud-Lequeux stationnaire est constitué d'un système d'équation (2.1) que l'on peut voir comme un système de deux équations à deux inconnues ϕ et p. Dans le chapitre 1, les démonstrations sont conçues de façon à court-circuiter l'inconnu p du problème, par l'intégration de l'équation différentielle de (2.1) et à ne raisonner qu'avec l'inconnue scalaire ϕ. Dans ce chapitre, nous ne raisonnons au contraire que sur l'inconnue p et ϕ n'apparaît qu'à travers son lien théorique de couplage avec p. À la suite du chapitre 1 nous nous sommes aperçus qu'il était plus pratique d'utiliser le paramètre y qui est un taux de cisaillement adimensionné plutôt que le paramètre b de Cancès, Catto et Gati,[16] car l'analyse du système (8)–(10) p. 7 se réduit à l'étude du système (2.1) qui ne fait plus intervenir que deux paramètres ; y et μ (la fonction ϕ est la même que celle définie dans le théorème 1.1 p. 39).

Les résultats principaux de ce chapitre sont le théorème 2.1 ainsi que son corollaire 2.1. Soulignons que le corollaire 2.1 est plus précis que le théorème analogue 1.2 du chapitre 1 : en effet, dans le corollaire 2.1, nous donnons un développement de la contrainte τ en série de Puiseux convergente de y alors que dans le théorème 1.2 nous n'en donnions qu'un équivalent.

Néanmoins, dans ce chapitre comme dans le chapitre 1, les énoncés comptent

en fait moins que les schémas de preuve utilisés pour les obtenir. Guidés tout de même par les résultats du chapitre 1, nous avons interprété la limite $y \to 0$ du système (2.1) comme pouvant être une limite singulière semblable à celle qui apparaît dans les problèmes de mécanique des fluides avec terme de pénalisation d'obstacle [2, 20, 12] : c'est du moins ce qui apparaît, si l'on remplace arbitrairement dans l'équation différentielle de (2.1), $\phi(y)$ par son équivalent obtenu dans la proposition 1.1. Dans ces modèles, l'objectif est de calculer le champ de vitesse u d'un fluide newtonien dans un domaine $\Omega \setminus \omega$ où ω s'interprète comme un obstacle à l'écoulement auquel le fluide, par exemple, adhère. Pour des raisons d'efficacité numérique, on cherche à calculer un champ de vitesse fictif dans Ω qui vaut idéalement u dans $\Omega \setminus \omega$ mais qui en réalité n'en n'est qu'une approximation u^ε. On calcule de fait u^ε en écrivant une équation de mécanique des fluides sur tout le domaine Ω modifié par un terme supplémentaire artificiel dit de pénalisation. De nombreux auteurs, notamment Fabrie, Carbou et Guès , ont développé des méthodes pour étudier la qualité de l'approximation de u par u^ε.

Dans le modèle d'Hébraud-Lequeux, nous pouvons interpréter le terme $\mathbf{1}_{\mathbf{R}\setminus[-1,1]}p$ comme étant un terme de pénalisation «naturelle» de l'«obstacle» $\mathbf{R}\setminus[-1,1]$. Nous avons donc décidé de nous approprier les méthodes mentionnées précédemment qui préconisent la description de u^ε par des termes qui décrivent une «couche limite» (d'origine numérique). Dans notre contexte, le petit paramètre ε est notre nombre de Weissenberg (ou cisaillement adimensionné) y, le rôle de «u^ε» est en fait joué par l'inconnu p, et u serait la solution limite de notre problème que nous ne connaissons pas.

Bien que nous soyons désormais guidés par des théories bien établies sur le développement en couches limites de ces types de problème, leur mise en en œuvre dans notre cas particulier ne va pas de soi, car nous ne voulons pas nous appuyer sur la proposition 1.1 : nous voulons développer une méthode qui puisse être utilisée sans connaissance *a priori* sur le modèle, car nous avons l'intention de l'appliquer à un modèle plus compliqué mais similaire (dans le chapitre 4), pour lequel nous ne possédons pas cette connaissance. Nous devons traiter en parallèle le problème du développement de ϕ en fonction de y. Ce qui est alors intéressant c'est que, bien que l'on sache qu'il faille regarder dans la direction des développements en couche limite, il nous manque *a priori* un élément important de ces développements qui est la taille de la couche limite. Nous ne savons pas non plus dans quelle échelle de y développer la solution car le problème ne s'écrit pas de façon immédiate comme un problème classique. Nous avons donc recours dans un premier temps à des formes de développements asymptotiques très générales que nous caractérisons à l'aide de la proposition 2.1, et il apparaît alors un changement de taille de couche limite et d'échelle de développement suivant la valeur de μ

qui préfigure la transition vitreuse sur μ. Bien que formelle, cette analyse est déjà très importante dans l'optique du chapitre 4.

Nous concluons ce chapitre par l'analyse de la convergence des développements formels que nous avons obtenus. Cette convergence est obtenue par une méthode de perturbation analytique d'opérateur, couplée à une application du théorème des fonctions implicites en version analytique. Cette méthode très efficace permet d'obtenir la convergence des développements, et ce, dans des espaces fonctionnels de fonctions à décroissance exponentielle. Ceci permet d'utiliser la définition (2.3) et d'obtenir le développement de la contrainte τ par intégration terme à terme des différents développements. Le corollaire 2.1 est donc gratuit, ce qui est à comparer avec la démonstration de (1.2).

Ce chapitre est tiré d'un article en cours de révision pour *SIAM J. Appl. Math.*, en collaboration avec Michael Renardy.

2.1 Introduction

Soft glassy materials are complex fluids which by definition exhibit a transition when a parameter goes through a critical value. This behaviour is very similar to the one of classical glasses in which case the parameter is simply the temperature of the glass. The class of materials we are interested in is formed of the so-called granular glasses. A granular glass is composed of "particles" dispersed in a Newtonian fluid: this is the case for suspensions of solid particles and for emulsions which are "particles" of a fluid dispersed in another immiscible fluid. In this setting, the parameter is related to the concentration of particles: as long as the particles are not too concentrated, the behavior of the material is Newtonian. But when the concentration reaches a certain value, the particles are so packed that the structure has to break before the material can flow. This leads to a stress threshold behavior similar to Herschel-Bulkley models.

One model available in the literature to describe this kind of phenomenon is the one introduced by HÉBRAUD and LEQUEUX in [37]. At the beginning, there was a kinetic-type of model for real glasses which was proposed by BOUCHAUD *et al.* in [11]. Then considering the aforementioned analogy between soft glasses and real glasses, a model was designed by SOLLICH *et al.* in [68] for soft glasses. Finally the Hébraud-Lequeux model was introduced as a simpler model taking the previous ideas into account.

In a previous paper [53], we mathematically proved that the Hébraud-Lequeux model (referred to as HL for the sake of brevity) describes the glass transition as was announced in HÉBRAUD's PHD thesis [36]. This work relied on analytical computations of the solutions of the model which was possible because HL was designed to describe simple shear flow and is thus, from a mathematical point of view, a 1d problem governed by an ODE. Thus all the computations can be done "by hand" (note that for given y and ϕ, equation (2.1) below is just an ODE with piecewise constant coefficients, which can be solved explicitly). But in an upcoming work [52], we intend to extend the model to multidimensional situations and thus study a model similar to HL but set on several dimension of space. This means that analytical solutions are not available anymore. This led us to search for other tools to prove the same results, techniques that would be more easily generalized to multidimensional situations. The tool we found to be appropriate are asymptotic expansions.

Let us introduce the model and our notations. We are interested in the stationary dimensionless version of the HL model. Here the unknown is p which is a probability density on the stress space. The stress variable will always be denoted σ. The small parameter is y. It is a dimensionless shear

rate and is chosen to be nonnegative. The glass parameter is denoted by μ. Finally, the model uses a function ϕ of y called the *fluidity*. Then the model reads:

$$\begin{cases} -\phi(y)\partial_\sigma^2 p + y\partial_\sigma p + \mathbf{1}_{[-1,1]^c} p = \dfrac{\phi(y)}{\mu}\delta_0, \\ p \in \mathrm{H}^1(\mathbf{R}), \\ p(\pm\infty) = 0, \\ p \geq 0, \\ \displaystyle\int_{\mathbf{R}} p(\sigma)\mathrm{d}\sigma = 1. \end{cases} \tag{2.1}$$

Here $\mathbf{1}_{[-1,1]^c}$ denotes the characteristic function of the complement of the interval $[-1,1]$ and δ_0 is the delta function located at the origin. The fluidity is not explicitly defined. It comes from the constraint on the integral of p. Indeed, if instead of $\phi(y)$ in the PDE we had a given constant Γ, then solving the boundary value problem is a simple matter. But since we have in addition the integral constraint, there is only one Γ that allows for solving the equation and the integral constraint simultaneously when $y > 0$. See Cancès, Catto and Gati [16] or [53] for further details on this question. On the other hand, by integrating the equation, one has the following connection between p and ϕ :

$$\frac{\phi}{\mu} = \int_{|\sigma|>1} p(\sigma)\mathrm{d}\sigma. \tag{2.2}$$

Finally, to connect more specifically to the physics of the phenomenon we are trying to model, we introduce the *macroscopic stress*

$$\tau = \int_{\mathbf{R}} \sigma p(\sigma)\mathrm{d}\sigma. \tag{2.3}$$

Then τ is only a function of y. In this setting the glass transition occurs at the critical value $1/2$: when $\mu > 1/2$, the behavior is Newtonian $\tau \sim \eta y$, when $\mu = 1/2$, we will have a power-law fluid with exponent $1/5$, that is $\tau \sim y^{1/5}$, and finally when $\mu < 1/2$, we obtain a Herschel-Bulkley fluid with exponent $1/2$, that is to say $\tau \sim \tau_0 + A\sqrt{y}$, where $\tau_0 > 0$ is called the *dynamic yield stress*. We note that the asymptotic expansions for p translate into a straightforward manner into expansions for τ, as long as we show convergence in a function space that embeds into a space for which $p \mapsto \int \sigma p$ is a continuous linear form.

The paper is organized as follows: in Section 2.2, we introduce the physical background of the model and the motivation for the equations. In Section

2.3, we discuss the limiting problem for $y = 0$ which provides the foundation for the asymptotic analysis. Our main result is stated in Section 2.4. Section 2.5 is devoted to the derivation of the asymptotic hierarchy. We explain how to find the appropriate scales of expansions and the sizes of the relevant boundary layers. In Section 2.6 we justify the formal expansions by an implicit function argument. In doing so, we find it advantageous to introduce a priori two small parameters $a = y/\phi(y)$ and $b = \sqrt{\phi(y)}$. This allows us to reduce our problem to a single equation of the form $F(\mu, a, b) = 0$. The behavior of ϕ as a function of y arises naturally from the analysis of this function.

2.2 Physical Background

2.2.1 Description

In this section we shall review the physical features behind the Hébraud-Lequeux model. The model describes what are called soft glassy materials. These materials are amorphous. For example, consider an emulsion, that is a material consisting of bubbles of one liquid plunged into another liquid and let us imagine that the bubbles do not coalesce. Then the disposition of the bubbles can be very complicated and does not follow any particular order. The rheology of these materials needs to take into account some of the complexity in the material. Indeed these kind of materials are sensitive to what can be called *the mechanical noise*: because of the composition of the material, what happens to the bubbles at some place can have have mechanical repercussions throughout all the material. Nevertheless, this noise must be taken into account in a manageable way. In the model by Bouchaud *et al* [11] or in SGR [68] the noise is taken into account *a priori* as a characteristic quantity of the material . In the HL model this is done by using a statistical approach which is simple but captures the basic physics of a typical soft glassy material. The noise can then be approached by mechanical considerations and is not "hidden" in the model. Only the intensity of the noise is characteristic of the material.

The model is restricted to simple shear flows. In classical rheology, when an "elementary" block of material undergoes a certain shear rate $\dot{\gamma}$, the continuous medium has a change in its stress σ to adapt to the shear rate so that the stress and the shear rate are always linked. The nature of this link defines the rheological properties of the material. One can then study a macroscopic sample (assuming the shear rate is constant throughout the sample) by mentally dividing it in "elementary" blocks. But for microscopi-

cally inhomogeneous materials like suspensions or emulsions this procedure is not relevant since elementary blocks are in all kinds of states.

The HL model acknowledges this difficulty by, in a sense, attributing a distribution of stresses to the "elementary" blocks for a given macroscopic shear rate. More accurately, the model describes a *typical* "elementary" block by giving it a distribution of stress p for a given shear rate that accounts for the distribution of stresses of all the "elementary" blocks (not typical ones but real ones) of a macroscopic sample. The HL model gives the evolution of this distribution in time. The quantity $p(t,\sigma)\mathrm{d}\sigma$ can be understood as the proportion of "elementary" blocks of a macroscopic sample that are in the stress state σ (with margin $\mathrm{d}\sigma$) at time t. It is consequently a probability density. The stress of the macroscopic sample at time t, which we denote by $\tau(t)$, is the average of all the contributions of the "elementary" blocks and is therefore given by the equation

$$\tau(t) = \int_{\sigma\in\mathbf{R}} \sigma p(t,\sigma)\mathrm{d}\sigma. \tag{2.4}$$

We note that formulating the model in terms of only one stress component is an oversimplification. Even if the flow is restricted to parallel shear, stress is a tensor with several components, and all of them have a statistical distribution. The formulation and analysis of such models will be addressed in future work. Even in the case of simple shear flow, they do not simply reduce to the original Hébraud-Lequeux model.

Let us now give the evolution equation of p. Suppose that at time t the shear rate throughout the sample is $\dot\gamma(t)$. Then we have

$$\partial_t p(t,\sigma) = -G_0\dot\gamma(t)\partial_\sigma p(t,\sigma) - \frac{1}{T_0}\mathbf{1}(\sigma)_{[-\sigma_c,\sigma_c]^c} p(t,\sigma) + \Gamma(p)(t)\delta_0(\sigma) + \alpha\Gamma(p)(t)\partial_\sigma^2 p(t,\sigma), \tag{2.5}$$

where G_0, σ_c, T_0 and α are material constants respectively called elastic modulus, stress threshold, relaxation time and fragility. The term $\mathbf{1}_{[-\sigma_c,\sigma_c]^c}$ designates the characteristic function of the complement of the segment $[-\sigma_c,\sigma_c]$ in the real line. The term $\Gamma(p)(t)$ is called the *fluidity* and depends on the state of the sample in the following way:

$$\Gamma(p)(t) = \frac{1}{T_0}\int_{|\sigma|>\sigma_c} p(t,\sigma)\mathrm{d}\sigma. \tag{2.6}$$

2.2.2 Explanations of the Terms of the Equation

Let us now explain heuristically how the equation is motivated.

We take a macroscopic sample of N "elementary" blocks and for each of this blocks we note $\Sigma_i(t)$ its stress. We say that under the shear rate $\dot{\gamma}(t)$ the stress of an "elementary" block will evolve because of three effects:

Elastic gain: the first possibility is that the particular block behaves elastically which means that its stress will evolve linearly in time, as prescribed by Hooke's law of linear elasticity:

$$\Sigma_i(t + \mathrm{d}t) - \Sigma_i(t) = G_0\dot{\gamma}(t)\mathrm{d}t. \tag{2.7}$$

Physically, we could say that the local structure withstands the shear by increasing elastically its stress. For an emulsion it could correspond to bubbles deforming to take in the shear rate. Of course, the actual source of elastic forces in an emulsion is the surface tension on the interfaces, so the assumption of linear Hookean elasticity is a rather crude simplification.

Relaxation toward 0: when $|\Sigma_i|$ is larger than a maximal value σ_c then the local structure cannot bear the shear and locally breaks. By doing this the stress is released and we model this effect by an exponential decay toward 0 with rate T_0. For an emulsion this would be for example a bubble that cannot deform any longer and moves away from its position to find a place where it would be less deformed and thus less stressed. We call this a *relaxation event*. Note that the fluidity is thus the time rate of relaxation events.

Rearrangements: when the structure breaks it induces rearrangements on neighboring blocks. One can think for example that, in the case of an emulsion, when a bubble moves away because of the relaxation event it lets its place to another bubble which, in turn, lets its place to another one and so on. We model this on a typical "elementary" block by adding a Brownian motion that accounts for the contribution of all the rearrangements around it. Of course the more relaxation events there are, the more rearrangements there can be and the more this effect will be important. So the intensity of the Brownian motion will be proportional to the total number of relaxation event and we call α/T_0 the proportionality constant. When α is small, then there needs to be a lot of relaxation events for the rearrangement to be perceived and on the contrary, if α is large then a few relaxation events will induce lots of rearrangements everywhere. This can be interpreted as follow: rearrangements are by nature local (in space). If α is small then it means that the rearrangements will take place on a very small area

around the relaxation event. So, for a given block, the extra stress due to rearrangement will be small because the block does not see the blocks that are far from it. On the other hand, if α is large, then even a few relaxation events will have consequences on a lot of blocks even far from the origin. In this interpretation, α is a measure of the fragility of the structure: when α is small, a break somewhere in the structure will have little repercussions which means that the structure is robust. On the other hand, if α is large, then a small break at some place will induce a lot of breaks throughout the structure and the structure can indeed be called fragile.

2.2.3 Dimensionless Equation

It is usually easier to analyze models such as (2.5) by rescaling variables. To do that we need to choose a scale for all the variable. For the stress variable, we choose the scale given by the stress threshold σ_c so we set $\sigma' = \sigma/\sigma_c$. The relaxation time T_0 provides a time scale.

Since p is a stress density, its dimension is the inverse of a stress. It is thus natural to introduce $p'(t', \sigma') = \sigma_c p(t'T, \sigma'\sigma_c)$. Note also that when changing variables we have $\delta_0(\sigma) = (1/\sigma_c)\delta_0(\sigma/\sigma_c)$. One can check that p' follows the following equation:

$$\partial_{t'} p'(t', \sigma') = -\frac{G_0}{\sigma_c}(T_0\dot{\gamma}(t'T_0))\partial_{\sigma'} p'(t', \sigma') - \mathbf{1}(\sigma')_{[-1,1]^c} p'(t', \sigma') + \Gamma'(p')(t')\delta_0(\sigma') + \frac{\alpha}{\sigma_c^2}\Gamma'(p')(t')\partial^2_{\sigma'} p'(t', \sigma'), \quad (2.8)$$

where

$$\Gamma'(p')(t') = \int_{|\sigma'|>1} p'(t', \sigma')\mathrm{d}\sigma'.$$

We also have, by this change of variables,

$$\int_{\sigma' \in \mathbf{R}} p'(t', \sigma')\mathrm{d}\sigma' = 1.$$

We thus define two dimensionless numbers: $\lambda = G_0/\sigma_c$, and what we call the *glass parameter*, $\mu = \alpha/\sigma_c^2$. In the sequel, we drop the primes in the variables and on the unknowns.

In this paper, we focus on the stationary equation, i.e. all variables are independent of time. This results in the following model (in dimensionless form):

$$0 = -\lambda(T_0\dot{\gamma})\partial_\sigma p(\sigma) - \mathbf{1}(\sigma)_{[-1,1]^c}p(\sigma) + \Gamma(p)\delta_0(\sigma) + \mu\Gamma(p)(t)\partial_\sigma^2 p(\sigma).$$

We note that the shear rate appears only in the combination $\lambda T_0\dot{\gamma}$. This dimensionless combination is referred to as a Weissenberg number, and it is what we have denoted by y in our analysis. Also, we use $\phi = \mu\Gamma$ instead of Γ, which is the diffusion coefficient of the equation. That is how we find (2.1) from (2.5).

2.2.4 Heuristic Considerations

The essential dimensionless parameter in the equations is therefore the glass transition parameter μ. Let us assess the relevance of this parameter. If μ is small, we have elastic behavior until $|\sigma|$ exceeds 1, and then we have relaxation. The result of this is a yield stress behavior; since a critical stress must be reached before relaxation can occur, the fluid has to overcome this critical stress to flow, no matter how small the shear rate is. On the other hand, if μ is large, the random effect of rearrangements can lead to stresses exceeding the critical stress. The distribution of microstresses becomes broad, and relaxation always occurs. In this scenario, the yield stress disappears, and the fluid can flow at any shear rate. Below, we shall specifically quantify these phenomena.

2.3 Behavior at Main Order

In this section we shall briefly discuss the "fundamental" solutions that govern the limiting behavior of System (2.1) in the limit $y = 0$. As the glass transition implies, there are three possible regimes. The first one is the Newtonian regime. In this regime the material constantly undergoes breaks and rearrangements (a process sometimes known as *rejuvenation* see Picard, Ajdari, Bocquet and Lequeux [59]), even in the limit of vanishing shear rate. We thus expect at the main order a stationary stress distribution which is non zero for $|\sigma| > 1$. The specific expression is obtained by setting $y = 0$ in the governing equation, while we expect a nonzero limit (which is to be determined) for $\phi(y)$. In the sequel we use the notations

$$q = p|_{]-1,1[}, \qquad r_g = p|_{]-\infty,-1[} \qquad r_d = p|_{]1,+\infty[},$$

and we use $\overline{Q}^0$,$\overline{R}_g^0$ and $\overline{R}_d^0$ for the leading order of q, r_g and r_d respectively. In the Newtonian regime the stationary distribution at main order is governed by the following equations:

$$\begin{cases} -\mu\overline{c}_0\partial_\sigma^2\overline{Q}^0 = \overline{c}_0\delta_0, \\ -\mu\overline{c}_0\partial_\sigma^2\overline{R}_g^0 + \overline{R}_g^0 = 0, \\ -\mu\overline{c}_0\partial_\sigma^2\overline{R}_d^0 + \overline{R}_d^0 = 0, \\ \overline{Q}^0(-1) = \overline{R}_g^0(-1), \\ \overline{Q}^0(1) = \overline{R}_d^0(1), \\ \partial_\sigma\overline{Q}^0(-1) = \partial_\sigma\overline{R}_g^0(-1), \\ \partial_\sigma\overline{Q}^0(1) = \partial_\sigma\overline{R}_d^0(1), \\ \displaystyle\int_{-1}^{1}\overline{Q}^0(\sigma)\mathrm{d}\sigma + \overline{c}_0 = 1, \\ \overline{c}_0 \neq 0. \end{cases} \tag{2.9}$$

This problem is simply (2.1) with $y = 0$ and $\phi/\mu = \overline{c}_0$ when split into the three intervals $]-\infty, -1[$, $]-1, 1[$ and $]1, +\infty[$. The explicit solution of this system, which can be found in [16, 53], is

$$\begin{aligned} \overline{Q}^0(\sigma) &= \begin{cases} \dfrac{\sigma+1}{2\mu} + \dfrac{1}{2}\sqrt{\dfrac{\overline{c}_0}{\mu}} & \text{if } \sigma < 0 \\ \dfrac{1-\sigma}{2\mu} + \dfrac{1}{2}\sqrt{\dfrac{\overline{c}_0}{\mu}} & \text{if } \sigma > 0 \end{cases} \\ \overline{R}_g^0(\sigma) &= \frac{1}{2}\sqrt{\frac{\overline{c}_0}{\mu}}\exp\left(\frac{\sigma+1}{\sqrt{\overline{c}_0\mu}}\right) \\ \overline{R}_d^0(\sigma) &= \frac{1}{2}\sqrt{\frac{\overline{c}_0}{\mu}}\exp\left(-\frac{\sigma-1}{\sqrt{\overline{c}_0\mu}}\right) \end{aligned} \tag{2.10}$$

where $\overline{c}_0$ satisfies the following equation (which is a statement of the integral constraint),

$$\overline{c}_0 + \sqrt{\frac{\overline{c}_0}{\mu}} + \frac{1}{2\mu} = 1, \tag{2.11}$$

and has thus the following solution

$$\overline{c}_0 = 1 - \frac{1}{2\mu}\sqrt{4\mu - 1}.$$

As announced, $\overline{R}_g^0 > 0$ and $\overline{R}_d^0 > 0$ and since the function obtained by gluing the previous pieces together is even, there is no stored stress in this fundamental problem. Indeed applying formula (2.3) to this function gives 0. Finally we remark that if $\mu \leq 1/2$ then (2.11) does not have a positive

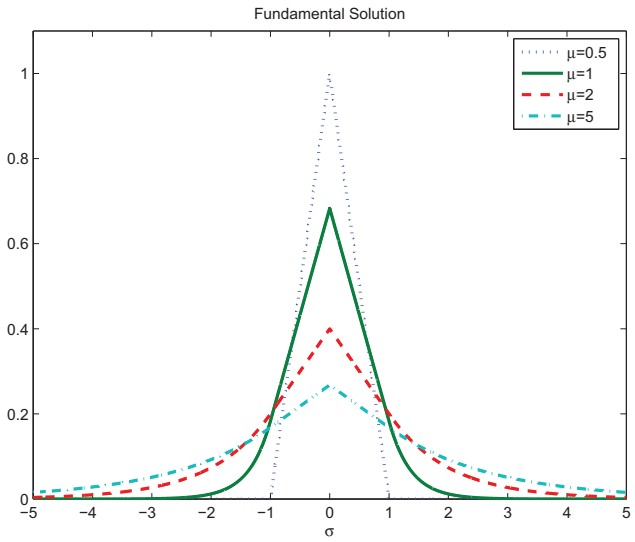

Figure 2.1: Examples of fundamental solutions for $\mu \geq 1/2$

solution and that is why Problem (2.9) cannot be the fundamental problem of (2.1) when $\mu \leq 1/2$.

The second regime is the jammed regime. In this regime, the effect of rearrangements is not strong enough to take the local stress beyond the threshold. At the limit, all the blocks are trapped in states that no longer allow relaxation events. As y becomes smaller, the elastic mechanism becomes weaker and cannot bring the stress high enough for relaxations to occur. In the end the stationary distribution of stress reflects that fact since $\overline{R}_g^0 = \overline{R}_d^0 = 0$. However, our analysis can give information on the inner distribution of stress "at the limit". This means that if we knew that a soft glassy material, in the jammed state, had been put to rest through a sequence of decreasing shear rate, with enough time to reach the stationary state at each step, then we would be able to compute the complete distribution of stress in the material. Note that without the history of the preparation of the material sample, we would not be able to distinguish between any distributions of stress which does not allow relaxation events. Indeed, if we set $y = \phi(y) = 0$, then all the terms in (2.1) vanish in the inner region, and we obtain absolutely no information. We can, however, obtain a meaningful limit by assuming that $\phi(y)$ is proportional to y, and then dividing the equation by y. If we set $\phi(y) = \mu c_1 y$, we obtain the following problem for $\overline{Q}^0$:

$$\begin{cases} -\mu c_1 \partial_\sigma^2 \overline{Q}^0 + \partial_\sigma \overline{Q}^0 = c_1 \delta_0, \\ \overline{Q}^0(\pm 1) = 0, \\ \displaystyle\int_{-1}^{1} \overline{Q}^0(\sigma) \mathrm{d}\sigma = 1, \\ c_1 \neq 0. \end{cases} \tag{2.12}$$

For this system, $\overline{Q}^0$ can be computed in terms of c_1 and the integral constraint gives us an equation on c_1. Namely we have:

$$\overline{Q}^0(\sigma) = \begin{cases} \dfrac{c_1 \left(1 - \exp\left(-\dfrac{1}{\mu c_1}\right)\right)}{\exp\left(\dfrac{1}{\mu c_1}\right) - \exp\left(-\dfrac{1}{\mu c_1}\right)} \left(\exp\left(\dfrac{\sigma+1}{\mu c_1}\right) - 1\right) & \text{if } \sigma \in]-1, 0[\\ \dfrac{c_1 \left(\exp\left(\dfrac{1}{\mu c_1}\right) - 1\right)}{\exp\left(\dfrac{1}{\mu c_1}\right) - \exp\left(-\dfrac{1}{\mu c_1}\right)} \left(1 - \exp\left(\dfrac{\sigma-1}{\mu c_1}\right)\right) & \text{if } \sigma \in]0, 1[\end{cases} \tag{2.13}$$

and c_1 is fixed by the following equation (which again is a statement of the integral constraint),

$$c_1 \tanh\left(\frac{1}{2\mu c_1}\right) = 1. \tag{2.14}$$

If we multiply this equation by μ and study $x \mapsto x \tanh(1/(2x))$ it is easy to see that it does not have a solution if $\mu \geq 1/2$ and that is why Problem (2.12) cannot serve as a fundamental problem for this range of μ. Finally, the solution is clearly not even and using (2.3) on $\overline{Q}^0$ instead of p one can compute a positive value τ_0. This value is called the *dynamic yield stress*.

The final regime is the transition regime which is in between the two previous regimes. Its governing equations would be:

$$\begin{cases} -\mu \partial_\sigma^2 \overline{Q}^0 = \delta_0, \\ \overline{Q}^0(\pm 1) = 0, \\ \displaystyle\int_{-1}^{1} \overline{Q}^0(\sigma) \mathrm{d}\sigma = 1. \end{cases} \tag{2.15}$$

This limit is obtained under the assumption that $\phi(y) \to 0$, but $\phi(y)/y \to \infty$ as $y \to 0$. The exact behavior of $\phi(y)$ is not obtained at this level, and can only be determined by considering higher orders in the expansion. This will be pursued further in Section 2.5.

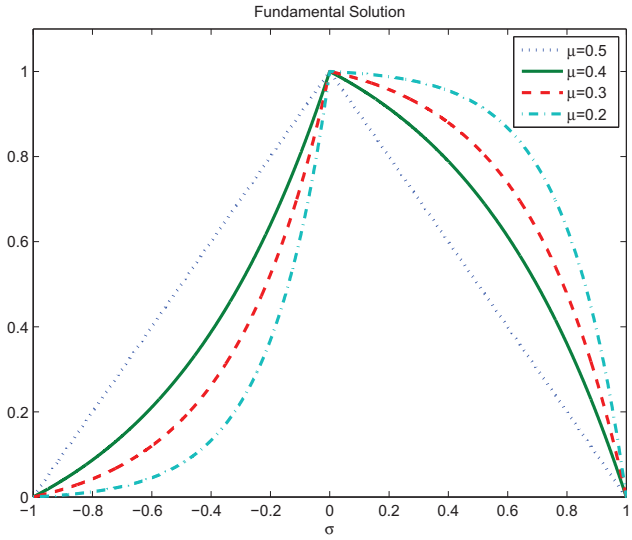

Figure 2.2: Examples of fundamental solutions for $\mu \leq 1/2$

However, it is easily seen that System (2.15) can only be solved when $\mu = 1/2$ by the function

$$\overline{Q}^0(\sigma) = \begin{cases} \sigma + 1, & \text{if } \sigma \in [-1, 0], \\ 1 - \sigma, & \text{if } \sigma \in [0, 1]. \end{cases} \tag{2.16}$$

As we can see this solution is really in between the two previous regimes: its support is $[-1, 1]$ so it is in a jammed state as are the fundamental solutions of the the $\mu < 1/2$ case. However the function is even as in the $\mu > 1/2$ case and as such, does not store any stress.

2.4 Reformulation of the Problem and Main Result

At the start of this study we were inspired by the similarity of the problem given by the system (2.1) with the problem of stationary Navier-Stokes equations with a penalization term to take into account an obstacle in viscous flows studied by Angot, Bruneau and Fabrie, [2], Carbou and Fabrie [20], or Carbou [19] in the context of porous materials, or the problem of wave equations with a penalization term studied by Fornet and Guès [30]

and FORNET [29, 28]. This encouraged us to see if the same methods could be adapted to our problem. In the HL setting, the obstacle would be the exterior of the $[-1,1]$ interval.

The first thing to do is to separate what happens inside and outside the obstacle. This means we rewrite (2.1) with unknowns

$$q = p|_{]-1,1[}, \qquad r = p|_{[-1,1]^c},$$

and obtain

$$-\phi(y)\partial_\sigma^2 q + y\partial_\sigma q = \frac{\phi(y)}{\mu}\delta_0 \qquad \text{in }]-1,1[, \tag{2.17a}$$

$$-\phi(y)\partial_\sigma^2 r + y\partial_\sigma r + r = 0 \qquad \text{in } [-1,1]^c, \tag{2.17b}$$

$$r(\pm\infty) = 0, \tag{2.17c}$$

$$q \geq 0, \tag{2.17d}$$

$$r \geq 0, \tag{2.17e}$$

$$r(\pm 1) = q(\pm 1), \tag{2.17f}$$

$$\partial_\sigma r(\pm 1) = \partial_\sigma q(\pm 1), \tag{2.17g}$$

$$\int_{|\sigma|>1} r(\sigma)\mathrm{d}\sigma + \int_{-1}^{1} q(\sigma)\mathrm{d}\sigma = 1. \tag{2.17h}$$

We refer to (2.17f) and (2.17g) as the *transmission conditions* and (2.17h) as the *integral constraint*.

Now our main result can be stated:

Theorem 2.1. *The solution of* (2.17a)–(2.17h)*, for small* y*, can be expanded in a* convergent *series whose terms can be described in terms of boundary layers. Moreover the expansion changes if the parameter* μ *changes, which leads more precisely to the following discussion:*

if $\mu > 1/2$**,** *there is no boundary layer terms (*$\overline{Q}$ *and* $\overline{R}$ *are functions of* σ*) and we have*

$$q = \overline{Q}^0 + y\overline{Q}^1 + y^2\overline{Q}^2 + \cdots,$$
$$r = \overline{R}^0 + y\overline{R}^1 + y^2\overline{R}^2 + \cdots,$$

and consequently

$$\frac{\phi}{\mu} = \overline{c}_0 + \overline{c}_1 y + \overline{c}_2 y^2 + \cdots.$$

if $\mu < 1/2$, *the boundary layer is of size* $y^{1/2}$ *and*

$$q = \overline{Q}^0 + y^{1/2}\overline{Q}^1 + y\overline{Q}^2 + \cdots,$$
$$r = \sqrt{y}R^1 + yR^2 + \cdots,$$

and consequently

$$\frac{\phi}{\mu} = c_1 y + c_2 y^{3/2} + \cdots,$$

with R^k *depending on* $(|\sigma| - 1)/y^{1/2}$.

if $\mu = 1/2$, *the boundary layer is of size* $y^{1/5}$ *and*

$$q = \overline{Q}^0 + y^{1/5}\overline{Q}^1 + y^{2/5}\overline{Q}^2 + \cdots,$$
$$r = y^{2/5}R^2 + y^{3/5}R^3 + \cdots,$$

and consequently

$$\frac{\phi}{\mu} = c_2 y^{4/5} + c_3 y + \cdots,$$

with R^k *depending on* $(|\sigma| - 1)/y^{2/5}$.

Using the previous theorem, the following result related to the macroscopic stress may be deduced:

Corollary 2.1. *The previous expansions converge in a space in which the application* $p \mapsto \int_{\mathbf{R}} \sigma p$ *is a continuous linear form. Thus by a simple integration we have the following expansions:*

if $\mu > 1/2$, *the stress expands as*

$$\tau = \eta_0 y + \eta_1 y^2 + \ldots$$

if $\mu < 1/2$, *the stress expands as*

$$\tau = \tau_0 + A_0\sqrt{y} + \ldots$$

if $\mu = 1/2$, *the stress expands as*

$$\tau = B_0 y^{1/5} + B_1 y^{2/5} + \ldots$$

The various constants (which may be 0 except for the first one of those we have indicated) can be computed in terms of the profiles of the expansion of q and r.

Section 2.5 is devoted to understanding from a formal point of view where the boundary layers come from, starting from an *a priori* unknown boundary layer expansion (meaning that we will not prescribe the size of the boundary layer nor the scale of the expansion). We will then obtain the equations of the profile in each case. This method is fairly general and may be applied in multi dimensional generalizations and the equations of profile can be useful for numerical purposes.

Even though this section does not contain any proof of convergence, one could follow up with a convergence proof based on existence and uniqueness of the profiles and estimation of the remainder at a given order, in a manner similar to Fabrie and Boyer [12]). However in Section 2.6 we shall give a simpler proof which exploits the fact that the problem is more easily analyzed in a two parameter setting. In this setting, $a = y/\phi(y)$ and $b = \sqrt{\phi(y)}$ are treated a priori as independent parameters. It turns out that the solution of the differential equation is actually an analytic function of a and b. The proof uses perturbation theory. One of the essential differences between the one-dimensional and multi-dimensional case is that the limit $b \to 0$ becomes a singular perturbation problem in several dimensions. The perturbation argument would therefore become more complicated, and the solution would depend only smoothly, but not analytically, on b. In a second step, we analyze the remaining equation resulting from the integral constraint. This is a finite dimensional problem of the form $F(\mu, a, b) = 0$. The implicit function theorem can be used to establish a relationship between a and b which naturally yields the expansions of Theorem 2.1.

2.5 Derivation of the Asymptotic Hierarchy

In this section we shall show the formal computations that will be justified by the next section. The formal computations are of interest in their own right, since the appropriate ansatz is not obvious *a priori*. Of course the results described by Hébraud and Lequeux in [37] and proved in [53] were a powerful guide. Yet they do not give the actual ansatz. The transitional case $\mu = 1/2$ was especially hard to devise.

2.5.1 Ansatz

To describe the boundary layer which lies in the exterior domain $[-1,1]^c$, we need the distance to the boundary $\{-1,1\}$ and we call this distance θ_e, which is simply

$$\theta_e(\sigma) = |\sigma| - 1.$$

We make the following ansatz for q and r:

$$q(\sigma) = \sum_{k=0}^{+\infty} y^{k/s} \overline{Q}^k(\sigma), \tag{2.18a}$$

$$r(\sigma) = \sum_{k=0}^{+\infty} y^{k/s} \overline{R}^k(\sigma) + y^{k/s} R^k\left(\mathrm{sign}(\sigma), \frac{\theta_e(\sigma)}{y^{l/s}}\right), \tag{2.18b}$$

which implies that ϕ/μ has the following expansion in view of (2.2):

$$\frac{\phi(y)}{\mu} = \sum_{k=0}^{+\infty} \tilde{c}_k y^{k/s}. \tag{2.18c}$$

Here l and s are two integers satisfying $1 \leq l \leq s$. We have also introduced:

$$\tilde{c}_k = \begin{cases} \overline{c}_k, & \text{if } 0 \leq k \leq l-1, \\ \overline{c}_k + c_{k-l}, & \text{if } k \geq l, \end{cases}$$

with

$$\overline{c}_k = \int_{|\sigma|>1} \overline{R}(\sigma)\mathrm{d}\sigma, \quad c_k = \int_0^{+\infty} y^{(k+l)/s}[R^k(-1,z) + R^k(1,z)]\mathrm{d}z. \tag{2.19}$$

We recall that in a boundary layer setting we have, from a formal point of view, the property:

$$\forall k \, \forall m \quad \lim_{z\to\infty} \left|\partial_z^m R^k(\pm 1, z)\right| = 0. \tag{2.20}$$

In more details we have the following:

Proposition 2.1 (Necessary form of the ansatz)**.** *The parameters in the previous ansatz in each case can only be:*

if $\mu > 1/2$**:** *we have $s = 1$ and no boundary layer, which means l is undefined and all the R^k are zero;*

if $\mu < 1/2$**:** *we have* $s = 2$ *and* $l = 1$*, which means that the boundary layer is of size* $y^{1/2}$*. In the exterior all the* $\overline{R}^k$ *are zero;*

if $\mu = 1/2$**:** *we have* $s = 5$ *and* $l = 2$ *which means that the boundary layer is of size* $y^{2/5}$ *while the expansion is in powers of* $y^{1/5}$*. In the exterior all the* $\overline{R}^k$ *are again zero.*

What we imply by necessary conditions is that taking other parameters will rapidly lead to ill-posed problems for the profiles, even at the leading order. Another detail to note is that for $\mu < 1/2$ for instance one could take $s = 4$ and $l = 2$ but this would lead to the same expansion with a lot of coefficients (half in fact) simply vanishing. We have indicated the choices of parameters that lead to the minimum of "trivially zero" terms.

The interest of this proposition is that its proof gives a methodology to find the size of the boundary layer when you have no *a priori* knowledge (from physics or elsewhere) to guide you. We have of course in mind our multidimensional generalization of the HL model for which we lack this kind of information.

Before we can prove this proposition, we need to derive the equations solved by the profiles.

2.5.2 Equations of Profile

We now put these ansaetze in (2.17a)-(2.17h) and assemble the terms of the same formal order. We obtain the following hierarchy of equations.

Equation (2.17a): We put the ansatz (2.18a) and the ansatz (2.18c) in (2.17a):

$$\begin{aligned} 0 \le k \le s-1: \quad & -\mu \sum_{k'=0}^{k} \tilde{c}_{k'} \partial_\sigma^2 \overline{Q}^{k-k'} = \tilde{c}_k \delta_0, \\ s \le k: \quad & -\mu \sum_{k'=0}^{k} \tilde{c}_{k'} \partial_\sigma^2 \overline{Q}^{k-k'} + \partial_\sigma \overline{Q}^{k-s} = \tilde{c}_k \delta_0. \end{aligned} \tag{2.21a}$$

Equation (2.17b): We put the ansatz (2.18b) and the ansatz (2.18c) in (2.17b). We can then separate in these equations the equations obeyed by the $\overline{R}^k$ and those obeyed by the R^k by using the property stated in Eq. (2.20).

We then obtain:

$$\begin{aligned}
-2l \le k \le -1 : \quad & -\mu \sum_{k'=0}^{k+2l} \tilde{c}_{k'} \partial_z^2 R^{k+2l-k'} = 0, \\
0 \le k \le s-l-1 : \quad & -\mu \sum_{k'=0}^{k+2l} \tilde{c}_{k'} \partial_z^2 R^{k+2l-k'} + R^k = 0, \\
s-l \le k : \quad & -\mu \sum_{k'=0}^{k+2l} \tilde{c}_{k'} \partial_z^2 R^{k+2l-k'} + R^k = -\theta_e' \partial_z R^{k-s+l},
\end{aligned} \tag{2.21b}$$

and

$$\begin{aligned}
0 \le k \le s-1 : \quad & -\mu \sum_{k'=0}^{k} \tilde{c}_{k'} \partial_\sigma^2 \overline{R}^{k-k'} + \overline{R}^k = 0, \\
s \le k : \quad & -\mu \sum_{k'=0}^{k} \tilde{c}_{k'} \partial_z^2 \overline{R}^{k-k'} + \overline{R}^k = -\partial_\sigma \overline{R}^{k-s}.
\end{aligned} \tag{2.21c}$$

Equation (2.17c): With (2.20) in mind, Eq. (2.17c) only tells us

$$0 \le k : \qquad \overline{R}^k(\pm\infty) = 0. \tag{2.21d}$$

Equation (2.17f): The continuity relation translates into

$$0 \le k : \qquad \overline{Q}^k(\pm 1) = \overline{R}^k(\pm 1) + R^k(\pm 1, 0). \tag{2.21e}$$

Equation (2.17g): The continuity of the derivative translates into (given that θ_e' is non zero):

$$0 \le k \le l-1 : \quad 0 = \partial_z R^k(\pm 1, 0), \tag{2.21f}$$

$$0 \le k : \qquad \partial_\sigma \overline{Q}^k(\pm 1) = \partial_\sigma \overline{R}^k(\pm 1) + \theta_e'(\pm 1) \partial_z R^{k+l}(\pm 1, 0). \tag{2.21g}$$

Equation (2.17h): Finally we get from Eq. (2.17h) the following constraints for the profile:

$$\begin{aligned}
k = 0 : \quad & \int_{-1}^{1} \overline{Q}^0(\sigma) \mathrm{d}\sigma + \frac{\tilde{c}_0}{\mu} = 1, \\
k > 0 : \quad & \int_{-1}^{1} \overline{Q}^k(\sigma) \mathrm{d}\sigma + \frac{\tilde{c}_k}{\mu} = 0.
\end{aligned} \tag{2.21h}$$

Influence of Eqs. (2.17d) *and* (2.17e): The two conditions (2.17d) and (2.17e) translate into the positivity of the lowest order term of the expansions (2.18a) and (2.18b). Moreover, by taking into account (2.19), this also means that the first nonzero $\tilde{c}_k$ must be positive.

2.5.3 Proof of Proposition 2.1

Now that we have the equations solved by the profiles, we can turn to the proof of Prop. th:ch2:necessary. We break it down into several steps.

Lemma 2.1. *If $\tilde{c}_0 \neq 0$ then all the R^k are necessarily zero (thus l is undefined).*

Proof. We argue by induction. Take $k = -2l$ in (2.21b) and $k = 0$ in (2.21f) and in (2.20). Then the problem solved by R^0 is

$$\begin{cases} \forall z > 0 \quad -\mu\tilde{c}_0\partial_z^2 R^0(\pm 1, z) = 0, \\ \qquad\qquad -\partial_z R^0(\pm 1, 0) = 0, \\ \qquad\qquad R^0(\pm 1, +\infty) = 0. \end{cases}$$

whose only solution is $R^0 = 0$. Now suppose $R^0, \cdots, R^{p-1}$ are identically 0 for $1 \leq p$. Then take $k = -2l + p$ in (2.21b). We find that R^p satisfies the equation

$$-\mu\tilde{c}_0\partial_z^2 R^p = 0,$$

i.e. $\partial_z^2 R^p = 0$. But since from (2.20) $\partial_z R^p \to 0$ as z tends to infinity then we find $\partial_z R^p = 0$ for all z. Then again $R^p \to 0$ at infinity and R^p is identically 0. □

Now we look at the other case when $\tilde{c}_0 = 0$.

Lemma 2.2. *If $\tilde{c}_0 = 0$ then necessarily*

1. *$\overline{R}^k$ is identically 0 (and thus so is $\overline{c}_k$) for all k,*
2. *$c_1, \ldots, c_{l-1}$ are 0 and c_l cannot be 0,*
3. *$R^0, \ldots, R^{l-1}$ are all identically zero.*

Proof. The first point is proved by induction. Taking (2.21c) for $k = 0$ gives

$$-\mu\tilde{c}_0\partial_z^2\overline{R}^0 + \overline{R}^0 = 0,$$

and since $\tilde{c}_0 = 0$ we have $\overline{R}^0 = 0$. The induction is then clear since all profile $\overline{R}^k$ will satisfy the same equation.

To prove the second point, introduce m the index of the first non zero c_k and suppose $0 \leq m \leq l - 1$. Then take (2.21b) with $k = m - l$ which is the first non trivially satisfied equation for the R^k. Since $m \leq l - 1$ then we have $m - l \leq -1$. Provide for this equation the boundary condition given by

(2.21f) with $k = 0$ and the property (2.20), and this leads to the following problem for R^0:

$$\begin{cases} \forall z > 0 \quad -\mu c_m \partial_z^2 R^0(\pm 1, z) = 0, \\ \qquad\qquad\qquad -\partial_z R^0(\pm 1, 0) = 0, \\ \qquad\qquad\qquad R^0(\pm 1, +\infty) = 0, \end{cases}$$

which can only be satisfied by the null function. All following R^k will then satisfy the same problem and be consequently 0 and thus so is R^m. This is contradictory since c_m is supposed to be nonzero and the integral of R^m..

Suppose now $m \geq l + 1$. Once again we argue by induction that all R^k are identically 0 which leads to a contradiction with $c_m \neq 0$. Take $k = 0$ in (2.21b) and you find that $R^0 = 0$ because all the coefficients in the sum are 0 due to the fact that the first index for which $\tilde{c}_k$ is non zero is $l + m$. Then suppose $R^0, \ldots, R^{p-1}$ are all identically zero and take $k = p$ in (2.21b). When we look at

$$\sum_{k'=0}^{p+2l} \tilde{c}_{k'} \partial_z^2 R^{p+2l-k'},$$

we see that if $k' \leq m+l-1$, then $\tilde{c}_{k'} = 0$, and if $k' \geq m+l$, then $p+2l-k' \leq p-(m-l)$, and thus $\partial_z^2 R^{p+2l-k'} = 0$, so that the sum is in fact 0. And if $p \geq 0$, then we can conclude $R^p = 0$.

Finally suppose $m = l$. By taking $k = 0$ in (2.21b) and in (2.21f) and then using the fact that we have $\tilde{c}_0 = \cdots = \tilde{c}_{2l-1} = 0$ we find that the problem solved by R^0 is

$$\begin{cases} \forall z > 0 \quad -\mu c_l \partial_z^2 R^0(\pm 1, z) + R^0(\pm 1, z) = 0, \\ \qquad\qquad\qquad\qquad -\partial_z R^0(\pm 1, 0) = 0, \\ \qquad\qquad\qquad\qquad R^0(\pm 1, +\infty) = 0, \end{cases}$$

which once again can only be solved by the null function. Argue by induction to find that $R^1, \ldots, R^{l-1}$ all satisfy the same problem as R^0 and are then identically 0 □

The fact that $\tilde{c}_{2l}$ is the first nonzero term of the expansion of ϕ is not surprising since in the equation of r you would want to balance the second order derivative with the zeroth order term to have an exponentially fast decay at infinity and when the coefficient in front of the second order derivative is of order y^α this can only be achieved if the boundary layer size is $y^{\alpha/2}$.

Now we complete the proof of the proposition.

Lemma 2.3. *If $\tilde{c}_0 \neq 0$ then the fundamental problem is well-posed if and only if $\mu > 1/2$. In this case s can be taken as one.*

Proof. Now we can look at the problem satisfied by $\overline{Q}^0$, $\overline{R}^0$ and $\overline{c}_0 = \tilde{c}_0$. We take $k = 0$ in (2.21a) and in (2.21c) and $k = -2l$ in (2.21b) for the equations and complete with the transmission condition from (2.21e) and (2.21g) with $k = 0$ and finally $k = 0$ in (2.21h). This leads to Problem (2.9) whose solution is given by (2.10).

Now we show that for $k = 1 + ns$ to $k = s - 1 + ns$ and for $n \geq 0$ the problem solved by $\overline{Q}^k$, $\overline{R}^k$, and $\overline{c}_k = \tilde{c}_k$ is solved by the trivial solution (0, 0, 0). We argue by induction on n. Let us look at the case $n = 0$. We argue by induction on k. The problem solved by $\overline{Q}^1$, $\overline{R}^1$, $\overline{c}_1$, is

$$\begin{cases} -\mu\bar{c}_0\partial_\sigma^2\overline{Q}^1 = \overline{c}_1\delta_0 + \mu\bar{c}_1\partial_\sigma^2\overline{Q}^0, \\ -\mu\bar{c}_0\partial_\sigma^2\overline{R}^1 + \overline{R}^1 = \mu\bar{c}_1\partial_\sigma^2\overline{R}^0, \\ \overline{Q}^1(\pm 1) = \overline{R}^1(\pm 1), \\ \partial_\sigma\overline{Q}^1(\pm 1) = \partial_\sigma\overline{R}^1(\pm 1), \\ \displaystyle\int_{-1}^{1} \overline{Q}^1(\sigma)\mathrm{d}\sigma + \frac{\overline{c}_1}{\mu} = 0. \end{cases}$$

Now using the fundamental problem we see that $\overline{c}_1\delta_0 + \mu\bar{c}_1\partial_\sigma^2\overline{Q}^0 = 0$. It is now clear that the trivial solution satisfies this problem. We can see now that for $k = 2, \cdots, s-1$, $\overline{Q}^k$, $\overline{R}^k$, $\overline{c}_k$ satisfies

$$\begin{cases} -\mu\bar{c}_0\partial_\sigma^2\overline{Q}^k = \overline{c}_k\delta_0 + \mu\bar{c}_k\partial_\sigma^2\overline{Q}^0 = 0, \\ -\mu\bar{c}_0\partial_\sigma^2\overline{R}^k + \overline{R}^k = \mu\bar{c}_k\partial_\sigma^2 Rb^0, \\ \overline{Q}^k(\pm 1) = \overline{R}^k(\pm 1), \\ \partial_\sigma\overline{Q}^k(\pm 1) = \partial_\sigma\overline{R}^k(\pm 1), \\ \displaystyle\int_{-1}^{1} \overline{Q}^k(\sigma)\mathrm{d}\sigma + \frac{\overline{c}_k}{\mu} = 0, \end{cases}$$

which is again satisfied by the trivial (0, 0, 0) solution. Now let us assume that we have proved our result for $n = 0, \cdots, p-1$. We prove that $\overline{Q}^{1+ps}$, $\overline{R}^{1+ps}$, $\overline{c}_{1+ps}$ is trivial. The other cases can be deduced by induction in the same fashion that in the $n = 0$ case. The equation solved by $\overline{Q}^{1+ps}$ is (2.21a) with $k = 1 + ps \geq s$ which is:

$$-\mu\sum_{k'}^{1+ps} \overline{c}_{k'}\partial_\sigma^2\overline{Q}^{1+ps-k'} + \partial_\sigma\overline{Q}^{1+ps-s} = \overline{c}_{1+ps}\delta_0.$$

Now $\overline{Q}^{1+(p-1)s}$ is identically 0 by hypothesis so $\partial_\sigma \overline{Q}^{1+ps-s}$ is zero. And if we consider the sum, the potentially non zero coefficients are $\overline{c}_0$, $\overline{c}_s$, ..., $\overline{c}_{ps}$ and also $\overline{c}_{1+ps}$. But for $k \geq 1$, $\overline{c}_{ks}$ is multiplied by $\partial_\sigma^2 \overline{Q}^{1+(p-k)s}$ which is zero by hypothesis. So the equation on $\overline{Q}^{1+ps}$ is really only:

$$-\mu \overline{c}_0 \partial_\sigma^2 \overline{Q}^{1+ps} = \overline{c}_{1+ps}\delta_0 + \mu \overline{c}_{1+ps} \partial_\sigma^2 \overline{Q}^0 = 0.$$

when using the fundamental problem. In the same way the equation in $\overline{R}^{1+ps}$ reduces to:

$$-\mu \overline{c}_0 \partial_\sigma^2 \overline{R}^{1+ps} + \overline{R}^{1+ps} = \mu \overline{c}_{1+ps} \partial_\sigma^2 \overline{R}^0,$$

which means that once again we can take $\overline{Q}^{1+ps} = 0$, $\overline{R}^{1+ps} = 0$ and thus $\overline{c}_{1+ps} = 0$. Finally only the multiples of s are potentially nonzero and we can minimize the number of equations by taking $s = 1$. □

The fact that we use the analytical solution of the fundamental problem seems contradictory to our intent not to compute solutions explicitly. But what we want to avoid is computing the analytical solution of the exact initial problem. We believe that it will be in our reach to do exact computations on the fundamental problem even in several space dimensions.

Lemma 2.4. *If $\tilde{c}_0 = 0$ and $2l \geq s$, then $\mu < 1/2$, and one can take $l = 1$ and $s = 2$.*

Proof. Since $\tilde{c}_0 = 0$, we know that we must have $c_l \neq 0$. Once again we look at the fundamental problem. Since $\overline{R}^0$ and R^0 are both zero, $\overline{Q}^0$ must vanish on the boundary of $[-1, 1]$. Finally with $\tilde{c}_0 = 0$, $\overline{Q}^0$ must be of integral 1. Now there are two possibilities. If $2l > s$ then the first non trivial equation featuring $\overline{Q}^0$ is for (2.21a) with $k = s$ and is simply $\partial_\sigma \overline{Q}^0 = 0$. This leads to a contradiction because $\overline{Q}^0$ would then be a constant which, given the boundary conditions, is 0, which is incompatible with the constraint. Thus we must have $2l = s$.

Then the equation on $\overline{Q}^0$ comes from (2.21a), $k = 2l$ and, sums up to System (2.12). Its solution is given by Eq. (2.13) and in particular we have $\mu < 1/2$.. We still have to see what l or s is. The first boundary profile to be non zero is R^l and it gives boundary conditions to the problem of $\overline{Q}^l$. It is then easy to see that to minimize the number of non trivial problems one can take $l = 1$ and thus $s = 2$. □

Lemma 2.5. *If $\tilde{c}_0 = 0$ and $2l + 1 \leq s$ then*

1. $\mu = 1/2$,

2. $l \geq 2$ *and* $2s = 5l$,

3. one can take $l = 2$ *and* $s = 5$.

Proof. If we are in the conditions of the lemma then the fundamental problem is System (2.15). We have the fundamental solution given by (2.16), but not c_l, and the most difficult part is to find the right boundary layer size and expansion scale. To do that, we compute the first non trivial boundary layer profile. We take $k = 2l$ in (2.21b) (at this point it does not matter if $2l$ is lower or greater than $s-l$ because all the R^k are zero for $k < l$) and boundary condition (2.21g) to find that R^l satisfies:

$$\begin{cases} -\mu c_l \partial_z^2 R^l(\pm 1, \cdot) + R^l(\pm 1, \cdot) = 0, \\ \partial_z R^l(-1, 0) = 1, \\ \partial_z R^l(1, 0) = 1. \end{cases}$$

whose solution is $R^l(\pm 1, z) = \sqrt{\mu c_l} \exp(-z/\sqrt{\mu c_l})$.

Now let us examine the equations (2.21a) obeyed by $\overline{Q}^p$. The first equation to have $\overline{Q}^p$ in a nontrivial manner is for $k = 2l + p$ because the first nontrivial $\tilde{c}_k$ is for $k = 2l$. In this equation there are two possible "external forces". First are the boundary conditions (2.21e). The first non zero boundary condition for a $\overline{Q}^k$ are for $k = l$. The second "external force" is the term of the form ∂_σ^{k-s}. The first $\overline{Q}^k$ to have a non trivial term of this form is when $k = s$ that is for the equation introducing $\overline{Q}^{s-2l}$.

It is easy to see by induction that for $1 \leq k \leq \min(s - 2l, l) - 1$ the $\overline{Q}^k$ are zero because they have no "external force" and they actually follow a linear equation (also (2.21h) gives the constraint $\int_{-1}^{1} \overline{Q}^k(\sigma) \mathrm{d}\sigma = 0$ as long as $1 \leq k \leq 2l - 1$ which is of course satisfied by a trivial $\overline{Q}^k$).

If we had $l < s - 2l$ then we would have $2l + l \leq s - 1$ and $\overline{Q}^l$ would satisfy the following problem:

$$\begin{cases} -\mu c_l \partial_\sigma^2 \overline{Q}^l = 0, \\ \overline{Q}^l(\pm 1) = R^l(\pm 1, 0), \\ \int_{-1}^{1} \overline{Q}^l(\sigma) \mathrm{d}\sigma = 0. \end{cases}$$

Since we have $R^l(1, 0) = R^l(-1, 0) = \sqrt{\mu c_l}$ we clearly have $\overline{Q}^l(\sigma) = \sqrt{\mu c_l}$, but this leads to a contradiction between $c_l \neq 0$ and $\int_{-1}^{1} \overline{Q}^l(\sigma) \mathrm{d}\sigma = 0$. This

means we must have $s-2l \leq l$ and thus the first term to have an external force is $\overline{Q}^{s-2l}$, whose equation is given by (2.21a) with $k=s$. This leads to $\overline{Q}^{s-2l}$ to satisfy the problem

$$\begin{cases} -\mu c_l \partial_\sigma^2 \overline{Q}^{s-2l} + \partial_\sigma \overline{Q}^0 = 0, \\ \overline{Q}^{s-2l}(\pm 1) = R^l(\pm 1, 0), & \text{if } s-2l = l, \\ \overline{Q}^{s-2l}(\pm 1) = 0, & \text{if } s-2l < l, \\ \displaystyle\int_{-1}^{1} \overline{Q}^{s-2l}(\sigma)\mathrm{d}\sigma = 0. \end{cases}$$

We now prove that $s-2l$ cannot be l. If it were we could decompose $\overline{Q}^{s-2l}$ into a sum $A+B$ by linearity where we have

$$\begin{cases} -\mu c_l \partial_\sigma^2 A = 0, \\ A(\pm 1) = R^l(\pm 1, 0), \end{cases}$$

and

$$\begin{cases} -\mu c_l \partial_\sigma^2 B = -\partial_\sigma \overline{Q}^0, \\ B(\pm 1) = 0. \end{cases}$$

Since $R^l(1,0) = R^l(-1,0) = \sqrt{\mu c_l}$ we once again have $A = \sqrt{\mu c_l}$. Now since we have $\partial_\sigma \overline{Q}^0$ odd we have that B is the sum of the odd primitive of $1/(\mu c_l)\overline{Q}^0$ and of an affine function and considering the boundary condition B is in fact odd. This put together leads to a contradiction since we should have

$$\begin{aligned} 0 = \int_{-1}^{1} \overline{Q}^{s-2l}(\sigma)\mathrm{d}\sigma &= \int_{-1}^{1} A(\sigma)\mathrm{d}\sigma + \int_{-1}^{1} B(\sigma)\mathrm{d}\sigma \\ &= 2\sqrt{\mu c_l}, \end{aligned}$$

with $c_l \neq 0$. Thus $s-2l < l$. From $2l+1 \leq s \leq 3l-1$ we get $l \geq 2$. And we have that the problem satisfied by $\overline{Q}^{s-2l}$ is well posed. We actually need $\overline{Q}^{s-2l}$. One can prove that it is the function

$$\sigma \mapsto \begin{cases} \dfrac{1}{c_l}\sigma(\sigma+1), & \text{if } \sigma \in [-1,0], \\ \dfrac{1}{c_l}\sigma(1-\sigma), & \text{if } \sigma \in [-1,0]. \end{cases}$$

But c_l is still not defined! We thus push the study to the following non zero term. From the "external force" point of view, the boundary condition still

drives $\overline{Q}^l$ first. For the derivative it is $\partial_\sigma \overline{Q}^{s-2l}$ which appears first in the equation (2.21a) with $k = 2s - 2l$ which gives the equation of $\overline{Q}^{2s-4l}$.

What we prove now is that both "external forces" need to be active simultaneously to have a well posed problem. This leads to $l = 2s - 4l$ which is equivalent to $2s = 5l$. If $l < 2s - 4l$ then the problem satisfied by $\overline{Q}^l$ is now

$$\begin{cases} -\mu c_l \partial_\sigma^2 \overline{Q}^l = \mu c_{4l-s} \partial_\sigma^2 \overline{Q}^{s-2l}, \\ \overline{Q}^l(\pm 1) = R^l(\pm 1, 0), \\ \displaystyle\int_{-1}^{1} \overline{Q}^l(\sigma) \mathrm{d}\sigma = 0. \end{cases}$$

Since $\overline{Q}^{s-2l}$ is odd this "external force" does not contribute to the integral constraint. Moreover we can still lift the boundary condition with the constant function $\sqrt{\mu c_l}$. This leads to a contradiction between the integral vanishing and c_l being non zero. On the other hand if $2s - 4l < l$, then the problem solved by $\overline{Q}^{2s-4l}$ is

$$\begin{cases} -\mu c_l \partial_\sigma^2 \overline{Q}^{2s-4l} = \mu c_{s-l} \partial_\sigma^2 \overline{Q}^{s-2l} - \partial_\sigma \overline{Q}^{s-2l}, \\ \overline{Q}^{2s-4l}(\pm 1) = 0, \\ \displaystyle\int_{-1}^{1} \overline{Q}^{2s-4l}(\sigma) \mathrm{d}\sigma = 0. \end{cases}$$

Once again, $\partial_\sigma^2 \overline{Q}^{s-2l}$ being odd, $\displaystyle\int_{-1}^{1} \overline{Q}^{2s-4l}(\sigma) \mathrm{d}\sigma$ by linearity is really only $\displaystyle\int_{-1}^{1} C(\sigma) \mathrm{d}\sigma$ where C solves:

$$\begin{cases} -\mu c_l \partial_\sigma^2 C = -\partial_\sigma \overline{Q}^{s-2l}, \\ C(\pm 1) = 0. \end{cases}$$

If we multiply the equation for C by $(\sigma^2 - 1)/2$ and integrate twice by parts we find :

$$\mu c_l \int_{-1}^{1} C(\sigma) \mathrm{d}\sigma = -\int_{-1}^{1} \overline{Q}^{s-2l}(\sigma) \sigma \mathrm{d}\sigma.$$

Now using the expression of $\overline{Q}^{s-2l}$ one finds $\displaystyle\int_{-1}^{1} C(\sigma) \mathrm{d}\sigma = 1/(3c_l^2)$ and this cannot be 0. We then necessarily have $2s - 4l = l$ that is $2s = 5l$. It is left to the reader to see that $s = 5$ and $l = 2$ lead to the minimum of non trivial

profiles. One also finds that c_l satisfies the following equation,

$$2\sqrt{\mu c_l} - \frac{1}{3c_l^2} = 0$$

which leads to $c_l = 1/(3\sqrt{2})^{2/5}$. □

2.6 Justification of the Formal Expansions

2.6.1 Reformulation as a Two Parameter Problem

We shall now give a rigorous proof that the behavior of (2.17a)–(2.17h) is the one described by Theorem 2.1. For this, we first rewrite the system in new variables. We then explain the argument of the proof using some technical assumptions. We finally check that these assumptions are true (unique solvability of the fundamental problem, analyticity and derivatives of the implicit function).

Reformulation Through New Parameters. A crucial step in the analysis is to rewrite the system with new variables: instead of having y and ϕ we set

$$a = \frac{y}{\phi} \qquad \text{and } b = \sqrt{\phi}.$$

Let us remark that this kind of change of variable was also necessary in our previous paper [53] in order to study the behavior near the singularity $(y, \phi) = (0, 0)$. However, y and ϕ have clear physical meaning (the first is a shear rate, the second is the fluidity). We then define from the solution p the functions

$$\begin{aligned} q &= p_{|}[-1, 1], \\ r_d(\theta) &= p(1 + b\theta), && \text{for } \theta > 0, \\ r_g(\theta) &= p(-1 - b\theta), && \text{for } \theta > 0. \end{aligned}$$

In these variables Eq. 2.1 can be written:

$$-\partial_\sigma^2 q + a\partial_\sigma q = \frac{1}{\mu}\delta_0, \qquad \text{in }]-1,1[, \tag{2.22a}$$

$$-\partial_\theta^2 r_g - ab\partial_\theta r_g + r_g = 0, \qquad \text{in }]0,\infty[, \tag{2.22b}$$

$$-\partial_\theta^2 r_d + ab\partial_\theta r_d + r_d = 0, \qquad \text{in }]0,\infty[, \tag{2.22c}$$

$$r(\pm\infty) = 0, \tag{2.22d}$$

$$q \geq 0, \tag{2.22e}$$

$$r \geq 0, \tag{2.22f}$$

$$r_g(0) = q(-1), \tag{2.22g}$$

$$r_d(0) = q(1), \tag{2.22h}$$

$$-\partial_\theta r_g(0) = b\partial_\sigma q(-1), \tag{2.22i}$$

$$\partial_\theta r_d(0) = b\partial_\sigma q(1), \tag{2.22j}$$

$$b\int_0^{+\infty} r_g(\theta)\mathrm{d}\theta + b\int_0^{+\infty} r_d(\theta)\mathrm{d}\theta + \int_{-1}^{1} q(\sigma)\mathrm{d}\sigma = 1. \tag{2.22k}$$

A major advantage of this formulation is that the reformulated problem no longer is of a singularly perturbed nature. This is the deeper reason why in the formal expansion of the previous section there was never any true two-parameter series; either all the R^k or all the $\bar{R}^k$ were zero. In several dimensions, the singularly perturbed nature of the problem cannot be removed by a mere rescaling of the independent variable, and this will complicate the analysis. In particular, analyticity of the solution with respect to a and b as shown below cannot be expected.

Proof of Theorem 2.1. In terms of the two parameter expansion, the three cases encountered in the previous section are as follows:

1. $\mu > 1/2$: $a \to 0$, $b \to b_0 > 0$.
2. $\mu < 1/2$: $b \to 0$, $a \to a_0 > 0$.
3. $\mu = 1/2$: Both a and b tend to 0 and b is of the same order as a^2.

The structure of our argument essentially proceeds as follows: First we show that if either a or b is close to 0, we can solve the system (2.22a)-(2.22j) uniquely for q, r_d and r_g as functions of μ, a and b. The remaining equation (2.22k) is then of the form $F(\mu, a, b) = 0$. The function F depends analytically on its arguments.

Case $\mu > 1/2$. We can show that $\partial F/\partial b(0, b_0, \mu) \neq 0$, hence we solve the equation $F = 0$ for b: $b = g(\mu, a)$. In terms of y this reads $\sqrt{\phi(y)} =$

$g(\mu, y/\phi(y))$. We can now use the implicit function theorem again to solve for ϕ as an analytical function of y.

Case $\mu < 1/2$. We can show that $\partial F/\partial a(a_0, 0, \mu) \neq 0$, and hence solve for a: $a = g(\mu, b)$. In terms of the original variables, this reads $y = \phi(y)g(\mu, \sqrt{\phi(y)})$. We can now apply another implicit function argument to solve for $\sqrt{\phi(y)}$ as an analytical function of $\sqrt{y}$; the leading order term is $\sqrt{\phi(y)} \sim \sqrt{y/g(\mu, 0)} = \sqrt{y/a_0}$.

Case $\mu = 1/2$. For μ near $1/2$, we can solve F uniquely for μ: $\mu - 1/2 = g(a, b)$. This confirms that $\mu = 1/2$ is the only case in which $a = b = 0$. We shall show that, to leading order $g(a, b) = c_1 b - c_2 a^2$ with positive constants c_1 and c_2. Thus, at $\mu = 1/2$, we have a balance of b and a^2. If we fix μ at $1/2$, we can solve for b in terms of a:

$$b = \gamma_2 a^2 + \gamma_3 a^3 + ..., \qquad \gamma_2 = c_2/c_1.$$

Now we substitute $b = \beta y^{2/5}$, leading to $a = \beta^{-2} y^{1/5}$. We find the following new equation for β:

$$\beta = \gamma_2/\beta^4 + \gamma_3 y^{1/5}/\beta^6 + ...$$

Another implicit function argument shows that β is an analytical function of $y^{1/5}$, with leading term $\beta \sim (\gamma_2)^{1/5}$.

2.6.2 The Fundamental Problems

We are now exhibiting the three fundamental solutions we will perturb; that is, we will uniquely solve (2.22a)–(2.22j) for specific sets of the parameters (μ, a, b). Of course we will find the three fundamental problems (2.12), (2.10) and (2.15) rewritten in the new variables (without satisfying the integral constraint yet).

Set $a = 0$ in the previous equations and let us find μ and b that satisfy the equations. We can solve the ODEs and use the various constraints to set the integration constants. This leads to

$$\begin{aligned} q^{\mu,0,b}(\sigma) &= \begin{cases} \dfrac{1}{2\mu}(\sigma+1) + \dfrac{b}{2\mu}, & \text{if } \sigma \in]-1, 0[, \\ \dfrac{1}{2\mu}(1-\sigma) + \dfrac{b}{2\mu}, & \text{if } \sigma \in]0, 1[, \end{cases} \\ r_g^{\mu,0,b}(\theta) &= \frac{b}{2\mu} \exp(-\theta), \\ r_d^{\mu,0,b}(\theta) &= \frac{b}{2\mu} \exp(-\theta). \end{aligned} \tag{2.23}$$

This indeed gives back (2.10) when one sets $b = \sqrt{\mu \overline{c}_0}$.

On the other hand set $b = 0$. Then the equations of q on one hand and r_g, r_d on the other hand decouple. We can set $r_g = r_d = 0$ by linearity and this makes the problem set on the interval $[-1, 1]$ only, with homogeneous Dirichlet boundary conditions. This leads to

$$\begin{aligned} q^{\mu,a,0}(\sigma) &= \begin{cases} \dfrac{1-\exp(-a)}{\mu a(\exp(a)-\exp(-a))}\left(\exp(a(\sigma+1))-1\right), & \text{if } \sigma \in]-1,0[, \\ \dfrac{\exp(a)-1}{\mu a(\exp(a)-\exp(-a))}\left(1-\exp(a(\sigma-1))\right), & \text{if } \sigma \in]0,1[, \end{cases} \\ r_g^{\mu,a,0} &= 0, \\ r_d^{\mu,a,0} &= 0. \end{aligned} \tag{2.24}$$

We find (2.13) again when $a = 1/(\mu c_1)$. Finally, taking the limit $b \to 0$ in the first case or $a \to 0$ in the second one leads to the same solution for $a = b = 0$

$$q^{\mu,0,0}(\sigma) = \begin{cases} \dfrac{1}{2\mu}(\sigma+1), & \text{if } \sigma \in]-1,0[, \\ \dfrac{1}{2\mu}(1-\sigma), & \text{if } \sigma \in]0,1[, \end{cases}$$

which gives back (2.16) when we set $\mu = 1/2$.

2.6.3 Unique Solvability of the ODE system

We define the weighted Sobolev space

$$H^s_\epsilon(0,\infty) = \{u \mid \exp(\epsilon\theta)u(\theta) \in H^s(0,\infty)\}.$$

We fix a small $\epsilon > 0$, and we seek solutions (q, r_d, r_g) in $H^1(-1,1)\times(H^1_\epsilon(0,\infty))^2$. We can get rid of the weight $\exp(\epsilon\theta)$ by setting $r_{g,d} = \exp(-\epsilon\theta)s_{g,d}$. Moreover, we isolate the singularity of q at the origin by setting $\tilde{q}(\sigma) = q(\sigma) - (1-|\sigma|)/(2\mu)$. This leads to the new system

$$-\partial_\sigma^2\tilde{q} + a\partial_\sigma\tilde{q} = \frac{a}{2\mu}\operatorname{sign}\sigma \qquad \text{in }]-1,1[, \tag{2.25a}$$

$$-\partial_\theta^2 s_g - (ab-2\epsilon)\partial_\theta s_g + (1-\epsilon^2+ab\epsilon)s_g = 0 \qquad \text{in }]0,\infty[, \tag{2.25b}$$

$$-\partial_\theta^2 s_d + (ab-2\epsilon)\partial_\theta s_d + (1-\epsilon^2-ab\epsilon)s_d = 0 \qquad \text{in }]0,\infty[, \tag{2.25c}$$

$$s_g(0) = \tilde{q}(-1), \tag{2.25d}$$

$$s_d(0) = \tilde{q}(1), \tag{2.25e}$$

$$-\partial_\theta s_g(0) + \epsilon s_g(0) = b\partial_\sigma\tilde{q}(-1) + b/(2\mu), \tag{2.25f}$$

$$\partial_\theta s_d(0) - \epsilon s_d(0) = b\partial_\sigma\tilde{q}(1) - b/(2\mu). \tag{2.25g}$$

We now look for solutions in the function space

$$X = \{(\tilde{q}, s_d, s_g) \in H^2(-1,1)\times(H^2(0,\infty))^2 / \; s_g(0)-\tilde{q}(-1) = 0, s_d(0)-\tilde{q}(1) = 0\}.$$

Define Y as

$$Y = L^2(-1,1) \times (L^2(0,\infty))^2 \times (\mathbb{R})^2.$$

We define the operator $\mathcal{L}_{\varepsilon,a,b}$ from X to Y by

$$\begin{aligned}\mathcal{L}_{\varepsilon,a,b}(\tilde{q}, s_d, s_g) \;=\; & (-\tilde{q}'' + a\tilde{q}',\\ & -s_g'' - (ab-2\epsilon)s_g' + (1-\epsilon^2+ab\epsilon)s_g,\\ & -s_d'' + (ab-2\epsilon)s_d' + (1-\epsilon^2-ab\epsilon)s_d,\\ & -s_g'(0) + \epsilon s_g(0) - b\tilde{q}'(-1),\\ & s_d'(0) - \epsilon s_d(0) - b\tilde{q}'(1)).\end{aligned}$$

Let us note $E = \mathbf{R}\times\{0\}\cup\{0\}\times\mathbf{R}_+$. We claim the following Proposition.

Proposition 2.2.
- *For every $(a_0, b_0) \in E$ there exists an $\varepsilon_0 > 0$ and a neighborhood $\mathcal{V}$ of (a_0, b_0) in $\mathbf{R}\times\mathbf{R}_+$ such that for any $(\varepsilon, a, b) \in [0, \varepsilon_0[\times\mathcal{V}$ the operator $\mathcal{L}_{\varepsilon,a,b}$ is invertible.*
- *The mapping $(\mu, a, b) \mapsto (q^{\mu,a,b}, r_g^{\mu,a,b}, r_d^{\mu,a,b})$ is analytic.*

.

Proof. For the proof of the first point, it clearly suffices to consider $\epsilon = 0$ and either $a = 0$ or $b = 0$; the rest follows from analytic perturbation theory (see for instance KATO[43, ch VII, p. 365]). Indeed, because we removed the singularity at 0, $\mathcal{L}_{\varepsilon,a,b}$ is a bounded operator from X to Y. Moreover, for any $(\tilde{q}, s_d, s_g)$ in X and f in Y^*, $\langle f, \mathcal{L}_{\varepsilon,a,b}(\tilde{q}, s_d, s_g)\rangle_{Y^*,Y}$ is a polynomial in (ε, a, b) and thus $\mathcal{L}_{\varepsilon,a,b}$ is analytic as an operator.

If $\epsilon = b = 0$, the problems for $\tilde{q}$, s_g and s_d decouple, and the decoupled problems are easy to analyze: we solve elliptic ODEs with inhomogeneous Neumann boundary conditions for s_g and s_d and then use the values $s_g(0)$ and $s_d(0)$ in the boundary conditions for $\tilde{q}$. Now, let $\epsilon = a = 0$, $b > 0$. Note that for $(\tilde{q}, s_d, s_g) \in X$ we have the following Poincaré-type estimate:

$$\int_{-1}^{1} \tilde{q}(\sigma)^2 \mathrm{d}\sigma \le 4\int_{-1}^{1} (\tilde{q}'(\sigma))^2 \mathrm{d}\sigma + 4\int_0^{+\infty} (s_g'(\theta))^2 + s_g(\theta)^2 \mathrm{d}\theta.$$

It is then easily checked that the following elliptic estimate is true:

$$\int_{-1}^{1} (\tilde{q}'(\sigma))^2 \, d\sigma + \frac{1}{b}\int_0^{\infty} (s_g'(\theta))^2 + s_g(\theta)^2 + (s_d'(\theta))^2 + s_d(\theta)^2 \, \mathrm{d}\theta \le C \, \|f\|_Y^2 \, .$$

The operator $\mathcal{L}_{0,0,b}$ is then invertible by standard arguments using Lax-Milgram Theorem and regularity of elliptic operators.

The second point uses the fact that $\mathcal{L}^{-1}_{\varepsilon,a,b}$, as a function of a and b, is analytic, so is

$$(\mu, a, b) \mapsto (\frac{a}{2\mu} \operatorname{sign} \sigma, 0, 0, 0, 0, \frac{b}{2\mu}, -\frac{b}{2\mu}),$$

and finally so are the various change of variables. □

2.6.4 Derivatives of F

We now set

$$F(\mu, a, b) = \int_{-1}^{1} q(\sigma)\, d\sigma + b \int_0^\infty r_g(\theta)\, d\theta + b \int_0^\infty r_d(\theta)\, d\theta,$$

where q, r_d and r_g have been determined as solutions of the ODE system as discussed in the previous subsection.

If $a = 0$, we compute, using (2.23),

$$F(\mu, 0, b) = \frac{b + b^2}{\mu} + \frac{1}{2\mu}.$$

A nonnegative solution b_0 of the equation $F(\mu, 0, b_0) = 1$ exists if and only if $\mu \geq 1/2$. Moreover, we find

$$\begin{aligned} \frac{\partial F}{\partial b}(\mu, 0, b_0) &= \frac{1 + 2b_0}{\mu} > 0, \\ \frac{\partial F}{\partial \mu}(\mu, 0, b_0) &= -\frac{F(\mu, 0, b_0)}{\mu} = -\frac{1}{\mu} < 0. \end{aligned}$$

If $b = 0$, we calculate, using (2.24),

$$F(\mu, a, 0) = \frac{\tanh(a/2)}{a\mu}. \tag{2.26}$$

As a varies, this function decreases monotonically from a limit of $1/(2\mu)$ at $a = 0$ to zero as $a \to \infty$. Hence the equation $F(\mu, a_0, 0) = 1$ has a solution a_0 if and only if $\mu \leq 1/2$. The derivative $\partial F/\partial a(\mu, a, 0)$ is negative for $a > 0$, but $\partial F/\partial a(\mu, 0, 0) = 0$. Moreover, we find

$$\frac{\partial^2 F}{\partial a^2}(\mu, 0, 0) = -\frac{1}{12\mu} < 0. \tag{2.27}$$

This verifies all the sign properties of derivatives of F claimed above.

Chapitre 3

Comportement du modèle d'Hébraud-Lequeux à fort taux de cisaillement

Résumé du chapitre

Ce chapitre pourrait être considéré comme le pendant du chapitre 2 mais c'est en réalité son descendant. En effet, nous considérons le modèle d'Hébraud-Lequeux (3.1) mais cette fois dans la limite $y \to +\infty$. Nous choisissons l'approche du chapitre 2 qui consiste à chercher un développement asymptotique de p en fonction de $\varepsilon = 1/y$ pour en déduire par simple intégration un développement de la contrainte τ définie en fonction de p par (3.4). Le résultat «physique» du chapitre est l'équivalent de la contrainte donné dans le théorème 3.2 mais, de nouveau, l'énoncé existait déjà dans l'article d'Hébraud et Lequeux [37]. L'intérêt de ce chapitre est donc la démonstration de ce résultat *via* la proposition 3.1.

Du point de vue mathématique, la différence avec le chapitre 2 est que, d'une part, la singularité de la limite apparaît explicitement à travers le terme $(1/\varepsilon)\partial_\sigma p$ mais que, d'autre part, il n'y a plus de distinction à faire suivant la valeur de μ. C'est la traduction mathématique d'un phénomène physique général sur les matériaux vitreux : lorsque le matériau est suffisamment cisaillé il finit par s'écouler de façon newtonienne, indépendamment de sa température. La limite singulière est problématique car, à la limite, on devrait trouver p constant, et étant donné que p doit décroître à l'infini, p nul,. Ceci est bien évidemment incompatible avec la condition d'intégrale qui apparaît dans (3.1). Il faut donc travailler sans limite mais uniquement avec des équivalents qui ne passent pas à la limite. Ces difficultés sont cependant assez

classiques. En revanche, il faut, comme dans le chapitre 2, traiter l'interaction entre Γ et p qui existe à travers la condition d'intégrale prescrite. Ceci permet de trouver un développement asymptotique formel pour la solution p et pour Γ.

Nous avons opté dans ce chapitre pour une justification «classique» du développement asymptotique formel, qui consiste à étudier le problème vérifié par le reste, c'est-à-dire la différence entre la solution exacte et son asymptotique formelle. Nous avons en effet pensé que pour l'étude du modèle plus compliqué du chapitre 4, la méthode de perturbation analytique employée dans le chapitre 2 pourrait ne pas s'appliquer, faute de solutions assez fortes au modèle. La méthode d'analyse des restes, que nous employons ici, a des chances d'être plus versatile mais ne donne à l'évidence que des développements tronqués et non des séries convergentes. Ce qui est compliqué dans le cas du modèle d'Hébraud-Lequeux, c'est d'étudier le reste du développement de Γ. Pour lever cette difficulté, l'idée est de découpler l'équation différentielle de la contrainte. On obtient alors un système différentiel non contraint et on peut créer une fonction continue F, dont les racines donnent implicitement le paramètre de reste. On montre alors que F a une racine dans un intervalle contrôlé en fonction de ε par la perturbation singulière du système découplé. Ce chapitre contient donc bien *deux* analyses de perturbation singulière d'équation différentielle.

Ce chapitre est tiré d'un article soumis pour un numéro spécial de *Science China Mathematics*, dans le cadre de la *French-Chinese Summer School* sur *les effets de tenseur de contraintes sur les fluides*.

3.1 Introduction

We are interested in the behaviour at large shear rates of the Hébraud-Lequeux model (referred to as HL in the sequel for brevity), derived by Hébraud and Lequeux in [37]. This model is a Fokker-Planck-like model which aims at describing the behaviour of a generic soft glassy material. This model has been studied by various authors, both in its nonstationary version and its stationary one. One can cite Cancès, Catto and Gati [16] for a PDE approach of the well-posedness and Ben Alaya and Jourdain [5] for a stochastic analysis of the Cauchy problem. The well-posedness of the stationary problem has been adressed in [16] and [53]. The study of the glass transition in this model has been conducted in [53] with a direct approach which is very specific to the $1d$ setting of the HL model and was revisited in [54] with a more robust method on which this paper is modelled. The need for a robust approach to this question arise when we try to justify a multidimensional model generalizing the one of Hébraud and Lequeux in [55].

Let us now review the description of the HL model. In this model the state of a sample of the material undergoing a shear rate $\dot{\gamma}$ is described by means of a probability density p over the stress space. The stress of the sample is noted τ. Because of the elastoviscoplastic nature of soft glassy material, when submitted to a shear rate, we expect it to have a transitory phase followed by a sationary phase. The HL model can handle both regimes but we will be interested only on the final stationary phase. In this phase, p is a probability density which follows the following dimensionless equation:

$$\begin{cases} -\mu\Gamma\partial_\sigma^2 p + hp + y\partial_\sigma p = \Gamma\delta_0, \\ \displaystyle\int_{\mathbf{R}} p(\sigma)\mathrm{d}\sigma = 1, \\ p \geq 0, \end{cases} \tag{3.1}$$

where h stands for the characteristic function of the set $\mathbf{R} \setminus [-1, 1]$. The term δ_0 is the Dirac mass. The parameter y is a dimensionless shear rate $\dot{\gamma}/\dot{\gamma}_c$ where $\dot{\gamma}_c$ is a critical shear rate depending on the material. The positive real number μ is a material dimensionless constant describing the material with respect to the glass transition.

In [54] we proved that when the shear rate is small, that means when $y \ll 1$ we can get various behaviour for the model depensing on the value of μ. More precisely, we proved that when $\mu > 1/2$ the behaviour of the model is at main order the behaviour of a Newtonian fluid, when $\mu < 1/2$ the behaviour is the one of a threshold fluid of Hershell-Bulkley type and

when $\mu = 1/2$ we have a power-law fluid with exponent $1/5$. In the present paper we are interested in the large shear rate behaviour of the fluid, that is to say $y \gg 1$ and we will prove that the behaviour is the one of a Newtonian fluid independently of the value of μ, which is the experimental behaviour expected for soft glassy materials (see for instance Oswald [57]).

Finally Γ is called the *fluidity* and is related to the integral constraint $\int p = 1$. We can see by integrating the differential equation that

$$\Gamma = \int_{|\sigma|>1} p(\sigma)\mathrm{d}\sigma. \tag{3.2}$$

Because p is a probability density, Γ is none other than the probability to find $|\sigma| > 1$ and thus

$$0 \leq \Gamma \leq 1. \tag{3.3}$$

The stress of a sample of material in this model is recovered by

$$\tau = \int_{\mathbf{R}} \sigma p(\sigma)\mathrm{d}\sigma. \tag{3.4}$$

Our aim is to study the link between y, which is given, and τ, which is computed *via* (3.4) where p is the solution of (3.1). We have already done so in the limiting case $y \to 0$ in another paper [54] (with M. Renardy) and wish to understand the other limiting case $y \to +\infty$. For the sequel of the paper we note $y = 1/\varepsilon$.

We are thus interested in the behaviour of an elliptic ODE with a perturbation of the form $\partial_\sigma p/\varepsilon$. This problem often arises in the study of the asymptotic behaviour of various models. One can refer for instance to the vanishing Rossby number approximation in oceanography as described in Chemin, Desjardins, Gallagher and Grenier [22]. What is specific in our model is first that it is set in an unbounded domain while the singular limits we mentionned are set in bounded domains. The consequence is that, if we try to take the naïve limit $\varepsilon \to 0$, we end up with the limit equation $\partial_\sigma p = 0$ which has only 0 as a solution on an unbounded domain. This limit is not very rich to describe the limiting behaviour of the model. Moreover, the second specific feature of our model is that we have $\int p = 1$ which is true for all $\varepsilon > 0$ and must remain true at the limit. This is clearly incompatible with the naïve limit $p = 0$ that we just mentionned. This difficulty is related to the fact that, despite appearances, our problem is truly nonlinear and the integral constraint makes System (3.1) quite rigid.

To overcome these difficulties we must describe the solution of (3.1) more accurately than with just the naïve limit. This is why we decompose the

solution into three parts corresponding to the intervals $]-\infty,0[$, $]0,1[$ and $]1,+\infty[$ completed with transmission conditions at 0 and 1 which are given by the expected global regularity of the solution of (3.1). We will see that these three parts behave very differently when $\varepsilon \to 0$. The situation is a bit different from the limit $y \to 0$ we studied in [54] for which we divided in $]-\infty,-1[$, $]-1,1[$ and $]1,+\infty[$ in order to study the passage from a density with support in $\mathbf{R}$ to a density with support in $]-1,1[$.

To conlude this introduction we would also like to point out that we used here a standard method of *a priori* estimates on the remainder of the expansion of p to prove the "convergence" while in [54] we took advantage of the $1d$ setting to use the singular perturbation theory of KATO [43] and get directly the convergence of the asymptotic expansion. The method used in this paper can, however, be extended fairly straightforwardly, to multi dimensional version of the HL model.

3.2 Main Results

Let us first recall the well-posedness theorem on which the sequel of the study relies on:

Theorem 3.1. *The stationary Hébraud-Lequeux model,*

$$\begin{cases} -\mu\Gamma\partial_\sigma^2 p + hp + \dfrac{1}{\varepsilon}\partial_\sigma p = \Gamma\delta_0, \\ \displaystyle\int_{\mathbf{R}} p(\sigma)\mathrm{d}\sigma = 1, \end{cases} \tag{3.5}$$

has a unique solution $p \in \mathrm{H}^1(\mathbf{R})$ which decays exponentially when $|\sigma| \to +\infty$, for every $\varepsilon > 0$.

For the proof we refer to [16, 53]. We can now state the main result of this paper:

Theorem 3.2. *Let us note p the solution to (3.5) and τ given by (3.4) then for $\varepsilon \to 0$ we have*

$$\tau \sim \frac{1}{\varepsilon},$$

or more precisely

$$\tau = \frac{1}{\varepsilon} + \mathcal{O}(1).$$

For the material, this means that when the shear rate is large the rheological law is at main order the law of Newtonian fluid with a viscosity independent of μ. This theorem is the main goal of this paper but it will need some intermediate results. The main idea which we have already used in [54] is to work directly on p instead of working on τ. For p we have the following asymptotic result:

Proposition 3.1. *The solution p to the HL problem given by Theorem 3.1 can be expanded when $\varepsilon \to 0$ as $p = p^{\mathrm{app}} + p^{\mathrm{rem}}$,where p^{app} has the following expression:*

$$p^{\mathrm{app}} = \begin{cases} \varepsilon \exp\left(\dfrac{\sigma}{\mu\varepsilon}\right) & \text{if } \sigma \leq 0, \\ \varepsilon & \text{if } 0 \leq \sigma \leq 1, \\ \varepsilon \exp\left(-\varepsilon(\sigma - 1)\right) & \text{if } 1 \leq \sigma, \end{cases} \tag{3.6}$$

and p^{rem} verifies the following estimations:

$$\left\| \exp\left(-\frac{\cdot}{2\mu\varepsilon}\right) p^{\mathrm{rem}} \right\|_{\mathrm{L}^2(-\infty,0)} = \mathcal{O}(\varepsilon^{5/2}), \tag{3.7}$$

$$\|p^{\mathrm{rem}}\|_{\mathrm{L}^2(0,1)} = \mathcal{O}(\varepsilon^{3/2}), \tag{3.8}$$

$$\left\| \exp\left(\frac{\varepsilon}{2}(\cdot - 1)\right) p^{\mathrm{rem}} \right\|_{\mathrm{L}^2(1,+\infty} = \mathcal{O}(\varepsilon^{3/2}). \tag{3.9}$$

This asymptotic expansion relies on the following estimation on Γ:

Lemma 3.1. *The following expansion of the fluidity Γ is true:*

$$\Gamma = 1 + \mathcal{O}(\varepsilon). \tag{3.10}$$

This lemma only requires p^{app}. The scheme of proof is then the following:

1. Compute formally the main order of p, p^{app} and the remainder problem (3.25).
2. Prove Proposition 3.1 assuming Lemma 3.1. This Justifies the formal asymptotic expansion and also gives estimation on the remainder p^{rem}.
3. Prove Theorem 3.2.
4. Prove Lemma 3.1.

The organization of the paper follows the scheme of proof: we carry out the formal expansions in Section 3.3 and give the remainder problem in Section 3.4. Then we prove Estimations (3.7)-(3.8) assuming Lemma 3.1.

Then we use the estimations obtained to prove the Theorem in Section 3.5. Then to complete the proof we show Lemma 3.1 in Section 3.6. We prefered to delay the proof of Lemma 3.1 because it is a bit long and we did not wish to interrupt the proof of Theorem 3.2.

3.3 Formal Expansions

Since we are interested in what happens to the system when y is large, we set $y = 1/\varepsilon$ and study the behaviour as $\varepsilon \to 0^+$. As we did before for the low shear rate asymptotics, we use asymptotic expansions on p instead of working directly on τ. We get these asymptotics in a suitable space so that we can go from p to τ just by integrating the expansion of p against σ.

3.3.1 Rewriting of the System

We are interested in the limit behaviour as $\varepsilon \to 0$ of the model given by (3.5):

$$\begin{cases} -\mu\Gamma\partial_\sigma^2 p + hp + \dfrac{1}{\varepsilon}\partial_\sigma p = \Gamma\delta_0, \\ \displaystyle\int_{\mathbf{R}} p(\sigma)\mathrm{d}\sigma = 1. \end{cases} \tag{3.11}$$

For this study we have to rewrite the equations in terms of what happens on $\mathbf{R}_-^*$,$[0,1]$ and $]1,+\infty[$. We note

$$p_- = p_{|\mathbf{R}_-^*}, \qquad p_{+,i} = p_{|[0,1]} \qquad p_{+,e} = p_{|[1,+\infty[}.$$

We rewrite this system in terms of these new variables:

$$\begin{cases} -\mu\Gamma\partial_\sigma^2 p_- + hp_- + \dfrac{1}{\varepsilon}\partial_\sigma p_- = 0, \\ -\mu\Gamma\partial_\sigma^2 p_{+,i} + \dfrac{1}{\varepsilon}\partial_\sigma p_{+,i} = 0, \\ -\mu\Gamma\partial_\sigma^2 p_{+,e} + p_{+,e} + \dfrac{1}{\varepsilon}\partial_\sigma p_{+,e} = 0, \\ p_{+,i}(0) = p_-(0), \\ p_{+,e}(1) = p_{-,i}(1), \\ \partial_\sigma p_{+,i}(0) = \partial_\sigma p_-(0) - \dfrac{1}{\mu}, \\ \partial_\sigma p_{+,e}(1) = \partial_\sigma p_{+,i}(1), \\ \displaystyle\int_{-\infty}^0 p_-(\sigma)\mathrm{d}\sigma + \int_0^1 p_{+,i}(\sigma)\mathrm{d}\sigma + \int_1^{+\infty} p_{+,e}(\sigma)\mathrm{d}\sigma = 1. \end{cases} \tag{3.12}$$

Transmission conditions

$$p_{+,i}(0) = p_-(0),$$
$$p_{+,e}(1) = p_{-,i}(1),$$

come from the fact that p is continuous. The condition

$$\partial_\sigma p_{+,i}(0) = \partial_\sigma p_-(0) - \frac{1}{\mu},$$

takes into account the Dirac mass at 0 while the last transmission condition

$$\partial_\sigma p_{+,e}(1) = \partial_\sigma p_{+,i}(1),$$

comes from the fact that we assume $\partial_\sigma p$ to be continuous at 1 (nothing in (3.5) could balance a jump in the derivative at 1). Now we change variables to find the right profiles equation. We set

$$p_-(\sigma) = q_-\left(\frac{\sigma}{\varepsilon}\right), \qquad p_{+,i}(\sigma) = q_{+,i}(\sigma) + q_{bl}\left(\frac{1-\sigma}{\varepsilon}\right),$$
$$p_{+,e}(\sigma) = q_{+,e}(\varepsilon(\sigma-1)),$$

and we note z the variable of q_-,q_{bl} and $q_{+,e}$ (and also the one of $q_{+,i}$ for simplicity). As q_{bl} describes a boundary layer in the neighbourhood of $\sigma = 1$ we assume exponential decrease of q_{bl} and all its derivatives for all $z \neq 0$. We finally write the system which will allow us to compute the equations of the profile:

$$\begin{cases} -\frac{1}{\varepsilon^2}\mu\Gamma\partial_z^2 q_- + h_\varepsilon q_- + \frac{1}{\varepsilon^2}\partial_z q_- = 0, \\ -\mu\Gamma\partial_z^2 q_{+,i} + \frac{1}{\varepsilon}\partial_z q_{+,i} = 0, \\ -\mu\Gamma\partial_z^2 q_{bl} - \partial_z q_{bl} = 0, \\ -\mu\Gamma\varepsilon^2\partial_z^2 q_{+,e} + q_{+,e} + \partial_z q_{+,e} = 0, \\ q_{+,i}(0) + q_{bl}\left(\frac{1}{\varepsilon}\right) = q_-(0), \\ q_{+,e}(0) = q_{+,i}(1) + q_{bl}(0), \\ \partial_z q_{+,i}(0) - \frac{1}{\varepsilon}\partial_z q_{bl}\left(\frac{1}{\varepsilon}\right) = \frac{1}{\varepsilon}\partial_z q_-(0) - \frac{1}{\mu}, \\ \partial_z q_{+,e}(0) = \frac{1}{\varepsilon}\partial_z q_{+,i}(1) - \frac{1}{\varepsilon^2}\partial_z q_{bl}(0), \\ \varepsilon\int_{-\infty}^0 q_-(z)\mathrm{d}z + \int_0^1 q_{+,i}(z)\mathrm{d}z + \varepsilon\int_0^{1/\varepsilon} q_{bl}(z)\mathrm{d}z + \frac{1}{\varepsilon}\int_0^{+\infty} q_{+,e}(z)\mathrm{d}z = 1, \end{cases} \tag{3.13}$$

where we have defined

$$h_\varepsilon(z) = h(\varepsilon z).$$

Note that since $h = \mathbf{1}_{\mathbf{R}\setminus[-1,1]}$, we have

$$h_\varepsilon(z) = \begin{cases} 1 & \text{if } |z| \geq \dfrac{1}{\varepsilon}, \\ 0 & \text{otherwise.} \end{cases}$$

Now if the expansion we make is ever to be valid we must have q_- exponentially decreasing when z decreases to $-\infty$. Then if we consider the function $z \mapsto h_\varepsilon(z)\exp(z)$ then it is easy to see that it is exponentially small (ie $\sim \exp(-\lambda/\varepsilon)$ for some $\lambda > 0$) in any norm we could consider. Thus in the following we will treat all terms multiplied by h_ε to be smaller than any ε^k for any $k \geq 0$. As a remark we cannot do this on the other side and have to break it into the interior part $q_{+,i}$ and the exterior part $q_{+,e}$.

3.3.2 Ansaetze

We make the following ansaetze:

$$q_- = \varepsilon q_-^1 + \varepsilon^2 q_-^2 + \varepsilon^3 q_-^3 + \dots, \tag{3.14}$$

$$q_{+,i} = \varepsilon q_{+,i}^1 + \varepsilon^2 q_{+,i}^2 + \varepsilon^3 q_{+,i}^3 + \dots, \tag{3.15}$$

$$q_{bl} = \varepsilon^3 q_{bl}^3 + \varepsilon^4 q_{bl}^4 + \dots, \tag{3.16}$$

$$q_{+,e} = \varepsilon q_{+,e}^1 + \varepsilon^2 q_{+,e}^2 + \varepsilon^3 q_{+,e}^3 \dots. \tag{3.17}$$

Of course we could have put terms of order 0 for q_-, $q_{+,i}$ and $q_{+,e}$ and terms of order 0,1 and 2 for q_{bl}. When one deos that, by putting the ansaetze in the equations of (3.12), we would see that these terms must be 0; because they solve linear Dirichlet problems with no exterior forces. We recall that we have (3.2) which is the following consistency equation between Γ and p:

$$\Gamma = \int_{|\sigma|>1} p(\sigma)\mathrm{d}\sigma$$

which can be rewritten in terms of q_- and $q_{+,e}$

$$\Gamma = \frac{1}{\varepsilon}\int_0^{+\infty} q_{+,e}(z)\mathrm{d}z + \varepsilon \int_{-\infty}^{-1/\varepsilon} q_-(z)\mathrm{d}z.$$

With such an expression, if we assume enough regularity of the profiles (which will be checked after we have computed them), we can derive the following ansatz on Γ:

$$\Gamma = c_0 + c_1\varepsilon + c_2\varepsilon^2 + c_3\varepsilon^3 \dots. \tag{3.18}$$

with $\forall k, c_k = \int_0^{+\infty} q_{+,e}^{k+1}(z)\mathrm{d}z$ because, as we remarked, the second term is exponentially small.

3.3.3 Profiles

In this section we only compute the profiles q_-^k, $q_{+,i}^k$ and $q_{+,e}^k$ for $k = 1, 2$ even if we will in the end only use the approximation given by the terms of order 1. Indeed, it can be interesting to compare the terms of order 2, that we give here, to the approximation of (3.63) given in (3.67).

All we need to do is to plug (3.14) , (3.15) and (3.17) in (3.13) and identify the formal powers of ε.

Order ε.

We first look for $q_{+,e}^1$:

$$\begin{cases} \partial_z q_{+,e}^1 + q_{+,e}^1 = 0, \\ \int_0^{+\infty} q_{+,e}^1(z)\mathrm{d}z = 1, \end{cases}$$

which leads to

$$q_{+,e}^1(z) = \exp(-z). \tag{3.19}$$

We also have that $c_0 = 1$. Now we can look for $q_{+,i}^1$ which solves the following problem

$$\begin{cases} \partial_z q_{+,i}^1 = 0, \\ q_{+,i}^1(1) = 1, \end{cases}$$

whose solution is obviously given by

$$q_{+,i}^1 = 1 \tag{3.20}$$

identically. Finally we compute for q_-^1 which solves the problem:

$$\begin{cases} -\mu\partial_z^2 q_-^1 + \partial_z q_-^1 = 0, \\ q_-^1(0) = 1, \\ \partial_z q_-^1(0) = \dfrac{1}{\mu}, \end{cases}$$

whose solution is

$$q_-^1(z) = \exp(z/\mu). \tag{3.21}$$

Order ε^2. Once again we start from the right:

$$\begin{cases} \partial_z q^2_{+,e} + q^2_{+,e} = 0, \\ \displaystyle\int_0^{+\infty} q^2_+(z)\mathrm{d}z = -\int_0^1 q^1_{+,i}(z)\mathrm{d}z = -1, \end{cases}$$

whose solution is $q^2_{+,e}(z) = -\exp(-z)$. We also have $c_1 = -1$. We continue by correcting the derivative of the previous approximation with a boundary layer:

$$\begin{cases} -\mu\partial_z^2 q^3_{bl} - \partial_z q^3_{bl} = 0, \\ \partial_z q^3_{bl}(0) = -\partial_z q^1_{+,e}(0) = -(-1), \end{cases}$$

for which we have the solution $q^3_{bl}(z) = -\mu\exp(-z/\mu) + 1$ up to an additive constant. We choose to take this solution so that $q^3_{bl}(0) = 0$. Only now do we look for $q^2_{+,i}$:

$$\begin{cases} \partial_z q^2_{+,i} = 0, \\ q^2_{+,i}(1) = -1, \end{cases}$$

whose solution is $q^2_{+,i} = -1$. Now we can find the profile q^2_- by solving the problem

$$\begin{cases} -\mu\partial_z^2 q^2_- + \partial_z q^2_- = -\mu\partial_z^2 q^1_-, \\ q^2_-(0) = -1, \\ \partial_z q^2_-(0) = 0, \end{cases}$$

whose solution is $q^2_-(z) = (z/\mu - 1)\exp(z/\mu)$.

3.4 Proof of Proposition 3.1

To construct the main order of p in its behaviour as $\varepsilon \to 0$ we simply truncate the expansions of (3.14)-(3.17) at first order, replace q^1_-,$q^1_{+,i}$ and $q^1_{+,e}$ by the expressions given at (3.21),(3.20) and (3.19). We introduce the notation:

$$p^{\mathrm{app}}_-(\sigma) = \varepsilon q^1_-\left(\frac{\sigma}{\varepsilon}\right), \tag{3.22}$$

$$p^{\mathrm{app}}_{+,i}(\sigma) = \varepsilon q^1_{+,i}(\sigma), \tag{3.23}$$

$$p^{\mathrm{app}}_{+,e}(\sigma) = \varepsilon q^1_{+,e}(\varepsilon(\sigma - 1)), \tag{3.24}$$

and this gives the expression of p^{app} given in (3.6). Finally, we note $p^{\mathrm{rem}}_- = p_- - p^{\mathrm{app}}_-$, $p^{\mathrm{rem}}_{+,i} = p_{+,i} - p^{\mathrm{app}}_{+,i}$ and $p^{\mathrm{rem}}_{+,e} = p_{+,e} - p^{\mathrm{app}}_{+,e}$. We write the problem

solved by the remainder terms:

$$\begin{cases} -\mu\Gamma\partial_\sigma^2 p_-^{\rm rem} + h p_-^{\rm rem} + \dfrac{1}{\varepsilon}\partial_\sigma p_-^{\rm rem} = R_-, \\ -\mu\Gamma\partial_\sigma^2 p_{+,i}^{\rm rem} + \dfrac{1}{\varepsilon}\partial_\sigma p_{+,i}^{\rm rem} = 0, \\ -\mu\Gamma\partial_\sigma^2 p_{+,e}^{\rm rem} + p_{+,e}^{\rm rem} + \dfrac{1}{\varepsilon}\partial_\sigma p_{+,e}^{\rm rem} = R_{+,e}, \\ p_{+,i}^{\rm rem}(0) = p_-^{\rm rem}(0), \\ p_{+,e}^{\rm rem}(1) = p_{-,i}^{\rm rem}(1), \\ \partial_\sigma p_{+,i}^{\rm rem}(0) = \partial_\sigma p_-^{\rm rem}(0), \\ \partial_\sigma p_{+,e}^{\rm rem}(1) - \varepsilon^2 = \partial_\sigma p_{+,i}^{\rm rem}(1), \\ \displaystyle\int_{-\infty}^{0} p_-^{\rm rem}(\sigma){\rm d}\sigma + \int_0^1 p_{+,i}^{\rm rem}(\sigma){\rm d}\sigma + \int_1^{+\infty} p_{+,e}^{\rm rem}(\sigma){\rm d}\sigma = -\varepsilon + \mu\varepsilon^2 \end{cases} \tag{3.25}$$

where we have set

$$\begin{aligned} R_- &= \mu\Gamma\partial_\sigma^2 p_-^{\rm app} - h p_-^{\rm app} - \frac{1}{\varepsilon}\partial_\sigma p_-^{\rm app} \\ &= \left(\frac{\Gamma-1}{\mu\varepsilon} - \varepsilon h\right)\exp\left(\frac{\sigma}{\mu\varepsilon}\right), \end{aligned} \tag{3.26}$$

$$\begin{aligned} R_{+,e} &= \mu\Gamma\partial_\sigma^2 p_{+,e}^{\rm app} - p_{+,e}^{\rm app} - \frac{1}{\varepsilon}\partial_\sigma p_{+,e}^{\rm app} \\ &= \mu\Gamma\varepsilon^3\exp(-\varepsilon(\sigma-1)). \end{aligned} \tag{3.27}$$

Note, for example, that we obtain the last transmission condition by writing:

$$\partial_\sigma p_{+,e}(1) = \partial_\sigma p_{+,i}(1),$$

which becomes, using $p = p^{\rm app} + p^{\rm rem}$,

$$\partial_\sigma p_{+,e}^{\rm rem}(1) + \partial_\sigma p_{+,e}^{\rm app}(1) = \partial_\sigma p_{+,i}^{\rm rem}(1) + \partial_\sigma p_{+,i}^{\rm app}(1),$$

and thus, using the expressions of $p_{+,e}^{\rm app}$ and $p_{+,i}^{\rm app}$,

$$\partial_\sigma p_{+,e}^{\rm rem}(1) - \varepsilon^2 = \partial_\sigma p_{+,i}^{\rm rem}(1).$$

We will now prove the estimations (3.7)-(3.9) of Proposition 3.1. It is useful to introduce $\widetilde{p}_-^{\rm rem}$ and $\widetilde{p}_{+,e}^{\rm rem}$ defined through,

$$p_-^{\rm rem} = \exp\left(\frac{\sigma}{2\mu\varepsilon}\right)\widetilde{p}_-^{\rm rem}, \tag{3.28}$$

$$p_{+,e}^{\rm rem} = \exp\left(-\frac{\varepsilon}{2}(\sigma-1)\right)\widetilde{p}_{+,e}^{\rm rem}. \tag{3.29}$$

This allows us to take advantage of the exponential decay of the right-hand sides of (3.25) and explains the form of estimations (3.7) and (3.9): we are going to show that $\widetilde{p}_-^{\mathrm{rem}}$ and $\widetilde{p}_{+,e}^{\mathrm{rem}}$ are bounded in $\mathrm{L}^2(-\infty,0)$ and $\mathrm{L}^2(1,+\infty)$ respectively. We thus now rewrite the system we will study with the unknowns $\widetilde{p}_-^{\mathrm{rem}}$, $p_{+,i}^{\mathrm{rem}}$ and $\widetilde{p}_{+,e}^{\mathrm{rem}}$:

$$\begin{aligned}
\partial_\sigma p_-^{\mathrm{rem}}(\sigma) &= \exp\left(\frac{\sigma}{2\mu\varepsilon}\right)\left(\partial_\sigma \widetilde{p}_-^{\mathrm{rem}}(\sigma) + \frac{1}{2\mu\varepsilon}\widetilde{p}_-^{\mathrm{rem}}(\sigma)\right),\\
\partial_\sigma^2 p_-^{\mathrm{rem}}(\sigma) &= \exp\left(\frac{\sigma}{2\mu\varepsilon}\right)\left(\partial_\sigma^2 \widetilde{p}_-^{\mathrm{rem}}(\sigma) + \frac{1}{\mu\varepsilon}\partial_\sigma \widetilde{p}_-^{\mathrm{rem}}(\sigma) + \frac{1}{4\mu^2\varepsilon^2}\widetilde{p}_-^{\mathrm{rem}}(\sigma)\right),\\
\partial_\sigma p_{+,e}^{\mathrm{rem}}(\sigma) &= \exp\left(-\frac{\varepsilon}{2}(\sigma-1)\right)\left(\partial_\sigma \widetilde{p}_{+,e}^{\mathrm{rem}}(\sigma) - \frac{\varepsilon}{2}\widetilde{p}_{+,e}^{\mathrm{rem}}(\sigma)\right),\\
\partial_\sigma^2 p_{+,e}^{\mathrm{rem}}(\sigma) &= \exp\left(-\frac{\varepsilon}{2}(\sigma-1)\right)\left(\partial_\sigma^2 \widetilde{p}_{+,e}^{\mathrm{rem}}(\sigma) + \varepsilon\partial_\sigma \widetilde{p}_{+,e}^{\mathrm{rem}}(\sigma) + \frac{\varepsilon^2}{4}\widetilde{p}_{+,e}^{\mathrm{rem}}(\sigma)\right).
\end{aligned}$$

We then replace in (3.25) and simplify both sides by the appropriate exponential:

$$\begin{cases}
-\mu\Gamma\partial_\sigma^2 \widetilde{p}_-^{\mathrm{rem}} + \left(h + \dfrac{1}{2\mu\varepsilon^2}\left(1-\dfrac{\Gamma}{2}\right)\right)\widetilde{p}_-^{\mathrm{rem}} + \dfrac{1-\Gamma}{\varepsilon}\partial_\sigma \widetilde{p}_-^{\mathrm{rem}} = \widehat{R}_-,\\
-\mu\Gamma\partial_\sigma^2 p_{+,i}^{\mathrm{rem}} + \dfrac{1}{\varepsilon}\partial_\sigma p_{+,i}^{\mathrm{rem}} = 0,\\
-\mu\Gamma\partial_\sigma^2 \widetilde{p}_{+,e}^{\mathrm{rem}} + \left(\dfrac{1}{2} - \dfrac{\mu\Gamma\varepsilon^2}{4}\right)\widetilde{p}_{+,e}^{\mathrm{rem}} + \left(\dfrac{1}{\varepsilon} - \mu\Gamma\varepsilon\right)\partial_\sigma p_{+,e}^{\mathrm{rem}} = \widehat{R}_{+,e},\\
p_{+,i}^{\mathrm{rem}}(0) = \widetilde{p}_-^{\mathrm{rem}}(0),\\
\widetilde{p}_{+,e}^{\mathrm{rem}}(1) = p_{-,i}^{\mathrm{rem}}(1),\\
\partial_\sigma p_{+,i}^{\mathrm{rem}}(0) = \partial_\sigma \widetilde{p}_-^{\mathrm{rem}}(0) + \dfrac{1}{2\mu\varepsilon}\widetilde{p}_-^{\mathrm{rem}}(0),\\
\partial_\sigma \widetilde{p}_{+,e}^{\mathrm{rem}}(1) - \dfrac{\varepsilon}{2}\widetilde{p}_{+,e}^{\mathrm{rem}} - \varepsilon^2 = \partial_\sigma p_{+,i}^{\mathrm{rem}}(1),
\end{cases} \tag{3.30}$$

where

$$\widehat{R}_- = R_- \exp\left(-\frac{\sigma}{2\mu\varepsilon}\right) = \left(\frac{\Gamma-1}{\mu\varepsilon} - \varepsilon h\right)\exp\left(\frac{\sigma}{2\mu\varepsilon}\right), \tag{3.31}$$

$$\widehat{R}_{+,e} = R_{+,e}\exp\left(\frac{\varepsilon}{2}(\sigma-1)\right) = \mu\Gamma\varepsilon^3\exp\left(-\frac{\varepsilon}{2}(\sigma-1)\right). \tag{3.32}$$

We do an energy estimate on System (3.30). We multiply each equation by its unknown, integrate on its domain and sum all the obtained equalities:

$$\begin{aligned}
&\mu\Gamma\left(\int_{-\infty}^{0}(\partial_\sigma\widetilde{p}_-^{\mathrm{rem}})^2+\int_0^1(\partial_\sigma p_{+,i}^{\mathrm{rem}})^2+\int_1^{+\infty}(\partial_\sigma\widetilde{p}_{+,e}^{\mathrm{rem}})^2\right)\\
&\quad+\int_{-\infty}^{0}\left(h+\frac{1}{2\mu\varepsilon^2}\left(1-\frac{\Gamma}{2}\right)\right)(\widetilde{p}_-^{\mathrm{rem}})^2+\int_1^{+\infty}\left(\frac{1}{2}-\frac{\mu\Gamma\varepsilon^2}{4}\right)(\widetilde{p}_{+,e}^{\mathrm{rem}})^2\\
&\qquad-\mu\Gamma\partial_\sigma\widetilde{p}_-^{\mathrm{rem}}(0)\widetilde{p}_-^{\mathrm{rem}}(0)+\frac{\Gamma-1}{\varepsilon}\frac{p_-^{\mathrm{rem}}(0)^2}{2}\\
&-\mu\Gamma\partial_\sigma p_{+,i}^{\mathrm{rem}}(1)p_{+,i}^{\mathrm{rem}}(1)+\mu\Gamma\partial_\sigma p_{+,i}^{\mathrm{rem}}(0)p_{+,i}^{\mathrm{rem}}(0)+\frac{1}{\varepsilon}\left(\frac{p_{+,i}^{\mathrm{rem}}(1)^2}{2}-\frac{p_{+,i}^{\mathrm{rem}}(0)^2}{2}\right)\\
&\qquad\mu\Gamma\partial_\sigma\widetilde{p}_{+,e}^{\mathrm{rem}}(1)\widetilde{p}_{+,e}^{\mathrm{rem}}(1)-\left(\frac{1}{\varepsilon}-\mu\Gamma\varepsilon\right)\frac{\widetilde{p}_{+,e}^{\mathrm{rem}}(1)^2}{2}\\
&\qquad=\int_{-\infty}^{0}\widehat{R}_-\widetilde{p}_-^{\mathrm{rem}}+\int_1^{+\infty}\widehat{R}_{+,e}.
\end{aligned}\tag{3.33}$$

Then we use the various transmission conditions to simplify the left-hand side. For example we have:

$$\begin{aligned}
&-\mu\Gamma\partial_\sigma\widetilde{p}_-^{\mathrm{rem}}(0)\widetilde{p}_-^{\mathrm{rem}}(0)+\frac{1-\Gamma}{\varepsilon}\frac{p_-^{\mathrm{rem}}(0)^2}{2}+\mu\Gamma\partial_\sigma p_{+,i}^{\mathrm{rem}}(0)p_{+,i}^{\mathrm{rem}}(0)-\frac{1}{\varepsilon}\frac{p_{+,i}^{\mathrm{rem}}(0)^2}{2}\\
=&\mu\Gamma\widetilde{p}_-^{\mathrm{rem}}(0)\left(\partial_\sigma p_{+,i}^{\mathrm{rem}}(0)-\partial_\sigma\widetilde{p}^{\mathrm{rem}}(0)\right)+\left(\frac{1-\Gamma}{\varepsilon}-\frac{1}{\varepsilon}\right)\frac{p_-^{\mathrm{rem}}(0)^2}{2}\\
=&\mu\Gamma\widetilde{p}_-^{\mathrm{rem}}(0)\left(\frac{1}{\mu\varepsilon}\widetilde{p}_-^{\mathrm{rem}}(0)\right)-\frac{\Gamma}{\varepsilon}\frac{p_-^{\mathrm{rem}}(0)^2}{2}\\
=&0.
\end{aligned}\tag{3.34}$$

In the same way, the interface terms at $\sigma=1$ simplify except for a term $\mu\Gamma\varepsilon^2\widetilde{p}_{+,e}^{\mathrm{rem}}(1)$ which comes from the discrepancy in the derivative, $\partial_\sigma p_{+,e}^{\mathrm{rem}}(1)$ and $\partial_\sigma p_{+,i}^{\mathrm{rem}}(1)$. This term is actually of a high enough order for our purpose. Then we have the following inequality:

$$\begin{aligned}
&\mu\Gamma\left(\int_{-\infty}^{0}(\partial_\sigma\widetilde{p}_-^{\mathrm{rem}})^2+\int_0^1(\partial_\sigma p_{+,i}^{\mathrm{rem}})^2+\int_1^{+\infty}(\partial_\sigma\widetilde{p}_{+,e}^{\mathrm{rem}})^2\right)\\
&\quad+\int_{-\infty}^{0}\left(h+\frac{1}{2\mu\varepsilon^2}\left(1-\frac{\Gamma}{2}\right)\right)(\widetilde{p}_-^{\mathrm{rem}})^2+\int_1^{+\infty}\left(\frac{1}{2}-\frac{\mu\Gamma\varepsilon^2}{4}\right)(\widetilde{p}_{+,e}^{\mathrm{rem}})^2\\
&\qquad\le\mu\Gamma\varepsilon^2|\widetilde{p}_{+,e}^{\mathrm{rem}}(1)|+\left|\int_{-\infty}^{0}\widehat{R}_-\widetilde{p}_-^{\mathrm{rem}}\right|+\left|\int_1^{+\infty}\widehat{R}_{+,e}\widetilde{p}_{+,e}^{\mathrm{rem}}\right|.
\end{aligned}\tag{3.35}$$

Our goal is to bound by above every term in the right-hand side by terms appearing in the left hand side and by quantities independent of p^{rem}. Let us assume for now Lemma 3.1 which will be proved in Section 3.6.2. Recall also that we have $\Gamma \leq 1$ from (3.3). We now estimate the various terms.

Bound for $\left|\int_1^{+\infty} \widehat{R}_{+,e}\widetilde{p}^{\mathrm{rem}}_{+,e}\right|$.

Firstly we have by (3.3) and a direct computation of the integral that:

$$\left\|\widehat{R}_{+,e}\right\|_{\mathrm{L}^2(1,+\infty)} = \mathcal{O}(\varepsilon^{5/2}), \tag{3.36}$$

so that by Hölder and Young's inequality one may write:

$$\begin{aligned}\left|\int_1^{+\infty} \widehat{R}_{+,e}\widetilde{p}^{\mathrm{rem}}_{+,e}\right| &\leq \left\|\widehat{R}_{+,e}\right\|_{\mathrm{L}^2(1,+\infty)} \left\|\widetilde{p}^{\mathrm{rem}}_{+,e}\right\|_{\mathrm{L}^2(1,+\infty)} \\ &\leq \left(\frac{1}{\varepsilon^{1/2}}\left\|\widehat{R}_{+,e}\right\|_{\mathrm{L}^2(1,+\infty)}\right)\left(\varepsilon^{1/2}\left\|\widetilde{p}^{\mathrm{rem}}_{+,e}\right\|_{\mathrm{L}^2(1,+\infty)}\right) \\ &\leq \frac{1}{4\varepsilon}\left\|\widehat{R}_{+,e}\right\|^2_{\mathrm{L}^2(1,+\infty)} + \varepsilon\left\|\widetilde{p}^{\mathrm{rem}}_{+,e}\right\|^2_{\mathrm{L}^2(1,+\infty)} \\ &\leq \mathcal{O}(\varepsilon^4) + \varepsilon\left\|\widetilde{p}^{\mathrm{rem}}_{+,e}\right\|^2_{\mathrm{L}^2(1,+\infty)}.\end{aligned} \tag{3.37}$$

Bound for $\left|\int_{-\infty}^0 \widehat{R}_{-}\widetilde{p}^{\mathrm{rem}}_{-}\right|$.

By a direct computation of the integral we have on the one hand

$$\left\|\exp\left(\frac{\sigma}{2\mu\varepsilon}\right)\right\|_{\mathrm{L}^2(-\infty,0)} = \mathcal{O}(\varepsilon^{1/2}), \tag{3.38}$$

and on the other hand

$$\left\|h(\sigma)\exp\left(\frac{\sigma}{2\mu\varepsilon}\right)\right\|_{\mathrm{L}^2(-\infty,0)} = \mathcal{O}\left(\exp\left(\frac{-1}{\mu\varepsilon}\right)\right). \tag{3.39}$$

From Lemma 3.1 we have

$$\frac{\Gamma - 1}{\mu\varepsilon} = \mathcal{O}(1). \tag{3.40}$$

and these three equalities gives us

$$\left\|\widehat{R}_{-}\right\|_{\mathrm{L}^2(-\infty,0)} = \mathcal{O}(\varepsilon^{1/2}). \tag{3.41}$$

Again, this estimation and Hölder and Young inequalities give:

$$\begin{aligned}\int_{-\infty}^{0} \widehat{R}_- \widetilde{p}_-^{\mathrm{rem}} &\leq \left\| \widehat{R}_- \right\|_{\mathrm{L}^2(-\infty,0)} \left(\int_{-\infty}^{0} (\widetilde{p}_-^{\mathrm{rem}})^2 \right)^{1/2} \\ &\leq \left(\varepsilon \left\| \widehat{R}_- \right\|_{\mathrm{L}^2(-\infty,0)} \right) \frac{1}{\varepsilon} \left(\int_{-\infty}^{0} (\widetilde{p}_-^{\mathrm{rem}})^2 \right)^{1/2} \\ &\leq \mathcal{O}(\varepsilon^3) + \frac{1}{8\mu\varepsilon^2} \int_{-\infty}^{0} (\widetilde{p}_-^{\mathrm{rem}})^2. \end{aligned} \tag{3.42}$$

Bound for $\mu\Gamma\varepsilon^2|\widetilde{p}_{+,e}^{\mathrm{rem}}(1)|$.

By (3.3),$\mu\Gamma\varepsilon^2 = \mathcal{O}(\varepsilon^2)$, so all we need to do is to bound from above $|\widetilde{p}_{+,e}^{\mathrm{rem}}(1)|$. To do that, we of course use the embedding of $\mathrm{H}^1(1,+\infty)$ into $\mathrm{L}^\infty(1,+\infty)$ and note C_∞ the constant of this embedding. We then use Young inequality to get

$$\begin{aligned}\mu\Gamma\varepsilon^2|\widetilde{p}_{+,e}^{\mathrm{rem}}(1)| &\leq \mu\Gamma\varepsilon^{3/2} C_\infty \varepsilon^{1/2} \left(\int_1^{+\infty} (\partial_\sigma \widetilde{p}_{+,e}^{\mathrm{rem}})^2 + \int_1^{+\infty} (\widetilde{p}_{+,e}^{\mathrm{rem}})^2 \right)^{1/2} \\ &\leq \mu\Gamma \left(\varepsilon^3 C_\infty^2 + \varepsilon \left(\int_1^{+\infty} (\partial_\sigma \widetilde{p}_{+,e}^{\mathrm{rem}})^2 + \int_1^{+\infty} (\widetilde{p}_{+,e}^{\mathrm{rem}})^2 \right) \right) \\ &\leq \mathcal{O}(\varepsilon^3) + \mu\Gamma\varepsilon \int_1^{+\infty} (\partial_\sigma \widetilde{p}_{+,e}^{\mathrm{rem}})^2 + \mu\Gamma\varepsilon \int_1^{+\infty} (\widetilde{p}_{+,e}^{\mathrm{rem}})^2 \end{aligned}$$

Final Form of the Energy Inequality (3.35).

Since we have $\Gamma \leq 1$ by (3.3) and h nonnegative, we have

$$h + \frac{1}{2\mu\varepsilon^2} \left(1 - \frac{\Gamma}{2} \right) \geq \frac{1}{4\mu\varepsilon^2}. \tag{3.43}$$

Also, by Lemma 3.1 we have that $\Gamma \to 1$ when $\varepsilon \to 0$ so that we may assume $\Gamma \geq 1/2$ for ε small enough. With that we can bound from below the left-hand side of (3.35)

$$\mu\Gamma\left(\int_{-\infty}^{0}(\partial_\sigma\widetilde{p}_-^{\rm rem})^2+\int_0^1(\partial_\sigma p_{+,i}^{\rm rem})^2+\int_1^{+\infty}(\partial_\sigma\widetilde{p}_{+,e}^{\rm rem})^2\right)$$
$$+\int_{-\infty}^{0}\left(h+\frac{1}{2\mu\varepsilon^2}\left(1-\frac{\Gamma}{2}\right)\right)(\widetilde{p}_-^{\rm rem})^2+\int_1^{+\infty}\left(\frac{1}{2}-\frac{\mu\Gamma\varepsilon^2}{4}\right)(\widetilde{p}_{+,e}^{\rm rem})^2$$
$$\geq\frac{\mu}{2}\left(\int_{-\infty}^{0}(\partial_\sigma\widetilde{p}_-^{\rm rem})^2+\int_0^1(\partial_\sigma p_{+,i}^{\rm rem})^2+\int_1^{+\infty}(\partial_\sigma\widetilde{p}_{+,e}^{\rm rem})^2\right)$$
$$+\frac{1}{4\mu\varepsilon^2}\int_{-\infty}^{0}(\widetilde{p}_-^{\rm rem})^2+\int_1^{+\infty}\left(\frac{1}{2}-\frac{\mu\varepsilon^2}{4}\right)(\widetilde{p}_{+,e}^{\rm rem})^2.$$

We now bound from above the three terms of the right-hand side of (3.35) using (3.37)-(3.43) to obtain that

$$\mu\Gamma\varepsilon^2|\widetilde{p}_{+,e}^{\rm rem}(1)|+\left|\int_{-\infty}^{0}\widehat{R}_-\widetilde{p}_-^{\rm rem}\right|+\left|\int_1^{+\infty}\widehat{R}_{+,e}\widetilde{p}_{+,e}^{\rm rem}\right|$$
$$\leq\mathcal{O}(\varepsilon^3)+\frac{1}{8\mu\varepsilon^2}\int_{-\infty}^{0}(\widetilde{p}_-^{\rm rem})^2+\mu\varepsilon\int_1^{+\infty}(\partial_\sigma\widetilde{p}_{+,e}^{\rm rem})^2+(\mu+1)\varepsilon\int_1^{+\infty}(\widetilde{p}_{+,e}^{\rm rem})^2$$

We can now write the final form of the energy inequality:

$$\mu\left(\frac{1}{2}-\varepsilon\right)\int_1^{+\infty}(\partial_\sigma\widetilde{p}_{+,e}^{\rm rem})^2+\left(\frac{1}{2}-\frac{\mu\varepsilon^2}{4}-(\mu+1)\varepsilon\right)\int_1^{+\infty}(\widetilde{p}_{+,e}^{\rm rem})^2$$
$$+\frac{\mu}{2}\int_{-\infty}^{0}(\partial_\sigma\widetilde{p}_-^{\rm rem})^2+\frac{1}{8\mu\varepsilon^2}\int_{-\infty}^{0}(p_-^{\rm rem})^2+\frac{\mu}{2}\int_0^1(\partial_\sigma p_{+,i}^{\rm rem})^2\leq\mathcal{O}(\varepsilon^3).\quad(3.44)$$

Proof of Inequalities (3.7)-(3.8).

We can extract from (3.44) the following estimations:

$$\left\|\widetilde{p}_-^{\rm rem}\right\|_{\mathrm{L}^2(-\infty,0)}=\mathcal{O}(\varepsilon^{5/2}),\quad(3.45)$$
$$\left\|\widetilde{p}_{+,e}^{\rm rem}\right\|_{\mathrm{L}^2(1,+\infty}=\mathcal{O}(\varepsilon^{3/2}),\quad(3.46)$$

which are exactly (3.7) and (3.9). To complete the proof of Proposition 3.1 we need to show the estimation (3.8). Since we do not get it directly from (3.44) we have to use some kind of Poincaré inequality. For this we write, for $\sigma\in[0,1]$:

$$(p_{+,i}^{\rm rem})^2(\sigma)=\int_0^\sigma 2\partial_\sigma p_{+,i}^{\rm rem}(s)p_{+,i}^{\rm rem}(s)\mathrm{d}s+(p_{+,i}^{\rm rem}(0))^2.\quad(3.47)$$

We can now use the transmission condition of (3.25) to write:

$$\begin{aligned}(p^{\rm rem}_{+,i})^2(\sigma) &= \int_0^\sigma 2\sqrt{2}\partial_\sigma p^{\rm rem}_{+,i}(s)\frac{1}{\sqrt{2}}p^{\rm rem}_{+,i}(s)\mathrm{d}s + (p^{\rm rem}_-(0))^2\\ &\leq 2\int_0^\sigma (\partial_\sigma p^{\rm rem}_{+,i}(s))^2\mathrm{d}s + \frac{1}{2}\int_0^\sigma (p^{\rm rem}_{+,i}(s))^2\mathrm{d}s + \left(\int_{-\infty}^0 \partial_\sigma p^{\rm rem}_-\right)^2\\ &\leq 2\int_0^1 (\partial_\sigma p^{\rm rem}_{+,i})^2 + \frac{1}{2}\int_0^1 (p^{\rm rem}_{+,i})^2 + \left(\int_{-\infty}^0 \partial_\sigma p^{\rm rem}_-\right)^2.\end{aligned} \tag{3.48}$$

We now integrate this inequality between 0 and 1 to obtain:

$$\int_0^1 (p^{\rm rem}_{+,i})^2 \leq 4\int_0^1 (\partial_\sigma p^{\rm rem}_{+,i})^2 + 2\left(\int_{-\infty}^0 \partial_\sigma p^{\rm rem}_-\right)^2. \tag{3.49}$$

Now from (3.44) we already have:

$$\int_0^1 (\partial_\sigma p^{\rm rem}_{+,i})^2 = \mathcal{O}(\varepsilon^3). \tag{3.50}$$

Moreover, we have seen that

$$\partial_\sigma p^{\rm rem}_- = \exp\left(\frac{\sigma}{2\mu\varepsilon}\right)\left(\partial_\sigma \widetilde{p}^{\rm rem}_-(\sigma) + \frac{1}{2\mu\varepsilon}\widetilde{p}^{\rm rem}_-(\sigma)\right).$$

and by (3.44) we have both

$$\left\|\frac{1}{2\mu\varepsilon}\widetilde{p}^{\rm rem}_-\right\|_{\mathrm{L}^2(-\infty,0)} = \mathcal{O}(\varepsilon^{3/2}), \tag{3.51}$$

$$\left\|\partial_\sigma \widetilde{p}^{\rm rem}_-\right\|_{\mathrm{L}^2(-\infty,0)} = \mathcal{O}(\varepsilon^{3/2}), \tag{3.52}$$

so that by Hölder inequality,

$$\begin{aligned}\int_{-\infty}^0 \partial_\sigma p^{\rm rem}_- &= \int_{-\infty}^0 \exp\left(\frac{\sigma}{2\mu\varepsilon}\right)\left(\partial_\sigma \widetilde{p}^{\rm rem}_-(\sigma) + \frac{1}{2\mu\varepsilon}\widetilde{p}^{\rm rem}_-(\sigma)\right)\mathrm{d}\sigma\\ &\leq \left(\int_{-\infty}^0 \exp\left(\frac{\sigma}{\mu\varepsilon}\right)\right)^{1/2}\left\|\partial_\sigma \widetilde{p}^{\rm rem}_- + \frac{1}{2\mu\varepsilon}\widetilde{p}^{\rm rem}_-\right\|_{\mathrm{L}^2(-\infty,0)}\\ &\leq (\mu\varepsilon)^{1/2}\left(\left\|\partial_\sigma \widetilde{p}^{\rm rem}_-\right\|_{\mathrm{L}^2(-\infty,0)} + \left\|\frac{1}{2\mu\varepsilon}\widetilde{p}^{\rm rem}_-\right\|_{\mathrm{L}^2(-\infty,0)}\right),\end{aligned} \tag{3.53}$$

and thus we have:

$$\left(\int_{-\infty}^0 \partial_\sigma p^{\rm rem}_-\right)^2 = \mathcal{O}(\varepsilon^4). \tag{3.54}$$

Consequently we have

$$\int_0^1 (p_{+,i}^{\mathrm{rem}})^2 = \mathcal{O}(\varepsilon^3), \tag{3.55}$$

that is (3.8). We have thus proved Proposition 3.1.

On a side note, the two equalities,

$$\partial_\sigma p_-^{\mathrm{rem}}(\sigma) = \exp\left(\frac{\sigma}{2\mu\varepsilon}\right)\left(\partial_\sigma \widetilde{p}_-^{\mathrm{rem}}(\sigma) + \frac{1}{2\mu\varepsilon}\widetilde{p}_-^{\mathrm{rem}}(\sigma)\right),$$
$$\partial_\sigma p_{+,e}^{\mathrm{rem}}(\sigma) = \exp\left(-\frac{\varepsilon}{2}(\sigma-1)\right)\left(\partial_\sigma \widetilde{p}_{+,e}^{\mathrm{rem}}(\sigma) - \frac{\varepsilon}{2}\widetilde{p}_{+,e}^{\mathrm{rem}}(\sigma)\right),$$

the energy estimate (3.44) and (3.8) prove that we also have the estimation

$$\|p - p^{\mathrm{app}}\|_{\mathrm{H}^1(\mathbf{R})} = \mathcal{O}(\varepsilon^{3/2}). \tag{3.56}$$

3.5 Proof of Theorem 3.2

In this section, we deduce Theorem 3.2 from Proposition 3.1, which was proved in the previous section.

Let us note first that by a direct computation we can show that:

$$\int_{\sigma\in\mathbf{R}} \sigma p^{\mathrm{app}}(\sigma)\mathrm{d}\sigma \sim \frac{1}{\varepsilon}. \tag{3.57}$$

All that is left to prove is that the stress attached to the remainder is $\wr(1/\varepsilon)$.

We use the symbol $A \lesssim B$ to express that there is a positive constant C *independent of* ε, such that

$$A \leq C \cdot B.$$

Since we have a weighted control of the norm of p_-^{rem} and $p_{+,e}^{\mathrm{rem}}$, we can use the following inequalities, which are true for small ε:

$$\begin{aligned}\left|\int_{-\infty}^0 \sigma p_-^{\mathrm{rem}}(\sigma)\mathrm{d}\sigma\right| &\leq \left(\int_{-\infty}^0 \sigma^2 \exp\left(\frac{\sigma}{\mu\varepsilon}\right)\mathrm{d}\sigma\right)^{1/2} \left\|\widetilde{p}_-^{\mathrm{rem}}\right\|_{\mathrm{L}^2(-\infty,0)} \\ &\lesssim (\mu\varepsilon)^{3/2}\left\|\widetilde{p}_-^{\mathrm{rem}}\right\|_{\mathrm{L}^2(-\infty,0)}, \end{aligned} \tag{3.58}$$

$$\begin{aligned}\left|\int_1^{+\infty} \sigma p_{+,e}^{\mathrm{rem}}(\sigma)\mathrm{d}\sigma\right| &\leq \left(\int_1^{+\infty} \sigma^2 \exp\left(-\varepsilon(\sigma-1)\right)\mathrm{d}\sigma\right)^{1/2} \left\|\widetilde{p}_-^{\mathrm{rem}}\right\|_{\mathrm{L}^2(1,+\infty)} \\ &\lesssim \frac{1}{\varepsilon^{3/2}}\left\|\widetilde{p}_-^{\mathrm{rem}}\right\|_{\mathrm{L}^2(1,+\infty)}, \end{aligned} \tag{3.59}$$

We also have

$$\begin{aligned}\left|\int_0^1 \sigma p_{+,i}^{\mathrm{rem}}(\sigma)\mathrm{d}\sigma\right| &\leq \left(\int_0^1 \sigma^2\right)^{1/2} \left\|p_{+,i}^{\mathrm{rem}}\right\|_{\mathrm{L}^2(0,1)} \\ &\lesssim \left\|p_{+,i}^{\mathrm{rem}}\right\|_{\mathrm{L}^2(0,1)}\end{aligned} \tag{3.60}$$

Then it suffices to combine inequalities (3.58) with (3.7), (3.59) with (3.9) and (3.60) with (3.8) to obtain:

$$\left|\int_{\sigma\in\mathbf{R}} \sigma p^{\mathrm{rem}}(\sigma)\mathrm{d}\sigma\right| \leq \mathcal{O}(1), \tag{3.61}$$

so that we have the expansion

$$\tau = \frac{1}{\varepsilon} + \mathcal{O}(1), \tag{3.62}$$

and Theorem 3.2.

3.6 Proof of Lemma 3.1

This section is devoted to the proof of Lemma 3.1. What's interesting is that the proof of this lemma requires the study of a singular limit by itself. Indeed to gain an estimation on Γ we need to approximate the remainder problem (3.25) by a linear approximate remainder problem (3.63). Contrary to what happens in the small shear rate limit we carried out in [54] the expansion of p and τ are uniform in μ and, as such, much simpler.

Let us first introduce the approximate remainder problem and explain its link to System (3.25): we define the functions $\pi_-^{C,\varepsilon}$, $\pi_{+,i}^{C,\varepsilon}$ and $\pi_{+,e}^{C,\varepsilon}$ to be the solutions of the following system,

$$\begin{cases} -\mu(1+C\varepsilon)\partial_\sigma^2\pi_-^{C,\varepsilon} + h\pi_-^{C,\varepsilon} + \dfrac{1}{\varepsilon}\partial_\sigma\pi_-^{C,\varepsilon} = \overline{R}_-, \\ -\mu(1+C\varepsilon)\partial_\sigma^2\pi_{+,i}^{C,\varepsilon} + \dfrac{1}{\varepsilon}\partial_\sigma\pi_{+,i}^{C,\varepsilon} = 0, \\ -\mu(1+C\varepsilon)\partial_\sigma^2\pi_{+,e}^{C,\varepsilon} + \pi_{+,e}^{C,\varepsilon} + \dfrac{1}{\varepsilon}\partial_\sigma\pi_{+,e}^{C,\varepsilon} = \overline{R}_{+,e}, \\ \pi_{+,i}^{C,\varepsilon}(0) = \pi_-^{C,\varepsilon}(0), \\ \pi_{+,e}^{C,\varepsilon}(1) = \pi_{+,i}^{C,\varepsilon}(1), \\ \partial_\sigma\pi_{+,i}^{C,\varepsilon}(0) = \partial_\sigma\pi_-^{C,\varepsilon}(0), \\ \partial_\sigma\pi_{+,e}^{C,\varepsilon}(1) - \varepsilon^2 = \partial_\sigma\pi_{+,i}^{C,\varepsilon}(1), \end{cases} \tag{3.63}$$

where

$$\overline{R}_- = \left(\frac{C}{\mu} - \varepsilon h\right) \exp\left(\frac{\sigma}{\mu\varepsilon}\right), \tag{3.64}$$

$$\overline{R}_{+,e} = \mu(1 + C\varepsilon)\varepsilon^3 \exp(-\varepsilon(\sigma - 1)). \tag{3.65}$$

We also define the two variable function

$$F(C, \varepsilon) = \int_{-\infty}^{0} \pi_-^{C,\varepsilon} + \int_0^1 \pi_{+,i}^{C,\varepsilon} + \int_1^{+\infty} \pi_{+,i}^{C,\varepsilon} + \varepsilon - \mu\varepsilon^2. \tag{3.66}$$

Replace, in (3.63), C by Γ^{rem} and the system becomes (3.25) without the integral constraint. Thus the solution to (3.63) with $C = \Gamma^{\text{rem}}$, which is by definition $\pi^{\Gamma^{\text{rem}},\varepsilon}$ is also the solution to (3.25) p^{rem}. Consequently the integral constraint of (3.25) is exactly the equation $F(\Gamma^{\text{rem}}, \varepsilon) = 0$. Conversely, for any C verifying $F(C, \varepsilon) = 0$ we have that $\pi^{\text{rem},C,\varepsilon}$ satisfies completely the problem (3.25), including the integral constraint and thus we have $C = \Gamma^{\text{rem}}$. This argument relies on the unique solvability of (3.25) for fixed ε or, equivalently, on the unique solvability of (3.5). This property has already been proved in [16] or [53].

Let us first state that we have the analogous to Proposition 3.1 for (3.63). Since there will be a boundary layer on the left side of $\sigma = 1$ we introduce θ, a $\mathcal{C}^\infty$ localization function which is 1 on $[1/2, 1]$, 0 on $[0, 1/3]$ and strictly increasing on $]1/3, 1/2[$. Then we have the following approximation result:

Proposition 3.2. *The solution to the remainder problem* (3.63) *noted by* $(\pi_-^{C,\varepsilon}, \pi_{+,i}^{C,\varepsilon}, \pi_{+,e}^{C,\varepsilon})$ *can be expanded, when* $\varepsilon \to 0$, *as* $\pi^{C,\varepsilon} = \pi^{C,\varepsilon,\text{app}} + \pi^{C,\varepsilon,\text{rem}}$ *where:*

$$\begin{aligned}
\pi_-^{C,\varepsilon,\text{app}}(\sigma) &= C\varepsilon^2 \left(1 - \frac{C\sigma}{\mu\varepsilon}\right) \exp\left(\frac{\sigma}{\varepsilon}\right), \\
\pi_{+,i}^{C,\varepsilon,\text{app}}(\sigma) &= C\varepsilon^2 + \mu\varepsilon^3\theta(\sigma) \left(1 - \exp\left(\frac{\sigma - 1}{\mu\varepsilon}\right)\right), \\
\pi_{+,e}^{C,\varepsilon,\text{app}}(\sigma) &= C\varepsilon^2 \exp\left(-\varepsilon(\sigma - 1)\right),
\end{aligned} \tag{3.67}$$

with the following estimations:

$$\begin{aligned}
\left\| \exp\left(-\frac{\cdot}{2\mu\varepsilon}\right) \pi_-^{C,\varepsilon,\text{rem}} \right\|_{\text{L}^2(-\infty,0)} &= \mathcal{O}(\varepsilon^{7/2}), \\
\left\| \pi_{+,i}^{C,\varepsilon,\text{rem}} \right\|_{\text{L}^2(0,1)} &= \mathcal{O}(\varepsilon^{5/2}), \\
\left\| \exp\left(\frac{\varepsilon}{2}(\cdot - 1)\right) \pi_{+,e}^{C,\varepsilon,\text{rem}} \right\|_{\text{L}^2(1,\infty)} &= \mathcal{O}(\varepsilon^{5/2}).
\end{aligned}$$

We will prove this proposition in Section 3.6.1. From this proposition we can deduce the following result which will be detailed in Section 3.6.2.

Proposition 3.3. *For a fixed C we have:*

$$F(C,\varepsilon) = (C+1)\varepsilon + \mathcal{O}(\varepsilon^2).$$

Because of the linear and elliptic nature of (3.63) it is clear that F must be at least continuous in C, ε in the domain $1 + C\varepsilon > 0$. Let us fix two constant numbers C_1 and C_2 such that $C_1 < -1 < C_2$. Then because of Proposition 3.3 and because F is continuous there is an interval $]0, \varepsilon_0[$ on which we have

$$\forall \varepsilon \in]0, \varepsilon_0[, \quad F(C_1,\varepsilon) < 0 < F(C_2,\varepsilon).$$

Now for any fixed $\varepsilon \in]0, \varepsilon_0[$ we use the continuity in C of F and the intermediate value theorem to affirm that there must be a 0 of $F(\cdot,\varepsilon)$ on the interval $[C_1, C_2]$. But as we pointed out, the only 0 that $F(\cdot,\varepsilon)$ has is Γ^{rem}. Consequently,

$$\forall \varepsilon \in]0, \varepsilon^0[, \quad C_1 < \Gamma^{\mathrm{rem}} < C_2,$$

which is exactly what Lemma 3.1 states.

Remark. Note that $C = -1$ makes $F(C,\varepsilon)$ vanish for $\varepsilon \to 0$ faster than any other value of C and indeed one could prove by expanding p at a higher order that we formally have $\Gamma = 1 - \varepsilon + \mathcal{O}(\varepsilon^2)$ and also that $p^{\mathrm{app}} + \pi^{-1,\varepsilon,\mathrm{app}}$ is the second order expansion of p.

3.6.1 Proof of Proposition 3.2

This section is devoted to construct an approximation to System (3.63) and to estimate the remainder of this approximation. It is very similar to Sections 3.3 and 3.4.

To find the asymptotic behaviour of $\pi^{C,\varepsilon}$ we once again change variable and set, now classically:

$$\pi_-^{C,\varepsilon}(\sigma) = \chi_-\left(\frac{\sigma}{\varepsilon}\right), \qquad \pi_{+,i}^{C,\varepsilon}(\sigma) = \chi_{+,i}(\sigma) + \chi_{bl}\left(\frac{1-\sigma}{\varepsilon}\right),$$
$$\pi_{+,e}^{C,\varepsilon}(\sigma) = \chi_{+,e}(\varepsilon(\sigma-1)),$$

so that the functions χ_-, $\chi_{+,i}$, χ_{bl} and $\chi_{+,e}$ satisfy the following problem:

$$\begin{cases} -\mu(1+C\varepsilon)\partial_z^2\chi_- + \varepsilon^2 h_\varepsilon \chi_- + \partial_z\chi_- = \varepsilon^2\left(\dfrac{C}{\mu} - \varepsilon h_\varepsilon\right)\exp\left(\dfrac{z}{\mu}\right), \\ -\mu(1+C\varepsilon)\partial_\sigma^2\chi_{+,i} + \dfrac{1}{\varepsilon}\partial_\sigma\chi_{+,i} = 0, \\ -\mu(1+C\varepsilon)\partial_z^2\chi_{bl} - \partial_z\chi_{bl} = 0, \\ -\mu\varepsilon^2(1+C\varepsilon)\partial_z^2\chi_{+,e} + \chi_{+,e} + \partial_z\chi_{+,e} = \mu(1+C\varepsilon)\varepsilon^3\exp(-z), \\ \chi_{+,i}(0) + \chi_{bl}\left(\dfrac{1}{\varepsilon}\right) = \chi_-(0), \\ \chi_{+,e}(0) = \chi_{+,i}(1), \\ \partial_\sigma\chi_{+,i}(0) = \dfrac{1}{\varepsilon}\partial_z\chi_-(0), \\ \varepsilon\partial_z\chi_{+,e}(0) - \varepsilon^2 = \partial_\sigma\chi_{+,i}(1) - \dfrac{1}{\varepsilon}\partial_z\chi_{bl}, \end{cases} \tag{3.68}$$

and assume an expansion of the form

$$\begin{aligned} \chi_- &= \varepsilon^2\chi_-^1 + \varepsilon^2\chi_-^2 + \varepsilon^3\chi_-^3 + \dots, \\ \chi_{+,i} &= \varepsilon^2\chi_{+,i}^1 + \varepsilon^2\chi_{+,i}^2 + \varepsilon^3\chi_{+,i}^3 + \dots, \\ \chi_{bl} &= \varepsilon^3\chi_{bl}^3 + \varepsilon^4\chi_{bl}^4 + \dots, \\ \chi_{+,e} &= \varepsilon^2\chi_{+,e}^1 + \varepsilon^2\chi_{+,e}^2 + \varepsilon^3\chi_{+,e}^3 \dots. \end{aligned}$$

Recall that, to obtain, (3.25) we used a truncation at order ε of the formal expansion of p, so that p^{rem} is formally of order ε^2. Now $\pi^{\mathrm{rem},C,\varepsilon}$ solves (3.63), a problem which is very similar to (3.25), and which is hopefully at the same formal ε order. It is thus natural to see that the first order of $\pi^{\mathrm{rem},C,\varepsilon}$ should be ε^2. The following analysis will prove that the previous formal expansions give the correct ansaetze.

One interesting point here is that when solving the profile equations for (3.13), we start with $\sigma > 1$ because the most singular term comes from equation

$$\varepsilon\int_{-\infty}^0 q_-(z)\mathrm{d}z + \int_0^1 q_{+,i}(z)\mathrm{d}z + \varepsilon\int_0^{1/\varepsilon} q_{bl}(z)\mathrm{d}z + \frac{1}{\varepsilon}\int_0^{+\infty} q_{+,e}(z)\mathrm{d}z = 1.$$

But such a constraint has disappeared in (3.68) and the most singular term now comes from

$$\partial_\sigma\chi_{+,i}(0) = \frac{1}{\varepsilon}\partial_z\chi_-(0),$$

and we solve from left ($\sigma < 0$) to right ($\sigma > 1$). It is then not difficult to see that the lowest order approximation of $\pi^{C,\varepsilon}$ is formally given by

$$\pi_-^{C,\varepsilon,\mathrm{app}}(\sigma) = C\varepsilon^2 \left(1 - \frac{C\sigma}{\mu\varepsilon}\right) \exp\left(\frac{\sigma}{\varepsilon}\right), \tag{3.69}$$

$$\pi_{+,i}^{C,\varepsilon,\mathrm{app}}(\sigma) = C\varepsilon^2 + \mu\varepsilon^3\theta(\sigma)\left(1 - \exp\left(\frac{\sigma-1}{\mu\varepsilon}\right)\right), \tag{3.70}$$

$$\pi_{+,e}^{C,\varepsilon,\mathrm{app}}(\sigma) = C\varepsilon^2 \exp\left(-\varepsilon(\sigma-1)\right). \tag{3.71}$$

These expressions should be compared to the second order profiles given in Section 3.3.3. We now again set $\pi^{C,\varepsilon,\mathrm{rem}} = \pi^{C,\varepsilon} - \pi^{C,\varepsilon,\mathrm{app}}$. Then $\pi_-^{C,\varepsilon,\mathrm{rem}}$,$\pi_{+,i}^{C,\varepsilon,\mathrm{rem}}$ and $\pi_{+,e}^{C,\varepsilon,\mathrm{rem}}$ solve the following problem:

$$\begin{cases} -\mu(1+C\varepsilon)\partial_\sigma^2\pi_-^{C,\varepsilon,\mathrm{rem}} + h\pi_-^{C,\varepsilon,\mathrm{rem}} + \dfrac{1}{\varepsilon}\partial_\sigma\pi_-^{C,\varepsilon,\mathrm{rem}} = \widetilde{R}_-, \\ -\mu(1+C\varepsilon)\partial_\sigma^2\pi_{+,i}^{C,\varepsilon,\mathrm{rem}} + \dfrac{1}{\varepsilon}\partial_\sigma\pi_{+,i}^{C,\varepsilon,\mathrm{rem}} = \widetilde{R}_{+,i}, \\ -\mu(1+C\varepsilon)\partial_\sigma^2\pi_{+,e}^{C,\varepsilon,\mathrm{rem}} + \pi_{+,e}^{C,\varepsilon,\mathrm{rem}} + \dfrac{1}{\varepsilon}\partial_\sigma\pi_{+,e}^{C,\varepsilon,\mathrm{rem}} = \widetilde{R}_{+,e}, \\ \pi_{+,i}^{C,\varepsilon,\mathrm{rem}}(0) = \pi_-^{C,\varepsilon,\mathrm{rem}}(0), \\ \pi_{+,e}^{C,\varepsilon,\mathrm{rem}}(1) = \pi_{+,i}^{C,\varepsilon,\mathrm{rem}}(1), \\ \partial_\sigma\pi_{+,i}^{C,\varepsilon,\mathrm{rem}}(0) = \partial_\sigma\pi_-^{C,\varepsilon,\mathrm{rem}}(0), \\ \partial_\sigma\pi_{+,e}^{C,\varepsilon,\mathrm{rem}}(1) = \partial_\sigma\pi_{+,i}^{C,\varepsilon,\mathrm{rem}}(1), \end{cases} \tag{3.72}$$

where

$$\widetilde{R}_- = -C\left(\frac{\sigma}{\mu^2} + \frac{C\varepsilon}{\mu}\right)\exp\left(\frac{\sigma}{2\mu\varepsilon}\right) - \left(C\varepsilon^2\left(1 - \frac{\sigma}{\mu\varepsilon}\right) + \varepsilon\right) h \exp\left(\frac{\sigma}{2\mu\varepsilon}\right), \tag{3.73}$$

$$\widetilde{R}_{+,i} = -\mu\varepsilon^2\theta' + \mu^2\varepsilon^3\theta'' + 3\mu\varepsilon^2\theta'\exp\left(\frac{\sigma-1}{\mu\varepsilon}\right) - \mu^2\varepsilon^3\theta''\exp\left(\frac{\sigma-1}{\mu\varepsilon}\right), \tag{3.74}$$

$$\widetilde{R}_{+,e} = \mu\varepsilon^3(1+C\varepsilon)\exp\left(-\frac{\varepsilon}{2}(\sigma-1)\right) + C\varepsilon^4(1+C\varepsilon)\exp\left(-\frac{\varepsilon}{2}(\sigma-1)\right). \tag{3.75}$$

Let us again introduce

$$\begin{aligned} \pi_-^{C,\varepsilon,\mathrm{rem}} &= \exp\left(\frac{\sigma}{2\mu\varepsilon}\right)\widetilde{\pi}_-^{C,\varepsilon,\mathrm{rem}}, \\ \pi_{+,e}^{C,\varepsilon,\mathrm{rem}} &= \exp\left(-\frac{\varepsilon}{2}(\sigma-1)\right)\widetilde{\pi}_{+,e}^{C,\varepsilon,\mathrm{rem}}. \end{aligned} \tag{3.76}$$

We are going to prove that $\widetilde{\pi}_-^{C,\varepsilon,\mathrm{rem}}$ and $\widetilde{\pi}_{+,e}^{C,\varepsilon,\mathrm{rem}}$, are in $\mathrm{L}^2(-\infty,0)$ and $\mathrm{L}^2(1,+\infty)$ respectively. Let us write the problem solved by $\widetilde{\pi}_-^{C,\varepsilon,\mathrm{rem}}$, $\pi_{+,i}^{C,\varepsilon,\mathrm{rem}}$ and $\widetilde{\pi}_{+,e}^{C,\varepsilon,\mathrm{rem}}$:

$$\begin{cases} -\mu(1+C\varepsilon)\partial_\sigma^2\widetilde{\pi}_-^{C,\varepsilon,\mathrm{rem}} + \left(h + \dfrac{1}{4\mu\varepsilon^2} - \dfrac{C}{4\mu\varepsilon}\right)\widetilde{\pi}_-^{C,\varepsilon,\mathrm{rem}} - \dfrac{C}{\mu}\partial_\sigma\widetilde{\pi}_-^{C,\varepsilon,\mathrm{rem}} = \widetilde{R}_-, \\ -\mu(1+C\varepsilon)\partial_\sigma^2\pi_{+,i}^{C,\varepsilon,\mathrm{rem}} + \dfrac{1}{\varepsilon}\partial_\sigma\pi_{+,i}^{C,\varepsilon,\mathrm{rem}} = \widetilde{R}_{+,i}, \\ -\mu(1+C\varepsilon)\partial_\sigma^2\widetilde{\pi}_{+,e}^{C,\varepsilon,\mathrm{rem}} + \left(\dfrac{1}{2} - \dfrac{\mu(1+C\varepsilon)\varepsilon^2}{4}\right)\widetilde{\pi}_{+,e}^{C,\varepsilon,\mathrm{rem}} \\ \qquad + \left(\dfrac{1}{\varepsilon} - \mu(1+C\varepsilon)\varepsilon^2\right)\partial_\sigma\widetilde{\pi}_{+,e}^{C,\varepsilon,\mathrm{rem}} = \widetilde{R}_{+,e}, \\ \pi_{+,i}^{C,\varepsilon,\mathrm{rem}}(0) = \widetilde{\pi}_-^{C,\varepsilon,\mathrm{rem}}(0), \\ \widetilde{\pi}_{+,e}^{C,\varepsilon,\mathrm{rem}}(1) = \pi_{+,i}^{C,\varepsilon,\mathrm{rem}}(1), \\ \partial_\sigma\pi_{+,i}^{C,\varepsilon,\mathrm{rem}}(0) = \partial_\sigma\widetilde{\pi}_-^{C,\varepsilon,\mathrm{rem}}(0) + \dfrac{1}{2\mu\varepsilon}\widetilde{\pi}_-^{C,\varepsilon,\mathrm{rem}}(0), \\ \partial_\sigma\widetilde{\pi}_{+,e}^{C,\varepsilon,\mathrm{rem}}(1) - \dfrac{\varepsilon}{2}\widetilde{\pi}_{+,e}^{C,\varepsilon,\mathrm{rem}}(1) = \partial_\sigma\pi_{+,i}^{C,\varepsilon,\mathrm{rem}}(1). \end{cases} \tag{3.77}$$

Now we can obtain the same kind of energy estimate as (3.35):

$$\begin{aligned} \mu(1+C\varepsilon)\left(\int_{-\infty}^0(\partial_\sigma\widetilde{\pi}_-^{C,\varepsilon,\mathrm{rem}})^2 + \int_0^1(\partial_\sigma\pi_{+,i}^{C,\varepsilon,\mathrm{rem}})^2 + \int_1^{+\infty}(\partial_\sigma\widetilde{\pi}_{+,e}^{C,\varepsilon,\mathrm{rem}})^2\right) \\ + \frac{1}{8\mu\varepsilon^2}\int_{-\infty}^0(\widetilde{\pi}_-^{C,\varepsilon,\mathrm{rem}})^2 + \frac{1}{2}\int_1^{+\infty}(\widetilde{\pi}_{+,e}^{C,\varepsilon,\mathrm{rem}})^2 \\ \leq \int_{-\infty}^0\widetilde{R}_-\widetilde{\pi}_-^{C,\varepsilon,\mathrm{rem}}\pi_{+,i}^{C,\varepsilon,\mathrm{rem}} + \int_0^1\widetilde{R}_{+,i} + \int_1^{+\infty}\widetilde{R}_{+,e}\widetilde{\pi}_{+,e}^{C,\varepsilon,\mathrm{rem}}, \end{aligned} \tag{3.78}$$

Once again we can absorb the right-hand side into the left hand side by noting that:

$$\left\|\widetilde{R}_-\right\|_{\mathrm{L}^2(-\infty,0)} = \mathcal{O}(\varepsilon^{3/2}), \tag{3.79}$$

$$\left\|\widetilde{R}_{+,e}\right\|_{\mathrm{L}^2(1,\infty)} = \mathcal{O}(\varepsilon^{5/2}), \tag{3.80}$$

$$\left\|\widetilde{R}_{+,i}\right\|_{\mathrm{L}^2(0,1)} = \mathcal{O}(\varepsilon^2). \tag{3.81}$$

Also note that we have the following *a priori* estimate:

$$\begin{aligned}
\int_0^1 (\pi_{+,i}^{C,\varepsilon,\mathrm{rem}})^2 &\lesssim (\pi_{+,i}^{C,\varepsilon,\mathrm{rem}}(0))^2 + \int_0^1 (\partial_\sigma \pi_{+,i}^{C,\varepsilon,\mathrm{rem}})^2 \\
&\lesssim \left(\int_{-\infty}^0 \partial_\sigma \pi_-^{C,\varepsilon,\mathrm{rem}}\right)^2 + \int_0^1 (\partial_\sigma \pi_{+,i}^{C,\varepsilon,\mathrm{rem}})^2 \\
&\lesssim \left(\int_{-\infty}^0 \partial_\sigma \left(\exp\left(\frac{\sigma}{2\mu\varepsilon}\right)\widetilde{\pi}_-^{C,\varepsilon,\mathrm{rem}}\right)\right)^2 + \int_0^1 (\partial_\sigma \pi_{+,i}^{C,\varepsilon,\mathrm{rem}})^2 \\
&\lesssim \left(\int_{-\infty}^0 \exp\left(\frac{\sigma}{2\mu\varepsilon}\right)\left(\partial_\sigma \widetilde{\pi}_-^{C,\varepsilon,\mathrm{rem}} + \frac{1}{2\mu\varepsilon}\widetilde{\pi}_-^{C,\varepsilon,\mathrm{rem}}\right)\right)^2 \\
&\qquad + \int_0^1 (\partial_\sigma \pi_{+,i}^{C,\varepsilon,\mathrm{rem}})^2 \\
&\lesssim \varepsilon^{1/2}\left(\int_{-\infty}^0 (\partial_\sigma \widetilde{\pi}_-^{C,\varepsilon,\mathrm{rem}})^2 + \frac{1}{4\mu\varepsilon^2}\int_{-\infty}^0 (\widetilde{\pi}_-^{C,\varepsilon,\mathrm{rem}})^2\right) \\
&\qquad + \int_0^1 (\partial_\sigma \pi_{+,i}^{C,\varepsilon,\mathrm{rem}})^2.
\end{aligned} \tag{3.82}$$

When we combine the previous estimations, we obtain for ε small enough,

$$\begin{aligned}
\int_{-\infty}^0 (\partial_\sigma \widetilde{\pi}_-^{C,\varepsilon,\mathrm{rem}})^2 + \int_0^1 (\partial_\sigma \pi_{+,i}^{C,\varepsilon,\mathrm{rem}})^2 + \int_1^{+\infty} (\partial_\sigma \widetilde{\pi}_{+,e}^{C,\varepsilon,\mathrm{rem}})^2 \\
+ \frac{1}{\mu\varepsilon^2}\int_{-\infty}^0 (\widetilde{\pi}_-^{C,\varepsilon,\mathrm{rem}})^2 + \frac{1}{2}\int_1^{+\infty} (\widetilde{\pi}_{+,e}^{C,\varepsilon,\mathrm{rem}})^2 \\
\leq \mathcal{O}(\varepsilon^5),
\end{aligned} \tag{3.83}$$

which in turn gives the following estimate:

$$\left\|\widetilde{\pi}_-^{C,\varepsilon,\mathrm{rem}}\right\|_{\mathrm{L}^2(-\infty,0)} = \mathcal{O}(\varepsilon^{7/2}), \tag{3.84}$$

$$\left\|\pi_{+,i}^{C,\varepsilon,\mathrm{rem}}\right\|_{\mathrm{L}^2(0,1)} = \mathcal{O}(\varepsilon^{5/2}), \tag{3.85}$$

$$\left\|\widetilde{\pi}_{+,e}^{C,\varepsilon,\mathrm{rem}}\right\|_{\mathrm{L}^2(1,\infty)} = \mathcal{O}(\varepsilon^{5/2}), \tag{3.86}$$

and thus ends the proof of Proposition 3.2

3.6.2 Proof of Lemma 3.1

Using the expressions in (3.67) in (3.66), we can now expand $F(C,\varepsilon)$:

$$\begin{aligned}
F(C,\varepsilon) &= \int_{-\infty}^{0} \pi_{-}^{C,\varepsilon} + \int_{0}^{1} \pi_{+,i}^{C,\varepsilon} + \int_{1}^{+\infty} \pi_{+,i}^{C,\varepsilon} + \varepsilon - \mu\varepsilon^2 \\
&= \int_{-\infty}^{0} \pi_{-}^{C,\varepsilon,\mathrm{rem}} + \int_{0}^{1} \pi_{+,i}^{C,\varepsilon,\mathrm{rem}} + \int_{1}^{+\infty} \pi_{+,i}^{C,\varepsilon,\mathrm{rem}} \\
&\quad + \int_{-\infty}^{0} \pi_{-}^{C,\varepsilon,\mathrm{app}} + \int_{0}^{1} \pi_{+,i}^{C,\varepsilon,\mathrm{app}} + \int_{1}^{+\infty} \pi_{+,i}^{C,\varepsilon,\mathrm{app}} + \varepsilon - \mu\varepsilon^2 \\
&= \int_{-\infty}^{0} \pi_{-}^{C,\varepsilon,\mathrm{rem}} + \int_{0}^{1} \pi_{+,i}^{C,\varepsilon,\mathrm{rem}} + \int_{1}^{+\infty} \pi_{+,i}^{C,\varepsilon,\mathrm{rem}} \\
&\quad + 2C\mu\varepsilon^3 + C\varepsilon^2 + \varepsilon^3 \int_{0}^{1} \theta(\sigma) \left(1 - \exp\left(\frac{\sigma-1}{\mu\varepsilon}\right)\right) \mathrm{d}\sigma + C\varepsilon + \varepsilon - \mu\varepsilon^2
\end{aligned} \tag{3.87}$$

Let us first note that

$$\theta(\sigma) \left(1 - \exp\left(\frac{\sigma-1}{\mu\varepsilon}\right)\right)$$

is bounded by 1 on $[0,1]$ so that

$$\varepsilon^3 \int_{0}^{1} \theta(\sigma) \left(1 - \exp\left(\frac{\sigma-1}{\mu\varepsilon}\right)\right) \mathrm{d}\sigma = \mathcal{O}(\varepsilon^3). \tag{3.88}$$

We now estimate the integrals of $\pi_{-}^{C,\varepsilon,\mathrm{rem}}$, $\pi_{+,i}^{C,\varepsilon,\mathrm{rem}}$ and $\pi_{+,e}^{C,\varepsilon,\mathrm{rem}}$. Since Proposition 3.2 gives us the order of the respective L^2 norms of $\widetilde{\pi}_{-}^{C,\varepsilon,\mathrm{rem}}$ and $\widetilde{\pi}_{+,e}^{C,\varepsilon,\mathrm{rem}}$, we can use them in the estimation of

$$\int_{-\infty}^{0} \pi_{-}^{C,\varepsilon,\mathrm{rem}} + \int_{0}^{1} \pi_{+,i}^{C,\varepsilon,\mathrm{rem}} + \int_{1}^{+\infty} \pi_{+,i}^{C,\varepsilon,\mathrm{rem}}.$$

Indeed we use Hölder Inequality to get the following estimates

$$\begin{aligned}\int_{-\infty}^{0} \pi_{-}^{C,\varepsilon,\mathrm{rem}} &= \int_{-\infty}^{0} \exp\left(\frac{\sigma}{\mu\varepsilon}\right) \widetilde{\pi}_{-}^{C,\varepsilon,\mathrm{rem}} \\ &\lesssim \varepsilon^{1/2} \left\| \widetilde{\pi}_{-}^{C,\varepsilon,\mathrm{rem}} \right\|_{\mathrm{L}^2(-\infty,0)} \lesssim \mathcal{O}(\varepsilon^3), \end{aligned} \tag{3.89}$$

$$\int_{0}^{1} \pi_{+,i}^{C,\varepsilon,\mathrm{rem}} \lesssim \left\| \pi^{C,\varepsilon,\mathrm{rem}} \right\|_{\mathrm{L}^2(0,1)} \lesssim \mathcal{O}(\varepsilon^{5/2}), \tag{3.90}$$

$$\begin{aligned}\int_{1}^{+\infty} \pi_{+,e}^{C,\varepsilon,\mathrm{rem}} &= \int_{1}^{+\infty} \exp\left(\frac{\varepsilon}{2}(\sigma-1)\right) \widetilde{\pi}_{+,e}^{C,\varepsilon,\mathrm{rem}} \\ &\lesssim \frac{1}{\varepsilon^{1/2}} \left\| \widetilde{\pi}_{+,e}^{C,\varepsilon,\mathrm{rem}} \right\|_{\mathrm{L}^2(1,\infty)} \lesssim \mathcal{O}(\varepsilon^2). \end{aligned} \tag{3.91}$$

since, by explicit integration, we get

$$\begin{aligned}\left\| \exp\left(\frac{\cdot}{2\mu\varepsilon}\right) \right\|_{\mathrm{L}^2(-\infty,0)} &= (\mu\varepsilon)^{1/2}, \\ \left\| \exp\left(\frac{\varepsilon}{2}(\cdot-1)\right) \right\|_{\mathrm{L}^2(+1,\infty)} &= \frac{1}{\varepsilon^{1/2}}. \end{aligned}$$

Finally we have

$$\int_{-\infty}^{0} \pi_{-}^{C,\varepsilon,\mathrm{rem}} + \int_{0}^{1} \pi_{+,i}^{C,\varepsilon,\mathrm{rem}} + \int_{1}^{+\infty} \pi_{+,i}^{C,\varepsilon,\mathrm{rem}} = \mathcal{O}(\varepsilon^2). \tag{3.92}$$

Now we use (3.88) and (3.92) in (3.87) to obtain:

$$F(C,\varepsilon) = (C+1)\varepsilon + \mathcal{O}(\varepsilon^2), \tag{3.93}$$

which is exactly what Proposition 3.3 states.

Chapitre 4

Un modèle autoconsistant pour les flots multidimensionnels de matériaux vitreux

Résumé du chapitre

Dans ce chapitre, nous essayons de répondre à une question posée au tout début de ce travail de thèse, et qui était aussi l'un des points centraux à étudier par l'équipe du projet ANR Maniphyc : quels modèles «à fluidité» peut-on écrire pour les fluides vitreux dans des configurations d'écoulement générales (dans la suite il nous arrivera de dire par abus de langage, multidimensionnels) ? Beaucoup d'approches sont pertinentes pour répondre à cette question, que ce soit l'écriture de modèles très généraux comportant de nombreux paramètres et d'une approche par assimilation de données et problème inverse ou l'écriture de modèles phénoménologiques multidimensionnels. Nous nous sommes modestement restreints à la question suivante : peut-on écrire un modèle basé sur les mêmes idées physiques que le modèle d'Hébraud-Lequeux, multidimensionnel et physiquement admissible ? Ce chapitre présente le fruit de nos réflexions, encore incomplètes, sur le sujet.

Ce chapitre contient en fait deux parties : une partie de modélisation où nous construisons le modèle multidimensionnel (4.5) en ajoutant essentiellement des ingrédients pour prendre en compte la question de l'objectivité : nous devons écrire un modèle qui donne une loi de comportement indépendante du référentiel d'observation. L'objectivité matérielle est une question absente de l'étude des modèles en cisaillement simple car les changements de référentiels sont triviaux dans ce cas. Dans des géométries générales, on a beaucoup plus de liberté de mouvement ce qui se traduit par des contraintes

supplémentaires sur les équations. Il faut noter que notre modèle répond à ce problème uniquement lorsque le flot ambiant est incompressible. Ce n'est toutefois pas une restriction très importante car c'est le cas des matériaux auquel le modèle pourrait s'appliquer.

Fidèle à la philosophie développée dans l'introduction de ce manuscrit, nous avons voulu démontrer mathématiquement que ce modèle, tout comme son aîné le modèle d'Hébraud-Lequeux, rendait compte d'une transition vitreuse similaire. C'est à cet effet que nous avons développé les outils des chapitres 2 et 3 : nous voulions obtenir un moyen d'étudier la transition vitreuse suffisamment souple pour s'adapter au modèle (4.5).

La bonne nouvelle, c'est qu'on peut dire aujourd'hui que la méthodologie du chapitre 2 s'applique avec quelque succès dans le cas plus général du modèle (4.5) : nous réussissons à prouver qu'au niveau formel il n'existe que trois types de développement asymptotique valables pour notre modèle et ce sous des hypothèses qui englobent une large classe d'écoulement. C'est l'objet du premier point du théorème 4.1. Il est assez étonnant de voir que ces développements ont les mêmes caractéristiques en terme d'échelles de développement et en terme de tailles de couche limite que les développements du théorème 2.1. Les calculs pour obtenir ces développements sont toutefois beaucoup plus compliqués dans le cas de la transition (4.30) et nécessitent d'analyser finement les symétries des solutions des équations de profil.

Néanmoins le théorème 4.1 reste, pour le moment, plus faible que son homologue d'Hébraud-Lequeux à cause de son point deux. Nous ne sommes pas encore capables d'associer une unique forme de développement à un ensemble de température. La raison de cette insuffisance est la nécessité de montrer la monotonie d'une fonction $F(\nu)$ dont on ne connaît pas l'expression analytique. Dans le cas du modèle d'Hébraud-Lequeux, nous étions capables de trouver l'expression analytique de l'analogue de la fonction $F(\nu)$ et ensuite par une simple étude de fonction de montrer sa croissance. Pour l'instant nous ne sommes capables que de calculer les limites de la fonction F.

Enfin une autre insuffisance de l'étude est l'absence de justification des développements asymptotiques. Notons toutefois que nous avons restreint le cadre fonctionnel de notre étude, en vue d'effectuer cette justification dans l'avenir.

Ce chapitre est constitué d'une première version d'un article écrit en collaboration avec Michael Renardy.

This the first version of an upcoming paper in collaboration with Michael Renardy paper has two parts: the first part is concerned with the modelling of a full tensorial model which keeps the main features of the so-called Hébraud-Lequeux (HL) model for Soft Glassy Material (Hébraud and Lequeux [37]); the second part is devoted to give some mathematical justification to the relevance of our model following the method we developped for HL in [54].

4.1 Modelization

4.1.1 Historical Background

In this article we are interested in the modelling soft glassy materials. Soft glassy materials are named after glasses because they exhibit similar behaviour: very complicated free energy landscapes and a transitional behaviour akin to phase transition. Soft glassy materials can be loosely described as "particles" dispersed inside a Newtonian fluid which may be liquid or gas. When the particles are solids we obtain what are called suspensions, when the particles are liquid bubbles we obtain emulsions. Foams and granular flows may also enter this category

Numerous models exist to describe specific materials: one can cite the model by Jop, Forterre and Pouliquen [40] for dense granular flows or the one by Bénito, Bruneau, Colin, Gay and Molino [6] for foams and emulsions. We want to call these two particular models *tensorial* or *multidimensional* models because they give constitutional equations that are not subject to any geometrical constraint on the flow type: the constitutional law links the full stress tensor to kinetic quantities such as the deformation tensor, the mass density or the temperature.

On the other hand we have models for generic Soft Glassy Material derived from the analogy between Soft Glassy Material and real molecular glasses. The first to have been concieved was by P. Sollich, Lequeux, Hébraud and Cates and simply called SGR (for Soft Glassy Rheology) [68] and was originally a model restricted to simple shear (as is customary in rheology). This model was later generalized to a tensorial version by M. E. Cates and P. Sollich [21]. However this model suffers from one drawback: the constitutive relation depends on an *ad hoc* phenomenological parameter (an effective temperature) which is hard to interpret. This is why Hébraud and Lequeux came up with a modified version of the SGR model [37] whose parameter have a more direct physical interpretation. However this model is designed for simple shear and this article is an attempt to give a tensorial

version of this model.

4.1.2 Scalar and Tensorial Model

Let us precise what we mean by tensorial or simple shear model. It is well known that in a continuous medium there is a tensor T, that is a field of $d \times d$ matrices (d is the space dimension) which describes the internal force that keeps the medium continous. This tensor is called the *stress* tensor. Physically speaking, if an element of surface $\mathrm{d}S$ with orientation n is placed at x then the force that the surface undergoes from one side to the other is $T(x)n\mathrm{d}S$. As a consequence, noting ρ the mass density and u is the Eulerian field of velocity, the conservation of momentum reads:

$$\rho(\partial_t u + u \cdot \nabla u) = \operatorname{div} T,$$

where the divergence of a matrix tensor is the vector of the divergence of its lines.

A constitutive law for a continuous material is a relation between T and kinetic quantities. For instance Newton law of simple fluids reads

$$T = -p_h(\rho, \theta)Id + \lambda(\rho, \theta)(\operatorname{div} u)Id + 2\mu(\rho, \theta)D(\nabla u) \tag{4.1}$$

where θ is the temperature, λ and μ are the viscosities and

$$D(\nabla u) = \frac{1}{2}(\nabla u + (\nabla u)^T)$$

is the *deformation rate* tensor. The term p_h is the *hydrostatic pressure* a given function. Combining this constitutive law with conservation of mass, momentum and energy yields the so-called Compressible Navier-Stokes Equations.

However it is classical in rheology to start the construction of a model by restricting to what is called a *simple shear* situation or *Couette flow*: in this thought experiment, a single small block of material is uniformly sheared. Typically the top surface of the block is displaced in a predefined direction while the bottom surface is kept motionless. In this situation, there is an invariant direction that makes us consider the material as two dimensional. Let us note x and y the plane containing our material. Then we can define x as the shear direction and y as its orthogonal. In this configuration, the velocity field has the special form $u = (\dot{\gamma}(t)y, 0)$. In this configuration, $\dot{\gamma}(t)$ is the *shear rate* and scales as the inverse of a time. We then suppose that no quantity depends on x and the conservation of momentum reads:

$$\rho\partial_t u^x = \partial_y T_{12}. \tag{4.2}$$

As we can see the mechanical effect of the stress in this configuration is given only by one of the component of the stress tensor. Consequently, if in our modelling we restrict ourselves to simple shear situation we only have to give a law linking T_{12} and $\dot{\gamma}$ to describe the flow situation. In this case T_{12} is usually called *the* stress and is a single scalar which we will note τ in the sequel. Examples of laws in this case are for example Newton's law for fluids,

$$\tau = \eta\dot{\gamma}, \tag{4.3}$$

or Hooke's law for linear elasticity

$$\tau = G_0\gamma \tag{4.4}$$

where $\gamma = \int_0^t \dot{\gamma}(t)\mathrm{d}t$ is called the *shear*. Another form of Hooke's law is $\dot{\tau} = G_0\dot{\gamma}$.

The simple shear can be set up experimentally very easily which is why rheologist will often model simple shear laws. However, simple shear do not give the full mechanical behaviour of a material. Think of the Newtonian case of (4.1): a Newtonian fluid has two distinct viscosities usually noted μ and λ but a simple shear flow of a Newtonian flow can only give an information on μ. To have specific information on λ one has to take into account compressible flows of the material. The situation for glassy material is a little different here since we will only be interested in incompressible flows. Yet we cannot exclude that simple shear flows can only see a part of the rheological properties of soft glassy materials. Having a model that can describe any type of flows can overcome this lack of information.

Another motivation for designing multidimensional models comes from experimentation. Not so much is known on multidimensional flows of glassy materials, in part due to the lack of a simple theoretical model to compare the results to.

We end this section by stating that, unfortunately, going from a simple shear model is not a standardized task.

4.1.3 The Simple Shear Hébraud-Lequeux Model

We will now review the (HL) model which is the foundation of our model. The HL model comes from the mean field theory and describes the state of the material at a mesoscopic model and then take some average of this mesoscopic description to give the properties of the material at the macroscopic scale. From a mathematical point of view the model is given by a Fokker-Planck type of equation:

$$\begin{aligned}\partial_t p(t,\sigma) =& -G_0\dot\gamma(t)\partial_\sigma p - \frac{1}{T_0}H(|\sigma|-\sigma_c)p(t,\sigma)\\ &+\Gamma(p(t))\delta(\sigma)+\alpha\Gamma(p(t))\partial^2_\sigma p(t,\sigma),\\ \Gamma(p) =& \frac{1}{T_0}\int H(|\sigma|-\sigma_c)p(t,\sigma)\mathrm{d}\sigma, \qquad \int_{\sigma\in\mathbf{R}} p(t,\sigma)\mathrm{d}\sigma = 1\end{aligned}$$

Let us now describe this equation. First note that p is a function of the time t and of a variable σ which has nothing to do with space but is rather a "mesoscopic stress". Then σ_c and α are constants depending on the fluid: σ_c is a stress threshold above which the fluid relax in a zero stress state with typical time T_0 (H designates the Heaviside function) and α acts as a control parameter: the higher α, the less the fluid can structrure itself and the more it behaves like a Newtonian fluid.

The idea behind this model is to imagine that in the material is composed of mesoscopic particles which undergo the shear rate $\dot\gamma(t)$. Each of these particle has its own stress. Then $p(t,\sigma)\mathrm{d}\sigma$ is the classicaly the numer of particles whose stress is around σ with latitude $\mathrm{d}\sigma$. Now when submitted to a shear rate $\dot\gamma(t)$ the stress of a particle evolves with the following rule: if it is smaller than the stress threshold σ_c then it evolves linearly in time. This behaviour is called an elastic behaviour since it mimics the behaviour of macroscopic elastic Hookean solids. If the stress grows beyond σ_c then the particle wil enter into a relaxation phase and its stress will exponentially decrease to 0. The last mechanism is the following: when a particle relaxes to 0 it will induce a modification of the stress to all the other particles. This accounts for the plastic behaviour of the material.

The equation gives the mesoscopic state p. The average procedure we mentionned allows to recover the macroscopic stress τ by

$$\int_{\sigma\in\mathbf{R}} \sigma p(t,\sigma)\mathrm{d}\sigma.$$

For more details on the underlying physical ideas, we refer to [37] and [54].

4.1.4 Full Tensorial Modelization

Let us introduce here our new model. Since this is a first attempt we have made simplificating assumptions. Our model only works for velocitiy fields

u which are incompressible. As such the Cauchy stress tensor, be it "mesoscopic" or "macroscopic" should be traceless. However we will set our model on the full space of symmetric matrices. We Note Σ the "mesoscopic" variable. The state is still described by a probability density p with respect to the Lebesgue measure on the symmetric matrices (all the technical details can be found on Section ?). The norm used is $|\Sigma|^2 = Tr(\Sigma\Sigma^T)$. The variable x is the space position and as such a vector of $\mathbf{R}^3$. The equation reads:

$$\begin{aligned}\partial_t p(t,x,\Sigma) + u\cdot\nabla_x p - g_a(\Sigma,\nabla u):\nabla_\Sigma p = \\ -2G_0 D(\nabla u):\nabla_\Sigma p(t,x,\Sigma) \\ -\frac{\mathbf{1}_{|\Sigma|>\sigma_c}(\Sigma)}{T_0}p(t,x,\Sigma) + \Gamma(p)(t,x)\rho(\Sigma) \\ +\alpha\Gamma(p)(t,x)\Delta_\Sigma p(t,x,\Sigma) \quad (4.5)\end{aligned}$$

with $g_a(T,\nabla u) = TW(\nabla u) - W(\nabla u)T - a(D(\nabla u)T + TD(\nabla u))$ and $D(M)$, $W(M)$ are the symmetric and skew-symmetric part of the matrix M. The operators Δ_Σ and ∇_Σ are described below. ρ is a radial density probability with compact support in the ball $\{|\Sigma| < \sigma_c\}$, replacing the Dirac mass that was in the $1d$ model.

In this section we explain how we designed the model 4.5. The main difficulty to extend to a multidimensional setting is the need for frame invariance. This problem already arises when one tries to extend the simple Maxwell model for viscoelastic fluids. It is a model for Couette flows and when one tries to extend it to multidimensional setting one realises that the most direct generalization violates the frame invariance. The same problem will arise here.

The frame invariance is the statement that when working in different frames one should observe the same behaviour of the material. Consequently the equations of state of a material should be independent of the frame. A change of frame is roughly a rotation of the physical space of matrix Q. Let us note $x^* = Qx$. When one changes frame, the stress Σ at point x is transformed in to Σ^* at point x^* with the following matricial relation $\Sigma^* = Q\Sigma Q^T$. Now when we want to write equations involving the stress or quantities related to the stress we have to be careful to use quantities that do not depend on the frame.

Let us note $\mathcal{S}_d$ the vector space of d-dimensionned symmetric space which we call the stress space (d is equal to 2 or 3 which means that the stress space is of dimension n equal respectively to 3 or 6). For a given symmetric matrix $S \in \mathcal{S}_d$ we note by $|S|^2$ the following Euclidean norm:

$$|S|^2 = \sum_i S_{ii}^2 + 2\sum_{i<j} S_{ij}^2 = Tr(SS^T). \tag{4.6}$$

We note that this norm is frame indifferent for the stress space. For Q in $\mathcal{O}_d$ (the set of orthogonal matrices) we note ϕ_Q the isomorphism of the space of d-by-d symmetric matrices defined by $\phi_Q(\Sigma) = Q\Sigma Q^T$.Then we have

$$\begin{aligned} |\Sigma^*|^2 &= Tr(\Sigma^*(\Sigma^*)^T) \\ &= Tr(Q\Sigma Q^T(Q\Sigma Q^T)^T) \\ &= Tr(Q\Sigma Q^T Q\Sigma^T Q^T) \\ &= Tr(\Sigma\Sigma^T) \\ &= |\Sigma|^2 \end{aligned} \tag{4.7}$$

since $Q^T = Q^{-1}$. Thus ϕ_Q is a metric preserving isomorphism. We can also show that $\det\phi_Q = (\det Q)^{d+1}$. When d is odd we then have $\det\phi_Q = 1$ and then ϕ_Q is a rotation in the space $(\mathcal{S}_d, |\cdot|)$. For the sake of brevity we shall call ϕ_Q a rotation in stress space even if d is even.

We will now look for a density of probability $p(t, x, \Sigma)$ over S_d. The extra stress tensor will be computed by the formula

$$T(t, x) = \int \Sigma p(t, x, \Sigma)\mathrm{d}\Sigma \tag{4.8}$$

where the measure $\mathrm{d}\Sigma$ is simply $\prod_{i\leq j} \mathrm{d}\Sigma_{ij}$ (a measure which is actually invariant by rotation in stress space). We extend the relaxation part by virtually the same formula than in one dimension except that for incompressible flows only the deviatoric part of the stress matrix should be taken into account. For any symmetric matrix Σ we will note by Σ_{dev} the deviatoric part of the matrix: $\Sigma_{\mathrm{dev}} = \Sigma - (Tr\Sigma)/dId$ ($\Sigma \mapsto \Sigma_{\mathrm{dev}}$ is the orthogonal projection onto the space of traceless matrices). We now note $\Gamma(p) = \int_{|\Sigma_{\mathrm{dev}}|>\sigma_c} p(t, x, \Sigma)\mathrm{d}\Sigma$ and the relaxation part becomes:

$$-\frac{\mathbf{1}_{|\Sigma_{\mathrm{dev}}|>\sigma_c}(\Sigma)}{T_0} p(t, x, \Sigma) + \Gamma(p)(t, x)\rho(\Sigma). \tag{4.9}$$

For technical and possibly modelization reason we do not want necessarily to put the Dirac mass so we put instead ρ which is a rotation invariant measure with compact support in the set $\{|\Sigma| \leq \sigma_c\}$. We subsequently note $\mathcal{M}$ the set of these measures. We replace the diffusion by a Laplacian-like operator.

We want a differential operator which is invariant through the group that preserves the Euclidean norm (and henceforth verifies invariance through a frame change). The operator is then

$$\Delta_\Sigma p = \sum_{i=1}^{3} \partial^2_{\Sigma_{ii}} p + 1/2 \sum_{i<j} \partial^2_{\Sigma_{ij}}, \tag{4.10}$$

and the diffusion then becomes

$$\alpha\Gamma(p)\Delta_\Sigma p. \tag{4.11}$$

Now for the elastic part we just want to obtain Hooke's law for linear elasticity so we put:

$$2G_0 D(u) : \nabla_\Sigma p. \tag{4.12}$$

so that when we integrate against Σ we obtain $G_0 D(u)$ where : is the usual tensor contraction $A : B = \sum_{i,j} A_{ij} B_{ij}$ (see below). Finally we have to treat the time derivative. As usual we have to use an objective time derivative and for that we have to add terms to the equation because we need to make sure that the resulting tensor is frame indifferent. Along the line of the Upper-convected Maxwell (UCM) model, we want the inertial part to look like :

$$\frac{\mathrm{d}T}{\mathrm{d}t} + g_a(T, \nabla u) = \partial_t T + u \cdot \nabla_x T + g_a(T, \nabla u), \tag{4.13}$$

where $g_a(T, \nabla u) = TW(\nabla u) - W(\nabla u)T - a(D(\nabla u)T + TD(\nabla u))$ with $D(\nabla u) = (\nabla u + (\nabla u)^T)/2$ and $W(\nabla u) = (\nabla u - (\nabla u)^T)/2$ and $a \in [-1, 1]$. Actually when the flow is incompressible (i.e. when we have $\operatorname{div} u = Tr(D(\nabla u)) = 0$ the same derivative can be used at the mesoscopic level. Indeed, let us consider the term $g_a(\Sigma, \nabla u) : \nabla_\Sigma p$. It is composed of terms of the form $M\Sigma : \nabla_\Sigma p$ or $\Sigma M : \nabla_\Sigma p$ where M is a traceless matrix (either because M is skew-symmetric or because its trace is $\operatorname{div} u = 0$). Now multiply by Σ and integrate over stress space. Using Einstein's summation convention we have:

$$\begin{aligned}
\left[\int_\Sigma (M\Sigma : \nabla_\Sigma p(\Sigma))\, \Sigma \mathrm{d}\Sigma\right]_{ij} &= \int_\Sigma M_{kl}\Sigma_{lm}\partial_{\Sigma_{km}} p(\Sigma)\Sigma_{ij}\mathrm{d}\Sigma \\
&= -\int_\Sigma M_{kl} p(\Sigma)\partial_{\Sigma_{km}}(\Sigma_{ij}\Sigma_{lm})\mathrm{d}\Sigma \\
&= -\int_\Sigma M_{il} p(\Sigma)\Sigma_{lj}\mathrm{d}\Sigma - \int_\Sigma M_{ll} p(\Sigma)\Sigma_{ij}\mathrm{d}\Sigma
\end{aligned} \tag{4.14}$$

This yields the following matrix relation:

$$\int_{\Sigma} M\Sigma : \nabla_{\Sigma} p \Sigma \mathrm{d}\Sigma = -MT - Tr(M)T \tag{4.15}$$

Incidently this proves that when one integrates $-G_0 D(\nabla u) : \nabla_{\Sigma} p$ against Σ one finds $2G_0 D(\nabla u)T$ as in the UCM Model. Now as we noted, the matrix we consider are traceless so if we integrate the term $g_a(\Sigma, \nabla u) : \nabla_{\Sigma} p$ against Σ we find $-g_a(T, \nabla u)$. We can also note another fact on the term $g_a(\Sigma, \nabla u) : \nabla p$: its integral is 0 under the constraint that $\operatorname{div} u$ is 0. Indeed if we integrate one of the terms of $g_a(\Sigma, \nabla u) : \nabla p$ as we did before but without multiplying by Σ we obtain:

$$\begin{aligned} \int_{\Sigma} \left(M\Sigma : \nabla_{\Sigma} p(\Sigma)\right) \mathrm{d}\Sigma &= \int_{\Sigma} M_{ik} \Sigma_{kj} \partial_{\Sigma_{ij}} p(\Sigma) \mathrm{d}\Sigma \\ &= -\int_{\Sigma} M_{ii} p(\Sigma) \mathrm{d}\Sigma \end{aligned} \tag{4.16}$$

which yields the general relation:

$$\int_{\Sigma \in \mathbf{R}^n} g_a(\Sigma, \nabla u) : \nabla_{\Sigma} p(\Sigma) \mathrm{d}\Sigma = 2a(\operatorname{div} u) \int_{\mathbf{R}^n} p. \tag{4.17}$$

We finally obtain the following model:

$$\begin{aligned} &\partial_t p(t,x,\Sigma) + u \cdot \nabla_x p - g_a(\Sigma, \nabla u) : \nabla_{\Sigma} p = \\ &-2G_0 D(\nabla u) : \nabla_{\Sigma} p(t,x,\Sigma) \\ &\qquad - \frac{\mathbf{1}_{|\Sigma| > \sigma_c}(\Sigma)}{T_0} p(t,x,\Sigma) + \Gamma(p)(t,x)\delta_0(\Sigma) \\ &\qquad\qquad + \alpha \Gamma(p)(t,x) \Delta_{\Sigma} p(t,x,\Sigma) \end{aligned}$$

with $g_a(T, \nabla u) = TW(\nabla u) - W(\nabla u)T - a(D(\nabla u)T + TD(\nabla u))$. Note that integrating this equation against one yields the general relation:

$$\partial_t \int p - 2a(\operatorname{div} u) \int p = \Gamma - \frac{1}{T_0} \int_{|\Sigma| > \sigma_c} p \tag{4.18}$$

and thus for divergence-free velocity fields the conservation of the integral of p is equivalent to the following relation between fluidity

$$\Gamma = \frac{1}{T_0} \int_{|\Sigma| > \sigma_c} p. \tag{4.19}$$

The situation is then exactly the same as in the one dimensional HL. Let us now rewrite the system in non dimensional variables. We set:

$$\Sigma' = \frac{\Sigma}{\sigma_c}, \qquad p' = \sigma_c^n p, \qquad \Gamma' = \int_{|\Sigma'|>1} p'(\Sigma')\mathrm{d}\Sigma', \tag{4.20}$$

for mesoscopic variables and

$$x' = \frac{x}{L}, \qquad t' = \frac{t}{T}, \qquad u' = \frac{T}{L}u \tag{4.21}$$

for macroscopic variables. Now introducing the three dimensionless numbers

$$\lambda = \frac{G_0}{\sigma_c}, \qquad We = \frac{T_0}{T}, \qquad \mu = \frac{\alpha}{\sigma_c^2}, \tag{4.22}$$

we rewrite the system as

$$\begin{aligned}\partial_t p(t,x,\Sigma) + u\cdot\nabla_x p - g_a(\Sigma,\nabla u) : \nabla_\Sigma p = \\ -2\lambda D(u) : \nabla_\Sigma p(t,x,\Sigma) \\ - \frac{\mathbf{1}_{|\Sigma|>1}(\Sigma)}{We} p(t,x,\Sigma) + \frac{1}{We}\Gamma(p)(t,x)\delta_0(\Sigma) \\ + \frac{\mu}{We}\Gamma(p)(t,x)\Delta_\Sigma p(t,x,\Sigma)\end{aligned} \tag{4.23}$$

completed with the constraint

$$\int_{\mathbf{R}^n} p = 1, \tag{4.24}$$

and some initial condition.

Let us point out that we work on the symmetric matrices space not the traceless symmetric one. With only minor changes we could work in this space (this would mean working in an $n-1$-dimensional space instead of an n-dimensional space with $n = d(d+1)/2$ and d is 2 or 3 and is the physical space dimension)

4.2 Main Results

To study the glass transition in our model is to study the low deformation rate limit of the stationary version of (4.23). The question is equivalent

to studying the limit as $\varepsilon \to 0$ of a solution p^ε (supposed to exist), of the following problem

$$\begin{cases} -\mu\Gamma^\varepsilon \Delta p^\varepsilon + \varepsilon \left(A\Sigma + A^0\right) \cdot \nabla p^\varepsilon + \mathbf{1}_{|\Sigma|>1}(\Sigma) p^\varepsilon = \Gamma^\varepsilon \rho, \\ \Gamma^\varepsilon = \displaystyle\int_{|\Sigma|>1} p^\varepsilon(\Sigma) \mathrm{d}\Sigma, \\ 2^{3/2} = \displaystyle\int_{\mathbf{R}^6} p^\varepsilon(\Sigma) \mathrm{d}\Sigma. \end{cases}$$

It is actually more convenient to work with the following equivalent system, where we have separated what happens inside and outside the unit ball.

$$\begin{cases} -\mu\Gamma^\varepsilon \Delta q^\varepsilon + \varepsilon(A\Sigma + A^0) \cdot \nabla q^\varepsilon = \Gamma^\varepsilon \rho & \text{in } |\Sigma| < 1, \\ -\mu\Gamma\varepsilon \Delta r^\varepsilon + \varepsilon(A\Sigma + A^0) \cdot \nabla r^\varepsilon + r^\varepsilon = 0 & \text{in } |\Sigma| > 1, \\ q^\varepsilon = r^\varepsilon & \text{on } |\Sigma| = 1, \\ \partial_n q^\varepsilon = \partial_n r^\varepsilon & \text{on } |\Sigma| = 1, \\ \displaystyle\int_{|\Sigma|\leq 1} q^\varepsilon(\Sigma) \mathrm{d}\Sigma + \int_{|\Sigma|>1} r^\varepsilon(\Sigma) \mathrm{d}\Sigma = 2^{3/2}. \end{cases} \tag{4.25}$$

Let us precise the mathematical setting. The analysis conducted in the paper is not fully justified for two reasons. Firstly, we assume existence and uniqueness of solutions of System (4.25) in a proper functional sense. This is not at all a light objection: even for the $1d$ model where we can compute the analytical solution of differential equations, the uniqueness of a solution satisfying the integral constraint requires a lot of heavy computations (see [53]). Secondly, we do not carry the usual remainder estimations to justify the asymptotic expansions we make. This second objection would not have a lot of meaning without the first objection taken care of first anyway.

On the other hand, we are not at a purely formal level either: we introduce thereafter a mathematical basis which allow us to justify the existence and assert the uniqueness of the terms of the formal asymptotic expansions.

This work could thus lay ground for a perfectly rigorous analysis in the following way: one could write a formal remainder problem and try to prove the wellposedness of this problem and then *define* the solution to System (4.25) for small ε to be the symptotic expansion plus the rest.

Let us start with two minimal hypotheses:

1. The measure ρ belongs to the space $\mathcal{M} \cap W^{-1,\beta}(B)$ for $1 < \beta \leq 2$.

2. $\Sigma \mapsto A\Sigma + A^0$ is a divergence-free vector field. All characteristic curves of points of the unit ball cross the unit sphere outwardly.

Hypothesis 1 allows for $\rho = \delta_0$. Moreover, the following system

$$\begin{cases} -\Delta E = \rho & \text{in } |\Sigma| \leq 1, \\ E = 0 & \text{on } |\Sigma| = 1. \end{cases} \tag{4.26}$$

defines a unique E in $\mathrm{W}_0^{1,\beta}(B)$ (see MEYERS, [49]). From E we define

$$\mu_c = 2^{-3/2} \int_{|\Sigma|\leq 1} E(\Sigma) \mathrm{d}\Sigma. \tag{4.27}$$

Let us now define Y, a space of function on the complementary of the unit ball so, that

1. Y is continuously embbedded in $\mathrm{L}^1(\bar{B}^c)$;
2. For every $f \in \mathrm{W}^{-1,\beta}(B)$ and every $\kappa > 0$ the problem

$$\begin{cases} -\kappa\Delta\bar{q} = f & \text{in } |\Sigma| < 1 \\ -\kappa\Delta\bar{r} + \bar{r} = 0 & \text{in } |\Sigma| > 1 \\ \bar{q} = \bar{r} & \text{on } |\eta| = 1 \\ \partial_\nu \bar{q} = \partial_\nu \bar{r} & \text{on } |\eta| = 1 \end{cases}$$

is well-posed in $\mathrm{W}^{1,\beta}(B) \times Y$.

If we follow [54, 55], we know that there must be a constant $\omega > 0$ so that we could take Y to be $\{u, \exp(\omega|\Sigma|)u \in \mathrm{W}^{1,\beta}(\bar{B}^c)\}$ but Properties 1 and 2 are the only one we really need.

Let us note $\theta_e(\Sigma) = |\Sigma| - 1$ the exterior distance to the unit sphere. Now the main result can be stated:

Theorem 4.1. *1. If a given solution $(q^\varepsilon, r^\varepsilon)$ of (4.25) is to have an asymptotic expansion with terms in $\mathrm{W}^{1,\beta}$ for q^ε and in Y for r^ε then this expansion can only be of one of the following types*

- *First type*

$$\begin{cases} q(\Sigma) = \overline{Q}^0 + \varepsilon\overline{Q}^1 + \varepsilon^2\overline{Q}^2 + \dots, \\ r(\Sigma) = \overline{R}^0 + \varepsilon\overline{R}^1 + \varepsilon^2\overline{R}^2 + \dots, \end{cases} \tag{4.28}$$

  where $\overline{Q}^k$ and $\overline{R}^k$ are functions of Σ.

- *Second type*

$$\begin{cases} q(\Sigma) = \overline{Q}^0 + \varepsilon^{1/2}\overline{Q}^1 + \varepsilon\overline{Q}^2 + \dots, \\ r(\Sigma) = \varepsilon^{1/2}R^1 + \varepsilon R^2 + \dots, \end{cases} \tag{4.29}$$

  where $\overline{Q}^k$ is a function of Σ and R^k is a function of $(\Sigma/|\Sigma|, \theta_e(\Sigma)/\varepsilon^{1/2})$.

- *Third type*

$$\begin{cases} q(\Sigma) = \overline{Q}^0 + \varepsilon^{1/5}\overline{Q}^1 + \varepsilon^{2/5}\overline{Q}^2 + \dots, \\ r(\Sigma) = \varepsilon^{2/5}R^2 + \varepsilon^{3/5}R^3 + \dots, \end{cases} \tag{4.30}$$

where $\overline{Q}^k$ *is a function of* Σ *and* R^k *is a function of* $(\Sigma/|\Sigma|, \theta_e(\Sigma)/\varepsilon^{2/5})$.

2. **If** $\mu > \mu_c$, *the expansion can only be of type* (4.28) *or* (4.29).
   If $\mu = \mu_c$, *the expansion can only be of type* (4.30) *or* (4.29).
   If $\mu < \mu_c$, *the expansion can only be of type* (4.29).

We remark that this theorem is weaker than its equivalent for the $1d$ model [54, Proposition 5.1] because we cannot restrain expansions of type (4.29) to the range of μ, $]0, \mu_c[$. The reason for that is made clear in Section 4.4.3

4.3 Formal Expansions for Small Deformation Rates

In this section we want to determine the behaviour of the model for small deformation rates. To keep it simple we study the stationary solution (no time dependence) with also a spatially homogeneous vector field (∇u is a constant matrix and there is no space dependence). We want to study the behaviour of the model around the rest state (corresponding to $\nabla u = 0$). For all classical rheological flow we can set $\nabla u = \varepsilon M$ where M is a given matrix and $\varepsilon \sim |\nabla u|$ is a positive number thought as small. For example for the $2d$ elongational flow we have $M = \begin{bmatrix} 1 & 0 & 0 \\ 0 & -1 & 0 \\ 0 & 0 & 0 \end{bmatrix}$ and $\varepsilon = |\dot{\varepsilon}| = |\nabla u|/\sqrt{2}$. Then what we want to study is

$$\begin{cases} -\dfrac{\mu}{We}\Gamma\Delta_\Sigma p + \varepsilon(2\lambda D(M) - g_a(\Sigma, M)) : \nabla_\Sigma p + \dfrac{1}{We}h(|\Sigma|)p = \dfrac{1}{We}\Gamma\delta_0 \\ \displaystyle\int_{\Sigma\in\mathcal{S}(\mathbf{R}^d)} p(\Sigma)\mathrm{d}\Sigma = 1 \end{cases} \tag{4.31}$$

4.3.1 Notations

We first have to rewrite the model with more suitable notations and variables.

Space and Operators.

Firslty we have to choose a basis to write the matrices Σ because the notations are not very convenient to do PDE analysis. We use the canonical basis of the space $\mathcal{S}(\mathbf{R}^3)$ to identify it with $\mathbf{R}^6$ via the map

$$\begin{pmatrix} \Sigma_1 \\ \vdots \\ \Sigma_6 \end{pmatrix} \mapsto \begin{pmatrix} \Sigma_1 & \Sigma_4 & \Sigma_5 \\ \Sigma_4 & \Sigma_2 & \Sigma_6 \\ \Sigma_5 & \Sigma_6 & \Sigma_3 \end{pmatrix}. \tag{4.32}$$

Through this identification, integration over the space of symmetric matrices is the same as integration over $\mathbf{R}^6$ with the Lebesgue measure $\mathrm{d}\Sigma_1 \cdots \mathrm{d}\Sigma_6$. By definition of the norm of the matrice we have

$$|\Sigma|^2 = \Sigma_1^2 + \Sigma_2^3 + \Sigma_3^2 + 2\Sigma_4^2 + 2\Sigma_5^2 + 2\Sigma_6^2, \tag{4.33}$$

so we finally set $\Sigma' \in \mathbf{R}^6$ in the following way:

$$\Sigma'_i = \Sigma_i, \tag{4.34}$$

for $i = 1, 2, 3$ and

$$\Sigma'_i = \sqrt{2}\Sigma_i, \tag{4.35}$$

for $i = 4, 5, 6$. Now rewriting the model with this new variables we have (dropping the prime)

$$\begin{cases} -\mu\Gamma\Delta p + We\varepsilon L(\Sigma, \nabla)p + h(|\Sigma|)p = \Gamma\rho \\ \displaystyle\int_{\Sigma\in\mathcal{S}(\mathbf{R}^d)} p(\Sigma)\mathrm{d}\Sigma = 2^{3/2} \end{cases} \tag{4.36}$$

where now $|\cdot|$ is the classical Euclidean norm on $\mathbf{R}^6$ and Δ is the classical Laplacian. The operator L is first order and its coefficients are affine functions of Σ. If we want we can write the operator $L(\Sigma, \nabla) = (A\Sigma + A^0)\cdot\nabla$ where A is a matrix over $\mathbf{R}^6$ and A^0 is a constant vector from $\mathbf{R}^6$. The general expression of A and A^0 in terms of M, a and λ are given in appendix.

Note one very important fact is that the matrice A is always traceless because M is, considering that we study incompressible flows.

Interior and Exterior Problem.

Following the ideas of the $1d$ model we write q for the interior part of p and r for its exterior part. We also take the Weissenberg number to be 1. If we write the system verified by q and r we find

$$
\begin{aligned}
&-\mu\Gamma\Delta q+\varepsilon L(\Sigma,\nabla)q=\Gamma\rho && \text{in } |\Sigma|<1, && (4.37)\\
&-\mu\Gamma\Delta r+\varepsilon L(\Sigma,\nabla)r+r=0 && \text{in } |\Sigma|>1, && (4.38)\\
&q=r && \text{on } |\Sigma|=1, && (4.39)\\
&\partial_n q=\partial_n r && \text{on } |\Sigma|=1, && (4.40)\\
&\int_{|\Sigma|\leq 1} q(\Sigma)\mathrm{d}\Sigma+\int_{|\Sigma|>1} r(\Sigma)\mathrm{d}\Sigma=2^{3/2}. && && (4.41)
\end{aligned}
$$

4.3.2 Ansaetze and Equations of Profile

We now introduce the function $\theta_e(\Sigma)=|\Sigma|-1$, the exterior distance to the unit sphere. We can now write some ansatz for q and r when ε goes to 0.

Notations for the Profiles We write

$$q(\Sigma)=\sum_k \varepsilon^{k/s}\overline{Q}^k(\Sigma), \tag{4.42}$$

$$r(\Sigma)=\sum_k \varepsilon^{k/s}\overline{R}^k(\Sigma)+\sum_k \varepsilon^{k/s}R^k\left(\Sigma,\frac{\theta_e(\Sigma)}{\varepsilon^{l/s}}\right), \tag{4.43}$$

$$\Gamma=\sum_k \tilde{c}_k\varepsilon^{k/s}. \tag{4.44}$$

The profiles R^k are boundary profiles depending on the direction $\eta=\Sigma/|\Sigma|$ and the fast variable $z=\theta_e(\Sigma)/\varepsilon^{l/s}$. We expect them to be exponentially decreasing at infinity in z and we make the following formal assumption:

$$\forall k,m,m',m''\geq 0,\ ||\Sigma|^m\nabla_\Sigma^{m'}\partial_z^{m'}R^k(\eta,z)|\rightarrow_{z\to 0}0 \tag{4.45}$$

We recall that we have the consistency relation $\Gamma=\displaystyle\int_{|\Sigma|>1} r(\Sigma)\mathrm{d}\Sigma$ so there is a relation between the coefficients $\tilde{c}_k$ and the profiles $\overline{R}^k$ and R^k. We can formally write

$$\begin{aligned}\int_{|\Sigma|>1} R^k\left(\frac{\Sigma}{|\Sigma|},\frac{\theta_e(\Sigma)}{\varepsilon^{l/s}}\right)\mathrm{d}\Sigma &= \int_1^{+\infty}\int_{|\eta|=1} R^k\left(\eta,\frac{\rho-1}{\varepsilon^{l/s}}\right)\rho^5\mathrm{d}\rho\mathrm{d}\eta,\\ &= \int_0^{+\infty}\int_{|\eta|=1} R^k(\eta,z)\,(1+\varepsilon^{l/s}z)^5\varepsilon^{l/s}\mathrm{d}z\mathrm{d}\eta,\\ &= \int_0^{+\infty}\int_{|\eta|=1} R^k(\eta,z)\sum_m\binom{m}{5}(\varepsilon^{l/s}z)^m\varepsilon^{l/s}\mathrm{d}z\mathrm{d}\eta,\\ &= \sum_{m=0}^{5} c_k^m\varepsilon^{(ml+l)/s},\end{aligned} \tag{4.46}$$

with

$$c_k^m = \int_{|\eta|=1}\int_0^{+\infty}\binom{m}{5}R^k(\eta,z)\,z^m\mathrm{d}z\mathrm{d}\eta. \tag{4.47}$$

We also define $\overline{c}_k$ to be

$$\overline{c}_k = \int_{|\Sigma|>1}\overline{R}^k(\Sigma)\mathrm{d}\Sigma. \tag{4.48}$$

Now using these newly defined coefficients, if we formally integrate (4.43) we obtain

$$\begin{aligned}\Gamma &= \sum_{k\geq 0}\overline{c}_k\varepsilon^{k/s} + \sum_{k\geq 0}\sum_{m=0}^{5} c_k^m\varepsilon^{(k+(m+1)l)/s}\\ &= \sum_{k\geq 0}\overline{c}_k\varepsilon^{k/s} + \sum_{m=0}^{5}\sum_{k\geq(m+1)l} c_{k-(m+1)l}^m\varepsilon^{k/s}.\end{aligned} \tag{4.49}$$

Consequently, given the definition of the expansion of Γ we find:

$$\tilde{c}_k = \begin{cases}\overline{c}_k & \text{if } k<l,\\ \overline{c}_k + \displaystyle\sum_{1\leq m'}^{\min(6,m)} c_{k-m'l}^{m'-1} & \text{if } ml\leq k<(m+1)l \text{ for } m\geq 1.\end{cases} \tag{4.50}$$

Equations of Profies.

We now put these ansaetze in (4.37)-(4.41) and assemble the terms of the same formal order. We obtain the following hierarchy of equations.

Equation (4.37): We put the ansatz (2.18a) and the ansatz (2.18c) in (4.37):

$$\begin{aligned} 0 \le k \le s-1 : \quad & -\mu \sum_{k'=0}^{k} \tilde{c}_{k'} \Delta \overline{Q}^{k-k'} = \tilde{c}_k \rho, \\ s \le k : \quad & -\mu \sum_{k'=0}^{k} \tilde{c}_{k'} \Delta \overline{Q}^{k-k'} + L(\Sigma, \nabla) \overline{Q}^{k-s} = \tilde{c}_k \rho. \end{aligned} \tag{4.51a}$$

Equation (4.38): We put the ansatz (2.18b) and the ansatz (2.18c) in (4.38). To do the computations we need some differential calculus formulae. Note f a function of $\Sigma \in \mathbf{R}^n$ and $z \in \mathbf{R}$. Then we have

$$\begin{aligned} \nabla \left(f\left(\frac{\Sigma}{|\Sigma|}, \frac{\theta_e(\Sigma)}{\varepsilon^{l/s}} \right) \right) &= \frac{1}{|\Sigma|} \nabla_{\tan} f\left(\frac{\Sigma}{|\Sigma|}, \frac{\theta_e(\Sigma)}{\varepsilon^{l/s}} \right) + \frac{1}{\varepsilon^{l/s}} \partial_z f\left(\frac{\Sigma}{|\Sigma|}, \frac{\theta_e(\Sigma)}{\varepsilon^{l/s}} \right) \frac{\Sigma}{|\Sigma|}, \\ \Delta \left(f\left(\frac{\Sigma}{|\Sigma|}, \frac{\theta_e(\Sigma)}{\varepsilon^{l/s}} \right) \right) &= \frac{1}{|\Sigma|^2} \Delta_{\tan} f\left(\frac{\Sigma}{|\Sigma|}, \frac{\theta_e(\Sigma)}{\varepsilon^{l/s}} \right) + \frac{1}{\varepsilon^{l/s}} \frac{n-1}{|\Sigma|} \partial_z f\left(\frac{\Sigma}{|\Sigma|}, \frac{\theta_e(\Sigma)}{\varepsilon^{l/s}} \right) \\ &\quad + \frac{1}{\varepsilon^{2l/s}} \partial_z^2 f\left(\frac{\Sigma}{|\Sigma|}, \frac{\theta_e(\Sigma)}{\varepsilon^{l/s}} \right). \end{aligned}$$

The formula is valid if we place ourselves in a space of dimension n but here $n = 6$. The operators $\nabla_{\tan}$ and $\Delta_{\tan}$ operate on the first component of f only. Their definitions is as follow:

$$(\nabla_{\tan}) f(\eta) = \Pi_{\eta^\perp} \nabla f, \tag{4.51b}$$

where $\Pi_{\eta^\perp}$ is the orthogonal projection onto the vector space $\{\eta\}^\perp$ and

$$(\Delta_{\tan} f)(\eta) = \mathrm{Tr}(\Pi_{\eta^\perp}^T \mathrm{d}^2 f(\eta) \Pi_{\eta^\perp}) + \nabla f \cdot \eta. \tag{4.51c}$$

Identifying formal powers of ε and using the formal decay of the boundary profiles one finds for the non BL terms :

$$\begin{aligned} 0 \le k < s : \quad & -\mu \sum_{k'=0}^{k} \tilde{c}_{k'} \Delta \overline{R}^{k-k'} + \overline{R}^k = 0 \\ s \le k : \quad & -\mu \sum_{k'=0}^{k} \tilde{c}_{k'} \Delta \overline{R}^{k-k'} + \overline{R}^k = -L(\Sigma, \nabla) \overline{R}^{k-s} \end{aligned} \tag{4.51d}$$

and for the boundary layer terms:

$$
\begin{aligned}
&-2l \le k < -l: \\
&\qquad -\mu \sum_{k'=0}^{k+2l} \tilde{c}_{k'} \partial_z^2 R^{k+2l-k'} = 0, \\
&-l \le k < 0: \\
&\qquad -\mu \sum_{k'=0}^{k+2l} \tilde{c}_{k'} \partial_z^2 R^{k+2l-k'} - \frac{5\mu}{|\Sigma|} \sum_{k'=0}^{k+l} \tilde{c}_{k'} \partial_z R^{k+l-k'}, \\
&\qquad = 0 \\
&0 \le k < s-l: \\
&\qquad -\mu \sum_{k'=0}^{k+2l} \tilde{c}_{k'} \partial_z^2 R^{k+2l-k'} - \frac{5\mu}{|\Sigma|} \sum_{k'=0}^{k+l} \tilde{c}_{k'} \partial_z R^{k+l-k'} \\
&\qquad -\frac{\mu}{|\Sigma|^2} \sum_{k'=0}^{k} \tilde{c}_{k'} \Delta_{\tan} R^{k-k'} + R^k = 0, \\
&s-l \le k < s: \\
&\qquad -\mu \sum_{k'=0}^{k+2l} \tilde{c}_{k'} \partial_z^2 R^{k+2l-k'} - \frac{5\mu}{|\Sigma|} \sum_{k'=0}^{k+l} \tilde{c}_{k'} \partial_z R^{k+l-k'} \\
&\qquad -\frac{\mu}{|\Sigma|^2} \sum_{k'=0}^{k} \tilde{c}_{k'} \Delta_{\tan} R^{k-k'} + R^k + L\left(\Sigma, \frac{\Sigma}{|\Sigma|}\right) \partial_z R^{k-(s-l)} = 0, \\
&s \le k: \\
&\qquad -\mu \sum_{k'=0}^{k+2l} \tilde{c}_{k'} \partial_z^2 R^{k+2l-k'} - \mu \sum_{k'=0}^{k+l} \tilde{c}_{k'} \frac{5}{|\Sigma|} \partial_z R^{k+l-k'} \\
&\qquad -\frac{\mu}{|\Sigma|^2} \sum_{k'=0}^{k} \tilde{c}_{k'} \Delta_{\tan} R^{k-k'} + R^k \\
&\qquad + L\left(\Sigma, \frac{\Sigma}{|\Sigma|}\right) \partial_z R^{k-(s-l)} + \frac{1}{|\Sigma|} L(\Sigma, \nabla_{\tan}) R^{k-s} = 0,
\end{aligned}
\tag{4.51e}
$$

Equation (4.39): The continuity relation translates into

$$
0 \le k: \qquad \overline{Q}^k(\eta) = \overline{R}^k(\eta) + R^k(\eta, 0) \qquad \forall \eta,\, |\eta| = 1. \tag{4.51f}
$$

Equation (4.40): The continuity of the derivative translates into (given that

θ'_e is non zero):

$$0 \leq k < l : \quad 0 = \partial_z R^k(\eta, 0) \qquad \forall \eta,\ |\eta| = 1, \quad (4.51g)$$

$$0 \leq k : \qquad \nabla \overline{Q}^k(\eta) \cdot \eta = \nabla \overline{R}^k(\eta) \cdot \eta + \partial_z R^{k+l}(\eta, 0) \quad \forall \eta,\ |\eta| = 1. \quad (4.51h)$$

Equation (4.41): Finally we get from Eq. (4.41) the following constraints for the profile:

$$\begin{aligned} k = 0 : \quad & \int_{-1}^{1} \overline{Q}^0(\sigma) \mathrm{d}\sigma + \tilde{c}_0 = 2^{3/2}, \\ k > 0 : \quad & \int_{-1}^{1} \overline{Q}^k(\sigma) \mathrm{d}\sigma + \tilde{c}_k = 0. \end{aligned} \quad (4.51i)$$

4.4 The Fundamental Problems

The first part of the proof of Theorem 4.1 is to look for the fundamental problems, that is the problems solved by the terms of lower order $\overline{Q}^0$, $\overline{R}^0$. First, we give here a proposition which tels us on which condition on the expansion of Γ^ϵ we will have boundary layer terms.

Proposition 4.1. *We have only one alternative:*

- *if* $\tilde{c}_0 \neq 0$ *all the* R^k *are identically* 0.
- *if* $\tilde{c}_0 = 0$ *all the* $\overline{R}^k$ *are identically* 0. *We also have that all the coefficients* $\tilde{c}_1, \ldots, \tilde{c}_{2l-1}$ *must be* 0 *while* $\tilde{c}_{2l}$ *must be positive. Finally we have that* $R^0, \ldots, R^{l-1}$ *must be identically* 0.

Proof. First let us assume that $\tilde{c}_0 \neq 0$. We can take Eq (4.51e) with $k = -2l$ which gives the equation

$$-\mu \tilde{c}_0 \partial_z^2 R^0 = 0 \quad (4.52)$$

which means that R^0 is affine in z but since R^0 must decay exponentially to 0 when z goes to infinity this gives $R^0 = 0$ identically. Now we see that since $\tilde{c}_0 \neq 0$ taking $k = -2l + p$ in Eq (4.51e) one finds the equation:

$$-\mu \tilde{c}_0 \partial_z^2 R^p = \text{terms involving profiles } R^j \text{ of order } j < p \quad (4.53)$$

which means that we can show by induction that all R^p are zero in the same way that we did for R^0. Now suppose $\tilde{c}_0 \neq 0$. We define K to be the first index for which $\tilde{c}_k$ is non zero and assume $K > 0$. Then firstly we have that all macroscopic profiles $\overline{R}^k$ are identically zero. Indeed the equation giving

the profiles $\overline{R}^k$ are (4.51d) and readily give $\overline{R}^k = 0$ by induction since in the sum $-\mu \sum_{k'=0}^{k} \tilde{c}_{k'} \Delta \overline{R}^{k-k'}$, either the coefficient is zero or the profile is identically zero. Consequently the $\overline{c}_k$ are also all 0. Now suppose $0 < K < 2l$. Then we can check that the equations (4.51e) satisfied by the R^k can be written as

$$
\begin{aligned}
&-\mu c_K \partial_z^2 R^0 = 0, \\
&-\mu c_K \partial_z^2 R^k = \text{terms involving profiles } R^j \text{ up to order } k-1,
\end{aligned}
$$

which given the decay rates asked of the profiles and with a clear induction implies that all R^k shoud be 0 which is contradictory to $\tilde{c}_K \neq 0$. So K must be greater or equal than $2l$. Let us show that it cannot be different from $2l$. Assume it is the case. Then by looking at (4.51e) for $k = 0$ to $k = K - 2l - 1$ we see that the equations only involve the coefficients up to $\tilde{c}_{K-1}$ which are all zero by our assumption. Then we have at least R^0 identically 0. Then we see that the equations for the following profiles are $R^k =$ terms involving profiles of lower order so that once again, by induction, all profiles are identically zero.

Thus we need to have $K = 2l$. Finally we prove that in this case we must have $R^0, \ldots, R^{l-1}$ equal to zero. Knowing the first non zero coefficient we can find the equation satisfied by these profiles. We have to take $k = 0$ to find the equation of R^0 which is

$$
-\mu \tilde{c}_{2l} \partial_z^2 R^0 + R^0 = 0. \tag{4.54}
$$

Now this equation is compatible with the decay rate we ask of the profile and give a solution of the form $A(\eta) \exp(-z/\sqrt{\mu \tilde{c}_{2l}})$. But considering the boundary condition (4.51h) we see that $\partial_z R^0$ must be 0 on the unit sphere so that A must be 0 actually be identically 0 and so is R^0. The same holds for $R^1, \ldots, R^{l-1}$ since they satisfy the same problem as R^0 with the same boundary conditions on the sphere. However we cannot apply this reasonning to R^l because its boundary condition is given by the trace of $\overline{Q}^0$ on the sphere in view of (4.51h). □

This second proposition will allow to distinguish all the fundamental problems

Proposition 4.2. *Only one of the three following possibilities can occur:*

Case 1: $\tilde{c}_0 \neq 0$ *and the fundamental problem is*

$$\begin{cases} -\mu\Delta\overline{Q}^0 = \rho & \text{in } |\Sigma| < 1 \\ -\mu\tilde{c}_0\Delta\overline{R}^0 + \overline{R}^0 = 0 & \text{in } |\Sigma| > 1 \\ \overline{Q}^0 = \overline{R}^0 & \text{on } |\eta| = 1 \\ \partial_\nu\overline{Q}^0 = \partial_\nu\overline{R}^0 & \text{on } |\eta| = 1 \\ \displaystyle\int_{|\Sigma|<1} \overline{Q}^0(\Sigma)\mathrm{d}\Sigma = 2^{3/2} - \tilde{c}_0 & \\ \tilde{c}_0 > 0 & \end{cases} \tag{4.55}$$

Case 2: $\tilde{c}_0 = 0$, $2l = s$ *and the fundamental problem is*

$$\begin{cases} -\mu\tilde{c}_{2l}\Delta\overline{Q}^0 + L(\Sigma,\nabla)\overline{Q}^0 = \tilde{c}_{2l}\rho & \text{in } |\Sigma| < 1, \\ \overline{Q}^0 = 0 & \text{on } |\Sigma| = 1, \\ \tilde{c}_{2l} > 0 & \\ \displaystyle\int_{|\Sigma|\leq 1} \overline{Q}^0(\sigma)\mathrm{d}\Sigma = 2^{3/2}. & \end{cases} \tag{4.56}$$

Case 3: $\tilde{c}_0 = 0$, $2l < s$ *and the fundamental problem is*

$$\begin{cases} -\mu\Delta\overline{Q}^0 = \rho & \text{in } |\Sigma| < 1, \\ \overline{Q}^0 = 0 & \text{on } |\Sigma| = 1, \\ \tilde{c}_{2l} > 0 & \\ \displaystyle\int_{|\Sigma|\leq 1} \overline{Q}^0(\sigma)\mathrm{d}\Sigma = 2^{3/2}. & \end{cases} \tag{4.57}$$

Proof. In the first and third cases there is nothing to prove. In the second case we need to prove that we cannot have $2l > s$ before writing the fundamental problem. Assume $2l > s$ then the equation defining $\overline{Q}^0$ is $L(\Sigma,\nabla)\overline{Q}^0 = 0$ completed with the boundary condition 0 on the unit sphere. Let us recall that for Theorem 4.1 we only consider the possibility that $\overline{Q}^0$ is in $\mathrm{W}^{1,\beta}$. Now we have the following lemma:

Lemma 4.1. *The problem*

$$\begin{cases} (A\Sigma + A^0)\cdot\nabla\bar{q} = 0 & \text{in } |\Sigma| < 1, \\ \bar{q} = 0 & \text{on } |\Sigma| = 1. \end{cases} \tag{4.58}$$

is well-posed on $\mathrm{W}_0^{1,\beta}(B)$ *(and thus* 0 *is the unique solution).*

The lemma comes from Hypothesis 2: because there are no stationary point for the characteristic system, the characteristic curves are locally parallelizable by a suitable transformation of space. Thus, Problem (4.58) falls back to studying

$$\begin{cases} \partial_{y_1} \tilde{q} = 0 & \text{in } y_1 > 0, \\ \tilde{q} = 0 & \text{on } y_1 = 0. \end{cases} \tag{4.59}$$

which clearly gives $\tilde{q} = 0$.

We can therefore conclude that $\overline{Q}^0 = 0$ and thus, that there is a contradiction between $\overline{Q}^0$ being zero and of integral $2^{3/2}$. Finally, if $2l \geq s$ then in fact $2l = s$. □

Now getting a hold on the fundamental problems is one thing but solving them is another matter. For example, as stated, Sys 4.57 is obviously ill-posed since we have absolutely no link between $\overline{Q}^0$ and $\tilde{c}_{2l}$ which could be any positive real for all we know at this point. Moreover, our ansaetze are not completely defined yet since we have not given l and s. Both these difficulties are solved by looking at several profiles and not only the fundamental one.

What we can do for the moment is to associate each of the fundamental problem to the range of μ for which it can be solved. This is given by the following proposition:

Proposition 4.3. *We have the following necessary or sufficent conditions of solvability of the fundamental problems:*

- *Sys 4.55 can only be solved if* $\mu > \mu_c$,
- *Sys 4.56 can be solved if* $\mu < \mu_c$,
- *Sys 4.57 can only be solved if* $\mu = \mu_c$,

We will prove each point separately.

4.4.1 Proof of Prop 4.3: Third Point

The third point is the easiest. Indeed considering the PDE and the boundary condition we immediately see that $\overline{Q}^0 = E/\mu$. Now if we plug it into the integral constraint we obtain an equation on μ which falls back to $\mu = \mu_c$.

4.4.2 Proof of Prop 4.3: First Point

Because of Hypothesis 1, (4.55) is radial. We are going to use this property to build a special radial solution exponentially decaying at infinity. We will assume that this solution is in Y (it is if we consider weighted Sobolev) so that by Property 2 it is the only solution. Plugging it into the integral constraint yields the condition $\mu > \mu_c$.

Analytical Form of the Solution of (4.55)

We claim that we can take the following expressions to solve the PDEs with continuity at the sphere and exponential decay at infinity.

$$\overline{Q}^0(\Sigma) = \frac{1}{\mu}E + p_0,$$
$$\overline{R}^0(\Sigma) = \frac{p_0}{\mathcal{B}(1/\sqrt{\mu\tilde{c}_0})}\mathcal{B}\left(\frac{|\Sigma|}{\sqrt{\mu\tilde{c}_0}}\right).$$

Here p_0 is a constant, here to adjust the values of $\overline{Q}^0$ and $\overline{R}^0$ along the sphere. We have noted $\mathcal{B}$ a Bessel potential given by

$$\mathcal{B}(\xi) = \int_0^\infty \frac{e^{-t}}{(4\pi t)^3}\exp\left(-\frac{\xi^2}{4t}\right)\mathrm{d}t. \tag{4.60}$$

Note that it can be expressed in terms of the modified Bessel function K_2 by the formula

$$\mathcal{B}(\xi) = \frac{1}{\xi^2}K_2(\xi), \tag{4.61}$$

where K_ν is defined as the unique solution of

$$x^2\frac{\mathrm{d}^2y}{\mathrm{d}x^2} + x\frac{\mathrm{d}y}{\mathrm{d}x} - (x^2+\nu^2)y = 0, \tag{4.62}$$

which decays exponentially at $+\infty$. The value of p_0 is given by

$$p_0 = \frac{\mathcal{B}(1/\sqrt{\mu\tilde{c}_0})}{|\mathcal{B}'(1/\sqrt{\mu\tilde{c}_0})|}\sqrt{\frac{\tilde{c}_0}{\mu}}|E'(1)|, \tag{4.63}$$

with the slight abuse of notation between $E(\Sigma)$ and $E(|\Sigma|)$. We have that $E'(1) = -1/\mathfrak{S}_5$: we just integrate the equation of E against the constant function 1 and we obtain $-\int_{|\Sigma|\leq 1}\partial_\nu E = \int_{|\Sigma|\leq 1}\rho$ and we use that the integral of ρ is 1 and that $\partial_\nu E = E'(1)$ on the sphere.

Expression of the integral constraint of (4.55).

The previous expressions give rise to a solution provided that the integral constraint is satisfied. This constraint is equivalent to the following equation on $\tilde{c}_0$:

$$\frac{1}{6}\frac{\mathcal{B}(1/\sqrt{\mu\tilde{c}_0})}{|\mathcal{B}'(1/\sqrt{\mu\tilde{c}_0})|}\sqrt{\frac{\tilde{c}_0}{\mu}}+\frac{1}{\mu}\int_{|\Sigma|\leq 1}E(\Sigma)\mathrm{d}\Sigma+\tilde{c}_0=2^{3/2}, \tag{4.64}$$

Let us recall that $\int E = 2^{3/2}\mu_c$. We now set $\nu_0 = \mu\tilde{c}_0$ and multiply the equation by μ to rewrite the equation as

$$\frac{1}{6}\frac{\mathcal{B}(1/\sqrt{\nu_0})}{|\mathcal{B}'(1/\sqrt{\nu_0})|}\sqrt{\nu_0}+\nu_0=2^{3/2}(\mu-\mu_c) \tag{4.65}$$

which is very similar to the equation we find in for the $1d$ model. Since the left-hand side is clearly positive a necessary condition to have a solution to the equation is for the right-hand side to be positive which yields the condition

$$\mu > \mu_c. \tag{4.66}$$

Moreover we introduce the function $\phi : \xi \mapsto \xi^2 + \xi\mathcal{B}(1/\xi)/(6|\mathcal{B}'(1/\xi)|)$ so that we are looking for a solution d_0 of $\phi(\sqrt{d_0}) = 2^{3/2}(\mu-\mu_c)$. The function ϕ is regular for $\xi \in]0,+\infty[$. Moreover we have $\phi(\xi) \geq \xi^2$ so that ϕ goes to $+\infty$ if $\xi \to +\infty$. We can have the behaviour of ϕ when ξ goes to 0^+ by examining the behaviour of $\mathcal{B}$ at $+\infty$. Using for example Laplace's method on $\mathcal{B}$ or classical estimates on K_2 yields the following estimation:

$$-\frac{\mathcal{B}(\omega)}{\mathcal{B}'(\omega)} \to_{\omega\to+\infty} 1, \tag{4.67}$$

so that we can conclude that ϕ vanished as ξ goes to 0. This means that we can always find at least one solution of this type. Note that contrary to the $1d$ case it is not clear at all that we can express analytically d_0 as a function of μ. To prove the uniqueness of such a solution we should prove that ϕ is strictly increasing. We do not have a formal proof but we provide Figure 4.1 as a strong hint that it is true.

4.4.3 Proof of Prop 4.3: Second Point

All we have to prove for this point, is that we can find a solution of (4.56) when $\mu < \mu_c$.

Let us intoduce the following problem:

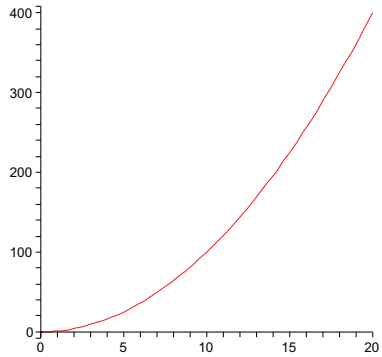

Figure 4.1: Plot of the function ϕ for ξ between 0 and 20 obtained with Maple

$$\begin{cases} -\nu\Delta H_\nu + L(\Sigma,\nabla)H_\nu = \nu\rho & \text{in } |\Sigma|<1, \\ H_\nu = 0 & \text{on } |\Sigma|=1, \end{cases} \tag{4.68}$$

Multiply the equation of (4.56) by μ and you find the equation of (4.68) where $\nu = \tilde{c}_{2l}\mu$. Consequently, we have solved our fundamental problem for a given μ if, and only if we can find a $\nu > 0$ such that $\displaystyle\int_{|\Sigma|\le 1} H_\nu = 2^{3/2}\mu$ and then, given this ν, set $\tilde{c}_{2l} = \nu/\mu$. The function H_ν, for $\nu > 0$, is actually uniquely defined because of

Lemma 4.2. *For every $f \in \mathrm{W}^{-1,\beta}(B)$ and every $\nu > 0$ the problem*

$$\begin{cases} -\nu\Delta H_\nu + (A\Sigma + A^0)\cdot\nabla H_\nu = f & \text{in } |\Sigma|<1, \\ H_\nu = 0 & \text{on } |\Sigma|=1, \end{cases}$$

is well-posed in $\mathrm{W}_0^{1,\beta}(B)$.

This lemma is a consequence of the ellipticity of the operator $-\nu\Delta + (A\Sigma + A^0)\cdot\nabla$ (see Agmon, Douglis and Nirenberg [1] Theorem 15.3' and 15.1").

So we can define the function $F(\nu) = \displaystyle\int_{|\Sigma|\le 1} H_\nu$ (since H_ν is in $\mathrm{L}^\beta(B)$. Let us prove:

Proposition 4.4. *For λ large enough (depending on M and a), F is a continuous function over $]0,+\infty[$ and $]0, 2^{3/2}\mu_c[\subset F(]0,+\infty[)$.*

It is clear that we have continuity of H_ν with respect to the $\mathrm{L}^1(B)$ strong topology in the domain $\nu > 0$ and thus F is continuous. All we have to do now is look at the limits of F with respect to $\nu \to +\infty$ and $\nu \to 0$ and apply the intermediate value theorem. The restriction in Theorem 4.1 comes from the fact that we do not know if F is monotone.

Limit of F when $\nu \to +\infty$.

Let us note that $H_\nu - E$ satisfies the following problem:

$$\begin{cases} -\Delta(H_\nu - E) + \dfrac{1}{\nu} L(\Sigma, \nabla)(H_\nu - E) = -\dfrac{1}{\nu} L(\Sigma, \nabla)E & \text{in } |\Sigma| < 1, \\ H_\nu - E = 0 & \text{on } |\Sigma| = 1, \end{cases} \tag{4.69}$$

We now estimate $\|H_\nu - E\|_{\mathrm{L}^\beta(B)}$. We note that since A is traceless, the operator $L(\sigma, \nabla)$ is actually skew-symmetric. Consequently we introduce the test function ψ:

$$\begin{cases} -\Delta\psi - \dfrac{1}{\nu} L(\Sigma, \nabla)\psi = |H_\nu - E|^{\beta-2}(H_\nu - E) & \text{in } |\Sigma| < 1, \\ \psi = 0 & \text{on } |\Sigma| = 1, \end{cases} \tag{4.70}$$

so that we have

$$\|H_\nu - E\|_{\mathrm{L}^\beta}^\beta \leq \frac{1}{\nu} \left| \int_B L(\Sigma, \nabla)E\psi \right| \leq \frac{1}{\nu} \|L(\Sigma, \nabla)E\|_{\mathrm{L}^\beta} \|\psi\|_{\mathrm{L}^{\beta'}}. \tag{4.71}$$

Finally we have the following elliptic estimation (again see [1]):

$$\|\psi\|_{\mathrm{L}^{\beta'}} \lesssim \left\| |H_\nu - E|^{\beta-2}(H_\nu - E) \right\|_{\mathrm{W}^{-1,\beta'}} \lesssim \left\| |H_\nu - E|^{\beta-2}(H_\nu - E) \right\|_{\mathrm{L}^{\beta'}}, \tag{4.72}$$

and we have $\left\| |H_\nu - E|^{\beta-2}(H_\nu - E) \right\|_{\mathrm{L}^{\beta'}} = \|H_\nu - E\|_{\mathrm{L}^\beta}^{\beta-1}$. Thus we can combine (4.71) and (4.72) to obtain the estimation:

$$\|H_\nu - E\|_{\mathrm{L}^\beta} \lesssim \frac{1}{\nu}. \tag{4.73}$$

so that H_ν converges to E in L^β when ν goes to infinity. We can deduce that $F(\nu) \to \displaystyle\int_{|\Sigma| \leq 1} E(\Sigma)\mathrm{d}\Sigma$ when ν goes to infinity so that by (4.27),

$$\lim_{\nu = +\infty} F(\nu) = 2^{3/2}\mu_c. \tag{4.74}$$

Limit of F when $\nu \to 0$.

For the other limit, the situation is a bit more intricate. We present two approaches to this problem. The first one relies on the classical method of *a priori* estimates in Hilbert spaces but is restricted to ρ in $\mathrm{W}^{-1,2}(B)$. The second one works for any ρ in $\mathcal{M} \cap \mathrm{W}^{-1,\beta}(B)$ but is more sophisticated.

What we are studying now is a singular limit of a diffusion-transport equation to a stationary transport equation for vanishing viscosity.

Both methods require the following lemma which, in a way, gives the structure of the underlying transport operator:

Lemma 4.3. *There is a regular function ζ, $\mathcal{C}^2$, such that we have the following estimates:*

$$m_1 \leq \zeta \leq m_2 \qquad -(A\Sigma + A^0)\cdot\nabla\zeta \geq m_3 \qquad |\nabla\zeta| \leq m_4 \qquad |\Delta\zeta| \leq m_5,$$

where m_i are positive constants.

First case: ρ is in H^{-1}.

The convergence :

Proposition 4.5. *Assume Lemma 4.3. Then the following bound on H_ν is true for ν small enough:*

$$\int_{|\Sigma|\leq 1} H_\nu(\Sigma)^2 \mathrm{d}\Sigma \leq \mathcal{O}(\nu).$$

We give here the details of this proposition for completeness sake but we actually are in a simpler situation than in Bresch and Simon [13] from where the proposition comes. We use ζH_ν as a test function (which considering the regularity of ζ is in $\mathrm{W}^{1,2}(B)$) and integrate by part the skew symmetric term. We find that we have

$$\begin{aligned}
&\nu\int_B \nabla H_\nu\cdot\nabla(\zeta H_\nu) + \int_B \zeta\left(A\Sigma+A^0\right)\cdot\nabla H_\nu H_\nu = \nu\langle\rho,\zeta H_\nu\rangle\\
\Leftrightarrow&\nu\int_B \zeta|\nabla H_\nu|^2 + \nu\int_B \nabla\zeta\cdot\nabla H_\nu H_\nu + \int_B \zeta\left(A\Sigma+A^0\right)\cdot\nabla H_\nu H_\nu = \nu\langle\rho,\zeta H_\nu\rangle\\
\Leftrightarrow&\nu\int_B \zeta|\nabla H_\nu|^2 + \nu\int_B \nabla\zeta\cdot\nabla H_\nu H_\nu - \frac{1}{2}\int_B \left(A\Sigma+A^0\right)\cdot\nabla\zeta|H_\nu|^2 = \nu\langle\rho,\zeta H_\nu\rangle.
\end{aligned} \tag{4.75}$$

Now using the properties of the function ζ we can bound by below the first two terms by:

$$\nu \int_B \zeta |\nabla H_\nu|^2 + \nu \int_B \nabla\zeta \cdot \nabla H_\nu H_\nu \geq \frac{\nu m_1}{2} \int_B |\nabla H_\nu|^2 - \nu m_4 \left\|\nabla H_\nu\right\|_{\mathrm{L}^2(B)} \left\|H_\nu\right\|_{\mathrm{L}^2(B)},$$
$$\geq \frac{\nu m_1}{2} \left\|\nabla H_\nu\right\|^2_{\mathrm{L}^2(B)} - \frac{\nu m_4^2}{2m_1} \left\|H_\nu\right\|^2_{\mathrm{L}^2(B)}, \tag{4.76}$$

and the third term is bounded from below by

$$-\frac{1}{2}\int_B \left(A\Sigma + A^0\right)\cdot\nabla\zeta |H_\nu|^2 \geq \frac{m_3}{2}\left\|H_\nu\right\|^2_{\mathrm{L}^2(B)}. \tag{4.77}$$

We now note that

$$\left\|\zeta H_\nu\right\|_{\mathrm{H}^1(B)} \leq C(m_1, m_2, m_4)\left\|H_\nu\right\|_{\mathrm{W}^{1,2}(B)}, \tag{4.78}$$

so that we can write

$$\begin{aligned}\nu\langle\rho, \zeta H_\nu\rangle &\leq C\nu \left\|\rho\right\|_{\mathrm{H}^{-1}(B)} \left\|H_\nu\right\|_{\mathrm{W}^{1,2}(B)} \\ &\leq \nu\frac{C^2}{m_1}\left\|\rho\right\|^2_{\mathrm{H}^{-1}(B)} + \nu\frac{m_1}{4}\left(\left\|H_\nu\right\|^2_{\mathrm{L}^2(B)} + \left\|\nabla H_\nu\right\|^2_{\mathrm{L}^2(B)}\right)\end{aligned} \tag{4.79}$$

Gathering all previous inequalities we finally have:

$$\nu\frac{m_1}{4}\left\|\nabla H_\nu\right\|^2_{\mathrm{L}^2(B)} + \left(\frac{m_3}{2} - \nu\left(\frac{m_4^2}{2m_1} + \frac{m_1}{4}\right)\right)\left\|H_\nu\right\|^2_{\mathrm{L}^2(B)} \leq \nu\frac{C^2}{m_1}\left\|\rho\right\|^2_{\mathrm{W}^{-1,2}(B)} \tag{4.80}$$

This inequality gives the convergence of H_ν to 0 in $\mathrm{L}^2(B)$ for small ν and thus the convergence of $F(\nu)$ to 0 as ν goes to 0.

This proposition works well when ρ is in $\mathrm{W}^{-1,2}$ because we can then use H_ν as a test function. But if ρ is in $\mathrm{W}^{-1,\beta}$ with $\beta < 2$ then we would want to use the test function $\zeta|H_\nu|^{\beta-2}H_\nu$ to obtain a similiar result. However when $\beta < 2$ this function is indeed in $\mathrm{L}^{\beta'}$ but not in $\mathrm{W}^{1,\beta'}_0(B)$ for the gradient cannot be in $\mathrm{L}^{\beta'}$.

Second case: ρ is in $\mathcal{M} \cap \mathrm{W}^{-1,\beta}$ for $1 < \beta < 2$.

We do an approximation argument in the following way: consider

$$-\nu\Delta H^j_\nu + (L(\Sigma, \nabla)\cdot\nabla)H^j_\nu = \nu\rho^j, \tag{4.81}$$

with Dirichlet boundary conditions, nonnegative ρ^j and smooth. By the maximum principle, H^j_ν is also nonnegative. Let ζ be a smooth function verifying the estimates of Lemma 4.3. Multiply the equation by ζ and integrate. We find, after integrating by parts,

$$-\nu \int_B (\Delta\zeta) H_\nu^j - \nu \int_{\partial B} \zeta \partial_n H_\nu^j - \int_B ((L(\Sigma,\nabla)\cdot\nabla)\zeta) H_\nu^j = \nu \int_B \rho^j \zeta. \quad (4.82)$$

On the left side, the first term is bounded from below by $-m_5\nu \int_B H_\nu^j$, the second term is nonnegative by the maximum principle, and the third term is bounded below by $m_3 \int_B H_\nu^j$. The right hand side is bounded by $m_2\nu \int_B \rho^j$. We conclude that

$$\int_B H_\nu^j \leq \frac{m_2\nu}{m_3 - m_5\nu} \int_B \rho^j. \quad (4.83)$$

This is true for any nonnegative function ρ^j. Now let $\rho^j tends to \rho$ when $j \to +\infty$. What we need is the convergence of both sides of (4.83) as $j \to +\infty$. The right-hand side can be written

$$\int_B \rho^j = \langle \rho^j, \mathbf{1} \rangle_{\mathcal{M},\mathcal{C}^0(\bar{B})}, \quad (4.84)$$

and as such converges to $\langle \rho, \mathbf{1} \rangle_{\mathcal{M},\mathcal{C}^0(\bar{B})}$. On the other hand we actually want to know if $\int_B H_\nu^j \to \int_B H_\nu$. We note first that since H_ν^j is positive, (4.83) gives us a uniform bound in L^1 when ν is fixed. Consequently any j-subsequence of (H_ν^j) weakly converges to a positive measure χ_ν. Moreover we have that

$$\chi_\nu(B) \leq \frac{m_2\nu}{m_3 - C_1\nu}, \quad (4.85)$$

so that $\chi_\nu(B)$ tends to 0 as $\nu \to 0$.

We now use the fact that when ν is fixed, the linear operator $(-\nu\Delta + L(\Sigma,\nabla))^{-1}$ is continuous over $\mathrm{W}^{-1,\beta}$ with value in $\mathrm{W}_0^{1,\beta}$ (which is another formulation for Lemma 4.2). Consequently H_ν^j converges to H_ν at least strongly in L^β and thus in L^1 when $j \to +\infty$. Which means that for *any* j-subsequence $\int_B H_\nu^j$ converges to $\int_B H_\nu$ and thus

$$\int_B H_\nu = \chi_\nu(B) \to_{\nu\to 0} 0. \quad (4.86)$$

Finally this shows that $F(\nu)$ goes to 0 as we announced.

Proof of Lemma 4.3

Now the question remains to find a suitable ζ. According to [13], such a function may be given by $\zeta(\Sigma) = l(\Sigma) + \zeta(\Sigma_+)$ where Σ_+ is the point of the characteristic line going through Σ on the sphere where the vector field is going outward and $l(\Sigma)$ is the length of the characteristic line from Σ_+ to Σ. This requires that all the characteristic curves define such a point Σ_+ which is the object of Hypothesis 2.

First, recall that we have made the hypothesis that in (4.23) we have $\nabla u = \varepsilon M$ ant that A is the matrix originating from the term $g_a(\Sigma, \nabla u)$ so that A depends on a and M. Recall also that A^0 comes from the term $2G_0 D(\nabla u)$ and that λ is the dimensionless counterpart of G_0, so that A^0 depends on λ (see also Appendix for the exact dependence of A and A^0 on the parameters λ, a and M).

We will prove the following proposition which gives a general result:

Proposition 4.6. *For every flow type M and for every a, there exists $\lambda_m \geq 0$, so that, for $\lambda \geq \lambda_m$, the characteristic curves of the vector field $\Sigma \mapsto A\Sigma + A^0$ cross the unit sphere outwardly.*

This proposition is essentially noting that the vector field depends very simply on λ since it only appears in $A^0 = \lambda\overline{A^0}$ where $\overline{A^0}$ does not depend on anything else than the given M. Consequently when λ is large, the vector field is in the limit a constant vector field and characteristic curves are parallel lines and the real characteristic curves should be near parallel ones, at least in a neighbourhood of the unit ball. In Section 4.6 we will study particular cases and give explicit lower bounds.

Proof of Proposition 4.6. We have to study the following Cauchy problem:

$$\begin{cases} \dfrac{\mathrm{d}\Sigma^\lambda(t)}{\mathrm{d}t} = A\Sigma^\lambda(t) + \lambda\overline{A^0}, \\ \Sigma^\lambda(0) = \Sigma_0 \in B. \end{cases} \tag{4.87}$$

We set $\Sigma^\lambda(t) = \overline{\Sigma^\lambda}(\lambda t)$ so that we have

$$\begin{cases} \dfrac{\mathrm{d}\overline{\Sigma^\lambda}(s)}{\mathrm{d}s} = \dfrac{1}{\lambda} A\overline{\Sigma^\lambda}(s) + \overline{A^0}, \\ \overline{\Sigma^\lambda}(0) = \Sigma_0 \in B. \end{cases} \tag{4.88}$$

The solution to this equation can be computed:

$$\begin{aligned}\overline{\Sigma^{\lambda}}(s) &= \exp\left(\frac{s}{\lambda}A\right)\Sigma_0 + \left(\int_0^s \exp\left(\frac{r}{\lambda}A\right)\mathrm{d}r\right)\overline{A^0} \\ &= \left(\exp\left(\frac{s}{\lambda}A\right) - Id\right)\Sigma_0 + \left(\int_0^s \exp\left(\frac{r}{\lambda}A\right)\mathrm{d}r - sId\right)\overline{A^0} + \Sigma_0 + s\overline{A^0}.\end{aligned} \tag{4.89}$$

We now remark that

$$\left\|\exp\left(\frac{s}{\lambda}A\right) - Id\right\| \leq \exp\left(\frac{|s|}{\lambda}\|A\|\right) - 1, \tag{4.90}$$

$$\left\|\int_0^s \exp\left(\frac{r}{\lambda}A\right)\mathrm{d}r - sId\right\| \leq \sum_{k=1}^{+\infty}\frac{|s|^{k+1}}{\lambda^k}\|A\|^k. \tag{4.91}$$

Thus if we define $\overline{\Sigma^{\mathrm{app}}}(s) = \Sigma_0 + s\overline{A^0}$ we have for any $C > 0$.

$$\left\|\overline{\Sigma^{\lambda}} - \overline{\Sigma^{\mathrm{app}}}\right\|_{\mathrm{L}^{\infty}(-C,C)} = \mathcal{O}\left(\frac{1}{\lambda}\right). \tag{4.92}$$

Note that this bound is uniform in $\Sigma_0 \in B$. Now take C such that $C\left\|\overline{A^0}\right\| - 1 > 3$ and for this C we can assure that $\left\|\overline{\Sigma^{\lambda}} - \overline{\Sigma^{\mathrm{app}}}\right\|_{\mathrm{L}^{\infty}(-C,C)} \leq 1$. Then we can prove that

$$\begin{aligned}\left\|\Sigma^{\lambda}(\pm C)\right\| &\geq \|\Sigma^{\mathrm{app}}(\pm C)\| - \left\|\Sigma^{\lambda}(\pm C) - \Sigma^{\mathrm{app}}(\pm C)\right\| \\ &\geq C\left\|\overline{A^0}\right\| - 1 - 1 \\ &\geq 2.\end{aligned} \tag{4.93}$$

The conclusion is thus that characteristic curves must cross the unit sphere at least twice which means at least once outwardly. □

4.5 Boundary Layer Sizes: The Transitional Case $\mu = \mu_C$

In the previous section, we have indentified which fundamental problem are possible. We have also given some constraints on the type of profiles we can find in the ansaetze and on the two parameters s and l. We have yet to find what values these parameter can take. Let us first admit the following result:

Proposition 4.7. *In Proposition 4.2,*

- *If we are in case 4.2 we can take $s = 1$.*
- *If we are in case 4.2 we can take $l = 1$ and $s = 2$.*

The proof uses exactly the same argument and computations that give the same result in the $1d$ case so we refer to [54]. Now we are left to prove:

Proposition 4.8. *In Proposition 4.2, if we are in case 4.2 we can take $l = 2$ and $s = 5$.*

This is also the same result as in the $1d$ case, however the proof is much more technical. Indeed in $1d$ we could compute the different profiles $\overline{Q}^k$ and R^k which we cannot do anymore. But from the proof in $1d$ we can see that what we mostly used is the symmetry of the solutions. We have to use the properties of the equations to find the same properties of symmetry. We also now have a first order operator with non constant coefficients to contend with.

4.5.1 Finding the First Exterior Problem

We start by computing the shape of the first exterior profile:

$$\begin{cases} -\mu\tilde{c}_{2l}\partial_z^2 R^l + R^l = 0 & \text{for all } |\eta| = 1 \text{ and } z > 0 \\ \partial_z R^l(\eta, 0) = \nabla \overline{Q}^0(\eta) \cdot \eta & \text{for all } |\eta| = 1 \end{cases} \tag{4.94}$$

Using that $\overline{Q}^0$ is radial, this leads to a radial profile of the form

$$R^l(\eta, z) = \frac{\sqrt{\mu\tilde{c}_{2l}}}{\mu \mathfrak{S}_5} \exp\left(-\frac{z}{\sqrt{\mu\tilde{c}_{2l}}}\right). \tag{4.95}$$

4.5.2 Second Interior Profile.

Equation of the Second Interior Profile

We now look for the first non trivial problem for $\overline{Q}^k$, $k > 0$. As in the $1d$ model we can see by a clear induction by taking (4.51a) with $k = 2l + p$ that for $p = 1, \ldots, \min(s - 2l, l)$, $\overline{Q}^p$ actually satisfies an elliptic linear equation with 0 as a right hand side and with Dirichlet condition on the boundary so it is necessarily zero. If $s - 2l > l$ then the first non trivial problem is the one for $\overline{Q}^l$ which is

$$\begin{cases} -\mu\tilde{c}_{2l}\Delta\overline{Q}^l = 0 & \text{in } |\Sigma| < 1, \\ \overline{Q}^l = R^l(0) & \text{on } |\Sigma| = 1, \\ \int_{|\Sigma|\leq 1} \overline{Q}^l(\sigma)\mathrm{d}\Sigma = 0. \end{cases} \tag{4.96}$$

The solution to this problem is clearly given by the constant function $R^l(0)$. But enforcing the integral constraint leads to $\tilde{c}_{2l} = 0$ which is forbidden. So we must have $s - 2l \leq l$. Suppose $s - 2l = l$. Then the problem satisfied by $\overline{Q}^{s-2l}$ is

$$\begin{cases} -\mu\tilde{c}_{2l}\Delta\overline{Q}^{s-2l} = -L(\Sigma,\nabla)\overline{Q}^0 & \text{in } |\Sigma| < 1, \\ \overline{Q}^{s-2l} = R^l(0) & \text{on } |\Sigma| = 1, \\ \int_{|\Sigma|\leq 1} \overline{Q}^{s-2l}(\sigma)\mathrm{d}\Sigma = 0. \end{cases} \tag{4.97}$$

We can get rid of the boundary condition by linearity so $\overline{Q}^{s-2l} = R^l(0) + G$ where G satisfies

$$\begin{cases} -\mu\tilde{c}_{2l}\Delta G = -L(\Sigma,\nabla)\overline{Q}^0 & \text{in } |\Sigma| < 1, \\ G = 0 & \text{on } |\Sigma| = 1, \end{cases} \tag{4.98}$$

Computation of the Integral of $\overline{Q}^{s-2l}$

We now introduce the test functions

$$\psi^0 = \frac{1}{12}(1 - |\Sigma|^2), \tag{4.99}$$

$$\psi = \frac{1}{12\mu\tilde{c}_{2l}}(1 - |\Sigma|^2). \tag{4.100}$$

This function can help us integrate G on the ball. Multiplying the equation on G by ψ and integrating by part twice yields

$$\int_{|\Sigma|\leq 1} G(\Sigma)(-\mu\tilde{c}_{2l}\Delta\psi(\Sigma))\mathrm{d}\Sigma = -\int_{|\Sigma|\leq 1} L(\Sigma,\nabla)\overline{Q}^0(\Sigma)\psi(\Sigma)\mathrm{d}\Sigma, \tag{4.101}$$

and one can check that $-\mu\tilde{c}_{2l}\Delta\psi = 1$. So to compute the integral of G we only need to compute $\int_{|\Sigma|\leq 1} L(\Sigma,\nabla)\overline{Q}^0(\Sigma)\psi(\Sigma)\mathrm{d}\Sigma$. But we have

$$\int_{|\Sigma|\leq 1} L(\Sigma,\nabla)\overline{Q}^0(\Sigma)\psi(\Sigma)\mathrm{d}\Sigma = \int_{r=0}^{1} \frac{1-r^2}{12\mu^2\tilde{c}_{2l}}\partial_r\overline{Q}^0(r)r^5\left(\int_{|\eta|=1}(A\eta + A^0)\cdot\eta\mathrm{d}\eta\right)\mathrm{d}r, \quad (4.102)$$

and the integral on the sphere is zero because A is traceless. This is the information we need (and is reminiscent of the fact that the similar term in the $1d$ model was odd and thus of zero integral [54]). Indeed we now have again a contradiction between $\tilde{c}_{2l} \neq 0$ and $\int \overline{Q}^{s-2l} = 0$. Consequently $s - 2l < l$ and in fact $\overline{Q}^{s-2l} = G$. In this case the function $\overline{Q}^{s-2l}$ finally satisfies the following:

$$\begin{cases} -\mu\tilde{c}_{2l}\Delta\overline{Q}^{s-2l} = -L(\Sigma,\nabla)\overline{Q}^0 & \text{in } |\Sigma| < 1, \\ \overline{Q}^{s-2l} = 0 & \text{on } |\Sigma| = 1, \end{cases} \quad (4.103)$$

4.5.3 Third Interior Profile.

Equation of the Third Interior Profile

We now look for the next non trivial problem. We can still look at the interior profiles, since we have not used the boundary condtion $R^l(0)$ yet. Suppose $l < 2s - 4l$. Then we have a problem on the profile $\overline{Q}^l$ which is

$$\begin{cases} -\mu\tilde{c}_{2l}\Delta\overline{Q}^l = \mu\tilde{c}_{5s-l}\Delta\overline{Q}^{s-2l}, \\ \overline{Q}^l(\eta) = R^l(0), \\ \int_{|\Sigma|\leq 1}\overline{Q}^l = 0. \end{cases} \quad (4.104)$$

This system has a solution $\overline{Q}^l = R^l(0) + (\tilde{c}_{5s-l}/\tilde{c}_{2l})\overline{Q}^{s-2l}$ and we know that the integral of $\overline{Q}^{s-2l}$ is 0 so whatever the value of $\tilde{c}_{5s-l}$ we still have a contradiction between $\int \overline{Q}^l = 0$ and $\tilde{c}_{2l} \neq 0$. So we must have $2s - 4l \leq l$ and the next profile to have a non trivial problem is $\overline{Q}^{2s-4l}$ which has equation

$$-\mu\tilde{c}_{2l}\Delta\overline{Q}^{2s-4l} = -L(\Sigma,\nabla)\overline{Q}^{s-2l} + \mu\tilde{c}_s\Delta\overline{Q}^{s-2l}, \quad (4.105)$$

and boundary condition 0 if $2s-4l<l$ and constant if $2s-4l=l$. We introduce a new temporary function $\widetilde{G}$ which satisfies the following:

$$\begin{cases} -\mu\tilde{c}_{2l}\Delta\widetilde{G} = -L(\Sigma,\nabla)\overline{Q}^{s-2l}, \\ \widetilde{G}(\eta)=0, \end{cases} \tag{4.106}$$

By linearity we can decompose the function

$$\overline{Q}^{2s-4l} = \mathbf{1}_{2s-4l=l}R^l(0) + \widetilde{G} + \frac{\tilde{c}_s}{\tilde{c}_{2l}}\overline{Q}^{s-2l}. \tag{4.107}$$

The first term takes into account the possibility of having a non zero boundary value if $2s-4l=l$ (the boundary value is zero if $2s-4l<l$)and the last two terms account for the two parts in the right hand side of the equation (4.105). To solve the problem on $\overline{Q}^{2s-4l}$ we have to check that $\displaystyle\int\overline{Q}^{2s-4l}$ is 0. But we have:

$$\int_{|\Sigma|\leq 1}\overline{Q}^{2s-4l}(\Sigma)\mathrm{d}\Sigma = 0 = \frac{\mathfrak{S}_5}{6}\mathbf{1}_{2s-4l=l}R^l(0) + \int_{|\Sigma|\leq 1}\widetilde{G}(\Sigma)\mathrm{d}\Sigma, \tag{4.108}$$

since we already know that the $\displaystyle\int\overline{Q}^{s-2l}$ is zero. Recall that the volume of the unit ball in dimension n is $\mathfrak{S}_{n-1}/n$. We thus have to compute the integral of $\widetilde{G}$. Using the test function ψ we know that the integral of $\widetilde{G}$ is equal to

$$\begin{aligned} \int_{|\Sigma|\leq 1}\widetilde{G} &= -\int_{|\Sigma|\leq 1} L(\Sigma,\nabla)\overline{Q}^{s-2l}(\Sigma)\psi(\Sigma)\mathrm{d}\Sigma \\ &= -\int_{|\Sigma|\leq 1}\left(A\Sigma + A^0\right)\cdot\nabla\overline{Q}^{s-2l}(\Sigma)\psi(\Sigma)\mathrm{d}\Sigma. \end{aligned} \tag{4.109}$$

We decompose $A = A^s + A^a$ where A^s is the symmetric part of A and A^a its skew-symmetric part. This decomposition is somewhat reminiscent of the decomposition of ∇u into its symmetric and skew-symmetric part in the study of the well posedness of some stationary Fokker-Planck equation arising in the study of polymeric fluid that is done by Jourdain, Le Bris, Lelièvre and Otto [42] or Arnold, Carillo and Manzini [3]. We can then write

$$A^s\Sigma + A^0 = \nabla\left(\frac{1}{2}A^s\Sigma\cdot\Sigma + A^0\cdot\Sigma\right), \tag{4.110}$$

and integrate by part to find:

$$\begin{aligned}
&-\int_{|\Sigma|\leq 1} L(\Sigma,\nabla)\overline{Q}^{s-2l}(\Sigma)\psi(\Sigma)\mathrm{d}\Sigma \\
=&-\int_{|\Sigma|\leq 1} \left(A\Sigma + A^0\right)\cdot\nabla\overline{Q}^{s-2l}(\Sigma)\psi(\Sigma)\mathrm{d}\Sigma \\
=&-\int_{|\Sigma|\leq 1} \nabla\left(\frac{1}{2}A^s\Sigma\cdot\Sigma + A^0\cdot\Sigma\right)\cdot\nabla\overline{Q}^{s-2l}(\Sigma)\psi(\Sigma)\mathrm{d}\Sigma \\
&-\int (A^a\Sigma)\cdot\nabla\overline{Q}^{s-2l}(\Sigma)\psi(\Sigma)\mathrm{d}\Sigma \\
=&\int_{|\Sigma|\leq 1}\left(\frac{1}{2}A^s\Sigma\cdot\Sigma + A^0\cdot\Sigma\right)\Delta\overline{Q}^{s-2l}\psi(\Sigma)\mathrm{d}\Sigma \\
&+\int_{|\Sigma|\leq 1}\left(\frac{1}{2}A^s\Sigma\cdot\Sigma + A^0\cdot\Sigma\right)\nabla\overline{Q}^{s-2l}\cdot\nabla\psi(\Sigma)\mathrm{d}\Sigma \\
&-\int_{|\Sigma|\leq 1}(A^a\Sigma)\cdot\nabla\overline{Q}^{s-2l}(\Sigma)\psi(\Sigma)\mathrm{d}\Sigma \\
=&\mathcal{I}_1+\mathcal{I}_2-\mathcal{I}_3
\end{aligned} \tag{4.111}$$

We now compute each of the $\mathcal{I}_k$ separately.

Computation of $\mathcal{I}_3$

We first note that

$$\mathcal{I}_3 = -\int \psi(\Sigma)\Sigma\cdot A^a\nabla\overline{Q}^{s-2l}(\Sigma)\mathrm{d}\Sigma$$

and using the the fact that, from (4.100), ψ is radial

$$\begin{aligned}
&=-\int_{|\Sigma|\leq 1}\nabla\left(\int^{|\Sigma|} r\psi(r)\mathrm{d}r\right)\cdot A^a\nabla\overline{Q}^{s-2l}(\Sigma)\mathrm{d}\Sigma \\
&=\int_{|\Sigma|\leq 1}\left(\int^{|\Sigma|} r\psi(r)\mathrm{d}r\right)\mathrm{div}\left(A^a\nabla\overline{Q}^{s-2l}\right)(\Sigma)\mathrm{d}\Sigma \\
&=0
\end{aligned} \tag{4.112}$$

because $\mathrm{div}\,(A^a\nabla\overline{Q}^{s-2l}) = A^a : \mathrm{d}^2\overline{Q}^{s-2l}$ and this contracted product is 0 since it is the contracted product of a symmetric matrix by a skew-symmetric one.

Computation of $\mathcal{I}_1$

We use the equation followed by $\overline{Q}^{s-2l}$ from (4.103) to write

$$\begin{aligned}\mathcal{I}_1 &= \int_{|\Sigma|\leq 1}\left(\frac{1}{2}A^s\Sigma\cdot\Sigma + A^0\cdot\Sigma\right)\frac{1}{\mu\tilde{c}_{2l}}\left(A\Sigma+A^0\right)\cdot\nabla\overline{Q}^0(\Sigma)\psi(\Sigma)\mathrm{d}\Sigma\\ &= \int_{|\Sigma|\leq 1}\left(\frac{1}{2}A^s\Sigma\cdot\Sigma + A^0\cdot\Sigma\right)\frac{1}{\mu\tilde{c}_{2l}}\left(A\Sigma+A^0\right)\cdot\left(\partial_r\overline{Q}^0(|\Sigma|)\frac{\Sigma}{|\Sigma|}\right)\psi(\Sigma)\mathrm{d}\Sigma\end{aligned} \tag{4.113}$$

We can simplify this last integral by using the change of variable $\Sigma\to-\Sigma$ to remove the odd part of the function. This leads to:

$$\begin{aligned}&\int_{|\Sigma|\leq 1}\left(\frac{1}{2}A^s\Sigma\cdot\Sigma + A^0\cdot\Sigma\right)\frac{1}{\mu\tilde{c}_{2l}}\left(A\Sigma+A^0\right)\cdot\left(\partial_r\overline{Q}^0(|\Sigma|)\frac{\Sigma}{|\Sigma|}\right)\psi(\Sigma)\mathrm{d}\Sigma\\ =&\frac{1}{2\mu\tilde{c}_{2l}}\int_{|\Sigma|\leq 1}\frac{\psi(\Sigma)\partial_r\overline{Q}^0(|\Sigma|)}{|\Sigma|}\left(A^s\Sigma\cdot\Sigma\right)^2\mathrm{d}\Sigma\\ &+\frac{1}{\mu\tilde{c}_{2l}}\int_{|\Sigma|\leq 1}\frac{\psi(\Sigma)\partial_r\overline{Q}^0(|\Sigma|)}{|\Sigma|}\left(A^0\cdot\Sigma\right)^2\mathrm{d}\Sigma\end{aligned} \tag{4.114}$$

We note that since A^s is symmetric we can use an orthogonal matrix to change variables and write:

$$\begin{aligned}&\frac{1}{2\mu\tilde{c}_{2l}}\int_{|\Sigma|\leq 1}\frac{\psi(\Sigma)\partial_r\overline{Q}^0(|\Sigma|)}{|\Sigma|}\left(A^s\Sigma\cdot\Sigma\right)^2\mathrm{d}\Sigma\\ =&\frac{1}{2\mu\tilde{c}_{2l}}\int_{|\Sigma|\leq 1}\frac{\psi(\Sigma)\partial_r\overline{Q}^0(|\Sigma|)}{|\Sigma|}\left(\sum_i\lambda_i\Sigma_i^2\right)^2\mathrm{d}\Sigma\\ =&\sum_{i,j}\lambda_i\lambda_j\frac{1}{2\mu\tilde{c}_{2l}}\int_{|\Sigma|\leq 1}\frac{\psi(\Sigma)\partial_r\overline{Q}^0(|\Sigma|)}{|\Sigma|}\Sigma_i^2\Sigma_j^2\mathrm{d}\Sigma,\end{aligned} \tag{4.115}$$

where the λ_i are the eigenvalues of the symmetric part of A. But it is clear that

$$\int_{|\Sigma|\leq 1}\frac{\psi(\Sigma)\partial_r\overline{Q}^0(|\Sigma|)}{|\Sigma|}\Sigma_i^2\Sigma_j^2\mathrm{d}\Sigma$$

does not depend on (i,j) when $i \neq j$ and does not depend on i when $i = j$. Therefore there are two constant

$$C = -\frac{1}{2\mu\tilde{c}_{2l}} \int_{|\Sigma|\leq 1} \frac{\psi(\Sigma)\partial_r \overline{Q}^0(|\Sigma|)}{|\Sigma|} \Sigma_1^2 \Sigma_2^2 \mathrm{d}\Sigma, \tag{4.116}$$

$$C' = -\frac{1}{2\mu\tilde{c}_{2l}} \int_{|\Sigma|\leq 1} \frac{\psi(\Sigma)\partial_r \overline{Q}^0(|\Sigma|)}{|\Sigma|} \Sigma_1^4 \mathrm{d}\Sigma, \tag{4.117}$$

$$\tag{4.118}$$

so that we have

$$\frac{1}{2\mu\tilde{c}_{2l}} \int_{|\Sigma|\leq 1} \frac{\psi(\Sigma)\partial_r \overline{Q}^0(|\Sigma|)}{|\Sigma|} \left(A^s\Sigma\cdot\Sigma\right)^2 \mathrm{d}\Sigma = -C\sum_i \lambda_i^2 - C'\sum_{i\neq j} \lambda_i\lambda_j. \tag{4.119}$$

We remark that since $\overline{Q}^0 = (1/\mu_c)E$ we have by maximum principle $\partial_r \overline{Q}^0 < 0$ and consequently, C and C' are positive.

Note that, because A^s is traceless when A is, we have $\sum_{i\neq j} \lambda_i\lambda_j = (\sum_i \lambda_i)^2 - \sum_i \lambda_i^2 = -\sum_i \lambda_i^2$. Finally we have

$$\frac{1}{2\mu\tilde{c}_{2l}} \int_{|\Sigma|\leq 1} \frac{\psi(\Sigma)\partial_r \overline{Q}^0(|\Sigma|)}{|\Sigma|} \left(A^s\Sigma\cdot\Sigma\right)^2 \mathrm{d}\Sigma = -(C - C')\sum_i \lambda_i^2. \tag{4.120}$$

Note that

$$2C - 2C' = -\frac{1}{2\mu\tilde{c}_{2l}} \int_{|\Sigma|\leq 1} \frac{\psi(\Sigma)\partial_r \overline{Q}^0(|\Sigma|)}{|\Sigma|} \left(\Sigma_1^4 + \Sigma_2^4 - 2\Sigma_1^2\Sigma_2^2\right) \mathrm{d}\Sigma \tag{4.121}$$

and thus $C - C'$ is positive. To clear out the complete dependence on the parameter we use $\overline{Q}^0 = (1/\mu)E$ and (4.100) can in fact say that we have:

$$\frac{1}{2\mu\tilde{c}_{2l}} \int_{|\Sigma|\leq 1} \frac{\psi(\Sigma)\partial_r \overline{Q}^0(|\Sigma|)}{|\Sigma|} \left(A^s\Sigma\cdot\Sigma\right)^2 \mathrm{d}\Sigma = -\frac{C_2}{\mu^3\tilde{c}_{2l}^2}\sum_i \lambda_i^2. \tag{4.122}$$

where now C_2 is a purely numerical constant with expression:

$$C_2 = -\frac{1}{2}\int_{|\Sigma|\leq 1} \frac{\psi^0(|\Sigma|)E'(|\Sigma|)}{|\Sigma|}\left(\Sigma_1^2 - \Sigma_2^2\right)^2 \mathrm{d}\Sigma$$

and using that $E' < 0$ and the expression of ψ_0 from (4.99)

$$= \frac{1}{24}\int_{|\Sigma|\leq 1} \frac{(1-|\Sigma|^2)|E'(|\Sigma|)|}{|\Sigma|}\left(\Sigma_1^2 - \Sigma_2^2\right)^2 \mathrm{d}\Sigma, \tag{4.123}$$

In the same fashion we have a purely numerical positive constant C_3 such that

$$-\frac{1}{\mu\tilde{c}_{2l}}\int_{|\Sigma|\leq 1} \frac{\psi(\Sigma)\partial_r\overline{Q}^0(|\Sigma|)}{|\Sigma|}\left(A^0\cdot\Sigma\right)^2 \mathrm{d}\Sigma = -\frac{C_3}{\mu^3\tilde{c}_{2l}^2}|A^0|^2. \tag{4.124}$$

where

$$C_3 = \frac{1}{12}\int_{|\Sigma|\leq 1} \frac{(1-|\Sigma|^2)|E'(|\Sigma|)|}{|\Sigma|}\Sigma_1^2 \mathrm{d}\Sigma. \tag{4.125}$$

Finally we have proven that we have

$$\mathcal{I}_1 = -\frac{1}{\mu^3\tilde{c}_{2l}^2}\left(C_2\sum_i \lambda_i^2 + C_3|A^0|^2\right). \tag{4.126}$$

Computation of $\mathcal{I}_2$

Recall that we have

$$\mathcal{I}_2 = \int_{|\Sigma|\leq 1}\left(\frac{1}{2}A^s\Sigma\cdot\Sigma + A^0\cdot\Sigma\right)\nabla\overline{Q}^{s-2l}\cdot\nabla\psi(\Sigma)\mathrm{d}\Sigma \tag{4.127}$$

We integrate by parts again:

$$\mathcal{I}_2 = -\int_{|\Sigma|\leq 1}\overline{Q}^{s-2l}\mathrm{div}\left(\left(\frac{1}{2}A^s\Sigma\cdot\Sigma + A^0\cdot\Sigma\right)\nabla\psi(\Sigma)\right)\mathrm{d}\Sigma. \tag{4.128}$$

With some elementary differential calculus we find

$$\mathrm{div}\left(\left(\frac{1}{2}A^s\Sigma\cdot\Sigma + A^0\cdot\Sigma\right)\nabla\psi(\Sigma)\right) = \frac{-7}{6\mu\tilde{c}_{2l}}\left(\frac{1}{2}A^s\Sigma\cdot\Sigma + A^0\cdot\Sigma\right) \tag{4.129}$$

and thus:

$$\mathcal{I}_2 = \frac{7}{6\mu\tilde{c}_{2l}} \int_{|\Sigma|\leq 1} \left(\frac{1}{2} A^s \Sigma \cdot \Sigma + A^0 \cdot \Sigma \right) \overline{Q}^{s-2l} \mathrm{d}\Sigma \tag{4.130}$$

We need to decompose into even and odd parts. Let us introduce the two functions G_1 and G_2 satisfying the following problems:

$$\begin{cases} -\mu\tilde{c}_{2l}\Delta G_1 = -\partial_r \overline{Q}^0(|\Sigma|)\dfrac{A^s\Sigma\cdot\Sigma}{|\Sigma|} & \text{in } |\Sigma| < 1, \\ G_1 = 0 & \text{on } |\Sigma| = 1, \end{cases} \tag{4.131}$$

and

$$\begin{cases} -\mu\tilde{c}_{2l}\Delta G_2 = -\partial_r \overline{Q}^0(|\Sigma|)\dfrac{A^0\cdot\Sigma}{|\Sigma|} & \text{in } |\Sigma| < 1, \\ G_2 = 0 & \text{on } |\Sigma| = 1, \end{cases} \tag{4.132}$$

If we sum the right-hand sides of the equation of G_1 and G_2 we find $-L(\Sigma, \nabla)\overline{Q}^0$ so that by linearity we have $\overline{Q}^{s-2l} = G_1 + G_2$.

Now we can use that G_1 is invariant through the change $\Sigma \to -\Sigma$ while under the same change G_2 is changed in $-G_2$ (this comes from the fact that this is true for their Laplacians). So we can split the integral in two terms:

$$\begin{aligned} \mathcal{I}_2 &= \frac{7}{6\mu\tilde{c}_{2l}} \int_{|\Sigma|\leq 1} \left(\frac{1}{2} A^s \Sigma \cdot \Sigma \right) G_1(\Sigma)\mathrm{d}\Sigma + \frac{7}{6\mu\tilde{c}_{2l}} \int_{|\Sigma|\leq 1} \left(A^0 \cdot \Sigma \right) G_2(\Sigma)\mathrm{d}\Sigma \\ &= \mathcal{J}_1 + \mathcal{J}_2. \end{aligned} \tag{4.133}$$

Computation of $\mathcal{J}_1$.

We now introduce an orthogonal matrix Q such that $Q^T A^s Q$ is a diagonal matrix. We change variables by setting $\Sigma = QS$ and consider the function G_1^* such that $G_1^*(S) = G_1(\Sigma)$. The function G_1^* thus satisfies the following equation:

$$-\mu\tilde{c}_{2l}\Delta G_1^* = -\sum_i \lambda_i \frac{\partial_r \overline{Q}^0(|S|)}{|S|} S_i^2. \tag{4.134}$$

Now introducing $\overline{G}_1$ which satisfies:

$$\begin{cases} -\Delta \overline{G}_1 = -\dfrac{E'(\sqrt{y^2 + |y'|^2})}{\sqrt{y^2 + |y'|^2}} y^2 \\ \overline{G}_1 = 0 \end{cases} \tag{4.135}$$

where (y, y') belongs in the unit ball of $\mathbf{R}^6$. $\overline{G}_1$ can be seen as a function of y and $|y'|$ or a vector function over the unit ball of $\mathbf{R} \times \mathbf{R}^5$. Note that $\overline{G}_1$ does not depend on any parameter. We can now write by linearity and using the fact that $\partial_r \overline{Q}^0 = (1/\mu)E'$,

$$G_1 = \frac{1}{\mu^2 \tilde{c}_{2l}} \sum_i \lambda_i \overline{G}_1(S_i, |\widehat{S}_i|)$$

where $\widehat{S}_i$ denotes any vector of $\mathbf{R}^5$ with components S_j with $j \neq i$.

Using now the matrix Q to change variable in the integral we can write:

$$\begin{aligned}
&\frac{7}{6\mu\tilde{c}_{2l}} \int_{|\Sigma|\leq 1} \left(\frac{1}{2} A^s \Sigma \cdot \Sigma\right) G_1(\Sigma) \mathrm{d}\Sigma = \frac{7}{12\mu\tilde{c}_{2l}} \int_{|S|\leq 1} \left(\sum_i \lambda_i S_i^2\right) G_1^*(S) \mathrm{d}S \\
=&\frac{7}{12\mu^3\tilde{c}_{2l}^2} \int_{|S|\leq 1} \left(\sum_i \lambda_i S_i^2\right) \left(\sum_j \lambda_j \overline{G}_1(S_j, |\widehat{S}_j|)\right) \mathrm{d}S \\
=&\frac{7}{12\mu^3\tilde{c}_{2l}^2} \sum_{i,j} \lambda_i \lambda_j \int_{|S|\leq 1} S_i^2 \overline{G}_1(S_j, |\widehat{S}_j|) \mathrm{d}S
\end{aligned} \tag{4.136}$$

Once again we see that $\displaystyle\int_{|S|\leq 1} S_i^2 \overline{G}_1(S_j, |\widehat{S}_j|)\mathrm{d}S$ does not depend on (i, j) if $i \neq j$ and on i for the terms $i = j$. This proves that there is a numerical constant

$$C_4 = \frac{7}{12} \int_{|S|\leq 1} (S_1^2 - S_2^2) \overline{G}_1(S_1, \widehat{S}_1) \mathrm{d}S. \tag{4.137}$$

so that

$$\frac{7}{12\mu\tilde{c}_{2l}} \int_{|\Sigma|\leq 1} \left(A^s \Sigma \cdot \Sigma\right) G_1(\Sigma) \mathrm{d}\Sigma = \frac{C_4}{\mu^3 \tilde{c}_{2l}^2} \sum_i \lambda_i^2. \tag{4.138}$$

To evaluate this integral we introduce the following test function:

$$\begin{aligned}
\chi_1(y, y') &= -\frac{3}{64} y^4 - \frac{7}{160} y^2 |y'|^2 + \frac{1}{24} y^2 + \frac{1}{320} |y'|^4 - \frac{1}{120} |y'|^2 + \frac{1}{192} \\
&= (1 - y^2 - |y'|^2) \left(\frac{3}{64} y^2 - \frac{1}{320} |y'|^2 + \frac{1}{192}\right),
\end{aligned} \tag{4.139}$$

where $y \in \mathbf{R}$ and $y' \in \mathbf{R}^5$. One can check that this function satisfies $-\Delta\chi_1 = y^2$ and χ_1 vanishes on the unit sphere. Now we have the following relation:

$$\int_{|S|\leq 1} (S_1^2 - S_2^2) \overline{G}_1(S_1, \widehat{S}_1) \mathrm{d}S = -\int_{|S|\leq 1} \frac{E'(|S|) S_1^2}{\sqrt{S_1^2 + |\widehat{S}_1|^2}} (\chi_1(S_1, \widehat{S}_1) - \chi_1(S_2, \widehat{S}_2)) \mathrm{d}S. \tag{4.140}$$

One can check using the definition of χ_1 that

$$\chi_1(S_1, \widehat{S}_1) - \chi_1(S_2, \widehat{S}_2) = \frac{1}{20}(S_1^2 - S_2^2)(1 - |S|^2), \tag{4.141}$$

so that what is left to compute is

$$\int_{|S|\leq 1} (S_1^2 - S_2^2)\overline{G}_1(S_1, \widehat{S}_1)\mathrm{d}S = -\int_{|S|\leq 1} \frac{E'(|S|)S_1^2(S_1^2 - S_2^2)(1 - |S|^2)}{20|S|}\mathrm{d}S. \tag{4.142}$$

Now using the change of variable which exchange the variables S_1 and S_2 and writing the average we have that the integral is also

$$\int_{|S|\leq 1} (S_1^2 - S_2^2)\overline{G}_1(S_1, \widehat{S}_1)\mathrm{d}S = -\int_{|S|\leq 1} \frac{E'(|S|)(S_1^2 - S_2^2)^2(1 - |S|^2)}{40|S|}\mathrm{d}S. \tag{4.143}$$

Therefore

$$C_4 = \frac{7}{480}\int_{|S|\leq 1} \frac{(S_1^2 - S_2^2)^2|E'(|S|)|}{|S|}(1 - |S|^2)\mathrm{d}S. \tag{4.144}$$

By comparing this expression with the expression of C_2 from (4.123) we have $C_4/C_2 = \dfrac{7}{480} \cdot 24 < 1$. This implies that $C_6 = C_2 - C_4 = \dfrac{3}{20}C_2 > 0$.

Computation of $\mathcal{J}_2$.

The integral $\mathcal{J}_2$ is treated using the same method. We introduce an orthogonal matrix Q^0 such that $(Q^0)^T A^0$ is the vector $(|A^0|, 0 \ldots, 0)$ and we write $S = Q^0\Sigma$ and $G_2^*(S) = G_2(\Sigma)$. We thus have by a change of variable that:

$$\mathcal{J}_2 = \frac{7}{6\mu\tilde{c}_{2l}}\int_{|\Sigma|\leq 1} \left(A^0 \cdot \Sigma\right) G_2(\Sigma)\mathrm{d}\Sigma = \frac{7|A^0|}{6\mu\tilde{c}_{2l}}\int_{|S|\leq 1} S_1 G_2^*(S)\mathrm{d}S, \tag{4.145}$$

and that

$$\begin{cases} -\mu\tilde{c}_{2l}\Delta G_2^* = -|A^0|\dfrac{\partial_r\overline{Q}^0(|S|)}{|S|}S_1 & \text{in } |\Sigma| < 1, \\ G_2^* = 0 & \text{on } |S| = 1, \end{cases} \tag{4.146}$$

so there is a numerical constant C_5 such that :

$$\frac{7}{6\mu\tilde{c}_{2l}}\int_{|\Sigma|\leq 1} \left(A^0 \cdot \Sigma\right) G_2(\Sigma)\mathrm{d}\Sigma = \frac{C_5}{\mu^3\tilde{c}_{2l}^2}|A^0|^2, \tag{4.147}$$

and this constant has the following expression:

$$C_5 = \frac{7}{6}\int_{|S|\leq 1} S_1\overline{G}_2(S_1, \widehat{S}_1)\mathrm{d}S, \tag{4.148}$$

where

$$\begin{cases} -\Delta\overline{G}_2 = -\dfrac{E'(\sqrt{y^2+|y'|^2})y}{\sqrt{y^2+|y'|^2}}, \\ \overline{G}_2 = 0. \end{cases} \tag{4.149}$$

We now introduce the test function $\chi_2(y,y') = \dfrac{1}{16}y(1-(y^2+|y'|^2))$ which satisfies $-\Delta\chi_2 = y$ and χ_2 vanishes on the sphere. Thus we have:

$$\begin{aligned} C_5 &= \frac{7}{6}\int_{|S|\leq 1} S_1\overline{G}_2(S_1,\widehat{S}_1)\mathrm{d}S \\ &= -\frac{7}{6}\int_{|S|\leq 1}\frac{E'(|S|)S_1}{|S|}\frac{S_1}{16}(1-|S|^2)\mathrm{d}S \\ &= \frac{7}{96}\int_{|S|\leq 1}\frac{|E'(|S||)(1-|S|^2)}{|S|}S_1^2\mathrm{d}S. \end{aligned} \tag{4.150}$$

Comparing C_5 to C_3 from (4.125) we can see that $C_5/C_3 = \dfrac{7}{96}\cdot 12 < 1$ and thus $C_7 = C_5 - C_3 > 0$.

Finally we have proven,

$$\mathcal{I}_2 = \frac{1}{\mu^3\tilde{c}_{2l}^2}\left(C_4\sum_i \lambda_i^2 + C_5|A^0|^2\right). \tag{4.151}$$

Conclusion on the Integral of $\widetilde{G}$.

Combining (4.109), (4.111), (4.112), (4.126) and (4.151) we finally obtain

$$\int_{|\Sigma|\leq 1}\widetilde{G}(\Sigma)\mathrm{d}\Sigma = -\frac{1}{\mu^3\tilde{c}_{2l}^2}((C_2-C_4)\sum_i\lambda_i^2 + (C_3-C_5)|A_0|^2), \tag{4.152}$$

and thus is strictly negative. This means that $2s-4l$ must be equal to l (that is $2s=5l$ as in the $1d$ case) for (4.108) to have a solution. Furthermore it is clear that to have the least number of trivial profiles one must take:

$$s = 5 \qquad\qquad l = 2.$$

Also we have that $\Gamma \sim \tilde{c}_{2l}\dot{\varepsilon}^{4/5}$. Note that the constant $\tilde{c}_{2l}$ depend on the quantities $\sum_i \lambda_i^2$ where λ_i are the eigenvalues of A^s which means that $\tilde{c}_{2l}$ depend on $A^s : A^s$. It also depends on $|A^0|^2$. We can explicit these two

quantities in terms of the matrix M which describes the rheological situation. We have:

$$A^s : A^s = 13a^2|D(M)|^2 + 5a^2|D(M) - \mathrm{diag}(M_{11}, M_{22}, M_{33})|^2 + |W(M)|^2$$
$$|A^0|^2 = 4\lambda^2|D(M)|^2$$

4.6 Examples

We have in mind three particular rheological configurations: the Couette flow and two types of elongational flows. We want to study the adequation of our model with the original model of Hébraudand Lequeux.

4.6.1 Couette Flow.

We are interested in comparing the results of our model with the original HL model. In stationary Couette flows we have seen that the velocity field has the form $u(x, y, z) = (\dot{\gamma}y, 0, 0)$. In this case we have

Elements of the Model

$$\nabla u = \begin{pmatrix} 0 & \dot{\gamma} & 0 \\ 0 & 0 & 0 \\ 0 & 0 & 0 \end{pmatrix}, \tag{4.153}$$

so, in the notations of Section 4.3, we have

$$M = \begin{pmatrix} 0 & 1 & 0 \\ 0 & 0 & 0 \\ 0 & 0 & 0 \end{pmatrix}. \tag{4.154}$$

This leads to a matrix A which is

$$A = \begin{pmatrix} 0 & 0 & 0 & \frac{\sqrt{2}}{2}(1+a) & 0 & 0 \\ 0 & 0 & 0 & \frac{\sqrt{2}}{2}(-1+a) & 0 & 0 \\ 0 & 0 & 0 & 0 & 0 & 0 \\ \sqrt{2}(-1+a) & \sqrt{2}(1+a) & 0 & 0 & 0 & 0 \\ 0 & 0 & 0 & 0 & 0 & 1+a \\ 0 & 0 & 0 & 0 & -1+a & 0 \end{pmatrix}, \tag{4.155}$$

and a vector

$$A^0 = (0, 0, 0, 2\sqrt{2}\lambda, 0, 0)^T. \tag{4.156}$$

The eigenvalues of A are in this case

$$\text{eigenvalues}(A) = \{0,\ 0,\ i\sqrt{2(1-a^2)},\ -i\sqrt{2(1-a^2)},\ i\sqrt{1-a^2},\ -i\sqrt{1-a^2}\}. \tag{4.157}$$

They are all purely imaginary or 0.

Estimation of λ_m of Prop 4.6

For Couette flows, we need to distinguish the different cases: $a = 0$, $0 < |a| < 1$ and $a = \pm 1$.

$a = \pm 1$

If $a = \pm 1$ then because of (4.157), all the eigenvalues of A are 0 while A is not 0. This means that the characteristic curves $\Sigma(t; \Sigma_0)$ are polynomials of t. Roughly this means that either Σ_0 is a stationary point or the characteristic line must cross the unit sphere when $t \to +\infty$ and $t \to -\infty$. Consequently, if we can ensure that no stationary point are located inside the ball, we are set.

Let us treat the case $a = 1$. In this case the matrix A falls to

$$A = \begin{pmatrix} 0 & 0 & 0 & \sqrt{2} & 0 & 0 \\ 0 & 0 & 0 & 0 & 0 & 0 \\ 0 & 0 & 0 & 0 & 0 & 0 \\ 0 & 2\sqrt{2} & 0 & 0 & 0 & 0 \\ 0 & 0 & 0 & 0 & 0 & 2 \\ 0 & 0 & 0 & 0 & 0 & 0 \end{pmatrix}. \tag{4.158}$$

We can give the expression of the characteristic curves:

$$\Sigma(t; \Sigma_0) = \Sigma_0 + t \begin{pmatrix} \sqrt{2}\Sigma_0^4 \\ 0 \\ 0 \\ 2\sqrt{2}(\Sigma_0^2 + \lambda) \\ 2\Sigma_0^6 \\ 0 \end{pmatrix} + t^2 \begin{pmatrix} 2(\Sigma_0^2 + \lambda) \\ 0 \\ 0 \\ 0 \\ 0 \\ 0 \end{pmatrix}. \tag{4.159}$$

Thus we can see that if $\lambda > 1$ then the characteristic curves go to infinity in both directions. The case $a = -1$ can be treated in the same way.

$0 < |a| < 1$

Considering (4.157), we now have the eigenvalues of a that are 0 or non zero and purely imaginary. More over we can see that the rank of A is 4, so that A is diagonable. This essentially means that some projections of the characteristic curves are ellipsis. Using that, we will then show that under a condition $\lambda > \lambda_m$ then the characteristic line must have a point outside the unit sphere. This means that the characteristic line must cross the boundary both inwardly and outwardly.

We note $\omega = \sqrt{1-a^2}$. Then one can show that the characteristic line can be decomposed as:

$$
\begin{aligned}
\Sigma^3(t;\Sigma_0) &= \Sigma_0^3 \\
\begin{pmatrix}\Sigma^5(t;\Sigma_0)\\ \Sigma^6(t;\Sigma_0)\end{pmatrix} &= \cos(\omega t)\begin{pmatrix}\Sigma_0^5\\ \Sigma_0^6\end{pmatrix} + \frac{\sin(\omega t)}{\omega}\begin{pmatrix}(1+a)\Sigma_0^6\\ (-1+a)\Sigma_0^5\end{pmatrix} \\
\begin{pmatrix}\Sigma^1(t;\Sigma_0)\\ \Sigma^2(t;\Sigma_0)\\ \Sigma^4(t;\Sigma_0)\end{pmatrix} &= \cos(\sqrt{2}\omega t)\begin{pmatrix}\Sigma_0^1\\ \Sigma_0^2\\ \Sigma_0^4\end{pmatrix} + \frac{\sin(\sqrt{2}\omega t)}{\sqrt{2}\omega}\begin{pmatrix}\frac{1}{\sqrt{2}}(1+a)\Sigma_0^4\\ \frac{1}{\sqrt{2}}(-1+a)\Sigma_0^4\\ \sqrt{2}(a-1)\Sigma_0^1 - \sqrt{2}(a+1)\Sigma_0^2\end{pmatrix} \\
&\quad - (1-\cos(\sqrt{2}\omega t))\begin{pmatrix}\frac{\lambda}{a}\\ \frac{\lambda}{a}\\ 0\end{pmatrix} + \frac{\sin(\sqrt{2}\omega t)}{\sqrt{2}\omega}\begin{pmatrix}0\\ 0\\ 2\sqrt{2}\lambda\end{pmatrix}
\end{aligned}
$$

It is possible to explicitly force the third part of the characteristic curves to reach a point outside the unit ball. Indeed we can write:

$$
\left\|(\Sigma^1,\Sigma^2,\Sigma^3)^T\right\| \geq \lambda(I_1(a)(1-\cos(\sqrt{2}\omega t)) + I_2(a)\left|\sin(\sqrt{2}\omega t)\right|) - I_3(a), \tag{4.160}
$$

where $I_1(a)$,$I_2(a)$ and $I_3(a)$ are positive function of $|a|$:

$$I_1(a) = \left\| \begin{matrix} \frac{1}{a} \\ \frac{1}{a} \\ 0 \end{matrix} \right\| = \frac{\sqrt{2}}{|a|}$$

$$I_2(a) = \frac{1}{\sqrt{2}\omega} \left\| \begin{matrix} 0 \\ 0 \\ 2\sqrt{2} \end{matrix} \right\| = \frac{2}{\omega}$$

$$I_3(a) \geq \left\| \begin{matrix} \frac{1}{\sqrt{2}}(1+a)\Sigma_0^4 \\ \frac{1}{\sqrt{2}}(-1+a)\Sigma_0^4 \\ \sqrt{2}(a-1)\Sigma_0^1 - \sqrt{2}(a+1)\Sigma_0^2 \end{matrix} \right\| + \left\| \begin{matrix} \Sigma_0^1 \\ \Sigma_0^2 \\ \Sigma_0^4 \end{matrix} \right\|$$

Since $I_1(a)(1-\cos(\sqrt{2}\omega t)) + I_2(a)\left|\sin(\sqrt{2}\omega t)\right|)$ is bounded from below by a positive constant, this means that we can impose $\left\|(\Sigma^1, \Sigma^2, \Sigma^3)^T\right\| > 1$ uniformly in Σ_0 by a condition of the type $\lambda > \lambda_m$.

$a = 0$

The previous argument does not apply since we have divided by a to make the vector B^0 such that $AB^0 = -A^0$. But we can also take the vector $B^0 = (0, 2\lambda, 0, 0, 0, 0)^T$ and the rest follows.

4.6.2 Elongational Flows

Elements of the Model

Elongational flow are classical rheological flows characterized by a diagonal deformation rate tensor. We distinguish two main types of elongationnal flows. The first kind is axisymmetric flow in which the velocity field has the expression $u(x, y, z) = (2\dot{\varepsilon}x, -\dot{\varepsilon}y, -\dot{\varepsilon}z)$ which leads to:

$$M = \begin{pmatrix} 2 & 0 & 0 \\ 0 & -1 & 0 \\ 0 & 0 & -1 \end{pmatrix}. \tag{4.161}$$

In this case the matrix A has the following expression:

$$A = \begin{pmatrix} 4a & 0 & 0 & 0 & 0 & 0 \\ 0 & -2a & 0 & 0 & 0 & 0 \\ 0 & 0 & -2a & 0 & 0 & 0 \\ 0 & 0 & 0 & 2a & 0 & 0 \\ 0 & 0 & 0 & 0 & 2a & 0 \\ 0 & 0 & 0 & 0 & 0 & -4a \end{pmatrix}, \tag{4.162}$$

The vector A^0 is also defined:

$$A^0 = (4\lambda, -2\lambda, -2\lambda, 0, 0, 0)^T. \tag{4.163}$$

We note immediately that the eigenvalues of A are in this case all real valued (or $A = 0$ if we take $a = 0$).

The second kind of elongational flow are planar elongational flow which have the velocity field $u(x, y, z) = (\dot{\varepsilon}x, -\dot{\varepsilon}y, 0)$. Thus

$$M = \begin{pmatrix} 1 & 0 & 0 \\ 0 & -1 & 0 \\ 0 & 0 & 0 \end{pmatrix}. \tag{4.164}$$

This leads to a matrix A which is

$$A = \begin{pmatrix} 2a & 0 & 0 & 0 & 0 & 0 \\ 0 & -2a & 0 & 0 & 0 & 0 \\ 0 & 0 & 0 & 0 & 0 & 0 \\ 0 & 0 & 0 & 0 & 0 & 0 \\ 0 & 0 & 0 & 0 & 2a & 0 \\ 0 & 0 & 0 & 0 & 0 & -2a \end{pmatrix}, \tag{4.165}$$

and a vector

$$A^0 = (2\lambda, -2\lambda, 0, 0, 0, 0)^T. \tag{4.166}$$

Estimation of λ_m in Prop 4.6

For the two elongational flows we want to study we have two possibilities: either $a = 0$ or $a \neq 0$. If $a = 0$ then the matrix A is 0. Then the transport vector field is the constant vector A^0 and the characteristic curves are straight lines with direction A^0 which means that we can take $\lambda_m = 0$ for Prop 4.6.

If $a \neq 0$ then the matrix A is diagonal. Moreover we can check that setting $B^0 = -\lambda/a(1, 1, 1, 0, 0, 0)^T$ we have a vector which verifies $AB^0 = -A^0$. This vector stands for the identity matrix in our choice of coordinates. Indeed we have the relation $g_a(Id, M) = 2aD(M)$. Thus the characteristic curves have the form $\Sigma(t; \Sigma_0) = \exp(tA)(\Sigma_0 - B^0) + B^0$. We now take λ large enough

so that $B^0 + \ker(A)$ does not meet the unit ball. It is possible since B^0 does not belong to $\ker(A)$. Then the characteristic curves satisfy the hypotheses of 4.6.

Appendix to chapter 4

Expressions of A and A^0

We have first before the rescaling of Σ the expression

$$
\begin{aligned}
&A = \begin{pmatrix} A_{11} & A_{12} \\ A_{21} & A_{22} \end{pmatrix}, \\
&A_{11} = \begin{pmatrix} 2aM_{11} & 0 & 0 \\ 0 & 2aM_{22} & 0 \\ 0 & 0 & 2aM_{33} \end{pmatrix}, \quad A_{12} = \begin{pmatrix} a_{11}^1 & a_{12}^1 & a_{13}^1 \\ a_{21}^1 & a_{22}^1 & a_{23}^1 \\ a_{31}^1 & a_{32}^1 & a_{33}^1 \end{pmatrix} \\
&A_{21} = \begin{pmatrix} a_{11}^2 & a_{12}^2 & a_{13}^2 \\ a_{21}^2 & a_{22}^2 & a_{23}^2 \\ a_{31}^2 & a_{32}^2 & a_{33}^2 \end{pmatrix} \qquad A_{12} = \begin{pmatrix} a_{11}^3 & a_{12}^3 & a_{13}^3 \\ a_{21}^3 & a_{22}^3 & a_{23}^3 \\ a_{31}^3 & a_{32}^3 & a_{33}^3 \end{pmatrix}
\end{aligned}
\tag{4.167}
$$

with

$$
\begin{aligned}
a^1_{11} &= M_{12} - M_{21} + a(M_{12} + M_{21}) \\
a^1_{12} &= M_{13} - M_{31} + a(M_{13} + M_{31}) \\
a^1_{13} &= 0 \\
a^1_{21} &= -(M_{12} - M_{21}) + a(M_{12} + M_{21})) \\
a^1_{22} &= 0 \\
a^1_{23} &= M_{23} - M_{32} + a(M_{23} + M_{32}) \\
a^1_{31} &= 0 \\
a^1_{32} &= -(M_{13} - M_{31}) + a(M_{13} + M_{31}) \\
a^1_{33} &= -(M_{23} - M_{32}) + a(M_{23} + M_{32}) \\
a^2_{11} &= -(M_{12} - M_{21}) + a(M_{12} + M_{21}) \\
a^2_{12} &= (M_{12} - M_{21}) + a(M_{12} + M_{21}) \\
a^2_{13} &= 0 \\
a^2_{21} &= -(M_{13} - M_{31}) + a(M_{13} + M_{31}) \\
a^2_{22} &= 0 \\
a^2_{23} &= (M_{13} - M_{31}) + a(M_{13} + M_{31}) \\
a^2_{31} &= 0 \\
a^2_{32} &= -(M_{23} - M_{32}) + a(M_{23} + M_{32}) \\
a^2_{33} &= (M_{23} - M_{32}) + a(M_{23} + M_{32}) \\
a^3_{11} &= 2a(M_{11} + M_{22}) \\
a^3_{12} &= M_{23} - M_{32} + a(M_{23} + M_{32}) \\
a^3_{13} &= M_{13} - M_{31} + a(M_{13} + M_{31}) \\
a^3_{21} &= -(M_{23} - M_{32}) + a(M_{23} + M_{32}) \\
a^3_{22} &= 2a(M_{11} + M_{33}) \\
a^3_{23} &= M_{12} - M_{21} + a(M_{12} + M_{21}) \\
a^3_{31} &= -(M_{13} - M_{31}) + a(M_{13} + M_{31}) \\
a^3_{32} &= -(M_{12} - M_{21}) + a(M_{12} + M_{21}) \\
a^3_{33} &= 2a(M_{22} + M_{33})
\end{aligned}
$$

We can also write the vector

$$A^0 = \begin{pmatrix} 2\lambda M_{11} \\ 2\lambda M_{22} \\ 2\lambda M_{33} \\ 2\lambda(M_{12} + M_{21}) \\ 2\lambda(M_{13} + M_{31}) \\ 2\lambda(M_{23} + M_{32}) \end{pmatrix}. \tag{4.168}$$

We now have to rescale Σ_4, Σ_5 and Σ_6. This amounts to multiply the matrix A_{12} by the factor $1/\sqrt{2}$ and the matrix A_{21} by the factor $\sqrt{2}$. Multiply by $\sqrt{2}$ also the last three rows of A^0.

Deuxième partie

Deux modèles mathématiques pour la biologie et la chimie

Chapitre 5

Diffusion d'espèces chimiques réagissant infiniment rapidement

Résumé du chapitre

Dans ce chapitre on s'intéresse au problème de la diffusion d'espèces réactives à travers la peau dans le contexte de la balnéothérapie. Ce problème est éminemment complexe et mélange, au moins, biochimie (préservation du soi, barrières de pH, osmose,...) et biomécanique (milieu poro-élastiques, tissus vivants, ...). Nous n'aborderons pas ce problème dans tous ses détails, loin s'en faut, mais nous proposons tout de même quelques réflexions sur les systèmes de réaction-diffusion qui, semble-t-il, n'ont pas été étudiées auparavant.

Notre optique est la suivante : nous nous intéressons principalement à la migration d'espèce chimique à travers la peau par diffusion. Bien que la peau soit de faible épaisseur, les distances à parcourir pour les ions et les molécules sont de taille macroscopique et par conséquent le temps de diffusion est lui aussi assez grand (ces notions seront précisées dans le chapitre). Par conséquent, si nous voulons suivre ces espèces le long de leur migration, nous ne pouvons pas pas nous permettre de descendre à des échelles de temps trop petites. D'un autre côté, les espèces ne font pas que diffuser, elles réagissent aussi entre elles. Or ces réactions sont très rapides ce qui a tendance à rendre le système mathématique de réaction-diffusion très raide. Et si l'échelle de temps est très grande, cela veut dire qu'«entre deux instants», le système a largement le temps de retourner à l'équilibre chimique. Pouvons-nous alors considérer que le système chimique est en permanence à l'équilibre ? Et si oui, comment rendre compte convenablement de ce fait mathématiquement et numériquement ? Ce sont les deux questions que nous allons aborder dans

ce chapitre.

À la première question nous n'apportons pas de réponse définitive. En effet, même si conceptuellement il paraît clair que, lorsque les échelles de temps entre réaction et diffusion sont suffisamment séparées, le système peut être considéré comme étant à l'équilibre chimique en permanence, évaluer en pratique le temps de réaction caractéristique de plusieurs réactions simultanées n'est pas toujours évident. Par conséquent, évaluer pour quelles espèces chimiques et quelles réactions un équilibre permanent est justifié n'est pas facile. Nous verrons cette difficulté numériquement sur l'exemple de la dissociation de l'eau. Cette difficulté est aussi liée à la complexité de la cinétique chimique en général car les données ne sont connues que dans certains contextes qui sont non transposables (par exemple la cinétique de la dissociation du dioxyde de carbone n'est pas du tout la même si l'on est dans une solution aqueuse «standard» ou dans la mer – voir par exemple Johnson [39])

En ce qui concerne la mise en œuvre pratique de l'hypothèse (en supposant qu'elle soit justifiée) nous proposons le système de réaction-diffusion (5.4) en le justifiant de trois façons différentes. Il faut noter que c'est dans cette hypothèse que les réactions sont *toutes* rapides que nous pouvons dériver ce modèle, ce qui simplifie considérablement l'étude. Contrairement à la situation «standarde» en réaction-diffusion, nous savons distinguer les échelles de temps *a priori*, et nous essayons de nous servir de cette information particulière dans notre modélisation et dans notre étude numérique. Ainsi, notre démarche est distincte de celle de Descombes et Massot dans [25], qui, au contraire, cherchent à démontrer l'efficacité de méthodes numériques dans des cas très généraux où le système chimique est si complexe, qu'il est illusoire d'espérer y distinguer ce qui est lent de ce qui est rapide.

Pour le moment, nous ne sommes pas en mesure d'en dire beaucoup sur les propriétés mathématiques du modèle en raison de sa nature non conservative. Tout ce que nous pouvons affirmer, c'est que le modèle respecte formellement l'équilibre.

Pour l'étude numérique d'un tel système nous proposons un schéma numérique basé sur les mêmes idées que le modèle continu et donné par (5.41)-(5.43). Nous comparons ce schéma au schéma de de diffusion/projection qui est parfois la seule approche disponible pour les problèmes dont la cinétique est inconnue ou trop raide. Notre schéma n'en est pas très éloigné en terme de complexité de mise en application et donne, à peu de frais, de meilleurs résultats comme nous l'illustrons dans le cas de la dissociation de l'eau. Puis nous donnons quelques résultats sur le système des carbonates dans un milieu inhomogène dans une version très simplifiée d'une séance de balnéothérapie.

Ce chapitre présente la version initiale d'un article en collaboration avec Yann Bouret et Stéphane Descombes.

5.1 Modelling hypotheses and General Formalism

In this article we want to study the diffusion of some reacting chemical species. Reaction-diffusion is a widely studied field of partial differential equations. We want to bring a new look at the numerical simulation of this problem by borrowing a concept of chemical kinetics which is commonly used in local systems (which means without the space dimension) but as not been tested on reaction-diffusion as far as our knowledge goes.

The main hypothesis of our model is the fact that we only have *two* time scales in our system: the first one would be the scale 1 which is the time scale of the diffusion process, and the second one would be the scale $1/\varepsilon$ of *all* the chemical reactions. In other words we consider on the one hand that the reactions are much faster than the diffusion and on the other hand that all the reaction take place at the same time scale.

Let us note immediately that these hypotheses are not empty: in Section 5.2 we will present two models to which our modelling can be applied. In fact our modelling is at least relevant for the broader class of *protic* reactions, namely reactions which involve the exchange of a proton H^+ from one molecule or ion to another.

5.1.1 Notations for the Chemistry

Let us now introduce some general notations that will be used throughout this article. The generality mainly serves the purpose of showing that our method is quite flexible.

We consider a general system of N chemical reactions involving M species (A_j). We note C_j the chemical activity of A_j which we consider to be equal to the concentration of A_j except if A_j is the solvant H_2O in which case its activity is simply 1 . An index i will always be used to refer to a reaction while an index j will always be used for a species. We write this chemical system under the compact form

$$\forall i, \sum_j \alpha_{ij} A_j \leftrightarrows \sum_j \alpha_{ij} A_j, \tag{5.1}$$

the (α_{ij}) being the reduced stoichiometric coefficients: α_{ij} is an integer, $\alpha_{ij} = 0$ if the species j is not involved in reaction i and the remaining (α_{ij}) do not have a common factor. The species appearing in the left-hand side of (5.1) are called the *reactants* of the i-th reaction and the species in the right-hand side are called the *products* of i. The algebraic stoichiometric coefficients can

now be defined by $\nu_{ij} = \alpha_{ij}$ if j is a product of i and $\nu_{ij} = -\alpha_{ij}$ otherwise. The N-by-M matrix $\nu = (\nu_{ij})$ defines the directions in which the law of mass conservation allows the system to evolve.

From the first and second principle of thermodynamics, every reaction i has an equilibrium constant noted K_i: the i-th reaction does not change the composition when the concentrations satisfy the following equation:

$$K_i = \prod_j C_j^{\nu_{ij}}. \tag{5.2}$$

It will be useful to introduce the following functions:

$$\Gamma_i = K_i \prod_{j,\text{reactant of } i} C_j^{|\nu_{ij}|} - \prod_{j,\text{product of } i} C_j^{|\nu_{ij}|}. \tag{5.3}$$

Indeed with our conventions we have: if $C_j > 0$ for all j then (5.2) is true if, and only if, $\Gamma_i = 0$. On the other hand the Γ_i are well defined when some of the concentrations are 0 while the right-hand side of (5.2) (called the *reaction quotient* is not. These singularities cannot happen if we consider a closed system undergoing only chemical process. However we are not in this case since we are not closed, and there are other physical processes to consider that allow the complete depletion of one species. That is why we will deal with Γ rather than the quotients of reaction.

We will also use extensively $\Phi = \mathrm{d}\Gamma = (\partial_{C_j}\Gamma_i)_{ij}$.

5.1.2 Notations for the Diffusion Process

We consider a very simplified diffusion process. Let us first note $\mathcal{D}_j$ the *free self-diffusion constant* of the species j. Those are well-known constants, easily found in the literature and some have been indicated in Table 5.1. However they are of little use by themselves in reality, for an ion cannot diffuse "by itself" alone: because the local electroneutrality must be preserved, when an ion wants to move, some counterion must move with it. If they do not have the same "speed" (*i.e* the same diffusion constant) then the faster one is slowed down compared to the theoretical "speed" it has by itself.

The easy way to circumvent this difficulty is to consider that every species has the same diffusion coefficient. In this case, the electroneutrality is always preserved. Another idea is that beside the reactive species we have selected, there are also spectator ions which are in charge of maintaining locally the electroneutrality. In this framework the medium in which the reaction-diffusion process takes place "knows" a way to maintain electroneutrality "in the background" and we do not have to take care of it ourselves.

This argument can be relevant in some context: for example in a biotissue there are always large quantities of non reactive counterions like Na^+, Cl^- and K^+. Finally, the most accurate way is to come back to the basics of diffusion: the existence of a diffusive flux $J_j = -\mathcal{D}_j \nabla C_j$ comes from a momentum balance between a fluid friction force and a potential force originating from the chemical potential. When charged species are in play, then one should take into account the electric Coulomb force. This results in a complicated right-hand side, beside the reaction term in the reaction-diffusion equation. Since we have in mind a problem coming from a physiological context, we will allow ourselves to bypass the electroneutrality of the reactional medium.

5.1.3 Continuous Model

We recall that our main hypothesis is that the chemical reaction all take place at a time scale which is much smaller than the time scale of any other process which all take place at the same macroscopic time scale. We now propose a model for the evolution of the composition of the medium in the limit of inifinitely fast reactions:

$$\partial_t \overrightarrow{C} = \left(I_M - \chi(\overrightarrow{C})\right)\left(\mathrm{div}\,(\mathcal{D}\nabla \overrightarrow{C}) + S(t;\overrightarrow{C})\right), \tag{5.4}$$

where $\mathcal{D} = \mathrm{diag}(\mathcal{D}_j)$ is the tensor form of the diffusion constants of the chemical species involved and χ is a local projection matrix defined by

$$\chi(\overrightarrow{C}) = \nu^T(\Phi(\overrightarrow{C})\nu^T)^{-1}\Phi(\overrightarrow{C}). \tag{5.5}$$

Of course this definition makes sense only when $\Phi(\overrightarrow{C})\nu^T$ is invertible which is true in practice for meaningful concentrations $\overrightarrow{C}$ (see (5.12) and (5.16) for a practical example of this fact). The term S (which will be 0 in the sequel) could represent any other macroscopic process such as, local modification of the composition (to modelize a sudden burst of chemical species) or advection by a given velocity field.

We said that $\chi(\overrightarrow{C})$ is a local projection matrix. This is true when $\Gamma = 0$ defines a real $M-N$-dimensional manifold (which we will assume). On the one hand, any v in $\ker(\Phi(\overrightarrow{C}))$ is also in the kernel of $\chi(\overrightarrow{C})$ and thus $\ker(\chi(\overrightarrow{C}))$ is at least of dimension $M-N$. On the other hand we clearly have $\chi(\overrightarrow{C})\nu^T = \nu^T$ and we can always assume ν^T to have maximal rank which is N. Otherwise it would mean that we could simplify our chemical system by removing some chemical reactions. Consequently $\chi(\overrightarrow{C})$ is the projection matrix onto $R(\nu^T)$ parallel to $\ker(\Phi(\overrightarrow{C}))$.

Section 5.2 describes an example that fits the general framework. Section 5.3 explains how we derive (5.4). Let us note that the principles behind this derivation are well-known in the local case but the application to the reaction diffusion context is new. Section 5.4 presents a numerical scheme which follows the same principles as the continous model. This scheme is then validated on an academic example. Finally we test its performance, compared to other traditional approaches.

5.2 Application to Balneotherapy

In balneotherapy, patients take bath in water naturally or artificially enriched in carbon dioxide CO_2. The purpose of these baths is usually to dilate the blood vessel contained in the skin in order to improve overall blood circulation. Carbon dioxide is known to have an effect on the dilatation of the vessels but is also very important in the regulatory process of the blood pH. On the other hand, the hydrostatic pressure of a water bath can be important, which means that patients with frail heart may not be able to bear it. Those people are thus usually treated in a CO_2-enriched atmosphere instead of a CO_2-enriched water bath. One question might then be: how to compare the efficiency of these two therapies? To answer this question, one has to be able to know precisely the concentration in or around the blood vessels as a function of time in both cases. This problem was pointed out to us by Bear and Bresch as they had tried to model this situation in an ultimately not published work [4]. What we propose in this article is a step in that direction, as we show how to study the diffusion of reactive species such as CO_2 in a possibly contrasted medium such as the skin layer. Let us now show how this situation enters in the general framework we have outlined in the previous section.

To study the balance of carbonated species we can consider the following two chemical scenarii:

1. Four species and two reactions. The species we will take into account are H^+, HO^-, CO_2 and HCO_3^-. These four species can undergo two chemical reactions:

$$H_2O \leftrightarrows H^+ + HO^-, \tag{5.6}$$
$$CO_2 + H_2O \leftrightarrows H^+ + HCO_3^-. \tag{5.7}$$

   The equilibrium constant of (5.6) is *water self-ionization constant* $K_w = 10^{-14}$ at 25 °C. The equilibrium constant of (5.7) is noted $K_1 = 4.47 \cdot 10^{-7}$ at 25 °C.

2. Five species and three reactions. We add CO_3^{2-} and the second dissociation:

$$HCO_3^- \leftrightarrows H^+ + CO_3^{2-}. \tag{5.8}$$

Th equilibrium constant is $K_2 = 4.69 \cdot 10^{-11}$ at 25 °C. Note that since $K_2 \sim 10^{-11}$, this reaction only matters when the pH is very high which shall not happen in biotissues. We merely introduced it for the academic purpose of testing our model in a wider context than the one we are really interested in.

The notations of Section 5.1 in the first scenario are thus

$$\Gamma(\overrightarrow{C}) = \begin{pmatrix} K_w - C_1C_2 \\ K_1C_3 - C_1C_4 \end{pmatrix}, \tag{5.9}$$

and

$$\nu = \begin{pmatrix} 1 & 1 & 0 & 0 \\ 1 & 0 & -1 & 1 \end{pmatrix}. \tag{5.10}$$

We also have

$$\Phi(\overrightarrow{C}) = \begin{pmatrix} -C_2 & -C_1 & 0 & 0 \\ -C_4 & 0 & K_1 & -C_1 \end{pmatrix}. \tag{5.11}$$

Finally one can check that

$$\det\left(\Phi(\overrightarrow{C})\nu^T\right) = K_1C_2 + K_1C_1 + C_1C_4 + C_1C_2 + C1^2, \tag{5.12}$$

so that $\Phi(\overrightarrow{C})\nu^T$ is invertible for admissible concentrations (which are non negative numbers) as long as C_1 or C_2 is non vanishing.

For the second scenario we have:

$$\Gamma(\overrightarrow{C}) = \begin{pmatrix} K_w - C_1C_2 \\ K_1C_3 - C_1C_4 \\ K_2C_4 - C_1C_5 \end{pmatrix}, \tag{5.13}$$

and

$$\nu = \begin{pmatrix} 1 & 1 & 0 & 0 & 0 \\ 1 & 0 & -1 & 1 & 0 \\ 1 & 0 & 0 & -1 & 1 \end{pmatrix}. \tag{5.14}$$

Moreover,

$$\Phi(\overrightarrow{C}) = \begin{pmatrix} -C_2 & -C_1 & 0 & 0 & 0 \\ -C_4 & 0 & K_1 & -C_1 & 0 \\ -C_5 & 0 & 0 & K_2 & -C_1 \end{pmatrix}, \tag{5.15}$$

and

$$-\det\left(\Phi(\overrightarrow{C})\nu^T\right) = 2K_1K_2 + C_1K_1K_2 + 2C_1C_4K_2 + C_1C_5K_1 + C_1C_2K_1 + C_1^2K_1 + 2C_1^2C_5 + C_1^2C_4 + C_1^2C_2 + C_1^3. \quad (5.16)$$

Again we see that $\Phi(\overrightarrow{C})\nu^T$ is invertible as long as C_1 or C_2 is non vanishing.

Now let us examine the pertinence of our two scale hypothesis. The two processes in competition are the diffusion through the skin layers and the chemical reactions. For the chemical species we consider we can estimate the characteristic time of diffusion by taking a typical thickness of the skin $L = 10^{-3}m$ and a typical free diffusion coefficient $D = 10^{-9}m^2s^{-1}$ (see Table 5.1) so that we get the typical diffusion time scale of $L^2/D = 10^3s$. By comparison the typical time scale of the chemical kinetics we consider is $10^{-9}s$. The hypothesis is fairly valid in this context.

Table 5.1: Free diffusion coefficients

Species	Diffusion coefficient (m^2s^{-1})
H^+	$9.3046 \cdot 10^{-9}$
HO^-	$5.2991 \cdot 10^{-9}$
CO_2	$1.9 \cdot 10^{-9}$
HCO_3^-	$1.4532 \cdot 10^{-9}$
CO_3^{2-}	$0.92221 \cdot 10^{-9}$

5.3 Three Ways into the Model

In this section we present the ideas that conducted us to study the model (5.4). The ideas developed here explain the numerical study.

5.3.1 Infinitesimal Local Modification

The first origin of the model is an argument that is widely used in numerical chemistry but has not been really tested (to our knowledge) in the context of reaction-diffusion.

Suppose that at time t and location x, $\overrightarrow{C}$ is at equilibrium and suppose that between time t and $t + \mathrm{d}t$ there is a modification $\mathrm{d}\overrightarrow{C}$ of the composition of the mix coming from the *outside*. Then since the chemical reactions

are infinitely fast, the reactions will advance simultaneously with the outside modification. This will result in the immediate apparition of another modification $\widetilde{\mathrm{d}\overrightarrow{C}}$. Because of the mass balance, this *inner* modification has necessarily the form $\widetilde{\mathrm{d}\overrightarrow{C}} = \nu^T \mathrm{d}\xi$. where $\mathrm{d}\xi$ is a vector whose components (one for each reaction) is the infinitesimal chemical extent. Consequently we can write:

$$\overrightarrow{C}(t+\mathrm{d}t, x) = \overrightarrow{C}(t,x) + \mathrm{d}\overrightarrow{C} + \nu^T \mathrm{d}\xi. \tag{5.17}$$

We now write that the constraint is preserved:

$$\begin{aligned} 0 = \Gamma(\overrightarrow{C}(t+\mathrm{d}t, x)) &= \Gamma(\overrightarrow{C}(t,x) + \mathrm{d}\overrightarrow{C} + \nu^T \mathrm{d}\xi) \\ &\approx \Gamma(\overrightarrow{C}(t,x)) + \Phi(\overrightarrow{C}(t,x))\mathrm{d}\overrightarrow{C} + \Phi(\overrightarrow{C}(t,x))\nu^T \mathrm{d}\xi \\ &\approx \Phi(\overrightarrow{C}(t,x))\mathrm{d}\overrightarrow{C} + \Phi(\overrightarrow{C}(t,x))\nu^T \mathrm{d}\xi. \end{aligned} \tag{5.18}$$

As we mentionned, we consider the matrix $\Phi(\overrightarrow{C})\nu^T$ to be invertible. We can thus compute

$$\mathrm{d}\xi = -(\Phi(\overrightarrow{C})\nu^T)^{-1}\Phi(\overrightarrow{C})\mathrm{d}\overrightarrow{C} \tag{5.19}$$

and when reinjecting one finds:

$$\overrightarrow{C}(t+\mathrm{d}t, x) = \overrightarrow{C}(t,x) + (I_M - \nu^T(\Phi(\overrightarrow{C})\nu^T)^{-1}\Phi(\overrightarrow{C}))\mathrm{d}\overrightarrow{C}. \tag{5.20}$$

This arguments remains valid for any modification of the mix (provided that it comes from the outside) and we can say that between t and $t+\mathrm{d}t$, because of the diffusion of the species, the local mix will be modified by an amount of $\mathrm{d}C = -\mathrm{div}\,(\mathcal{D}\nabla\overrightarrow{C})\mathrm{d}t$. Dividing by $\mathrm{d}t$ and taking the limit $\mathrm{d}t \to 0$ yields (5.4).

5.3.2 Lagrange Multipliers

Another way to see the previous argument is by writing a standard diffusion-reaction system:

$$\partial_t \overrightarrow{C} - \mathrm{div}\,(\mathcal{D}\nabla\overrightarrow{C}) = S, \tag{5.21}$$

where S are the (volumic) reaction source terms. Now once again, by following the laws of chemical kinetics, the source terms can only have the form $\nu^T\sigma$ where σ is a volumic density of reaction rate (one for each reaction).

Now since the reactions are infinitely fast, we are permanently on the equilibrium manifold defined by $\Gamma(\overrightarrow{C}) = 0$ and the reaction source terms are here to ensure that we stay on it: σ can thus be seen as a vector of unknown Lagrange multipliers associated to the constraint $\Gamma(\overrightarrow{C}) = 0$. Then the real system is a system with unknowns $\overrightarrow{C}$ and σ and equations

$$\begin{cases} \partial_t \overrightarrow{C} - \operatorname{div}(\mathcal{D}\nabla \overrightarrow{C}) = \nu^T \sigma, \\ \Gamma(\overrightarrow{C}) = 0. \end{cases} \tag{5.22}$$

If we now take a solution to the previous system then we can compute

$$0 = \partial_t \Gamma(\overrightarrow{C}) = \Phi(\overrightarrow{C})\partial_t \overrightarrow{C} = \Phi(\overrightarrow{C}) \left(\operatorname{div}(\mathcal{D}\nabla \overrightarrow{C}) + \nu^T \sigma \right). \tag{5.23}$$

Once again we can assume $\Phi(\overrightarrow{C})\nu^T$ is invertible so that we can express the reaction term as

$$\nu^T \sigma = -\nu^T (\Phi(\overrightarrow{C})\nu^T)^{-1} \Phi(\overrightarrow{C}) \operatorname{div}(\mathcal{D}\nabla \overrightarrow{C}), \tag{5.24}$$

and thus $\overrightarrow{C}$ also satisfies (5.4). Note that this is really the continuous version of the argument (5.18).

It is interesting to note that it is the elimination of the lagrangian multiplier σ that yields the non conservative form of the diffusion. This can happen in other contexts : for instance, Klak in [44] derives a non conservative diffusion system while studying compressible Navier-Stokes with small viscosities and a highly oscillating forcing term.

Note that invertly, if we take $\overrightarrow{C}$ to satisfy (5.4), and if we compute $\partial_t \Gamma(\overrightarrow{C})$, we find that

$$\begin{aligned} \partial_t \Gamma(\overrightarrow{C}) = \Phi(\overrightarrow{C})\partial_t \overrightarrow{C} &= \Phi(\overrightarrow{C})(I_M - \nu^T(\Phi(\overrightarrow{C})\nu^T)^{-1}\Phi(\overrightarrow{C}))\operatorname{div}(\mathcal{D}\nabla \overrightarrow{C}) \\ &= (\Phi(\overrightarrow{C}) - \Phi(\overrightarrow{C})\nu^T(\Phi(\overrightarrow{C})\nu^T)^{-1}\Phi(\overrightarrow{C}))\operatorname{div}(\mathcal{D}\nabla \overrightarrow{C}) \\ &= 0, \end{aligned} \tag{5.25}$$

so that if the initial data are on the equilibrium manifold, (5.4) guarantees that $\overrightarrow{C}$ stays on it for all time and consequently (5.4) and (5.22) are equivalent for good initial data.

5.3.3 Fast Chemistry Asymptotics

A third way to understand (5.4) is to consider a full reaction-diffusion system

$$\partial_t \overrightarrow{C}^\varepsilon - \operatorname{div}(\mathcal{D}\nabla \overrightarrow{C}^\varepsilon) = \nu^T \sigma(\overrightarrow{C}^\varepsilon). \tag{5.26}$$

and somehow quantify what fast chemical kinetics means. Note that σ has N components because σ_i is the reaction rate of the i-th reaction; the global (algebric) production rate of species j is then computed by $\sum_i \nu_{ij}\sigma_i$. It can be very hard in general to know the kinetic law, that is the exact expression of σ. One important case is the when the chemical system is known to be a *reactional mechanism*: when we deal with a reactional mechanism, we know there are two kinetic constants (scaling as the inverse of a time) k_i and k_{-i} such that

$$\sigma_i(\overrightarrow{C}) = k_{-i} \prod_{j,\text{productof}i} \overrightarrow{C}_j^{|\nu_{ij}|} - k_i \prod_{j,\text{reactantof}i} \overrightarrow{C}_J^{|\nu_{ij}|}. \tag{5.27}$$

The reaction constant is defined by $K_i = k_i/k_{-i}$ so that $\sigma_i = 0$ yields the usual equilibrium relation

$$K_i = \prod_j \overrightarrow{C}_j^{\nu_{ij}}. \tag{5.28}$$

The fast kinetics hypothesis we want to take into account could, in this case, be defined in the following way: $k_{\pm i} = k'_{\pm i}/\varepsilon$ with ε thought as small and $k'_{\pm i}$ of order 1. We then have $K_i = k'_i/k'_{-i}$. Note that with our notations, we can write

$$\sigma_i = k_i \left(K_i \prod_{j,\text{product of } i} \overrightarrow{C}_j^{|\nu_{ij}|} - \prod_{j,\text{reactant of } i} \overrightarrow{C}_j^{|\nu_{ij}|} \right) = k_i \Gamma_i = \frac{1}{\varepsilon} k'_i \Gamma_i. \tag{5.29}$$

Finally in the case of a reactional mechanism, Eq (5.28) can be written:

$$\partial_t \overrightarrow{C}^{\varepsilon} - \operatorname{div}(\mathcal{D}\nabla \overrightarrow{C}^{\varepsilon}) = \frac{1}{\varepsilon} \nu^T \operatorname{diag}(k'_i) \Gamma(\overrightarrow{C}^{\varepsilon}), \tag{5.30}$$

and we can study the limit $\varepsilon \to 0$. In the general case we write $\sigma = \sigma'/\varepsilon$.

For this kind of singular limit, we have to study the interplay between the singular term and the regular operator. Indeed, the limit (or at least lowest order term) must fall in the kernel of the singular operator which can be large – the limit is thus usually not completely defined at this stage. One has then to study the links between the limit and the higher order term to find a well-posed limit problem. In connection with diffusion equations one can mention the case of kinetic equations with singular collision kernels : Klak mentions several such examples in his Ph. D [44]. For instance, Degond, Goudon and Poupaud obtain a non linear (but conservative) diffusion term on the macroscopic density of a class of kinetic models in [23]. In this direction one

can also cite Besse and Goudon who obtain in [7] a macroscopic diffusion equation with a non local diffusion coefficient for some kinetic model (but once again, the equation is conservative).

In the framework of reaction-diffusion system, where the singular operator is of order zero, one can mention the article by Bothe, Pierre and Rolland [10] (cited in the lecture notes [60, Theorem 9]) where they prove the convergence (in L^2 in space and time) of System (5.26) with a right-hand side of the form (5.29) (for three species and one reaction) towards what they call a *cross-diffusion system*.

The question of the approximation of a reaction-diffusion system like (5.26) by a relaxed system is related to the problem of the *quasi steady-state approximation* (QSSA), where one removes the most unstable chemical species (they are supposed to have relaxed to equilibrium). The validity of such an approximation in local systems (governed by ODEs) has been studied by many authors. Yet in the framework of reaction-diffusion system much less is known and one can refer to [8] by Bisi, Conforto and Desvillettes for a rigorous proof of the validity of QSSA in one such system.

We make the ansatz that

$$\overrightarrow{C}^{\varepsilon} = \overrightarrow{C}^{0} + \varepsilon \overrightarrow{C}^{1} + \mathcal{O}(\varepsilon^2). \tag{5.31}$$

We now identify the first *two* orders of the formal expansion for small ε, that is order ε^{-1} and 1. This yields the relations

$$\begin{cases} \nu^T \sigma'(\overrightarrow{C}^{0}) = 0, \\ \partial_t \overrightarrow{C}^{0} - \operatorname{div}\left(\mathcal{D} \nabla \overrightarrow{C}^{0}\right) = \nu^T \mathrm{d}\sigma'(\overrightarrow{C}^{0}) \overrightarrow{C}^{1}. \end{cases} \tag{5.32}$$

We always assume ν to have maximum rank (which basically means we do not have written redundant chemical information and is true in our example) so that ν^T is one-to-one. Consequently we have $\sigma'(\overrightarrow{C}^{0}) = 0$ which is equivalent to $\sigma(\overrightarrow{C}^{0}) = 0$. Also, we note that System (5.32) has the same structure than System (5.22) when setting "$\sigma = \mathrm{d}\sigma'(\overrightarrow{C}^{0})\overrightarrow{C}^{1}$".

Let us make some remarks. First we note that in the case of a reactional mechanism the relation $\sigma(\overrightarrow{C}^{0}) = 0$ is equivalent to the relation $\Gamma(\overrightarrow{C}^{0}) = 0$. It is more advantageous to use this second formulation for two reasons. The first is that the expression of σ of (5.27) uses the values of k_i and k_{-i} which can be hard to obtain especially in the cases we are interested in, that is when they are very large. Invertly, the expression of Γ only uses the constants K_i which are more easily found. The second reason is that, when we cannot say that we deal with a real reactional mechanism, we cannot use (5.27) in (5.26) but we can *still* use $\Gamma = 0$ to describe the stationary equation. Another

remark is thus that, if we are not interested in the details of the chemistry, the formulation (5.4) is interesting because the detailed expression of σ is not needed; only the equilibrium is important and is easier to find.

5.4 Numerical Scheme

We are not able to do anything with the continuous model (5.4) yet, but we can use the ideas presented in Section 5.3 to design a numerical scheme which has good features and is fast enough. For the moment we restrict ourselves to a 1d geometry (given that the depth of the skin is much smaller than its longitudinal length scales). However we present here a method which can easily adapt to 2d or 3d geometries or to finite elements methods. We choose finite volumes because it allows to take easily into account spatial jumps in the diffusion coefficients.

5.4.1 Presentation of the Numerical Scheme

Construction of the Basic Finite Volume Numerical Scheme

Our base scheme here is of finite volume type. Let us briefly recall the how the scheme is designed for the standard diffusion equation.

Consider a given mesh (x_l) of the the unit interval (we consider that we have rescaled the equation so that the depth is 1) and a sequence of points $x_{l+1/2} \in [x_l, x_{l+1}]$. Let us also be given a time step δt. The medium is then divided in contiguous finite volumes $[x_l, x_{l+1}]$ which will be considered as small chemical reactors which are also exchanging chemical species through their border by diffusion. To find the finite volume formulation, take the continuous equation (f is given here)

$$\partial_t \overrightarrow{C} - \partial_x(\mathcal{D}\partial_x \overrightarrow{C}) = f, \tag{5.33}$$

and take its spatial average on a volume $[x_l, x_{l+1}]$. One obtains the following equation:

$$\begin{aligned}(x_{l+1} - x_l)\partial_t \left(\frac{1}{x_{l+1} - x_l} \int_{[x_l, x_{l+1}]} \overrightarrow{C}(t,x)\mathrm{d}x \right) \\ - (\mathcal{D}(x_{l+1})\partial_x \overrightarrow{C}(x_{l+1}) - \mathcal{D}(x_l)\partial_x \overrightarrow{C}(x_l)) = \int_{[x_l, x_{l+1}]} f(t,x)\mathrm{d}x.\end{aligned} \tag{5.34}$$

Let us note $\overrightarrow{C}^k_{l+1/2}$ an approximation of $\dfrac{1}{x_{l+1}-x_l}\displaystyle\int_{[x_l,x_{l+1}]}\overrightarrow{C}(k\delta t,x)\mathrm{d}x$. Now we consider that $\overrightarrow{C}^k_{l+1/2}\approx\overrightarrow{C}(k\delta t,x_{l+1/2})$ and what we have to do is to approximate the fluxes $\mathcal{D}(x_l)\partial_x\overrightarrow{C}(x_l)$ at the boundary of each finite volume. It is well known that a good approximation of these fluxes is given by:

$$F^k_l=\mathcal{D}_l\frac{1}{x_{l+1/2}-x_{l-1/2}}\left(\overrightarrow{C}^k_{l+1/2}-\overrightarrow{C}^k_{l-1/2}\right), \tag{5.35}$$

with D_l defined by

$$\frac{x_{l+1/2}-x_{l-1/2}}{\mathcal{D}_l}=\frac{x_l-x_{l-1/2}}{\mathcal{D}(x_{l-1/2})}+\frac{x_{l+1/2}-x_l}{\mathcal{D}(x_{l+1/2})}. \tag{5.36}$$

We also note $f^k_{l+1/2}$ a given approximation of the average of f at time t on the l-the finite volume. One last choice we have to make is the approximation of the time derivative for which we have basically to choices leading to an explicit

$$\overrightarrow{C}^{k+1}_{l+1/2}=\overrightarrow{C}^k_{l+1/2}+\frac{\delta t}{x_{l+1}-x_l}(F^k_{l+1}-F^k_l)+\delta t f^k_l \tag{5.37}$$

or an implicit in time scheme,

$$\overrightarrow{C}^{k+1}_{l+1/2}-\frac{\delta t}{x_{l+1}-x_l}(F^{k+1}_{l+1}-F^{k+1}_l)=\overrightarrow{C}^k_{l+1/2}+\delta t f^k_l. \tag{5.38}$$

The Constrained Finite Volume Scheme

Finite Volume Modification.

We consider now our situation under the form (5.22). If we apply the finite volume construction to our problem all we need to find are good approximations of the averages of $\nu^T\sigma$. If we note $\xi^k_{l+1/2}=\sigma^k_{l+1/2}\delta t$ we can write

$$\overrightarrow{C}^k_{l+1/2}=\overrightarrow{C}^{k-1}_{l+1/2}+\frac{\delta t}{x_{l+1}-x_l}(F_{l+1}-F_l)+\nu^T\xi^k_{l+1/2}. \tag{5.39}$$

However, we do not have an expression of $\nu^T\sigma$ which is only defined implicitly *via* the condition $\Gamma(\overrightarrow{C})=0$ and thus cannot compute analytically $\xi^k_{l+1/2}$. But we can see that the previous equation is exactly (5.17) with $\mathrm{d}C=\dfrac{\delta t}{x_{l+1}-x_l}(F_{l+1}-F_l)$. To approximate $\xi^k_{l+1/2}$, we follow Section 5.3.1 and reproduce the argument (5.18). This leads to the following approximation (which is the finite volume analogue of (5.19)):

$$\nu^T \xi^k_{l+1/2} = -\nu^T (\Phi(\overrightarrow{C}^{k-1}_{l+1/2})\nu^T)^{-1} \Phi(\overrightarrow{C}^{k-1}_{l+1/2}) \left[\frac{\delta t}{x_{l+1} - x_l} (F_{l+1} - F_l) \right] \quad (5.40)$$

In the sequel we choose to compute the diffusive fluxes F_l at time $k+1$ which leads to a semi-implicit scheme. Finally this leads to a linear system on $(\overrightarrow{C}^{k+1}_{l+1/2})_l$ which can be put under the form:

$$\overrightarrow{C}^{k+1}_{l+1/2} + \delta t (I_M - \chi(\overrightarrow{C}^k_{l+1/2})) \mathcal{L}[(\overrightarrow{C}^{k+1}_{l+1/2})_l] = \overrightarrow{C}^{k+1}_{l+1/2}, \quad (5.41)$$

where $\mathcal{L}$ is the linear operator (it is a matrix when we have chosen an ordering for $(\overrightarrow{C}^{k+1}_{l+1/2})_l$) that would appear in the unconstrained finite volume scheme.

Because we have a semi-implicit scheme, we have to solve a linear system to compute $\overrightarrow{C}^{k+1}$ while knowing $\overrightarrow{C}^k$. However, we do not have theoretical or numerical properties for the linear system that guarantees the non negativity of the resulting $\overrightarrow{C}^{k+1}$ (contrary to the usual diffusion). We are thus forced to add a time step adaptation procedure: if the solution is not non negative we retry with a smaller time step. Numerical experiments indicate that the non negativity is lost if the linear system has to take in strong gradients, which will be our case at the beginning of the simulations since we have initial datum that does not satisfy the boundary conditions. When the steep gradients have been smoothed out by the diffusion, we observe that the time step is as large as we want. We will thus have a *target* time step, that is a maximum time step allowed in the simulation which may not be the current time step in the beginning of the simulations.

Local Chemical Projection.

Because we have only made a first order approximation on the constraint, at time k we may be too far from the equilibrium manifold but first we must precise what "too far" means. To do this we come back to the reaction: in a local reactor (without diffusion) we know that when the chemical composition $(\overrightarrow{C}_j)$ is not at equilibrium, the chemical reactions will advance to a certain extent and this will result in a modification of each composition $(\delta\overrightarrow{C}_j)$ in order to bring back the chemical composition to equilibrium. Suppose we know how to compute exactly (δC_j) in a local reactor as a function of $(\overrightarrow{C}_j)$. Then we can compute for each species its relative modification $|\delta\overrightarrow{C}_j|/\overrightarrow{C}_j$: if the relative modification are all smaller than a given tolerance, say 10^{-4} for example, we can consider that we have not moved because the reaction would modify the composition only to the 4th digit. This means that we already were at equilibrium.

It remains to compute the modification of each reaction in a local reactor and usually this cannot be done analytically because it means computing the solution of a system of algebraic equation. However we do know that by the law of conservation of mass the modification has a certain structure and thus it exists an extent ξ_i for each reaction so, that the modification $\delta\overrightarrow{C}$ can only be of the form $\nu^T\xi$. We compute an approximation of the extent ξ via a Newton algorithm. Suppose initially the system has the composition $\overrightarrow{C}_0$. The extent ξ_i of each reaction is such that $\Gamma'(\xi) = \Gamma(\overrightarrow{C}_0 + \nu^T\xi) = 0$: Newton algorithm is thus the computation of a sequence ξ_n by the following scheme:

$$\begin{cases} \xi_0 = 0, \\ \xi_{n+1} = \xi_n - (\partial_\xi\Gamma'(\xi_n))^{-1}\Gamma'(\xi_n), \end{cases} \tag{5.42}$$

and we have $\partial_\xi\Gamma'(\xi_n) = \Phi(\overrightarrow{C}_0 + \nu^T\xi_n)\nu^T$. It is thus more convenient to compute $\overrightarrow{C}_n = \overrightarrow{C}_0 + \nu^T\xi_n$ through

$$\begin{cases} \overrightarrow{C}_0 = \overrightarrow{C}_0, \\ \overrightarrow{C}_{n+1} = \overrightarrow{C}_n - \nu^T(\Phi(\overrightarrow{C}_n)\nu^T)^{-1}\Gamma(\overrightarrow{C}_n), \end{cases} \tag{5.43}$$

Ideally we would define the extent $\xi = \lim_{n\to+\infty} \xi_n$ but it is well-known that Newton algorithm generically converge very fast. To determine the distance to the equilibrium we take the approximation given by the first step of Newton's algorithm:

$$\delta\overrightarrow{C}_0 = -\nu^T(\Phi(\overrightarrow{C}_0)\nu^T)^{-1}\Gamma(\overrightarrow{C}_0). \tag{5.44}$$

The criterion for a composition $\overrightarrow{C}$ to be at equilibrium (which is also the stop condition we implement on Newton's algorithm) is thus

$$\forall j,\ |\delta\overrightarrow{C}_j| \leq \delta_{\text{tol}}\overrightarrow{C}_j. \tag{5.45}$$

The complete scheme consist in doing one step of diffusion by (5.41) followed by a projection (5.43) until we satisfied in all control volumes te criterion (5.45). By design, the diffusion step sends us in the good direction so that the projection step should not be very stringent and with some heuristics may not need to be done every time step.

5.4.2 Validation of the Scheme on a Simpler Problem

We consider in this section only the water dissociation. We thus have only two chemical species H^+ and OH^- and one reaction that we write:

$$H_2O \leftrightarrows H^+ + OH^-. \tag{5.46}$$

The stoichiometric matrix is simply

$$\nu = \begin{pmatrix} 1 & 1 \end{pmatrix}, \tag{5.47}$$

and we set

$$\Gamma(\overrightarrow{C}) = K_w - C_1 C_2, \tag{5.48}$$

and

$$\Phi(\overrightarrow{C}) = (-C_2 - C_1). \tag{5.49}$$

We will compare our scheme to a reference solution given by a first order kinetics. Namely we set

$$\sigma(\overrightarrow{C}) = \begin{pmatrix} k_d - k_r \overrightarrow{C}_1 \overrightarrow{C}_2 \\ k_d - k_r \overrightarrow{C}_1 \overrightarrow{C}_2 \end{pmatrix} \tag{5.50}$$

and we compare our numerical scheme to the numerical solution of the system

$$\partial_t \overrightarrow{C}' - \Delta \overrightarrow{C}' = \sigma(\overrightarrow{C}'). \tag{5.51}$$

We take the values of the chemical constants from [27]:

$$k_d = 1.38 \cdot 10^{-3} mole \cdot L^{-1} \cdot s^{-1}, \quad k_r = 1.40 \cdot 10^{11} mole^{-1} \cdot L \cdot s^{-1}, \tag{5.52}$$

$$K_w = 1.00 \cdot 10^{-14} mole^2 \cdot s^{-2}. \tag{5.53}$$

We note that we have $|K_w - k_d/k_r|/Kw = 2\%$.

The numerical experiment is the following. We consider one medium of length one in which the two species have the same diffusion coefficients (with a dimensionless value of 1). In the medium, the chemical composition is

$$[H^+] = 3.98 \cdot 10^{-8} mole \cdot m^{-1}, \quad [OH^-] = 2.51 \cdot 10^{-7} mole \cdot m^{-1}, \tag{5.54}$$

which amounts to an equilibrium composition of initial $pH = 7.4$. On the boundaries we set artificial Dirichlet conditions corresponding to an equilibrium composition of $pH = 6.4$ on the left boundary and an equilibrium composition of $pH = 7$ on the right boundary.

In space we take 70 homogeneous finite volumes and the target time step is 10^{-2} (note that $\mathrm{d}t/\mathrm{d}x^2 = 49 \gg 1/2$). We do 100 iterations for a target ending time of about 1 (which corresponds to about $15mn$ of real time).

We run a simulation of the full reaction diffusion scheme and we find that the equilibrium constraint $\Gamma = 0$ is satisfied in the sense that we have defined

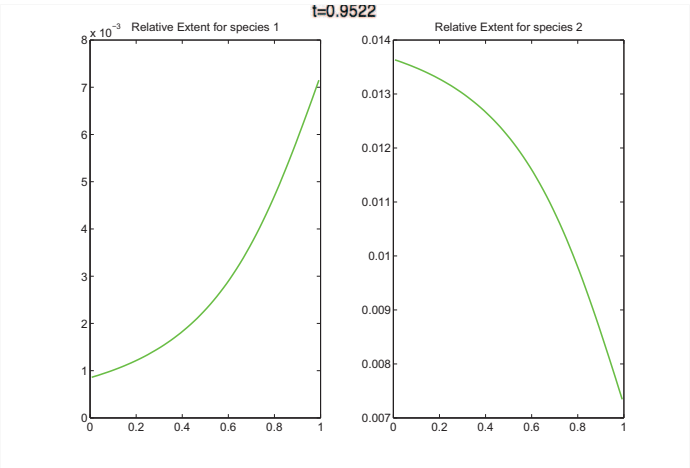

Figure 5.1: Distance to equilibrium of the reference solution in the sense of (5.44)

in (5.45) with a tolerance $\delta_{\text{tol}} = 10^{-2}$ as one can see on figure 5.4.2. This is actually limited by our choice of boundary conditions.

We thus took $\delta_{\text{tol}} = 10^{-2}$ in the simulation of our constrained scheme. Finally we also compare the reference solution to what we call the "free diffusion" scheme which consists of one step of free diffusion following (5.38) (with $f = 0$) and then a local chemical projection (5.43) (until (5.45) is satisfied everywhere). The full reaction-diffusion scheme and the free diffusion scheme are computed with the same timesteps as the one resulting from our constrained scheme. In Figure 5.2 we represent the L^2 norm in space of our constrained scheme and of the free-diffusion scheme relatively to the reference solution versus time. In blue we have our constrained scheme while in red is the curve for the free diffusion algorithm. We see that the relative errors is very small in the beginning. This is due to the fact that the timestep is initially reduced to 10^{-4}. After this initial adequation, we see that our scheme is twice as precise as the free diffusion scheme.

On the discussion of the validity of the hypothesis (of sufficiently fast reactions to consider permanent chemical equilibrium), let us note that the tolerance on the equilibrium condition must be specified by the reference solution. Indeed, if we compare the results of our scheme to the same reference solution, with the same timesteps and spacestep, but with different tolerance parameter δ_{tol}, the better solution is not the one with the stricter condition but the one with the same tolerance as the reference solution. We must thus find a heuristics (which probably lie in distance of the boundary and initial

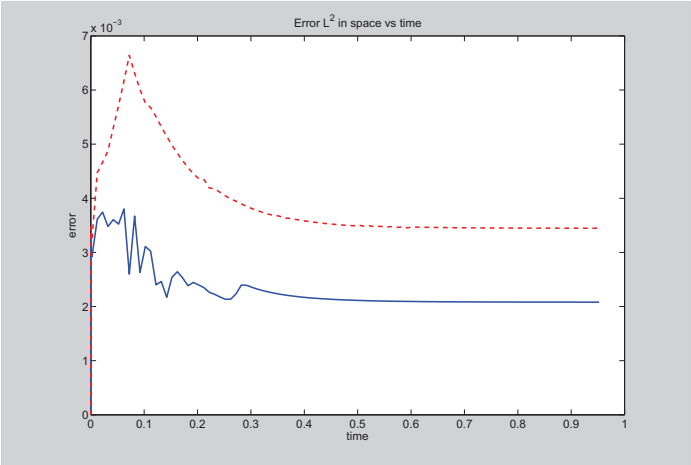

Figure 5.2: Relative error to the reference solution. In red is the free diffusion/projection scheme while in blue is our constrained scheme

data to the equilibrium) to set this parameter in our model.

5.4.3 Difficulties and Results of the Numerical Simulation of the "Balneotherapy"

Recall that in connection with balneotherapy, our aim is to give a model that can compute the concentration of a chemical species in the neighbourhood of the blood vessel, since an elevated concentration of CO_2 around the blood vessel could trigger a dilatation of the blood vessel. The numerical setting we envision for now is a $1d$ setting where space is supposed represents the depth of the skin. The skin itself is constituted of two layers with a jump in the porosity : the layer which is in contact with the bath (called the *epidermis*) is assumed to be much more dense than the second layer, *dermis*. In our model, the *dermis* is bounded by the *epidermis/dermis* interface on one side and by the blood vessel on the other side. This is of course, a great simplification of the biological reality but allows us to demonstrate that our scheme can handle space varying diffusion coefficients, as is customary with finite volume schemes.

Boundary conditions.

To complete the model, and make numerical simulations of it, one has to prescribed the boundary condition at the surface of the skin and at the blood vessel (the interface between the two skin layers being handled by a flux continuity condition which is implicit in the finite volume formulation (5.41)).

This is no trivial task for several reasons. To have an accurate boundary condition one should take into account the physics, or the chemistry, or the biology of the interface exchange of matter. While it is possible to experiment on the exchange between air and porous media (such as soil) to find some echange law and then transpose this law to the skin (forgetting that it is a biotissue and keeping only its porous property), it seems highly unlikely that such a procedure could give valid results at the skin blood vessel interface which has to be much more complex. One can think of the blood vessel as a resisting membrane (a possibility taken under consideration by Bear and Bresch), lessening the flux as the difference of concentrations from one side to the other becomes too large. This condition would take the form

- if $C_j^b \geq C_j^{b\,\min}$ we have the no-flux condition $D_j \partial_x C_j = 0$ through the membrane; C_j^b is the concentration of speicies number j in the blood vessels, and $C_j^{b\,min}$ is some specified minimum threshold on C_j^b;
- if $C_j^b < C_j^{b\,min}$, then

$$D_j \partial_x C_j = \frac{C_j - C_j^b}{r_j}, \tag{5.55}$$

where r_j would be the resistance of the membrane to species j. Possibly, this resistance to species j could be infinite and the no flux condition would be unconditional.

On the other hand, one could think that the blood vessel has a prescribed chemical composition that must not be tampered with by the outside, and consider this blood composition as a Dirichlet boundary condition. As far as our own knowledge goes, these two scenarios are equally valid (or more accurately, equally simplistic and unphysical).

For the moment, we do not have an answer to this problem. We can only say that, in our scheme, we can take into account several (if unrealistic) classical boundary conditions such as inhomogeneous Dirichlet or Neumann boundary condition.

Fluxes.

Another interrogation at this point is the notion of matter transport. Since the chemical species simultaneously diffuse and react how do we define the precise quantity that moved from place A to place B? Consider that A and B are the boundaries of the domain. and imagine that the solution reached a stationary regime. If we were in a purely diffusive scenario, then the stationary equation would be $-\partial_x(\mathcal{D}\partial_x \overrightarrow{C}) = 0$ and by integrating this equation over the interval $[A, B]$ yields that the outer flux at B must be equal

to the inner flux at A. This is not true anymore with (5.4) as the equation is not conservative!

Moreover consider the following setting : assume the chemistry reduces to two species a and b which reacts through $2a \leftrightarrows b$ for instance. Assume that the medium is at chemical equilibrium everywhere. Assume that, by exchanging matter with its neighbours, a given volume gains 1 unit of b and loses 2 units of a. When that happens, the equilibrium is broken and the volume reacts to regain it. But it is easy to see here that the chemical reaction will take the extra unit of b to produce the 2 missing units of a. Consequently, at the end of the reaction, the chemical composition of the volume is exactly the same. This means that there could be currents of matter in the medium which are not seen since the chemical composition does not evolve. Indeed, must we consider that the fluxes are 0 or not in the previous example?

In the end, our goal is to control the carbon dioxide in the vicinity of the blood vessel so we take exactly the quantity in the last finite volume as a function of time. But for now we would be unable to evaluate the flux at the blood vessel without introducing it explicitly in the model through a boundary condition.

Chapitre 6

Modélisation du phénomène d'interdigitation dans les sutures crâniennes

Résumé du chapitre

Ce chapitre est consacré au phénomène d'interdigitation des sutures. L'approche développée dans ce chapitre pourrait être décrite comme l'exact inverse de la démarche de [50] : dans cet article, Miura *et al.* prennent dans un premier temps acte du phénomène d'interdigitation. Puis par analogie avec les motifs labyrinthiques étudiés par Meron et Hagberg dans [35] ils suggèrent que le même système de réaction-diffusion doit gouverner le phénomène d'interdigitation. Enfin, ils donnent une interprétation possible des deux inconnues du sytème en lien avec les sutures. Pour éviter une complexité excessive, ils subordonnent la diffusion à un coefficient décroissant exponentiellement en temps.

Dans notre approche, nous partons de nos connaissances sur les sutures et sur les mécanisme qui participent à leur fonctionnement. D'une part nous décrivons un milieu biologique composé de trois espèces : les cellules mésenchymales (cellules formant le milieu de la suture), les ostéocytes (c'est-à-dire les cellules osseuses) et enfin les fibroblastes qui sont des chaînes protéinées très longues. Leur importance est capitale dans notre modèle, car ce sont les fibroblastes qui nous permettent de mettre en œuvre la mécanotransduction. En effet, de nombreuses études (voir par exemple [64]) ont montré que les contraintes mécaniques que subissaient le crâne (et donc les sutures) avaient une influence sur le développement des sutures. L'autre ingrédient que nous mettons donc dans notre modèle est ainsi la mécanique.

La façon dont nous couplons biologie et mécanique est l'élément déterminant dans le modèle. La biologie agit sur la mécanique car le milieu est hétérogène : en effet les joints que constituent les sutures sont beaucoup plus souples (c'est-à-dire élastiques) que les os. Cette différence entre sutures et os nous amène à considérer un matériau spatialement hétérogène. D'un autre côté, la mécanique agit sur la biologie au travers des fibroblastes. Il faut savoir que pour fabriquer du nouvel os, il faut d'abord que des cellules mésenchymales s'accumulent au voisinage de la berge avant de recevoir un signal chimique qui commande leur différenciation en ostéocyte. Or les cellules mésenchymale baignent dans un milieu comprenant entre autre les fibroblastes. Nous postulons que les cellules mésenchymales se déplacent plus facilement dans des tubes de fibroblastes que lorsqu'elles sont au milieu de chaînes sans orientation particulière, un phénomène appelé haptotaxis. La mécanotranduction se traduit alors par un alignement des fibroblastes en fonction des contraintes mécaniques subies localement.

Les règles que nous avons choisies pour cette orientation sont les suivantes : d'abord l'orientation des fibres se fait suivant les directions principales de contraintes ; si les contraintes principales sont de même signe alors il y a compétition entre les deux direction et c'est la contrainte principale la plus grande en valeur absolue qui l'emporte d'autant plus que le milieu est anisotrope. ; si les contraintes principales sont de signes opposées alors les effets se combinent et les fibres s'alignent suivant la direction de traction.

Avec tous ces ingrédients nous avons pu formuler un modèle d'évolution des berges suturales. Nous avons ensuite conçu un code à l'aide du langage *FreeFem++* pour tester notre modèle numériquement. Les tests numériques, suggèrent effectivement une instabilité à même d'expliquer le comportement tortueux des sutures. Nous pensons que cette instabilité est bien contenue dans le modèle et ne viens pas de défauts purement numériques : en effet, la déstabilisation de la berge semble se faire suivant certaines longueur d'ondes spatiales particulières. Une étude théorique de stabilité est en cours pour confirmer cette observation numérique.

Ce chapitre est une première version d'un article en collaboration avec Hossein Khonsari, Paul Tafforeau, Paul Vigneaux, Didier Bresch et Vincent Calvez. Cette collaboration est issue du projet *Sutures* du Cemracs 2009.

Important remark. This part corresponds to the first version of a paper under preparation. This is a joint work with three mathematicians but also with R.H. KHONSARI (Doctor working in department of craniofacial development (London)) and P. TAFFOREAU (Paleonthologue working in the European Synchrotron Radiation Facility (ESRF) (Grenoble)). This work corresponds to a subject proposed in CEMRACS by V. CALVEZ and R.H. KHONSARI.

6.1 Introduction

Craniofacial bones are united by sutures, which act as joints, absorb shocks during impacts (RAFFERTY *et al.*, 2003) [61] and work as intramembranous bone growth sites (OPPERMAN *et al.*, 2000) [56]. Sutures are delimited by two bony borders and contain an undifferentiated, osteogenic, mesenchyme (RICE *et al.*, 2008) [66]. The two borders of the suture are strongly interconnected by a dense network of collagen fibres (BYRON *et al.*, 2004) [15], (WARREN *et al.*, 2008) [71]. Bone deposition occurs on the borders of the sutures and is subjected to the influence of external mechanical stimuli (HERRING, 2008)[38]. During growth, sutures progressively develop a striking interdigitated pattern (RICE, 2008) [65], which has been modelled using a strictly chemical reaction-diffusion equation (MIURA *et al.*, 2009) [50] based on a Fitzhugh-Nagano instability ((HAGBERG *et al.*, 1994) [35]). Nevertheless, if morphogens are strong determinants of embryonic suture development(OPPERMAN *et al.*, 2000) [56], (RICE, 2008) [65], mechanical forces have to be taken into account in order to explain how sutures grow after birth and develop their peculiar architecture (HERRING, 2008) [38].

We approach this problem by using the geometrical data available on sutures as secondary confirmations of a mathematical model involving simple mechanotransduction processes. Sutures are known to interdigitate in the first weeks after birth (MIURA *et al.*, 2009) [50]. Bone deposition mainly occurs at the convexities of the interdigitations (BYRON *et al.*, 2004) [15], (SUN *et al.*, 2004) [69] while the convexities witness resorption (BYRON, 2006) [14]. Furthermore, collagen fibres radiated from the convexities to the concavities in the interdigitated areas (HERRING, 2008) [38], (KOLPAKOVA-HART *et al.*, 2008) [45].

We thus propose a model, aiming to find instabilities occurring during sutural growth which originate from a biological/mechanical coupling, without *a priori* geometrical hypotheses. We describe cellular events (proliferation, motion, differentiation) in a simple way involving a minimal number of parameters by a set of continuous equation (thus describing the whole system only at a macroscopic level). We consider two tissues with different mechan-

ical properties separated by sharp parallel boundaries: the bone, rigid, and the mesenchyme of the suture, softer.

6.2 Biomechanical modelling of a typical suture

As outlined in the introduction, our model is based on two pillars : biology on the one hand and mechanics on the other hand. Interestingly enough, each part does not have to be exceedingly complex in order to give rise to the aforementionned interdigitating instability. Moreover, by using simple models, the experimental data on sutures (such as the one which can be found in Table 6.1) can be used quite straightforwardly. Thus, we do not need to use many hidden parameters – still there are some parameters that have yet to be measured, since our model is not classical.

Let us first rapidly describe the basic geometrical assumptions. We consider the medium to be constituted by both the bone and the mesenchymal of the actual suture. The suture is thin compared to the characteristic length of the bone, yet not thin enough to be considered a one dimensional object. Our model was mainly conceived with sagittal suture in mind, but can probably adapted to any suture since we magnify on the neighbourhood of the suture : in our model the bone could be considered infinite outside of the suture (even though, it has of course be taken as finite in the numerical simulation).

We consider the medium to be $2d$ which seems fairly justify from the comparative length between the depth of the suture and the other length scale. However, we must point out that it is known that the complexity of the interdigitation pattern actually vary in depth. Also the hypothesis that the two bone fronts are facing each other in a planar configuration is not true as some overlapping can occur. The $2d$ hypothesis is thus a restriction but we must gain some insight on the general mechanism before going into the finer details of the suture interdigitating process.

6.2.1 Mechanical properties of the suture

We start by presenting the mechanical assumptions we have made on the sutures. The first hypothesis on the mechanical nature of the medium is that it can be described at a purely continuous level. Consequently, the bone occupies the space $\Omega_b \subset \mathbf{R}^2$ while the suture occupies the space $\Omega_m \subset \mathbf{R}^2$. This is clearly valid for the bone but means that some averaging of the local properties of the sutural part is implicitly done. We then assume that the model reacts mechanically as a simple elastic material (which means

that the material is mechanically isotropic) but the material constants that describe the material take into account the difference of medium between bone and suture – the material is an inhomogeneous Hookean elastic material. Some authors (HERRING , 2008) [38] have pointed out that the mechanical properties of sutures involve some kind of viscoelasticity. Without further details on the time scales at which this viscoelasticity comes into play, we assume that the elastic behaviour dominates and only consider elasticity. One last hypothesis on the mechanical properties of the medium is that the equations of motion for the medium are quasi-static. It is a classical assumption since we consider somewhat small samples of material.

With all these assumptions, the quantities of mechanical interests are the vector displacement u and the stress tensor σ and the governing equations are the quasistatic equations of motion :

$$\begin{cases} -\operatorname{div}\sigma = 0, \\ \sigma = \begin{pmatrix} \sigma_{xx} & \sigma_{xy} \\ \sigma_{xy} & \sigma_{yy} \end{pmatrix} = 2\mu \dfrac{\nabla u + (\nabla u)^T}{2} + \lambda \operatorname{div} u, \end{cases} \tag{6.1}$$

which when written as a system equation in u become the Lamé system. The strain is continuous at the bone/suture interfaces and the Lamé coefficients λ and μ are bivaluated, respectively (λ_o, μ_o) in the bone and (λ_m, μ_m) in the mesenchyme. Experimental data are often expressed in terms of Young's modulus E and Poisson's ratio (again see Table 6.1) and the Lamé coefficients are obtained from (E, ν) through

$$\lambda = \frac{E\nu}{(1+\nu)(1-2\nu)}, \qquad \mu = \frac{E}{2(1+\nu)}. \tag{6.2}$$

In the sequel, we take $\nu_o = \nu_m$ and $E_o \gg E_m$.

As can be seen in Eq. (6.1) we assume that there are no volumic force : the external forces only act through boundary conditions as if something actually acted on the bones' ends. Since we have an implicit thin layer approximation (as we consider the bones and suture to be $2d$) this may not be accurate (it actually may not be accurate on the real $3d$ medium).

Let us briefly discuss what we mean by external forces. We consider that the suture undergo external stress coming from essentially three sources the relative importance of which, depends on the location of the suture : intracranial pressure from brain development; mastication effects; impacts. Each of this effect is different and acts on the suture interdigitation complexity (HERRING, 2008) [38] : intracranial pressure is a quasistatic constant force; mastication effects are oscillatory in nature; impacts are brief and intense. One of the goals of our model is to be able to determine the influence

of each effect. For the moment we will only concentrate on the intracranial pressure (this is why our model is at the moment focused on the sagittal suture). This effect is modelled as a constant traction force on the boundary of the bone. Mathematically we write $\sigma n = Fn$ (where n is the normal vector to the lateral sides pointing outward) on the lateral sides of the bone, where $F > 0$ since we consider a traction. We assumed periodic boundary conditions on the other boundaries for mathematical and numerical simplicity.

6.2.2 Biological description of the suture

Bone.

We now give the description of the biological behaviour of the whole system. We first describe the bone part. Bone is created by differentiation of mesenchymal cells into osteocytes which in turn slowly mineralize to become actual bone. Our bone description will be very simple : bone will only consist of mineralized cells and as such is simply considered as any non biological material. However, we keep a trace of the "early osteocyte stage" by letting the bone interact with the suture through chemical signals.

Principles of bone formation.

The biological behaviour of the suture is richer even though in our description, we only take into account mesenchymal cells, described by their density ρ and fibroblasts (or collagen fibers) which are actually taken into account implicitly as one can see below. The description of the biology of the suture is restricted here to the description of bone formation from mesenchymal cells.

We adopt the following scenario : bone is made by differentiation of mesenchymal cells but this is the last stage. Before the differentiation can happen, the mesenchymal cell must first concentrate in the vicinity of the sutural borders and this is done by a proliferation mechanism. Note that the proliferation and differentiation are both controlled by a chemical signal (fgfr2) which diffuses from the bone edge which means that proliferation or differentiation can only happen to mesenchymal cell close enough to the border to sense this signal. Moreover, the proliferation can only start if there is already concentration of cells at the bone border and thus the first stage of the bone formation process, consists in the migration of the mesenchymal cell from the suture to the border. Our model focuses on the description of this early stage and on the way the mechanical effects act on it. Consequently, we "factor" the other stages into a single mesenchymal-to-bone process : as soon as the mesenchymal cells have sufficiently concentrated on the border to start the transformation process, we assume they turn to bone. It seems reasonable

to think that the full description of the transformation process would only impact the time scale of the interdigitation process – even though this impact could be important.

Haptotaxis.

The originality of our work lies in the following mechanism for cell migration towards suture borders. Since collagen fibers are long linear proteinic molecules, they can create some local anisotropy by orientating themselves. Moreover, when they have a collective orientation they form "tubes" inside which the mesenchymal cells can move more easily : this phenomenon is usually called *haptotaxis*. One can see on Fig. 6.5 mesenchymal cells (in black) deformed to move inside a fiber tube. However is is not clear experimentally wether the cells are just constricted by the network of fibers or if they are polarized to move inside the tube.

Note that, as far as we are concerned the cells move equally in both directions. Consequently, the mesenchymal cell density will follow the classical equation of motion :

$$\begin{cases} \partial_t \rho + \operatorname{div} j = 0 & \text{where } x \in \Omega_m \text{ and } t > 0, \\ j = -D_\rho \nabla \rho + \rho \mathcal{F}, \end{cases} \tag{6.3}$$

where $\mathcal{F}$ is the vector giving the preferential direction of movement (technically similar to chemotaxis – see Perthame [58] for a review on the modelling of chemotaxis by PDEs) taking into account the local collective fiber orientation (or lack of thereof). We also added some random motion for the cells.

Now we want to understand how this can make the mesenchymal cells go preferentially towards certain places of the borders and to do that, we must explain how the fibers "choose" to orientate (and define the vector $\mathcal{F}$).

Mechanotransduction on fibers.

In our model the state of fibers is subjected to two mechanisms. For the first one, we assume that the bone edge emits another chemical signal whose concentration is noted f which attracts the collagen fibers near the border. The higher the concentration, the more the fibers concentrate. We assume that the concentration of fibers is directly proportional to the concentration of the signal. Note that the behaviour f can classically be described by the following diffusion equation:

$$\begin{cases} -D_f \Delta f + \alpha f = 0 & \text{for } x \in \Omega_m, \\ f = 1 & \text{on the interface } x \in \partial\Omega, \end{cases} \tag{6.4}$$

where α is some degradation rate.

On the other hand, the fibers are also influenced by the *local mechanical stress*. This is maybe the key point because it is now that we couple mechanics with biology. We will encode the effect of mechanical stress on the orientation of fibers in a vector field $e(t,x)$: its norm will essentially encode how collectively orientated the fibers are (if the norm is small it means that the fibers are orientated independently of each others) and its direction the mean direction.

The fibers can be viewed as elastic rods that will align if one pulls on its edges. On the other hand, if one pushes instead of pulling, the rod will first compress but at some point will start buckling. When that happens the fiber tries to find a more suitable orientation to sustain the compression which is orthogonally to the compression direction. The local pushing or pulling is enforced in our model by saying that the fibers see the principal directions of stress. In an elastic material, the stress tensor is symmetric and consequently we can define two orthogonal principal directions e_1 and e_2 associated to two principal stresses, respectively σ_1 and σ_2 so that a small square whose edges are aligned with e_1 and e_2 feels pressure forces (pressure being algebric, this can be a tensile force or a compression force) that act on its edges. The principal stresses are easily computed in terms of the stress matrix component:

$$\sigma_{1,2} = \frac{\sigma_{xx} + \sigma_{yy} \pm \sqrt{(\sigma_{xx} - \sigma_{yy})^2 + 4\sigma_{xy}^2}}{2} \tag{6.5}$$

Consider such a cube which contains many collagen fibers. Imagine that the cubes has a pair of opposite edges on which the local stress pushes while on the other pair the local stress pulls: we decide, according to our previous observation, that the fibers will tend to collectively orientate themselves in the direction of pulling quite easily as both directions cooperate to set the orientation. On the other hand, if the local stress pushes or pulls on both pair of opposite edges, then the orientations of fibers in the cube will tend to decorrelate. Incidentally, the more isotropic the stress is, the more independent the orientations will become and hence the norm of e will be small. When the stress is not isotropic, the stronger principal stress (in absolute value) "wins the orientation battle" and we choose its principal direction as collective orientation, while making the norm of e comparatively smaller than in the "cooperative stress" scenario. We collect the previous rules in the following equation for e:

$$\begin{cases} e = G_-\left(\dfrac{\sigma_1}{\sigma_2}\right) e_1 & \text{if } 0 \le \sigma_2 \le \sigma_1 \\ e = G_-\left(\dfrac{\sigma_1}{\sigma_2}\right) e_2 & \text{if } \sigma_1 \le \sigma_2 \le 0 \\ e = G_+(\sigma_1, \sigma_2)\, e_2 & \text{if } \sigma_1 < 0 < \sigma_2 \\ e = G_+(\sigma_2, \sigma_1)\, e_1 & \text{if } \sigma_2 < 0 < \sigma_1 \end{cases} \tag{6.6}$$

The function G_- defined on $[1; +\infty)$ is increasing and satisfies $G_-(1) = 0$ (isotropic case) and $G_-(+\infty) = 1$ (anisotropic case). One can take for instance $G_-(r) = |\tanh r - 1|$. The function G_+ is defined by $G_+(\sigma_2, \sigma_2) = 1 + |\sigma_1| + |\sigma_2|$.

We can now give the expression of $\mathcal{F}$:

$$\mathcal{F} = (\nabla f \cdot e)\frac{e}{\|e\|}. \tag{6.7}$$

We have that $\mathcal{F}$ has the same direction that the local average fiber orientation and is proportional to both ∇f (which is proportional to the gradient of fiber concentration) as in chemotaxis but also to e so that $\mathcal{F}$ is small if the orientation of the fibers is random. Finally if the fibers are strongly orientated in one direction but the gradient of f that drives the mesenchymal cells is orientated orthogonally then the haptotaxis is also null.

The mechanisms of the complete model is summed up on Figure 6.1

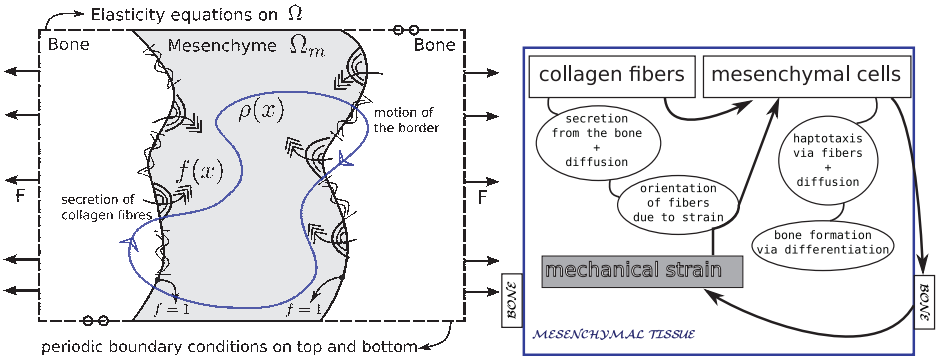

Figure 6.1: (Left) geometry + actors – (Right) actors and retroaction loop.

6.3 Simulations

6.3.1 Presentation of the model.

We used *FreeFEM++* in order to compute the distribution of the mesenchyme cells in the suture. The bulk of the numerical code is the numerical translation of Eqs. (6.1)–(6.6):

1. `Compute the displacement` $\mathbf{u}$ `due to the mechanical strain by Eq.`(6.1)`, using the previous space repartition of mesenchyme and bone as input`
2. `Compute the attracting signal/collagen concentration in the suture by Eq.`(6.4)
3. `Compute the haptotaxis vector` $\mathcal{F}$ `by Eqs.`(6.6) `and` (6.7)`, using the current stress` $\boldsymbol{\sigma}$ `and the current` f `as input`
4. `Compute the advancement of the distribution of mesenchymal cells in the suture by Eq.`(6.3)`, using the current` $\mathcal{F}$ `as input`
5. `Compute the displacement` $\mathbf{v}$ `of the interface and move the whole mesh accordingly`

Only the last point remains to be explained. As we explained, we do not consider the whole process of transformation of mesenchymal cell into bone : to us, bone is created and attached to the existing bone with the sole effect of displacing the interface between suture and bone. The mechanism of mesenchyme migration we have devised should lead to inhomogeneous cell concentration along the borders of the suture : points where the density has increased the most have more matter to turn into bone and thus the bone front should advance more rapidly. We thus add to our model the variable $\mathbf{v}$ which is the speed of the interface. Natural assumptions on $\mathbf{v}$ is that $\mathbf{v}$ is defined on the border only, and is normal to the border (the bone is created inside the suture). We take it to be proportional to the local value of ρ. Then we have to take into account that there is a mechanical displacement.

It is actually an open question to understand how the sutures maintain their existence since it is roughly governed by reaction-diffusion for the bone making which tends to close the suture and by mechanical displacement which (here) tends to open it. This should lead to either complete opening, closing (both of which are not observed at the time scales we are interested in or ever – at least for healthy individuals) or a perfect equilibrium between

the two which should reasonably be unstable and therefore is not a valid explanation. We have to take into account this difficulty but we have to find a way to maintain or suture long enough to observe the interdigitation phenomenon. What we do is that we correct the local value of the speed on the boundary, by its mean value (which we can compute since it is only linked to the value of the mesenchymal cell density on the border). In this way there must be some compensation between points on the border which is a way to implicitly take into account the mechanical displacement: we postulate the existence of an overall mechanism, yet to be explain, that takes both the mechanical displacement and the speed of bone formation and creates the effective speed of the bone/suture interface $\mathbf{v}$. The speed is then expanded in the whole mesenchymal domain with equation:

$$\begin{cases} -\Delta v + \nabla^{\perp} p = 0 \\ \operatorname{rot} v = 0, \text{for } x \in_{\Omega_m} \\ v \cdot t = 0 \\ v \cdot n = \rho - \dfrac{1}{|\Gamma|} \displaystyle\int_{\Gamma} \rho \mathrm{d}\gamma \text{ on } \Gamma = \partial\Omega_m. \end{cases} \tag{6.8}$$

This expansion is made for purely numerical reason (the use of `movemesh` in *FreeFem++*) but since it could affect the numerical results, we mention it. We made some numerical simulations using this code and realistic parameters of Table 6.1 which were extracted from previous studies.

Parameter	Value
Width of the suture	0.5 – 1 mm
Duration of constraint application	30 days
Frequency of masticatory forces	1 Hz
Traction force	100 kPa
Bone Young's modulus (E_o)	6.10^3 MPa
Mesenchyme Young's modulus (E_m)	50 MPa
Bone Poisson's ratio (n_o)	0.28
Mesenchyme Poisson's ratio (n_m)	0.28
Collagen diffusion (D_f)	0.25 mm^2/day
Collagen secretion (α)	1
Mesenchymal cells diffusion (D_ρ)	0.1 mm^2/day
Speed of deposition of bone on the border	0.1 mm/day

Table 6.1: Biological parameters.

6.3.2 Numerical results

Using biological parameters (table 6.1), we find that the model simulates the apparition of an instability starting from strictly parallel borders and evolves in a similar way as sutures do in the first months after birth (figure 6.2). Note that the destabilization originates from errors in the numerical computations (which, most probably, come from the use of an unstructured mesh). We only used classical iterative solvers for linear problems whose stability is not a concern (like GMRES) and our equations are not stiff or numerically difficult (even Eq. (6.3) which is the most unusual equation in our system is stabilized by the diffusion). This means that there is no reason to think that the overall numerical error is out of control. Consequently, the large destabilization we observe must have an origin coming from the coupling between the equation. We give a partial justification of this fact in Section 6.4.

We performed finite element analysis and showed that the concavities of interdigitations are the areas of maximal constraint (figure 6.3), which is in line with the fact that bone deposition occurs in strained areas (Byron *et al.*, 2004) [15].

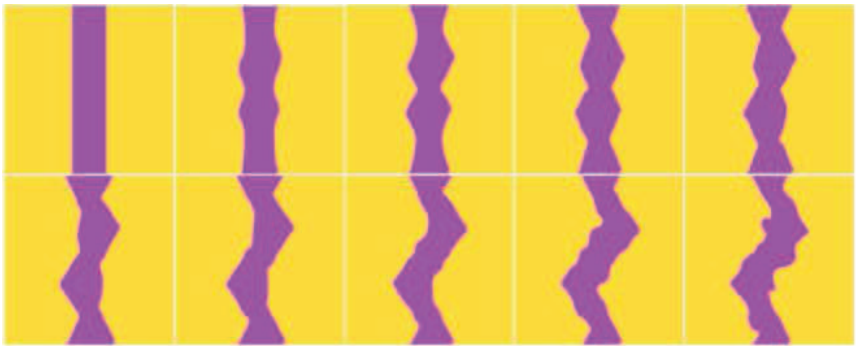

Figure 6.2: Mechanical instability during sutural growth when a quasi-static force is applied to the lateral borders of the domain.

We furthermore found that the model spontaneously predicts that bone deposition occurs on the tip of the interdigitations and that collagen fibres within the suture orientate in a radiating way at the zones of maximum curvature (figure 6.3). This is in accordance with the experimental data appearing in Fig 6.4 where the fibers can be seen in the turning points of the suture.

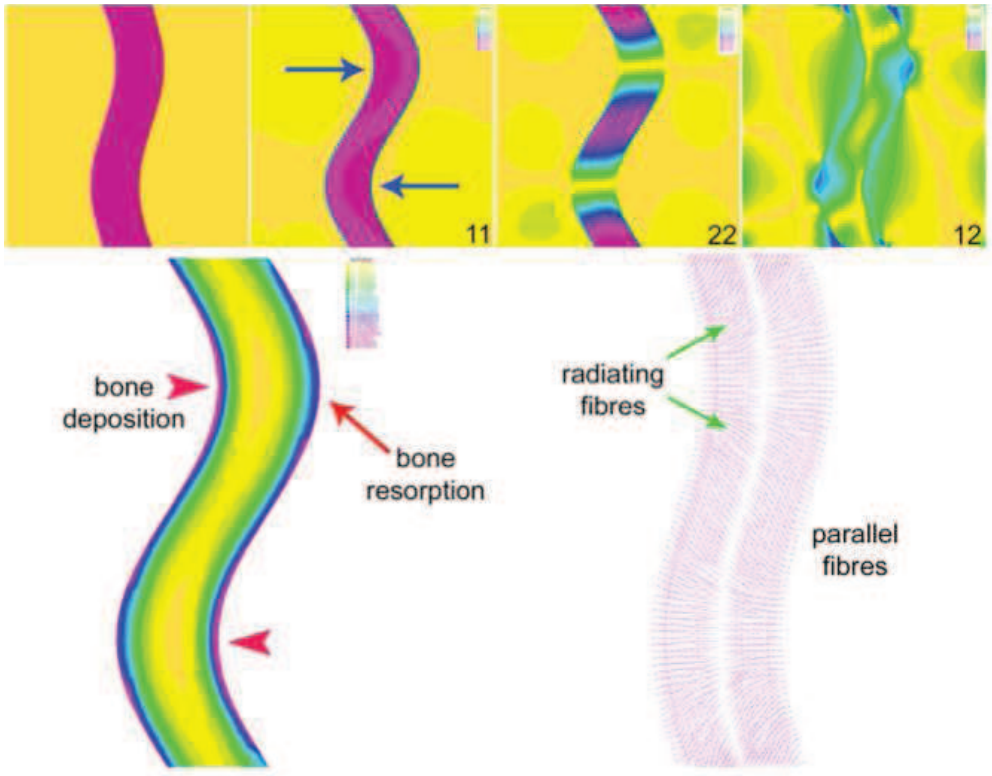

Figure 6.3: Finite element analysis performed on a simple sinusoidal shape with the physical characteristics of sutures predicts that the maximum of constraint affects the concavities of interdigitations along the x-axis. The 22 and 12 directions involve negligible constraints. The model predicts that bone deposition clearly predominates on concavities while convexities have no growth or resorption. The fibres spontaneously radiate across the suture from the concavities and are parallel in linear regions.

6.4 Analytic calculations

6.4.1 Presentation of the mathematical system

In this section we want to see if we can justify in some way the numerical instabilities that we have observed. Only in this section, and for the purpose of a simpler mathematical exposition, will we consider a somewhat simpler problem which should retain the main features of the suture model. The simplification lie in the fact that we consider only one interface between the mesenchyme (on the left of the interface) and bone (on the right). The inner biological bone creation mechanism is unchanged. However, for the

mechanical part we have to introduce some boundary condition at the border of the mesenchyme. Whatever boundary condition we would take would be unphysical in the context of a real suture. However, we are interested in the behaviour of the interface in the model and we expect that this behaviour to only depend on what is happening locally in the vicinity of the interface.

When the interface is a straight line (as in the numerical experiment of Section 6.3 whose results can be seen on Fig. 6.2) it is clear by symmetry that the solutions of our equations do not depend on the vertical variable y. Consequently, when starting from a straight interface, the interface should remain straight for all time. To investigate the instability of our model we start from an initially perturbed straight interface with a sine curve: as the straight interface has equation $x = 0$ (the left limit of the the suture is thus $x = -1$ and the right limit of the bone is $x = 1$), the perturbed interface has equation $x = \varepsilon \sin(ky)$ where ε is a small parameter. Using this interface as initial data we want to study the evolution of the amplitude of the interface with respect to k. Indeed, the results in Fig. 6.2 suggest that the destabilisation is not anarchical and that only specific wavelength could be affected by the instability.

6.4.2 Perturbed mechanical response

The numerical scheme of Section 6.3 suggest a "fixed-point procedure" to study the (non linear) coupling of our model. We thus start by computing the response in ε of the mechanical equations (6.1), that is the formal first order expansion of the solution. In time, we will insert the expansion we find in the equations governing the biology (6.3)–(6.7) and by computing the time evolution of the interface, maybe identify the complete instability mechanism

Let us describe the zeroth order term. As we mentioned, we have to take a boundary condition at $x = -1$ and we take, as in the real suture case, $\sigma n = Fn$. When $\varepsilon = 0$, due to the symmetry, the solution of (6.1) does not depend on the y variable and admit the following simple expression:

$$\begin{cases} \bar{u}^x_{g,d}(x,y) = \dfrac{F}{2\mu_{g,d} + \lambda_{g,d}} x \\ \bar{u}^y_{g,d}(x,y) = 0 \end{cases} \tag{6.9}$$

$$\overline{\boldsymbol{\sigma}} = \begin{pmatrix} F & 0 \\ 0 & 0 \end{pmatrix} \tag{6.10}$$

As we will need to study higher order term, we set $u = \bar{u} + \varepsilon \widetilde{u} + \mathcal{O}(\varepsilon^2)$ where $\widetilde{u}$ is independent of ε.

6.4.3 New variables

Now to study the perturbed solution, it is easier to change variables in order to get a problem with a fixed interface, especially since the coefficients of the Lamé equations are discontinuous at the interface. We thus set

$$x' = x - \varepsilon \sin(ky), \qquad y' = y. \tag{6.11}$$

Of course, after this change of variables, the boundaries $x = \pm 1$ become ε dependent in the x', y' variables. But as we mentioned, we are mainly interested at what happens at $x' = 0$. We thus completely "forget" the boundaries in the sequel. Our approximation will then not have the right order on the boundaries and that should be corrected but only with boundary layers which will not affect the solution near the interface. To keep the notation as light as possible, we will omit the primes in the equation and express everything in the new variables, except when we explicitely state otherwise.

We now set (in the new variables):

$$\widehat{u}^y_{g,d} = \widetilde{u}^y_{g,d}, \tag{6.12}$$

$$\widehat{u}^x_{g,d} = \widetilde{u}^x_{g,d} - \frac{F}{2\mu_{g,d} + \lambda_{g,d}} \sin(ky). \tag{6.13}$$

Note in (6.13) the second term coming from the change of variable. We now write the equations of these unknowns:

$$\begin{cases} (2\mu_{g,d} + \lambda_{g,d})\partial_{xx}\widehat{u}^x_{g,d} + (\mu_{g,d} + \lambda_{g,d})\partial_{xy}\widehat{u}^y_{g,d} + \mu_{g,d}\partial_{yy}\widehat{u}^x_{g,d} = 0, \\ \mu_{g,d}\partial_{xx}\widehat{u}^y_{g,d} + (\mu_{g,d} + \lambda_{g,d})\partial_{xy}\widehat{u}^x_{g,d} + (2\mu_{g,d} + \lambda_{g,d})\partial_{yy}\widehat{u}^y_{g,d} = 0, \end{cases} \tag{6.14}$$

together with the continuity condition at $x = 0$,

$$\begin{cases} \left[\widehat{u}^x + \dfrac{F}{2\mu + \lambda} \sin(ky)\right] = 0, \\ [\widehat{u}^y] = 0, \\ [-\left((2\mu + \lambda)\partial_x \widehat{u}^x + \lambda \partial_y \widehat{u}^y\right)] = 0, \\ \left[-\mu\left(\partial_x \widehat{u}^y + \partial_y \widehat{u}^x\right) + k\cos(ky)\dfrac{\lambda F}{2\mu + \lambda}\right] = 0. \end{cases} \tag{6.15}$$

In the previous expression the square brackets express the jump at $x = 0$ that is $[a] = a_d - a_g$ for any scalar function with value a_d on the right of the interface and a_g on the left.

6.4.4 First order perturbation: solving the differential equations (6.14)

We look for a solution satisfying the following ansatz:

$$\begin{cases} \widehat{u}^x = U^x(x)\sin(ky), \\ \widehat{u}^y = U^y(x)\cos(ky), \end{cases} \tag{6.16}$$

where U^x and U^y have the particular form:

$$U^x_g(x) = A_g \exp(kx) + C_g x \exp(kx), \tag{6.17}$$

$$U^y_g(x) = \left(A_g + \frac{3\mu+\lambda}{k(\lambda+\mu)} C_g\right)\exp(kx) + C_g x \exp(kx), \tag{6.18}$$

$$U^x_d(x) = B_d \exp(-kx) + D_d x \exp(-kx), \tag{6.19}$$

$$U^y_d(x) = \left(-B_d + \frac{3\mu+\lambda}{k(\lambda+\mu)} D_d\right)\exp(-kx) + -D_d x \exp(-kx). \tag{6.20}$$

These particular forms of U^x and U^y have two properties: firstly, then ensure that differential equations (6.14) are solved by $\widehat{u}^x$ and $\widehat{u}^y$; secondly they decrease in x in their respective neighbourhood of $x = 0$ (that is $x < 0$ for $U^{x,y}_g$ and $x > 0$ for $U^{x,y}_d$.

6.4.5 First order perturbation: satisfying conditions (6.15)

To determine the four scalar parameters A_g, B_d, C_g, and D_d we shall use the four continuity conditions (6.15) on the interface $x = 0$. They give :

- Continuity of displacement:

$$A_g = B_d + \left[\frac{F}{2\mu+\lambda}\right], \tag{6.21}$$

$$A_g + \left(\frac{3\mu+\lambda}{k(\lambda+\mu)}\right)_g C_g = -B_d + \left(\frac{3\mu+\lambda}{k(\lambda+\mu)}\right)_d D_d, \tag{6.22}$$

- Continuity of normal stress:

$$\begin{aligned} (2\mu+\lambda)_g(kA_g + C_g) - \lambda_g(kA_g + \alpha_g C_g) = \\ (2\mu+\lambda)_d(-kB_d + D_d) - \lambda_d(-kB_d + \alpha_d D_d), \end{aligned} \tag{6.23}$$

$$\begin{aligned} -\mu_g\left(kA_g + \alpha_g C_g + C_g\right) - \mu_g k A_g + k\left(\frac{\lambda F}{2\mu+\lambda}\right)_g = \\ -\mu_d\left(kB_d - \alpha_d D_d - D_d\right) - \mu_d k B_d + k\left(\frac{\lambda F}{2\mu+\lambda}\right)_d, \end{aligned} \tag{6.24}$$

where for brevity we have noted

$$\alpha = \frac{3\mu + \lambda}{\mu + \lambda}. \tag{6.25}$$

Equation (6.23) is equivalent to

$$2\mu_g k A_g + \left(\frac{2\mu^2}{\mu+\lambda}\right)_g C_g = -2\mu_d k B_d + \left(\frac{2\mu^2}{\mu+\lambda}\right)_d D_d, \tag{6.26}$$

whereas equation (6.24) is equivalent to

$$-2\mu_g k A_g - \left(\frac{2\mu^2}{\mu+\lambda} + 2\mu\right)_g C_g = -2\mu_d k B_d + \left(\frac{2\mu^2}{\mu+\lambda} + 2\mu\right)_d D_d + \left[\frac{k\lambda F}{2\mu+\lambda}\right]. \tag{6.27}$$

We can replace (6.26)-(6.27) with

$$-\mu_g C_g = -2\mu_d k B_d + \left(\frac{2\mu^2}{\mu+\lambda} + \mu\right)_d D_d + \frac{1}{2}\left[\frac{k\lambda F}{2\mu+\lambda}\right], \tag{6.28}$$

$$2\mu_g k A_g + \left(\frac{2\mu^2}{\mu+\lambda} + \mu\right)_g C_g = -\mu_d D_d - \frac{1}{2}\left[\frac{k\lambda F}{2\mu+\lambda}\right]. \tag{6.29}$$

From (6.21)-(6.22) we get (A_g, B_d):

$$2A_g = -\left(\frac{3\mu+\lambda}{k(\lambda+\mu)}\right)_g C_g + \left(\frac{3\mu+\lambda}{k(\lambda+\mu)}\right)_d D_d + \left[\frac{F}{2\mu+\lambda}\right], \tag{6.30}$$

$$2B_d = -\left(\frac{3\mu+\lambda}{k(\lambda+\mu)}\right)_g C_g + \left(\frac{3\mu+\lambda}{k(\lambda+\mu)}\right)_d D_d - \left[\frac{F}{2\mu+\lambda}\right]. \tag{6.31}$$

We can simplify (6.28)-(6.29), using

$$-\mu k \frac{3\mu+\lambda}{k(\lambda+\mu)} + \frac{2\mu^2}{\mu+\lambda} = -\mu\,.$$

We obtain

$$-\mu_g C_g = \mu_d \left(\frac{3\mu+\lambda}{\lambda+\mu}\right)_g C_g + \mu_d k \left[\frac{F}{2\mu+\lambda}\right] + \frac{1}{2}\left[\frac{k\lambda F}{2\mu+\lambda}\right], \tag{6.32}$$

$$\mu_g \left(\frac{3\mu+\lambda}{\lambda+\mu}\right)_d D_d = -\mu_d D_d - \mu_g k \left[\frac{F}{2\mu+\lambda}\right] - \frac{1}{2}\left[\frac{k\lambda F}{2\mu+\lambda}\right]. \tag{6.33}$$

Finally we have

$$C_g = -\frac{k}{\mu_g + \mu_d\alpha_g}\left(\mu_d\left[\frac{F}{2\mu+\lambda}\right] + \frac{1}{2}\left[\frac{\lambda F}{2\mu+\lambda}\right]\right) = \frac{kF}{\mu_g + \mu_d\alpha_g}\cdot\frac{\mu_d - \mu_g}{2\mu_g + \lambda_g}, \tag{6.34}$$

$$D_d = -\frac{k}{\mu_d + \mu_g\alpha_d}\left(\mu_g\left[\frac{F}{2\mu+\lambda}\right] + \frac{1}{2}\left[\frac{\lambda F}{2\mu+\lambda}\right]\right) = \frac{kF}{\mu_d + \mu_g\alpha_d}\cdot\frac{\mu_d - \mu_g}{2\mu_d + \lambda_d}, \tag{6.35}$$

and

$$\begin{aligned} A_g &= \frac{(\mu_d - \mu_g)F}{2}\left(\frac{\alpha_d}{(\mu_d + \mu_g\alpha_d)(2\mu_d + \lambda_d)} - \frac{\alpha_g}{(\mu_g + \mu_d\alpha_g)(2\mu_g + \lambda_g)}\right) \\ &\quad + \frac{1}{2}\left[\frac{F}{2\mu+\lambda}\right], \\ &= \frac{F}{2}\left(\frac{2\mu_d}{(\mu_d + \mu_g\alpha_d)(\mu_d + \lambda_d)} - \frac{2\mu_g}{(\mu_g + \mu_d\alpha_g)(\mu_g + \lambda_g)}\right), \end{aligned} \tag{6.36}$$

$$B_d = A_g - \left[\frac{F}{2\mu+\lambda}\right]. \tag{6.37}$$

6.4.6 First order perturbation : stress

We conclude, computing the linearized left stress tensor through its definition (6.1). However we do so *in the initial variables* in the (x, y) around $x = 0$:

$$\begin{aligned} (\sigma_g)_{xx} &= F + \varepsilon\left((2\mu_g + \lambda_g)(kA_g + C_g) - \lambda_g(kA_g + \alpha_g C_g)\right)\sin(ky), \\ &= F + \varepsilon\left(2\mu_g kA_g + \left(\frac{2\mu^2}{\mu+\lambda}\right)_g C_g\right)\sin(ky), \\ &= F + \varepsilon\left(-\mu_g C_g + \mu_g\alpha_d D_d + \mu_g\left[\frac{kF}{2\mu+\lambda}\right]\right)\sin(ky), \\ &= F + \varepsilon kF\Bigg(-\frac{2\mu_g\mu_d}{(\mu_g + \mu_d\alpha_g)(\mu_g + \lambda_g)} \\ &\quad + \frac{2\mu_g\mu_d}{(\mu_d + \mu_g\alpha_d)(\mu_d + \lambda_d)}\Bigg)\sin(ky), \end{aligned} \tag{6.38}$$

and

$$\begin{aligned} (\sigma_g)_{xy} &= \varepsilon\left(\mu_g kA_g + \mu_g kA_g + \mu_g\alpha_g C_g + \mu_g C_g\right)\cos(ky), \\ &= \varepsilon\left(-\mu_d D_d + \mu_g C_g - \frac{1}{2}\left[\frac{k\lambda F}{2\mu+\lambda}\right]\right)\cos(ky), \end{aligned} \tag{6.39}$$

Lastly,

$$\begin{aligned}
(\sigma_g)_{yy} &= \varepsilon\left(\lambda_g\left(kA_g + C_g\right) - (2\mu_g + \lambda_g)(kA_g + \alpha_g C_g)\right)\sin(ky) \\
&= \varepsilon\left(-2\mu_g k A_g + \left(\lambda_g - (2\mu_g + \lambda_g)\alpha_g\right) C_g\right)\sin(ky) \\
&= \varepsilon\Bigg(\left(\mu_g\alpha_g + \lambda_g - (2\mu_g + \lambda_g)\alpha_g\right) C_g - \mu_g\alpha_d D_d \\
&\quad - \mu_g\left[\frac{kF}{2\mu + \lambda}\right]\Bigg)\sin(ky) \\
&= \varepsilon\left(-3\mu_g C_g - \mu_g\alpha_d D_d - \mu_g\left[\frac{kF}{2\mu + \lambda}\right]\right)\sin(ky) \\
&= \varepsilon kF\Bigg(3\mu_g\frac{\mu_g - \mu_d}{(\mu_g + \mu_d\alpha_g)(2\mu_g + \lambda_g)} + \mu_g\alpha_d\frac{\mu_g - \mu_d}{(\mu_d + \mu_g\alpha_d)(2\mu_d + \lambda_d)} \\
&\quad - \mu_g\left[\frac{1}{2\mu + \lambda}\right]\Bigg)\sin(ky) \\
&= \varepsilon kF\left(\frac{\mu_g}{2\mu_g + \lambda_g}\cdot\frac{4\mu_g - \frac{2\lambda_g}{\mu_g + \lambda_g}\mu_d}{\mu_g + \mu_d\alpha_g} - \frac{2\mu_g\mu_d}{(\mu_d + \mu_g\alpha_d)(\mu_d + \lambda_d)}\right)\sin(ky) \\
&= \varepsilon kF\left(\frac{2\mu_g^2 + (\mu_g - \mu_d)\frac{2\mu_g\lambda_g}{2\mu_g + \lambda_g}}{(\mu_g + \mu_d\alpha_g)(\mu_g + \lambda_g)} - \frac{2\mu_g\mu_d}{(\mu_d + \mu_g\alpha_d)(\mu_d + \lambda_d)}\right)\sin(ky)
\end{aligned} \tag{6.40}$$

As a preparation for the study of the instability on the full system, we compute the first order expansions of the principal stress and their associated principal direction. The eigenvalues, given through (6.5), are at order $\mathcal{O}(\varepsilon)$:

$$\sigma_1 = F + \varepsilon kF\left(-\frac{2\mu_g\mu_d}{(\mu_g + \mu_d\alpha_g)(\mu_g + \lambda_g)} + \frac{2\mu_g\mu_d}{(\mu_d + \mu_g\alpha_d)(\mu_d + \lambda_d)}\right)\sin(ky)\,,$$

$$\sigma_2 = \varepsilon kF\left(\frac{2\mu_g^2 + (\mu_g - \mu_d)\frac{2\mu_g\lambda_g}{2\mu_g + \lambda_g}}{(\mu_g + \mu_d\alpha_g)(\mu_g + \lambda_g)} - \frac{2\mu_g\mu_d}{(\mu_d + \mu_g\alpha_d)(\mu_d + \lambda_d)}\right)\sin(ky)\,.$$

Remark that σ_{xy} does not enter into account before order ε^2. It is also mandatory to compute the eigenvectors in order to determine the orientation of fibers. However the expressions of the coefficients of the various expansions are getting increasingly complicated to write and in order to understand the instability we have to know the signs of such expression which is not clear in general. Since our goal is to study the problem for the parameters of Table 6.1 we make in the sequel the following simplifications : $\nu_g = \nu_d$ and $E_g/E_d \to 0$. Under this hypotheses we find the following expansions:

$$\sigma_1 \approx F + \varepsilon k F \frac{2(1-2\nu)}{3-4\nu}\sin(ky)$$
$$\sigma_2 \approx -\varepsilon k F \frac{2\nu(1-2\nu)(1+\nu)}{(1-\nu)(3-4\nu)}\sin(ky)$$

and

$$\sigma_{xy} \approx -\frac{\varepsilon k F}{3-4\nu}\cos(ky).$$

Therefore $\sigma_1 > 0$ and depending on y we find two possibilities $0 < \sigma_2 < \sigma_1$ and $\sigma_2 < 0 < \sigma_1$. Thus fibres are oriented in the e_1 direction where e_1 is the vector with horizontal component given by $\sigma_1 - \sigma_2$ and the vertical one given by σ_{xy}. The main order related to σ_{xy} give us exactly the behavior simulated in Fig. 6.3.

6.5 Biomedical comments related to modelization

The central hypothesis in our model is that the information about external force is transmitted to the suture via the orientation of the collagen fibres. In order to confirm the role of mechanotransduction on suture patterning and collagen fibre orientation, we used a mouse with a conditional knock-out of Pkd2 in neural crest cells (Pkd2$^{fl/fl}$;Wnt1-Cre). Pkd1 and Pkd2 form a complex working as a calcium channel activated by the bending of primary cilia and are expressed by osteoprogenitor cells within sutures (Kolpakova-Hart *et al.*, 2008) [45]. In the fronto-maxillary suture, the lack of Pkd2, and thus defective mechanotransduction, lead to a failure of suture patterning and to abnormal collagen fibre disposition across the suture (figure 6.4.

The hypothesis on the migration of mesenchyme cells along collagen fibres spanning across the suture was confirmed by using an adult R26R;Wnt1-Cre mouse. The mesenchyme of the sagittal suture derives from neural crest cells but the parietal bones are mesoderm derivatives. We could thus clearly visualise the orientation of mesenchyme cells within the suture using a LacZ-staining in R26R;Wnt1-Cre mice. We found that mesenchyme cells are oriented in the same direction as the collagen fibres crossing the suture (figure 6.5).

6.5.1 Conclusion

Finally, the model we propose simulates the morphological characteristics of adult sutures using mechanical feed-back only and the small number of

Figure 6.4: Fronto-nasal suture in adult wild-type (CD1) and Pkd2$^{fl/fl}$;Wnt1-Cre mice. Picrosirius staining. The absence of a gene involved in mechanotransduction leads to abnormal suture patterning and wrong collagen fibre insertions (arrowheads). The bone is globally depleted in collagen.

crucial hypothesis we made (importance of mechanotransduction, migration along the fibres) are corroborated by data from transgenic mice and high resolution imaging.

Pattern formation involves a combination of chemical and physical processes. Most of the current research on suture maintenance and on craniosynostosis focuses on the molecular factors involved in bone proliferation and differentiation.

Our model illustrates the patterning ability of simple mechanical processes. Mechanotransduction could act upstream in several very common pathological situations such as deformational plagiocephalies or occlusal disorders due to maxillary malposition, where there are striking and unexplained individual variations and differences in responses to external stimuli.

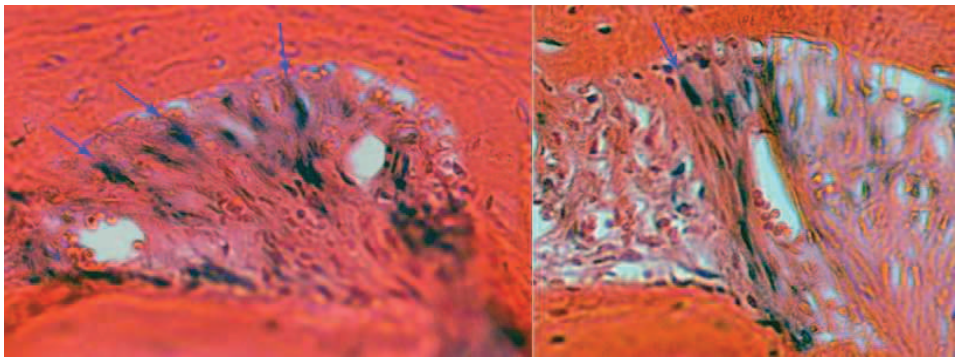

Figure 6.5: $\beta-$galactosidase positive neural crest derived mesenchyme cells in the sagittal suture are oriented following the collagen fibres spanning across the suture (arrows).

Conclusion et perspectives

Matériaux vitreux

Dans cette thèse, nous nous sommes essentiellement attelés à l'étude de modèles cinétiques pour les matériaux vitreux : le modèle d'Hébraud-Lequeux ainsi que l'une de ses extensions possibles que nous sommes en train de développer. Nous avons montré que l'on pouvait faire une étude mathématique complète de la transition vitreuse dans ce type de modèle. Rappelons que la transition vitreuse se caractérise par un changement de comportement asymptotique pour petits taux de cisaillement de la loi rhéologique du matériau.

Nous avons tout d'abord montré cette transition vitreuse en calculant rigoureusement l'équivalent de la contrainte en fonction de la température de transition. Pour ce faire, nous avons utilisé une méthode que l'on pourrait dire *en dimension finie* : après intégration de l'équation différentielle du modèle, l'analyse s'est ramenée à des études de fonctions d'une seule variable réelle et de courbes du plan. D'une part, nous avons dû déterminer le comportement asymptotique d'une fonction définie par le théorème des fonctions implicites, au voisinage d'un point où la fonction génératrice est très singulière. D'autre part, nous avons dû étudier le comportement d'une fonction de deux variables le long de la courbe connue implicitement.

Nous avons ensuite changé de point de vue et adopté un point de vue *en dimension infinie*. Nous avons étendu le résultat précédent en calculant, non plus un équivalent de la contrainte en fonction du taux de cisaillement, mais un développement asymptotique à tout ordre, et même un développement en série de Puiseux convergente. À cette fin, nous avons employé la technique des développements asymptotiques en *couches limites* inspirés de l'étude de la pénalisation d'obstacle en mécanique des fluides. Bien que l'idée originelle d'employer ce type de développement soit liée aux comportements asymptotiques trouvés précédemment, cette démonstration est complètement autonome. Le développement en série convergente s'obtient par des techniques de perturbations analytiques à la Kato. Nous avons pu montrer la puissance de

cette approche en l'adaptant de façon très naturelle à l'étude du comportement pour grands taux de cisaillement pour le modèle d'Hébraud-Lequeux, et ainsi retrouver le comportement newtonien du matériau, indépendamment de sa température.

Enfin, nous avons également conçu un modèle de matériau vitreux pour écoulements généraux et non plus limités à l'écoulement de cisaillement simple. Nous avons adapté la généralisation du modèle de Maxwell au cas du modèle d'Hébraud-Lequeux pour prendre en compte la propriété d'objectivité des lois rhéologiques, que nous écrivons directement au niveau mésoscopique. Nous avons pu partiellement appliquer la méthodologie développée sur le modèle d'Hébraud-Lequeux pour montrer que notre modèle avait, au moins d'un point de vue formel, des propriétés semblables de transition vitreuse, et donc, valider (partiellement) la démarche de construction de notre modèle.

Dans l'avenir, il y a plusieurs points qu'il serait intéressant de développer à partir de ce travail. Tout d'abord, nous aimerions évidemment compléter l'étude de notre modèle d'écoulement général sur deux points. Tout d'abord montrer, même au niveau formel, que notre modèle a exactement le même type de transition vitreuse que son aîné car, pour le moment, il existe peut-être certaines gammes de températures dans lesquelles le modèle pourrait avoir plusieurs types de comportement à faible taux de cisaillement. Ensuite, nous souhaiterions aussi rendre notre analyse rigoureuse en adaptant le raisonnement de perturbation analytique que nous avons construit pour le modèle d'Hébraud-Lequeux. Ceci fournirait aussi un théorème d'existence pour petit taux de cisaillement.

Par ailleurs, nous aimerions mieux comprendre la transition vitreuse en ne considérant plus uniquement le régime stationnaire du modèle d'Hébraud-Lequeux, mais aussi le régime transitoire. En effet, la transition vitreuse provient d'un ralentissement de la dynamique d'évolution du matériau lors du refroidissement : dans le contexte des modèles de piège, le système se retrouve de plus en plus piégé dans des puits d'énergie libre de plus en plus profonds et dont le système met de plus en plus de temps à sortir. Mathématiquement, il s'agirait d'étendre les résultats de Cancès et Le Bris [18] de convergence en temps longs de la solution du modèle d'Hébraud-Lequeux évolutionnaire, qui s'appuient sur la méthode de dissipation d'entropie telle que développée par Desvillettes et Villani dans [26].

Enfin nous aimerions faire des ponts entre le modèle d'Hébraud-Lequeux et d'autres modèles car le modèle d'Hébraud-Lequeux a une carence importante par rapport au comportement expérimental des matériaux vitreux : ceux-ci présentent des bandes de cisaillement (*shear-banding* en anglais), c'est-à-dire que le matériau, soumis à une contrainte homogène, présente

deux phases localisées en espace, l'une dans laquelle le matériau s'écoule et l'autre dans laquelle le matériau est au repos. Le modèle d'Hébraud-Lequeux ne permet pas de rendre compte de ce phénomène. Les bandes de cisaillement peuvent provenir d'une instabilité due à la plasticité à haute déformation dans le matériau qui amplifie la non uniformité et les défauts locaux (Tzavaras [70]). Les bandes de cisaillement sont donc liées à des propriétés non locales dans le matériau qu'il faut ajouter au modèle d'Hébraud-Lequeux, ce qu'ont fait Bocquet, Adjari et Colin dans [9]. D'autre part, il existe des modèles dits «sur réseau» développés par Picard, Adjari, Bocquet et Lequeux [59] dans lesquels les matériaux sont discrétisés en blocs, et les interactions entre blocs, écrites explicitement. Dans ces modèles, on distingue en général trois temps caractéristiques pour piloter les différents effets qui agissent sur la contrainte locale (contre un seul dans le modèle d'Hébraud-Lequeux). Faire des liens entre ces modèles discrétisés et les modèles continus pourrait permettre de mieux comprendre les mécanismes à l'œuvre dans les matériaux vitreux.

Biologie et chimie

Dans le domaine de la chimie, nous avons proposé une façon d'aborder les problèmes de réaction-diffusion dans laquelle toute la partie réactive est supposée *a priori* infiniment rapide par rapport à la diffusion. Nous avons alors montré comment cette hypothèse pouvait être prise en compte dans l'écriture des équations par un multiplicateur de Lagrange dans le terme source. Surtout, nous avons montré qu'on pouvait s'appuyer sur ce raisonnement continu pour construire un schéma numérique performant, qui permet d'éviter de traiter la raideur du système tout en gardant une partie de la phénoménologie au niveau numérique.

Par la suite nous aimerions poursuivre ce travail dans plusieurs directions. Tout d'abord comparer notre schéma numérique à l'approche relaxée de Guermond et Minev qui, sur le système de Navier-Stokes incompressible, traitent la contrainte à l'aide d'une équation de relaxation modifiée [34]. Nous aimerions aussi pouvoir étudier réellement le modèle continu, ce qui pourrait éventuellement se faire à l'aide du calcul pseudo-différentiel. Enfin nous aimerions pouvoir développer l'aspect biologique du problème de la balnéothérapie afin d'obtenir un modèle complet de la diffusion des ions à travers la peau.

Enfin, en ce qui concerne les sutures, nous avons proposé un modèle d'interaction original pour rendre compte de l'interdigitation au cours du

développement des sutures crâniennes. Ce modèle couple des mécanismes biologiques et mécaniques simples mais qui conduisent à une instabilité qui peut expliquer l'origine de l'interdigitation, en tout cas si on s'appuie sur les simulations numériques de ce modèle.

Dans la suite, nous pensons améliorer notre compréhension des phénomènes d'évolution des sutures, d'une part en achevant l'étude mathématique de l'instabilité que nous n'avons pu que commencer au cours de cette thèse et, d'autre part en revenant sur le problème du maintien dans le temps des sutures. En effet, nous avons expliqué que les sutures avaient un temps de vie «anormalement élevé» pour un phénomène gouverné mécaniquement par la convection du milieu, et biologiquement par des phénomènes de diffusion : on s'attend, avec ces ingrédients, à ce que la suture s'ouvre complètement, ou fusionne complètement ce qui n'est pas ce qu'on observe dans la réalité. Si nous pouvions trouver de nouvelles idées pour leur comportement biomécanique qui permettent de stabiliser l'écart entre les berges, nous obtiendrions un modèle complet d'évolution des sutures. Ceci permettrait par la suite d'étudier quels sont les facteurs qui interviennent dans cette évolution, et ainsi, peut-être, ouvrir de nouvelles voies dans le traitement des pathologies liées au développement anormal des sutures.

Annexe A

Résumé de modélisation des matériaux

Dans ce chapitre, nous allons rappeler des notions élémentaires de modélisation pour les milieux continus, les matériaux simples et complexes avec évidemment une mention spéciale pour les matériaux vitreux. Nous tirons cette présentation essentiellement de [57] ainsi que d'autres sources comme des notes de cours non publiées de Didier Bernardin dans le cadre de l'école de printemps du GDR Matériaux vitreux, ainsi que du texte des exposés du Séminaire Poincaré «Bourbaphy» numéro XIII intitulé *Verres et grains*.

A.1 Matériaux continus

A.1.1 Définition du tenseur des contraintes

Commençons par quelques généralités sur les matériaux simplement *continus*, c'est-à-dire des matériaux qui occupent des volumes de l'espace ambiant (éventuellement l'espace ambiant pourra être considéré comme bidimensionnel). Du simple fait qu'ils sont continus, ces matériaux possèdent des forces internes qui ont une forme très particulière et que l'on représente de la façon suivante : on place une petite surface $\mathrm{d}S$ (ou courbe en $2d$) orientée par un vecteur normal n en un point x du matériau et on note $\mathrm{d}T(x,n)$ la force interne qu'exerce un côté de la surface sur l'autre côté ; on peut, en fait, démontrer qu'il existe un tenseur appelé *tenseur des contraintes* (tenseur est pour nous un raccourci pour «champ de matrice») et souvent noté $\sigma(x)$ tel que

$$\mathrm{d}T(x,n) = \sigma(x)\mathrm{d}Sn. \tag{A.1}$$

La dimension des composantes du tenseur des contraintes est donc celle d'une pression (elles s'expriment donc en Pa ou MPa).

A.1.2 Symétrie du tenseur des contraintes

On peut exprimer, à partir du tenseur des contraintes σ, les couples internes qui s'exercent dans le matériau. En général, ces couples sont nuls : soit à cause des symétries internes du matériau, soit parce que l'energie nécessaire pour obtenir ces couples est trop importante (c'est le cas notamment des solides cristallins car un couple doit distordre tout le réseau du cristal). Dans ces cas-là, le tenseur des contraintes est symétrique (c'est-à-dire qu'en tout point x la matrice σ est symétrique). Il peut arriver néanmoins que les couples internes ne soient pas nuls auquel cas le tenseur des contraintes n'est pas symétrique : c'est le cas notamment de certains cristaux liquides.

A.2 Matériaux déformables

On ne considèrera dans la suite que des matériaux déformables. En effet, le mouvement des matériaux continus indéformables peut s'étudier par décomposition en mouvement du centre de masse d'un côté et rotation propre de l'autre. Un tel mouvement est dès lors appelé mouvement rigide ; il est caractérisé par la trajectoire d'un point quelconque et par la matrice décrivant la rotation au cours du temps.

A.2.1 Descriptions eulérienne et lagrangienne

Il y a essentiellement deux grands types d'approche des mouvements de matériaux continus. L'approche dite *lagrangienne* consiste à repérer chaque point du matériau (on dit souvent *particule*) au temps initial et ensuite à suivre le mouvement de chacun des points individuellement. Dans cette approche, la vitesse d'une particule est toujours facilement accessible, tandis que sa position nécessite la connaissance de toute la trajectoire. L'approche dite *eulérienne* consiste à fixer un référentiel d'observation unique. La vitesse en un point x donné du référentiel à un instant donné t est alors la vitesse de la particule qui se trouvait au point x à l'instant t.

Le lien entre les quantités lagrangiennes et eulériennes se font donc grâce aux trajectoires.

A.2.2 Quantités cinématiques importantes

Pour étudier le mouvement des matériaux déformables, on utilise l'approche lagrangienne : il faut repérer à chaque instant le matériau par rapport à une configuration de base Ω_0 qui est la position qu'occupe le matériau à l'instant initial. À un instant t de son mouvement, le matériau occupe la configuration Ω_t. On note maintenant $\phi_t : \Omega_0 \to \Omega_t$ le *déplacement absolu* du matériau entre les configurations Ω_0 et Ω_t. Notons immédiatement qu'on a $\phi_0 = id\Omega_0$. On ne considère ici que des déplacements réversibles (ϕ_t est un difféomorphisme) quasistatiques (ϕ_t dépend régulièrement du temps). Si on se donne X une particule appartenant à Ω_0, la courbe de l'espace $t \mapsto \phi_t(X)$ est donc la trajectoire eulérienne de la particule X. Le déplacement ϕ_t est la quantité centrale lorsque l'on étudie les solides élastiques. À partir de ϕ on peut construire le champ de vecteur eulérien du mouvement qui est la quantité centrale dans l'étude des fluides : pour x apprtenant Ω_t on définit

$$u(t,x) = \dot{\phi}_t(\phi_t^{-1}(x)) \tag{A.2}$$

où le point désigne la dérivée par rapport à t des quantités lagrangiennes (on notera ∂_t pour la dérivée par rapport au temps des quantités eulériennes).

Puisque l'on étudie des matériaux déformables, il faut pouvoir quantifier la déformation. Pour cela, on étudie la modification locale des distances et des angles au cours du mouvement : on se donne deux instants $t' < t$, deux vecteurs élémentaires $\mathrm{d}x'_1$ et $\mathrm{d}x'_2$ au voisinage d'un point x' de $\Omega_{t'}$, et on imagine que x', $x'+\mathrm{d}x'_1$ et $x'+\mathrm{d}x'_2$ sont attachés au solide. On peut commencer par repérer la trajectoire de ces trois points en écrivant

$$\begin{aligned}
&x' = \phi_{t'}(X), && \text{où } X = \phi_{t'}^{-1}(x'),\\
&x' + \mathrm{d}x'_1 = \phi_{t'}(X_1), && \text{où } X_1 = \phi_{t'}^{-1}(x' + \mathrm{d}x'_1),\\
&x' + \mathrm{d}x'_2 = \phi_{t'}(X_2), && \text{où } X_2 = \phi_{t'}^{-1}(x' + \mathrm{d}x'_2).
\end{aligned}$$

À l'instant t, ces trois points se retrouvent en x, $x + \mathrm{d}x_1$ et $x + \mathrm{d}X_2$ avec pour chacun l'expression :

$$\begin{aligned}
&x = \phi_t(X)\\
&\mathrm{d}x_1 = \phi_t(X_1) - \phi_t(X)\\
&\mathrm{d}x_2 = \phi_t(X_2) - \phi_t(X).
\end{aligned}$$

Puisqu'on suppose $\mathrm{d}x'_1$ et $\mathrm{d}x'_2$ infiniments petits, on ne garde qu'au premier ordre :

$$\mathrm{d}x_1 \cdot \mathrm{d}x_2 = \mathrm{d}x_1'^{\,T} \left(\left(\mathrm{d}_{x'} \left(\phi_t \circ \phi_{t'}^{-1} \right) \right)^T \mathrm{d}_{x'} \left(\phi_t \circ \phi_{t'}^{-1} \right) \right) \mathrm{d}x_2' \tag{A.3}$$

On note en général

$$F_{t'}(t, x') = \mathrm{d}_{x'}(\phi_t \circ \phi_{t'}^{-1}) \tag{A.4}$$

le gradient de déformation relatif et $C_{t'} = F_{t'}^T F_{t'}$ le tenseur de *Cauchy-Green droit*. Il y a déformation si le tenseur de Cauchy-Green est différent de l'identité (dans le cas contraire, les angles et les distances sont conservés à l'ordre principal). On peut donc introduire le tenseur des déformations de *Green-Lagrange*,

$$E_{t'} = \frac{1}{2}(C_{t'} - Id), \tag{A.5}$$

comme mesure locale de la déformation du matériau.

Mais il faut remarquer que l'on aurait pu renverser le point de vue : on se place au point x à l'instant t, on se donne deux vecteurs élémentaires $\mathrm{d}x^1$ et $\mathrm{d}x^2$ et on cherche à savoir de combien a changé le produit scalaire depuis l'instant $t' < t$. En adaptant l'argument précédent, on en vient à définir le tenseur de Cauchy-Green gauche $B_{t'} = F_{t'} F_{t'}^T$ ainsi que le tenseur des déformation d'*Euler-Almansi* $(1/2)(Id - B_t^{-1} \circ (\phi_{t'} \circ \phi_t^{-1}))$.

Il existe, en fait, de nombreuses mesures pertinentes des déformations (on aurait pu étudier le changement de petites surfaces plongées dans le matériau) et on aurait aussi pu choisir le tenseur de *Piola* $1/2(Id - C^{-1})$ ou le tenseur de *Finger*

$$H_{t'}(t, x') = \frac{1}{2} \left(B_{t'}(t, x') - Id \right), \tag{A.6}$$

dont nous reparlerons plus bas.

Il faut néanmoins dire que si l'on s'appuie non pas sur le mouvement ϕ_t mais sur le déplacement $\xi = \phi_t - id$ et que l'on suppose que les déformations sont petites ($\|\mathrm{d}_X \xi\| \ll 1$), tous les tenseurs précédents se réduisent au *tenseur des petites déformations* ε

$$\varepsilon = \frac{1}{2} \left(\mathrm{d}_X \xi + (\mathrm{d}_X \xi)^T \right). \tag{A.7}$$

On peut notamment en déduire que le taux de déformation instantané est $2D(\nabla u)(t, x)$ à l'instant t.

A.2.3 Équations de la mécanique

Pour trouver les équations de la mécanique pour un matériau continu, on considère un élément quelconque V_0 dans Ω_0 que l'on suit au cours de son mouvement (on note alors $V_t = \phi_t(V_0)$. On obtient ainsi un système fermé auquel on peut appliquer les principes de la mécanique newtonienne. Ainsi les équations de la mécanique des milieux continus s'écrivent naturellement dans une optique eulérienne.

On note ρ la densité volumique de masse (eulérienne) du matériau. La conservation de la masse de V_0 au cours du temps prend la forme :

$$\int_{V_t} (\partial_t \rho + \operatorname{div}(\rho u)) \mathrm{d}x = 0.$$

Cette équation devant être vérifiée pour tout volume V_t, on en déduit l'équation de conservation de la masse dite aussi équation de continuité :

$$\partial_t \rho + \operatorname{div}(\rho u) = 0, \tag{A.8}$$

en tout point de Ω_t.

On écrit ensuite l'égalité entre la variation de quantité de mouvement et la puissance des forces qui s'exercent sur un volume en mouvement. C'est ici que l'on distingue force externe volumique f, forces externes surfaciques f et forces internes qui, comme le montre l'équation (A.1), sont de nature surfacique. On obtient alors, de la même façon que précédemment, l'équation suivante :

$$\partial_t(\rho u) + \operatorname{div}(\rho u \otimes u) = f + \operatorname{div}\sigma. \tag{A.9}$$

C'est la forme la plus générale de l'équation de conservation de la quantité de mouvement (parfois appelée très abusivement équation des moments). En général il faut ensuite ajouter une équation thermodynamique sur l'entropie du système mais nous n'évoquerons que des système isothermes.

Dans la suite, sauf mention explicite du contraire, nous nous limiterons au cas où ρ est une constante (arbitrairement fixée à 1). Dans ce cas, on déduit de (A.8) que le champ de vitesse u vérifie la condition d'incompressibilité $\operatorname{div} u = 0$.

A.3 Matériaux simples : lois linéaires

Résoudre les équations de la mécanique revient à chercher les inconnues ρ et u des équations (A.8) et (A.9), ce qui requiert évidemment de connaître f et σ. Le terme f peut être considéré comme connu puisqu'il s'agit de la

densité de forces extérieures mais nous devons expliciter ce que vaut σ en fonction de (ρ, u), ce qui revient à déterminer une équation constitutive pour le matériau. Trouver des lois constitutives de matériaux est l'objet de la rhéologie.

A.3.1 Le cisaillement simple

En rhéologie, il y a un type d'écoulement qui a une très grande importance dans la pratique : l'écoulement en cisaillement simple. Il y a écoulement en cisaillement simple lorsque le champ de vitesse du matériau a, dans un repère orthonormé, la forme $u(t,x,y,z) = (\dot{\gamma}(t)y, 0, 0)$; dans cette expression, $\dot{\gamma}(t)$ s'appelle le taux de cisaillement. Dans ce cas, il est naturel de supposer par symétrie que toutes les quantités physiques en jeu ne dépendent ni de x ni de z. Le tenseur des taux de déformations a alors l'expression très simple :

$$2D(\nabla u) = \dot{\gamma}(t) \begin{pmatrix} 0 & 1 & 0 \\ 1 & 0 & 0 \\ 0 & 0 & 0 \end{pmatrix} \tag{A.10}$$

La quantité γ est naturellement appelé cisaillement.

En supposant qu'il n'y a pas de forces extérieures, l'équation de conservation de la quantité de mouvement se réduit à l'équation différentielle :

$$\ddot{\gamma} y = \partial_y \sigma_{12}. \tag{A.11}$$

Ainsi lorsque l'on se restreint à l'étude des écoulements en cisaillement simple, on peut se contenter de ne donner que la loi constitutive de σ_{12} qui, souvent, prend alors abusivement le nom de contrainte (ou de contrainte scalaire) et nous la noterons comme c'est l'habitude σ.

Les écoulements en cisaillement simple sont particulièrement étudiés car il est très facile de les mettre en place expérimentalement dans ce que l'on appelle les rhéomètres.

A.3.2 Lois élémentaires de rhéologie

La modélisation des matériaux continus commence à la fin du XVII^e siècle avec les travaux de Newton en mécanique des fluides et de Hooke en élasticité des solides. Ces deux savants laisseront leur nom aux toutes premières et néanmoins fondamentales lois constitutives de matériau : on parle de fluide newtonien et de solide hookéen. La loi de Hooke met en relation la contrainte σ avec le cisaillemen γ au moyen d'une constante de proportionnalité G appelé *module d'élasticité* :

$$\sigma = G\gamma. \tag{A.12}$$

On visualise cette loi dans un diagramme (γ, σ) ou dans un diagramme (t, σ) en supposant $\dot{\gamma}$ constant.

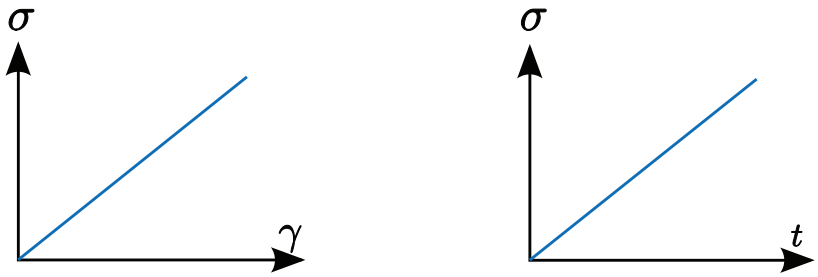

Courbe de réponse — Courbe d'écoulement à $\dot{\gamma}$ fixé

FIG. A.1: Description de la loi de Hooke

La loi de Newton, quant à elle, met en relation la contrainte avec le taux de déformation $\dot{\gamma}$ au moyen d'une constante de proportionnalité η appelée *viscosité* de cisaillement :

$$\sigma = \eta\dot{\gamma}. \tag{A.13}$$

On visualise cette loi dans un diagramme $(\dot{\gamma}, \sigma)$ (appelé courbe de flot) ou, de nouveau, dans un diagramme (t, σ) dans la figure A.2.

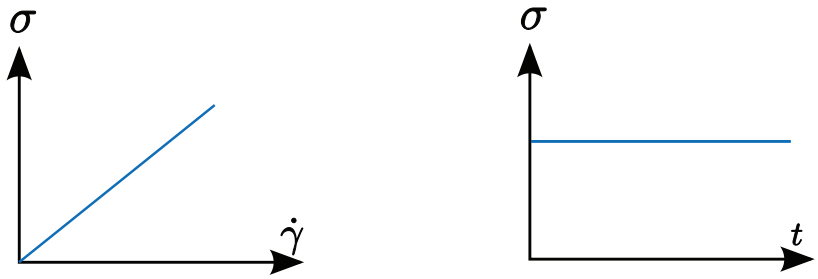

Courbe de flot — Courbe d'écoulement à $\dot{\gamma}$ fixé

FIG. A.2: Description de la loi de Newton

Leurs travaux seront améliorés par la suite, notamment au XIX^e siècle, par Navier pour l'élasticité et par Navier et Stokes en mécanique des fluides, ce qui aboutira par exemple à l'équation fondamentale de la mécanique des fluides, l'équation de Navier-Stokes. Cette équation, bien qu'étant en un sens

la plus simple que l'on puisse écrire pour un fluide, est encore loin d'avoir livré tous ses secrets, comme le rappelle l'existence d'un prix du millénaire pour qui arrivera à démontrer le caractère globalement bien posé des solutions de cette équation.

Malgré les grands services que peuvent rendre les deux modèles précités, on s'est rendu compte que les modèles de Hooke et de Newton ne rendaient pas compte de tous les comportements observables des matériaux. Tout d'abord Maxwell a réalisé à la fin du XIX^e siècle que la distinction entre solide élastique d'une part et fluide visqueux de l'autre n'était pas aussi nette qu'on pouvait le penser et, même, que tous les fluides tenaient des deux formes simultanément : c'est le concept de fluide *viscoélastique*. Maxwell introduit à cette occasion une échelle caractéristique de temps T_0 au-dessous de laquelle le comportement est élastique et au-dessus de laquelle il est fluide. Ce modèle prend alors la forme suivante :

$$T_0\dot{\sigma} + \sigma = \eta\dot{\gamma}. \tag{A.14}$$

Comme on peut le voir sur la figure A.3, le matériau répond comme un solide de Hooke pour des temps courts de l'ordre de T_0, puis adopte le comportement d'une fluide de Newton aux temps longs.

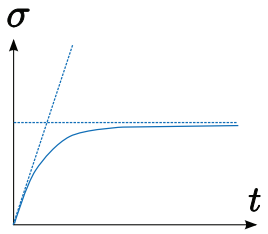

FIG. A.3: Courbe d'écoulement à $\dot{\gamma}$ fixé

Dans l'eau, ce temps caractéristique T_0 est de l'ordre de $10^{-12}s$, ce qui fait qu'on n'observera jamais le comportement élastique de l'eau. En revanche, la glace a, elle, un temps caractéristique de $10^4 s$ ce qui explique que l'on peut marcher sur les glaciers (car un pas ne dure que quelques secondes – une durée très inférieure au temps caractéristique) mais que les glaciers s'écoulent aussi sur les temps longs (créant les vallées glaciaires). Parallèlement, il existe des matériaux qui se comporteront comme des fluides aux temps courts et des solides élastiques aux temps longs (modèle de Kelvin-Voigt) :

$$\sigma = G(\gamma + T_0\dot{\gamma}). \tag{A.15}$$

Notons que cette loi peut se décrire comme une décomposition additive de la contrainte en une partie élastique $G\Gamma$ et une partie fluide $GT_0\dot{\gamma}$.

La viscoélasticité montre que certaines propriétés des matériaux sont d'origine dynamique. Par conséquent, s'intéresser uniquement à des régimes stationnaires peut faire perdre de l'information. Elle met aussi en évidence à quel point la notion d'échelle est centrale. Néanmoins ces effets peuvent toujours être décrits à l'aide de lois constitutives linéaires (les équations de Navier-Stokes sont non-linéaires mais la loi constitutive sous-jacente de Newton est bel et bien une loi linéaire ; l'effet non-linéaire a une origine cinétique).

De nombreux autres modèles linéaires peuvent être construits pour rendre compte de la viscoélasticité, parmi lesquel citons le modèle de Jeffreys

$$T_0\dot{\sigma} + \sigma = \eta(T_1\ddot{\gamma} + \dot{\gamma}), \tag{A.16}$$

dont l'une des généralisations multidimensionnelles est l'un des modèles les plus connus dans le domaine des fluides complexes, le modèle d'Oldroyd-B (A.51).

Dans la suite, nous parlerons de fluide lorsque, pour un taux de cisaillement donné, le matériau subit une contrainte donnée et nous parlerons de solide (sous-entendu élastique) lorsque, pour un cisaillement donné, la contrainte est fixée.

A.4 Matériaux complexes : lois non linéaires

D'autres effets intéressants et assez communs sont en revanche de nature non linéaire.

A.4.1 Rhéofluidification et rhéoépaississement

Si l'on considère simplement une loi $\sigma = \sigma(\dot{\gamma})$, nous obtenons une loi de fluide complexe. Nous pouvons choisir de la voir comme $\sigma = \eta(\dot{\gamma})\dot{\gamma}$ c'est-à-dire comme un fluide quasi newtonien dont la viscosité dépendrait du taux de cisaillement vu par le fluide. On obtient ainsi deux types de comportements, la *rhéofluidification* lorsque $\eta(\dot{\gamma})$ diminue, et le *rhéoépaississement* dans le cas contraire d'une viscosité qui croît. Les fluides très complexes peuvent avoir un comportement rhéofluidifiant dans certaines gammes de taux de cisaillement et rhéoépaississant dans d'autres (par exemple, le sang).

Une classe de modèle pour les fluides rhéofluidifiants/rhéoépaississants est donnée par les lois de puissances $\eta(\dot{\gamma}) = A\dot{\gamma}^{n-1}$: lorsque $n < 1$ le fluide est rhéofluidifiant alors que si $n > 1$ le fluide est rhéoépaississant.

A.4.2 Effet de seuil

Un autre effet typiquement non linéaire est l'effet de *seuil* tel que mis en évidence par Bingham au début du XX^e siècle. Il a remarqué que certains fluides ne s'écoulaient pas tant qu'ils n'étaient pas suffisamment forcés. C'est un effet analogue au frottement de Coulomb entre deux solides. Au-delà de cette contrainte seuil σ_c, le fluide peut s'écouler à l'aide d'une loi linéaire et on obtient la loi de Bingham :

$$\begin{aligned} &|\sigma| \leq \sigma_c, \quad \dot{\gamma} = 0, \\ &\dot{\gamma} \neq 0, \qquad \sigma = \eta\dot{\gamma} + \sigma_c. \end{aligned} \tag{A.17}$$

La courbe de flot d'un tel fluide est donnée figure A.4.

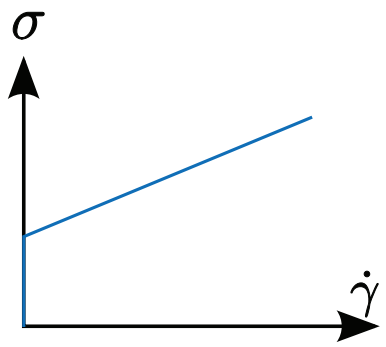

FIG. A.4: Courbe de flot du modèle de Bingham

On peut aussi coupler l'effet de seuil avec des comportements de lois de puissance : on obtient alors les modèles d'Herschel-Bulkley,

$$\begin{cases} \dot{\gamma} = 0, & \sigma \leq \sigma_0 \\ \sigma = \sigma_0 + A\dot{\gamma}^n, & \dot{\gamma} > 0 \end{cases} \tag{A.18}$$

dont on peut voir les courbes de flots figure A.5.

Nous devons faire deux remarques sur les modèles à seuil. Tout d'abord, il faut bien comprendre que la branche verticale au dessus de $\dot{\gamma} = 0$ fait partie intégrante de la courbe de flot ; la loi de comportement est bel et bien multivaluée. La contrainte n'est pas uniquement définie tant que le fluide ne s'écoule pas : c'est un comportement parfaitement rigide. Ainsi le matériau peut passer brusquement d'un comportement de solide rigide à celui de fluide : c'est un comportement idéalisé et en pratique le fluide réagit élastiquement plutôt que de façon rigide.

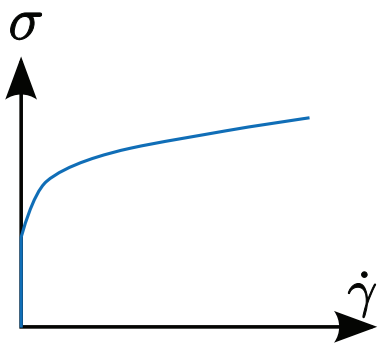

FIG. A.5: Courbe de flot d'un modèle d'Herschel-Bulkley

La deuxième remarque est que la notion de seuil n'est définie qu'à la précision des appareils de mesures. Expérimentalement, il n'est pas possible descendre en dessous d'un certain taux de cisaillement minimal non nul (ce que nous pourrions appeler la résolution de l'appareil). Par conséquent, il est impossible en pratique de distinguer un fluide à seuil d'un fluide à très forte viscosité (mais finie) à faible cisaillement.

Comme exemples de fluide à seuil, on peut citer le dentifrice et la peinture. Notons que l'effet de seuil peut être nuisible comme bénéfique. Il est par exemple plus coûteux de faire s'écouler un fluide à seuil dans un tuyau puisqu'il faut lui appliquer une contrainte plus forte que pour un fluide sans seuil. En revanche, il est heureux que la peinture soit un fluide à seuil car on peut l'appliquer sur un mur en la cisaillant d'un coup de pinceau, mais le cisaillement naturel imposé par la force de gravitation ne la fait pas couler.

A.5 Écoulements généraux de fluides

Dans cette dernière section nous ne considèrerons que des fluides complexes.

A.5.1 Changement de référentiels

Nous allons nous intéresser dans cette section au principe d'objectivité qui pose que les lois de comportement doivent être indépendantes du référentiel dans lequel on les écrit. Ainsi le comportement d'un matériau donné sera observé de la même façon par tous les observateurs.

Supposons que, dans un référentiel de référence, un point ait les coordonnées x et que, dans un référentiel en mouvement par rapport au référentiel

de référence, le même point ait les coordonnées x^*. On déduit x^* de x par un mouvement rigide, c'est-à-dire par la composée d'une rotation Q qui dépend du temps et d'une translation a (qui dépend aussi du temps) :

$$x^* = \Psi_t(x) = a(t) + Q(t)x. \tag{A.19}$$

Par conséquent, si dans le référentiel de référence le matériau a un mouvement donné par $(\phi_t)_{t\geq>0}$, dans le référentiel en mouvement il aura le mouvement donné par la famille

$$\phi_t^*(X) = \psi(t, \phi_t(X)), \tag{A.20}$$

où on a supposé, pour simplifier, que $\Psi_0 = Id$. Exprimons maintenant le champ de vitesse dans le référentiel en mouvement :

$$u^*(t, x^*) = \dot{a}(t) + \dot{Q}(t)\Psi_t^{-1}(x^*) + Q(t)u(t, \Psi_t^{-1}(x^*)). \tag{A.21}$$

Nous en déduisons que nous avons la relation

$$\mathrm{d}_{x^*}u^*(t, x^*) = \dot{Q}(t)Q(t)^T + Q(t)\partial_x u(t, \Psi_t^{-1}(x^*))Q(t)^T, \tag{A.22}$$

dont nous déduisons la relation entre les tenseurs des taux de déformations :

$$\begin{aligned} 2D(\nabla_{x^*}u^*) &= \dot{Q}(t)Q(t)^T + Q(t)\dot{Q}(t)^T + 2Q(t)D(\nabla_x u(t, \Psi_t^{-1}(x^*))Q(t)^T \\ &= (Q(t)Q(t)^T)' + 2Q(t)D(\nabla_x u(t, \Psi_t^{-1}(x^*))Q(t)^T \\ &= 2Q(t)D(\nabla_x u(t, \Psi_t^{-1}(x^*))Q(t)^T, \end{aligned} \tag{A.23}$$

puisque, $Q(t)$ étant une matrice de rotation, on a $Q(t)Q(t)^T = Id$ pour tout t.

Étudions maintenant l'effet d'un changement de référentiel sur le tenseur des contraintes. On s'appuie pour cela sur la notion de puissance des forces internes : la puissance instantanée qu'exerce les forces internes à l'intérieur d'une partie $\mathcal{O}$ dans le référentiel de référence est donnée par la formule

$$\mathcal{P}(\mathcal{O}, u) = \int_{\mathcal{O}} \sigma(t, x) : D(\nabla_x u)(t, x)\mathrm{d}x, \tag{A.24}$$

et dans le référentiel en mouvement par

$$\mathcal{P}^*(\mathcal{O}^*, u^*) = \int_{\mathcal{O}^*} \sigma^*(t, x^*) : D(\nabla_{x^*}u^*)(t, x^*)\mathrm{d}x^*, \tag{A.25}$$

où l'on a évidemment noté $\mathcal{O}^* = \Psi(t, \mathcal{O})$ et σ^* le tenseur des contrainte du matériau dans le référentiel en mouvement. Dans ces formules nous avons noté ":" le produit scalaire des tenseurs symétriques qui a pour définition

$$A : B = Tr(AB).$$

Nous écrivons maintenant que, d'après le principe d'objectivité, nous devons avoir $\mathcal{P}(\mathcal{O}, u) = \mathcal{P}^*(\mathcal{O}^*, u^*)$. D'autre part, en faisant un changement dans l'intégrale, nous obtenons :

$$\begin{aligned}\mathcal{P}^*(\mathcal{O}^*, u^*) &= \int_{\mathcal{O}^*} \sigma^*(t, x^*) : D(\nabla_{x^*} u^*)(t, x^*) \mathrm{d}x^* \\ &= \int_{\mathcal{O}} \sigma^*(t, \Psi_t(x)) : D(\nabla_{x^*} u^*)(t, \psi(t, x)) \mathrm{d}x\end{aligned}$$

car ψ_t préserve le volume

$$\begin{aligned}&= \int_{\mathcal{O}} \sigma^*(t, \Psi_t(x)) : Q(t) D(\nabla_x u)(t, x) Q(t)^T \mathrm{d}x \text{ d'après (A.23)} \\ &= \int_{\mathcal{O}} Tr(\sigma^*(t, \Psi_t(x))^T Q(t) D(\nabla_x u)(t, x) Q(t)^T) \mathrm{d}x \\ &= \int_{\mathcal{O}} Tr(Q(t)^T \sigma^*(t, \Psi_t(x)) Q(t) D(\nabla_x u)(t, x)) \mathrm{d}x.\end{aligned} \tag{A.26}$$

Ainsi nous obtenons,

$$\sigma(t, x) = Q(t)^T \sigma^*(t, \Psi_t(x)) Q(t), \tag{A.27}$$

ou de manière équivalente

$$\sigma^*(t, x^*) = Q(t) \sigma(t, \Psi_t^{-1}(x^*)) Q(t)^T. \tag{A.28}$$

A.5.2 Version tensorielle des lois de Newton et Hooke

Pour obtenir la forme tensorielle des deux lois élémentaires (A.12) et (A.13) on généralise l'idée que :

- dans le cas des solides élastiques simples, le tenseur des contraintes est linéaire par rapport aux déformations,
- dans le cas des fluides simples, le tenseur des contraintes est linéaire par rapport au taux de déformation.

Cas des fluides

Commençons par la loi de Newton. Pour les fluides, d'une manière générale, on décompose le tenseur des contraintes sous la forme

$$\sigma = -\pi_h \, Id + \widetilde{\sigma}, \tag{A.29}$$

où π_h désigne ce que l'on appelle en général la *pression hydrostatique*. Il existe parfois une certaine ambiguïté dans la définition de la pression, donc précisons quel sens nous donnons à la décomposition (A.29) : pour nous $\widetilde{\sigma}$ n'est pas nécessairement à trace nulle. Quel est l'intérêt alors de distinguer une partie diagonale au tenseur des contraintes ? L'important, pour nous, est que, d'une part, π_h ne dépend pas du champ de vitesse eulérien u, et que, d'autre part, $\widetilde{\sigma}$ doit être nul lorsque le champ de vitesse u est constant (donc nul à un changement de référentiel galliléen près). Ce que nous disons, en imposant *a priori* la décomposition (A.29), c'est que, lorsque le fluide est au repos, le champ de force interne s'exerce de façon normale ($T(x,n)//n$) ou autrement dit, qu'il n'existe pas de frottement tangentiel entre deux sous-parties du fluide en contact.

Nous prolongeons alors la loi de Newton (A.13) en imposant d'abord que $\widetilde{\sigma}$ soit linéaire en fonction du taux de déformation $D(\nabla u)$ (puisque $D(\nabla u)$ est comme nous l'avons dit la généralisation naturelle de $\dot{\gamma}$). Écrire une relation linéaire entre le tenseur des contraintes σ et le tenseur des taux de déformation c'est écrire que chaque coefficient $\widetilde{\sigma}_{ij}$ de $\widetilde{\sigma}$ s'écrit comme une combinaison linéaire des coefficients A_{kl} de $D(\nabla u)$. Il existe donc *a priori* des coefficients η_{ij}^{kl} (formant ce qu'on peut appeler un tenseur de viscosité) tels que :

$$\forall i,j \qquad \sigma_{ij} = \sum_{k,l} \eta_{ij}^{kl} A_{kl}. \tag{A.30}$$

On voit donc qu'en toute généralité, il existe en fait 81 viscosités pour un fluide. On peut réduire ce nombre en remarquant que $\widetilde{\sigma}$ et A sont des tenseurs symétriques ce qui implique, par conséquent, que l'on a $\eta_{ij}^{kl} = \eta_{ij}^{lk}$ et $\eta_{ij}^{kl} = \eta_{ji}^{kl}$ ce qui laisse tout de même 36 coefficients. Nous rajoutons alors l'hypothèse que le fluide est isotrope, ce qui signifie que son groupe de symétrie est le groupe de toutes les rotations de l'espace : on peut tourner un échantillon de fluide isotrope dans tous les sens sans arriver à en distinguer des propriétés différentes. En faisant cette hypothèse et en exploitant ces nouvelles symétries, on réduit le nombre de viscosités à seulement deux, que nous notons μ et λ et l'équation (A.30) se réécrit de façon compacte :

$$\widetilde{\sigma} = 2\mu D(\nabla u) + \lambda Tr(D(\nabla u))\, Id = 2\mu D(\nabla u) + \lambda(\operatorname{div} u)\, Id. \tag{A.31}$$

En utilisant (A.29) et (A.32) on obtient le tenseur des contraintes complet :

$$\sigma = (-\pi_h + \lambda(\operatorname{div} u))\, Id + 2\mu D(\nabla u). \tag{A.32}$$

Notons que dans cette équation, π_h, μ et λ sont des coefficients qui ne dépendent que de la densité de masse ρ. Lorsque l'équation (A.32) est couplée avec les équations (A.8) et (A.9), on obtient le célèbre système de Navier-Stokes compressible (barotrope car on ne prend pas en compte la température).

Cas des solides élastiques

Intéressons-nous maintenant à la loi de Hooke. Nous devons écrire une loi linéaire entre le tenseur des contraintes et le tenseur de déformation. Dans la loi de Hooke, c'est la propriété de linéarité qui prédomine et nous choisissons comme tenseur des déformations le tenseur des petites déformations ε. Ajoutons de nouveau la propriété d'isotropie pour le matériau et nous obtenons la loi de Hooke généralisée :

$$\sigma(t, X) = 2\mu D(\nabla_X \xi) + \lambda \nabla_X \xi, \tag{A.33}$$

où λ et μ sont les coefficients de Lamé du matériau.

A.5.3 Dérivées temporelles objectives

Après avoir expliqué comment les changements de référentiels affectaient les quantités mécaniques comme le champ de vitesse et le tenseur des contraintes, nous allons montrer comment ils affectent les équations constitutives elles-mêmes sur l'exemple du modèle de Maxwell.

Considérons l'équation différentielle (A.14) définissant le modèle de viscoélasticité de Maxwell en cisaillement simple et essayons de voir si nous pouvons écrire un modèle semblable qui soit valable quelle que soit la forme du champ de vitesse u. Le plus simple semble, d'une part, de remplacer la contrainte de cisaillement par le tenseur des contraintes lui-même et, d'autre part, de remplacer le taux de cisaillement par le tenseur des taux de déformations complet $2D(\nabla_x u)$. Le cisaillement simple supprimant le terme de convection pour des raisons géométriques, nous le rajoutons pour les flots généraux. Ainsi, nous pourrions tenter de généraliser le modèle de Maxwell à l'aide du modèle différentiel donné par l'équation :

$$T_0(\partial_t \sigma + u \cdot \nabla \sigma) + \sigma = 2\eta D(\nabla_x u). \tag{A.34}$$

Par le principe d'objectivité, la loi constitutive doit être la même dans le référentiel en mouvement. Observons pourtant comment (A.34) se transforme sous l'effet du changement de référentiel :

$$\partial_t \sigma^* = \dot{Q}\sigma Q^T + Q\sigma\dot{Q}^T + Q(\partial_t\sigma + (\dot{Q}^T(x^* - a) - Q^T\dot{a}) \cdot \nabla_x \sigma)Q^T, \quad \text{(A.35)}$$

$$u^* \cdot \nabla_{x^*}\sigma^* = Q((Q^T\dot{a} + Q^T\dot{Q}Q^T(x^* - a) + u) \cdot \nabla\sigma)Q^T, \quad \text{(A.36)}$$

$$\partial_t \sigma^* + u^* \cdot \nabla_{x^*}\sigma^* = \dot{Q}\sigma Q^T + Q\sigma\dot{Q}^T + Q(\partial_t\sigma + u \cdot \nabla\sigma)Q^T. \quad \text{(A.37)}$$

Nous avons utilisé

$$Q^T\dot{Q}Q^T = -Q^TQ\dot{Q}^T = -\dot{Q}^T, \quad \text{(A.38)}$$

pour simplifier (A.37).

Nous voyons donc que, si on a (A.34) dans le référentiel de référence, nous avons en fait

$$T_0(\partial_t\sigma^* + u^* \cdot \nabla_{x^*}\sigma^*) + \sigma^* = 2\eta D(\nabla_{x^*}u^*) + \dot{Q}Q^T\sigma^* + \sigma^*Q\dot{Q}^T, \quad \text{(A.39)}$$

dans le référentiel en mouvement. L'équation constitutive n'est pas invariante par changement de référentiel, ce n'est donc pas une équation acceptable pour un modèle physique.

Pour se sortir de cette impasse, une manière de procéder est de passer par la forme intégrale de (A.14) : pour écrire la contrainte en fonction du taux de cisaillement, nous devons résoudre l'équation différentielle et nous obtenons (en posant $G = \eta/T_0$) :

$$\sigma = \int_{-\infty}^{t} G \exp\left(-\frac{t-t'}{T_0}\right)\dot{\gamma}(t')\mathrm{d}t'. \quad \text{(A.40)}$$

Dans cette intégrale, on voit apparaître $\dot{\gamma}(t')\mathrm{d}t'$ qui est le cisaillement infinitésimal au temps t'. Si nous intégrons par parties, nous pouvons faire apparaître le cisaillement relatif à deux instants $\gamma(t,t') = 1/2\int_{t'}^{t}\dot{\gamma}(t'')\mathrm{d}t''$. On obtient alors

$$\sigma = 2\eta\int_{-\infty}^{t}\exp\left(-\frac{t-t'}{T_0}\right)\gamma(t,t')\mathrm{d}t'. \quad \text{(A.41)}$$

Puisque $\gamma(t,t')$ est le cisaillement entre les instants t' et t, on peut généraliser l'équation précédente en remplaçant le cisaillement, par exemple par le tenseur de déformation relatif de Finger $H_{t'}$ défini par (A.6). Nous obtenons alors en variables lagrangiennes :

$$\sigma(t,X) = 2\eta \int_{-\infty}^{t} \exp\left(-\frac{t-t'}{T_0}\right) H_{t'}(t,\phi_{t'}(X))\mathrm{d}t'. \tag{A.42}$$

Maintenant nous dérivons cette équation par rapport au temps pour retrouver une formulation différentielle. Pour cela, nous aurons besoin de la dérivée de $F_{t'}(t,x')$ (défini par (A.4)) par rapport à t :

$$\begin{aligned}
\partial_t F_{t'}(t,x') &= \mathrm{d}_{x'}(\dot{\phi}_t \circ \phi_{t'}^{-1})(t,x') \\
&= \mathrm{d}_{x'}(\dot{\phi}_t \circ \phi_t^{-1} \circ \phi_t \circ \phi_{t'}^{-1})(t,x') \\
&= \mathrm{d}_x(\dot{\phi}_t \circ \phi_t^{-1})(t,\phi_t \circ \phi_{t'}^{-1}(x'))\mathrm{d}_{x'}\phi_t \circ \phi_{t'}^{-1})(t,x') \\
&= \mathrm{d}_x u(t,\phi_t \circ \phi_{t'}^{-1}(x'))F_{t'}(t,x'),
\end{aligned} \tag{A.43}$$

où on a utilisé la définition du champ de vitesse eulérien u donnée par (A.2). Ainsi, en utilisant la définition (A.6) du tenseur de Finger, on obtient :

$$\begin{aligned}
\partial_t H_{t'}(t,\phi_t'(X)) &= \frac{1}{2}(\partial_t F_{t'} F_{t'}^T + F_{t'}\partial_t F_{t'}^T) \\
&= \frac{1}{2}((\mathrm{d}_x u)F_{t'}F_{t'}^T + F_{t'}F_{t'}^T(\mathrm{d}_x u)^T) \\
&= (\mathrm{d}_x u)H_{t'} + H_{t'}(\mathrm{d}_x u)^T + \frac{1}{2}\left((\mathrm{d}_x u) + (\mathrm{d}_x u)^T\right) \\
&= (\mathrm{d}_x u)H_{t'} + H_{t'}(\mathrm{d}_x u)^T + D(\nabla_x u).
\end{aligned} \tag{A.44}$$

Maintenant nous pouvons dériver (A.42) par rapport à t et nous obtenons

$$\begin{aligned}
\dot{\sigma}(t,X) = 2\eta H_t(t,\phi_t(X)) - \frac{1}{T_0}\left(2\eta \int_{-\infty}^{t} \exp\left(-\frac{t-t'}{T_0}\right) H_{t'}(t,\phi_{t'}(X))\mathrm{d}t'\right) \\
+ 2\eta \int_{-\infty}^{t} \exp\left(-\frac{t-t'}{T_0}\right) \partial_t H_{t'}(t,\phi_{t'}(X))\mathrm{d}t'
\end{aligned} \tag{A.45}$$

Le premier terme est nul par définition de H et le second vaut $-1/T_0\sigma$.

Ainsi, nous nous apercevons que l'on peut généraliser le modèle de Maxwell en un modèle invariant par changement de référentiel par l'équation suivante :

$$T_0 \overset{\triangledown}{\sigma} + \sigma = 2GD(\nabla_x u), \tag{A.46}$$

où

$$\overset{\triangledown}{\sigma} = \partial_t \sigma + u \cdot \nabla_x \sigma - \nabla_x u \sigma - \sigma(\nabla_x u)^T, \tag{A.47}$$

désigne la dérivée temporelle *surconvectée* du tenseur σ. Pour cette raison, l'équation (A.46) est appelée modèle de Maxwell surconvecté. Ce modèle a été proposé par Oldroyd dans [51]. En fait, Oldroyd a montré qu'il existait plusieurs possibilités pour la généralisation du modèle de Maxwell par le choix d'une bonne dérivée temporelle pour les tenseurs : on peut choisir n'importe quelle dérivée de la forme

$$\frac{\mathcal{D}_a\sigma}{\mathcal{D}t} = \partial_t\sigma + u\cdot\nabla_x\sigma + \sigma W(\nabla u) - W(\nabla u)\sigma - a(D(\nabla u)\sigma + \sigma D(\nabla u)), \quad \text{(A.48)}$$

où l'on note $W(M)$ la partie antisymétrique de la matrice M et où a est un réel compris entre $[-1,1]$. Lorque $a=1$ on retrouve la dérivée surconvectée. Lorsque $a=-1$ on parle de dérivée sous-convectée : c'est le modèle que l'on obtient si on remplace le tenseur de Finger H par le tenseur de Green-Lagrange E dans (A.42). Lorsque $a=0$ on parle de dérivée corotationnelle ou de Jaumann. Pour voir que ces dérivées sont bien invariantes par changement de référentiel il suffit de calculer :

$$\sigma^* W(\nabla_{x^*}u^*) - W(\nabla_{x^*}u^*)\sigma^* = Q(\sigma W(\nabla u) - W(\nabla u)\sigma)Q^T - Q\sigma\dot{Q}^T - \dot{Q}\sigma Q^T, \quad \text{(A.49)}$$

$$D(\nabla_{x^*}u^*)\sigma^* + \sigma^* D(\nabla_{x^*}u^*) = Q(D(\nabla u)\sigma + \sigma D(\nabla u))Q^T. \quad \text{(A.50)}$$

La restriction sur a vient d'un changement de type : l'équation perd son hyperbolicité lorsque $|a|>1$ ce qui empêche de résoudre le problème de Cauchy (voir Joseph, Renardy et Saut [41]).

Comme nous l'avons annoncé précédemment, le modèle de Jeffreys (A.16) peut se généraliser de la même façon que le modèle de Maxwell. En utilisant la dérivée surconvectée, on obtient le célèbre modèle d'Oldroyd-B, très utilisé dans le domaine des polymères dilués et dans l'étude des bandes de cisaillement :

$$T_0\overset{\triangledown}{\sigma} + \sigma = 2\eta(T_1 D(\overset{\triangledown}{\nabla}_x u) + D(\nabla_x u)). \quad \text{(A.51)}$$

A.6 Quelques mots sur les fluides vitreux

La majeure partie de cette thèse étant consacrée à l'étude d'un modèle pour les matériaux vitreux mous, présentons-les rapidement. Nous renvoyons notamment aux thèses de Gati [31], Hébraud [36] et Goyon [33] pour de plus amples informations.

A.6.1 La transition vitreuse

On apprend très tôt que la matière se trouve sous trois états : solide, liquide ou gazeux. On apprend ensuite que les solides sont constitués d'atomes ou de molécules disposés sur un réseau (dit cristallin) alors que, dans les liquides, les molécules sont très libres, et s'agitent dans tous les sens, d'autant plus vite que la température est élevée. Il faut alors réaliser que, lorsqu'on refroidit un liquide, non seulement les molécules ralentissent, mais surtout elles s'ordonnent. On dit que les molécules gagnent un ordre de position. Contrairement à ce qu'on pourrait croire, les molécules ne font donc pas que ralentir «sur place» sans se préoccuper de leur environnement.

Il arrive pourtant que ce soit le cas. Dans certains processus de refroidissement, la dynamique moléculaire ralentit sans pour autant que les molécules ne s'ordonnent les unes par rapport aux autres. Le matériau a alors la structure microscopique d'un liquide mais s'écoule infiniment lentement à mesure que sa viscosité devient de plus en plus grande : à l'œil nu, il semble que, bien que fluide, le matériau ne s'écoule pas. Puisque de tels matériaux ne s'écoulent pas, on les considère comme solides mais, à cause de l'absence de structure cristalline, ce sont des solides amorphes. Les matériaux qui peuvent subir ces processus sont appelés verres. La figure A.6 décrit ce phénomène de transition vitreuse par rapport à un phénomène de cristallisation dans un diagramme température/énergie et dans un diagramme température/temps de relaxation.

Thermodynamiquement, les verres (en dessous de la température de transition vitreuse) sont piégés dans des états métastables d'énergie libre. Le temps de relaxation est devenu tellement grand qu'ils évoluent très lentement (on dit qu'ils vieillissent). À cause de leur absence de structure, on dit souvent que le matériau évolue dans un «paysage d'énergie libre» particulièrement chaotique avec de nombreux puits de potentiel et des barrières d'énergies petites et grandes.

A.6.2 Modèle de piège

Pour modéliser cette situation extrêmement complexe, Bouchaud, Comtet et Monthus ont proposé dans [11] de ne pas décrire l'intégralité du paysage d'énergie libre, mais de ne considérer que la distribution statistique des barrières d'énergie. Dans une approche de champ moyen, le système est décrit par la probabilité de se trouver dans un puits de profondeur énergétique e à l'instant t. Cette évolution se fait alors par l'équation suivante :

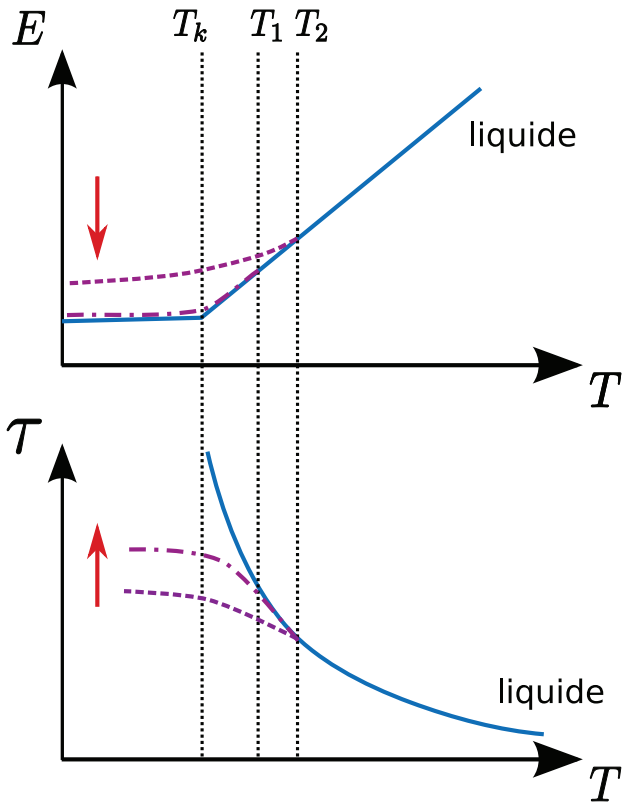

FIG. A.6: Refroidissement d'après J. Kurchan. Les flèches rouges indiquent l'évolution du matériau à basse température

$$\begin{aligned} \partial_t P(t,e) &= -\Gamma_0 \exp\left(-\frac{e}{x}\right) P(t,e) + \Gamma(t)\rho(e), \\ \Gamma(t) &= \Gamma_0 \int_{e\geq 0} \exp\left(-\frac{e}{x}\right) P(t,e)\mathrm{d}e. \end{aligned} \tag{A.52}$$

Dans le système (A.52), $\rho(e)$ est la distribution de barrière de potentiel et x est un paramètre qui joue le rôle d'une température (penser $x = k_b T$ où k_b est la constante de Boltzmann). Le premier terme décrit la possibilité pour le système de sortir de l'état e avec un temps de relaxation $1/\Gamma_0 \exp(e/x)$ tandis que le second terme décrit une répartition après franchissement de barrière avec une distribution ρ. Ce que BOUCHAUD *et al.* ont remarqué, c'est que lorsque la distribution de piège ρ était exponentielle de paramètre x_0, le système voyait bel et bien une transition vitreuse. On peut s'en rendre compte en essayant de calculer l'état d'équilibre du système, théoriquement

donné par

$$P_{\text{eq}}(e) = \frac{\Gamma_{\text{eq}}}{\Gamma_0} \exp\left(\frac{e}{x}\right) \rho(e), \tag{A.53}$$

où Γ_{eq} garantit que P_{eq} est d'intégrale 1. Lorsque $\rho(e) = x_0 \exp(-e/x_0)$, on voit que pour $x < x_0$ il n'y a en fait pas d'équilibre et le système évolue sans jamais s'arrêter tandis que lorsque $x > x_0$ un équilibre existe. On voit, d'autre part, que lorsque $x < x_0$ avec x s'appprochant de x_0 la distribution devient de plus en plus étalée et les puits de grandes profondeurs deviennent de plus en plus fréquents, piégant de plus en plus le système et ralentissant la dynamique.

A.6.3 Matériaux vitreux mous

C'est par analogie avec ce phénomène de transition vitreuse que Sollich, Cates, Lequeux, Hébraud et Cates ont conçu le modèle SGR pour les matériaux vitreux mous [68]. L'importance de cet article réside beaucoup dans l'unification qu'il fait de comportements qui apparaissent dans des matériaux très variés par analogie avec les verres. Les matériaux vitreux mous sont en général des dispersions, c'est-à-dire des matériaux composés d'un liquide newtonien qui contient des particules, solides (suspensions), liquides (emulsions) ou gazeuses (mousses). Notons que les matériaux granulaires (particules solides dans un gaz, en général l'air) partagent aussi certains comportements avec les matériaux vitreux mous.

Dans les matériaux vitreux mous (ou amorphes), ce sont les particules dispersées qui jouent le rôle des molécules en désordre. La température est alors liée à la concentration en particule. Lorsque la concentration est faible, les particules sont très libres de se mouvoir et leur influence se fait peu sentir : le matériau est presque newtonien. En revanche, lorsque la concentration est très élevée, les particules se gênent et une particule se retrouve piégée par ses voisines : avant que le matériau ne s'écoule, il faut entrer suffisamment d'énergie pour pouvoir briser les liens entre particules et le matériau est un fluide à seuil. Le fluide subit donc une transition en fonction de sa concentration comme résumé sur la figure A.7.

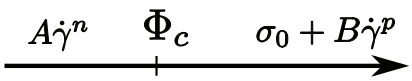

Fig. A.7: Transition vitreuse pour les matériaux vitreux mous

On peut décrire assez généralement le comportement microscopique d'un matériau amorphe. Parce qu'une particule est localement piégée par ses voisines, lorsqu'un élément de fluide est soumis à une contrainte externe, il commence par absorber élastiquement cette contrainte (par exemple en déformant les particules). Lorsque la limite d'élasticité est atteinte, les liens entre les particules vont se briser localement et se disposer différemment (on parle de réarrangement). Dans ce processus, la contrainte locale va pouvoir diminuer car le matériau trouve une configuration plus avantageuse. En revanche, les réarrangements créent un «bruit» mécanique qui va influer sur la contrainte des éléments voisins. Les trois comportements principaux possibles sont donc : déformation élastique, relaxation locale, bruit global.

A.6.4 Modèle SGR – modèle d'Hébraud-Lequeux

Sollich *et al.* ont proposé un modèle pour un matériau amorphe idéalisé basé sur celui de Bouchaud. Dans ce modèle, le système est décrit par sa distribution statistique d'energie libre, mais aussi de déformation possible $P(E, l, t)$:

$$\partial_t P = -\dot{\gamma}\partial_l P - \Gamma_0 \exp\left(-\frac{E - 1/2kl^2}{x}\right) P + \Gamma(t)\rho(E)\delta_0(l). \tag{A.54}$$

Le premier terme traduit la déformation élastique du système en augmentant l en fonction de la déformation locale. Le second terme est semblable à celui de (A.52) à la différence que cette barrière est réduite du fait de l'énergie élastique stockée $1/2kl^2$. Enfin, une fois la barrière d'énergie franchie, la déformation élastique relaxe vers 0 (à cause de la masse de Dirac en 0, $\delta_0(l)$) tandis que le système choisit une énergie suivant la distribution $\rho(E)$. Ce modèle prédit bien une transition vitreuse lorsque la distribution de puits est exponentielle.

Les modèles de Bouchaud *et al.* ou Sollich *et al.* s'appuient tous deux sur le paramètre x pour contrôler la transition vitreuse. Ainsi, le niveau de bruit est fixé grâce à un paramètre *ad hoc*. Or, dans les matériaux amorphes, le bruit est lié aux réarrangements et n'est donc pas connu *a priori* mais dépend de l'état du matériau lui-même.

C'est pourquoi Hébraud et Lequeux ont proposé un nouveau modèle dans [37], inspiré par le modèle SGR mais dans lequel le bruit mécanique est effectivement corrélé à l'état du système : le bruit mécanique est directement lié aux réarrangements qui surviennent dans le système (on parle de modèle *autoconsistant*). Le modèle est gouverné par l'équation cinétique suivante :

$$\partial_t p = -G_0\dot{\gamma}(t)\partial_\sigma p - \frac{1}{T_0}\mathbf{1}_{\mathbf{R}\setminus[-\sigma_c,\sigma_c]}p + \Gamma(t)\delta_0(\sigma) + \alpha\Gamma(t)\partial_{\sigma\sigma}p. \qquad \text{(A.55)}$$

Une description détaillée de ce modèle se trouve au chapitre 2.

Bibliographie

[1] Shmuel Agmon, Avron Douglis, and Louis Nirenberg. Estimates near the boundary for solutions of elliptic partial differential equations satisfying general boundary conditions. I. *Comm. Pure Appl. Math.*, 12 :623–727, 1959.

[2] Philippe Angot, Charles-Henri Bruneau, and Pierre Fabrie. A penalization method to take into account obstacles in incompressible viscous flows. *Numer. Math.*, 81(4) :497–520, 1999.

[3] Anton Arnold, José A. Carrillo, and Chiara Manzini. Refined long-time asymptotics for some polymeric fluid flow models. *Commun. Math. Sci.*, 8(3) :763–782, 2010.

[4] Jacob Bear and Didier Bresch. Modelling the transport of carbonic species through the human skin. part i : Conceptual and mathematical modelling. Personal communication to the author.

[5] Mohamed Ben Alaya and Benjamin Jourdain. Probabilistic approximation of a nonlinear parabolic equation occurring in rheology. *J. Appl. Probab.*, 44(2) :528–546, 2007.

[6] Sylvain Bénito, Charles-Henri Bruneau, Thierry Colin, Cyprien Gay, and François Molino. An elasto-visco-plastic model for immortal foams or emulsions. *Eur. Phys. J. E*, 25 :225–251, 2008.

[7] C. Besse and T. Goudon. Derivation of a non-local model for diffusion asymptotics—application to radiative transfer problems. *Commun. Comput. Phys.*, 8(5) :1139–1182, 2010.

[8] Marzia Bisi, Fiammetta Conforto, and Laurent Desvillettes. Quasi-steady-state appproximation for reaction-diffusion equations. accepted for publication in the Bulletin of the Institute of Mathematics, Academia Sinica.

[9] L. Bocquet, A. Colin, and A. Ajdari. Kinetic theory of plastic flow in soft glassy materials. *Phys. Rev. Lett.*, 103(3) :36001, 2009.

[10] Dieter Bothe, Michel Pierre, and Guillaume Rolland. Instantaneous limit for a reaction-diffusion system with fast reversible reaction. to appear.

[11] Jean-Phillipe. Bouchaud, Alain Comtet, and Cécile Monthus. On a dynamical model of glasses. *J. Phys. I France*, 5(12) :1521–1526, December 1995.

[12] Franck Boyer and Pierre Fabrie. *Éléments d'analyse pour l'étude de quelques modèles d'écoulements visqueux incompressibles*, volume 52 of *Mathématiques & Applications (Berlin) [Mathematics & Applications]*, chapter VI, pages xii+398. Springer, Berlin, 2006.

[13] Didier Bresch and Jacques Simon. Western boundary currents versus vanishing depth. *Discrete Contin. Dyn. Syst. Ser. B*, 3(3) :469–477, 2003.

[14] Craig D. Byron. Role of the osteoclast in cranial suture waveform patterning. *Anat. Rec.*, 288A(5) :552–563, 2006.

[15] Craig D. Byron, James Borke, Jack Yu, David Pashley, Christopher J. Wingard, and Mark Hamrick. Effects of increased muscle mass on mouse sagittal suture morphology and mechanics. *Anat. Rec.*, 279A(1) :676–684, 2004.

[16] Éric Cancès, Isabelle Catto, and Yousra Gati. Mathematical analysis of a nonlinear parabolic equation arising in the modelling of non-Newtonian flows. *SIAM J. Math. Anal.*, 37(1) :60–82 (electronic), 2005.

[17] Éric Cancès, Isabelle Catto, Yousra Gati, and Claude Le Bris. Well-posedness of a multiscale model for concentrated suspensions. *Multiscale Model. Simul.*, 4(4) :1041–1058 (electronic), 2005.

[18] Éric Cancès and Claude Le Bris. Convergence to equilibrium of a multiscale model for suspensions. *Discrete Contin. Dyn. Syst. Ser. B*, 6(3) :449–470 (electronic), 2006.

[19] Gilles Carbou. Penalization method for viscous incompressible flow around a porous thin layer. *Nonlinear Anal. Real World Appl.*, 5(5) :815–855, 2004.

[20] Gilles Carbou and Pierre Fabrie. Boundary layer for a penalization method for viscous incompressible flow. *Adv. Differential Equations*, 8(12) :1453–1480, 2003.

[21] Michael E. Cates and Peter Sollich. Tensorial constitutive models for disordered foams, dense emulsions and other soft non ergodic materials. *J. Rheol*, 48 :193–207, 2004.

[22] Jean-Yves Chemin, Benoît Desjardins, Isabelle Gallagher, and Emmanuel Grenier. *Mathematical geophysics*, volume 32 of *Oxford Lecture Series in Mathematics and its Applications*. The Clarendon Press Oxford University Press, Oxford, 2006. An introduction to rotating fluids and the Navier-Stokes equations.

[23] Pierre Degond, Thierry Goudon, and Frédéric Poupaud. Diffusion limit for nonhomogeneous and non-micro-reversible processes. *Indiana Univ. Math. J.*, 49(3) :1175–1198, 2000.

[24] Pierre Degond, Mohammed Lemou, and Marco Picasso. Viscoelastic fluid models derived from kinetic equations for polymers. *SIAM J. Appl. Math.*, 62(5) :1501–1519 (electronic), 2002.

[25] Stéphane Descombes and Marc Massot. Operator splitting for nonlinear reaction-diffusion systems with an entropic structure : singular perturbation and order reduction. *Numer. Math.*, 97(4) :667–698, 2004.

[26] Laurent Desvillettes and Cédric Villani. On the trend to global equilibrium in spatially inhomogeneous entropy-dissipating systems : the linear Fokker-Planck equation. *Comm. Pure Appl. Math.*, 54(1) :1–42, 2001.

[27] Manfred Eigen and Leo de Maeyer. Self-dissociation and protonic charge transport in water and ice. *Proc. Roy. Soc. London. Ser. A.*, 247(1251) :505–533, 1958.

[28] Bruno Fornet. Influence of boundary layers over the rate of convergence in a penalization method for a 1-d wave equation. *Comptes Rendus Mécanique*, 336(5) :454 – 457, 2008.

[29] Bruno Fornet. A Kreiss' symmetrizer domain penalization method. *Comm. Partial Differential Equations*, 33(7-9) :1549–1570, 2008.

[30] Bruno Fornet and Olivier Guès. Penalization approach to semi-linear symmetric hyperbolic problems with dissipative boundary conditions. *Discrete Contin. Dyn. Syst.*, 23(3) :827–845, 2009.

[31] Yousra Gati. *Analyse mathématique et simulations numériques d'un modèle de fluides complexes*. PhD thesis, École Nationale des Ponts et Chaussées, 2004.

[32] David Gérard-Varet. Formal derivation of boundary layers in fluid mechanics. *J. Math. Fluid Mech.*, 7(2) :179–200, 2005.

[33] Julie Goyon. *Matériaux amorphes : des solides qui coulent de façon collective*. PhD thesis, Université Bordeaux I, 2008.

[34] Jean-Luc Guermond and Peter D. Minev. A new class of fractional step techniques for the incompressible Navier-Stokes equations using direction splitting. *C. R. Math. Acad. Sci. Paris*, 348(9-10) :581–585, 2010.

[35] Aric Hagberg and Ehud Meron. From labyrinthine patterns to spiral turbulence. *Phys. Rev. Lett.*, 72(15) :2494–2497, Apr 1994.

[36] Pascal Hébraud. *Propriétés mécaniques des systèmes vitreux. L'exemple des émulsions concentrées.* PhD thesis, Université Louis Pasteur, 1998.

[37] Pascal Hébraud and François Lequeux. Mode-coupling theory for the pasty rheology of soft glassy materials. *Phys. Rev. Lett.*, 81(14) :2934–2937, Oct 1998.

[38] Susan W. Herring. Mechanical influences on suture development and patency. In David P. Rice, editor, *Craniofacial Sutures*, volume 12 of *Frontiers of Oral Biology*, pages 41–56. Karger, 2008.

[39] Kenneth S. Johnson. Carbon dioxide hydration and dehydration kinetics in seawater. *Limnol. Oceanogr.*, 27(5) :849–855, 1982.

[40] Pierre Jop, Yoël Forterre, and Olivier Pouliquen. A constitutive law for dense granular flows. *Nature*, 441 :727–730, 2006.

[41] Daniel D. Joseph, Michael Renardy, and Jean-Claude Saut. Hyperbolicity and change of type in the flow of viscoelastic fluids. *Arch. Rational Mech. Anal.*, 87(3) :213–251, 1985.

[42] Benjamin Jourdain, Claude Le Bris, Tony Lelièvre, and Félix Otto. Long-time asymptotics of a multiscale model for polymeric fluid flows. *Arch. Ration. Mech. Anal.*, 181(1) :97–148, 2006.

[43] Tosio Kato. *Perturbation theory for linear operators.* Classics in Mathematics. Springer-Verlag, Berlin, 1995. Reprint of the 1980 edition.

[44] Aurélien Klak. *Méthodes asymptotiques pour les équations de types Helmoltz et Navier-Stokes.* PhD thesis, Université Rennes I, 2011.

[45] Elona Kolpakova-Hart, Brandeis McBratney-Owen, Bo Hou, Naomi Fukai, Claudia Nicolae, Jing Zhou, and Bjorn R. Olsen. Growth of cranial synchondroses and sutures requires polycystin-1. *Dev. Biol.*, 321(2) :407 – 419, 2008.

[46] Claude Le Bris. *Systèmes multi-échelles*, volume 47 of *Mathématiques & Applications (Berlin) [Mathematics & Applications]*. Springer-Verlag, Berlin, 2005. Modélisation et simulation. [Modelling and simulation].

[47] Claude Le Bris and Tony Lelièvre. Micro-macro models for viscoelastic fluids : modelling, mathematics and numerics. 76A05, 35Q82, 65C05.

[48] Pierre-Louis Lions and Nader Masmoudi. Global solutions for some Oldroyd models of non-Newtonian flows. *Chinese Ann. Math. Ser. B*, 21(2) :131–146, 2000.

[49] Norman G. Meyers. An L^pe-estimate for the gradient of solutions of second order elliptic divergence equations. *Ann. Scuola Norm. Sup. Pisa (3)*, 17 :189–206, 1963.

[50] Takashi Miura, Chad A. Perlyn, Masato Kinboshi, Naomichi Ogihara, Mikiko Kobayashi-Miura, Gillian M. Morriss-Kay, and Kohei Shiota. Mechanism of skull suture maintenance and interdigitation. *J. Anat*, 215(6) :642–655, 2009.

[51] James G. Oldroyd. On the formulation of rheological equations of state. *Proc. Roy. Soc. London. Ser. A.*, 200 :523–541, 1950.

[52] Julien Olivier. Large shear rate behaviour for the hébraud-lequeux model. Submitted.

[53] Julien Olivier. Asymptotic analysis in flow curves for a model of soft glassy rheology. *Z. Angew. Math. Phys*, 61(3) :445–466, 2010.

[54] Julien Olivier and Michael Renardy. Glass transition seen through asymptotic expansions. Submitted.

[55] Julien Olivier and Michael Renardy. On the generalization of the hébraud-lequeux to multidimensional flows. In preparation.

[56] Lynne A. Opperman. Cranial sutures as intramembranous bone growth sites. *Dev. Dyn.*, 219(4) :472–485, 2000.

[57] Patrick Oswald. *Rhéophysique*. Échelles. Belin, Paris, 2005.

[58] Benoit Perthame. Pde models for chemotactic movements : Parabolic, hyperbolic and kinetic. *Appl. Math.*, 49 :539–564, 2004. 10.1007/s10492-004-6431-9.

[59] Guillemette Picard, Armand Ajdari, Lydéric Bocquet, and François Lequeux. Simple model for heterogeneous flows of yield stress fluids. *Phys. Rev. E*, 66(5) :051501, Nov 2002.

[60] Michel Pierre. Reaction-diffusion systems with positivity and mass control : Global existence and singular limits. Lecture notes of the 3rd Spring School *Analytical and Numerical Aspects of Evolution Equation* in Essen.

[61] Katherine L. Rafferty, Susan W. Herring, and Christopher D. Marshall. Biomechanics of the rostrum and the role of facial sutures. *J. Morphol.*, 257(1) :33, 2003.

[62] Michael Renardy. Local existence of solutions of the Dirichlet initial-boundary value problem for incompressible hypoelastic materials. *SIAM J. Math. Anal.*, 21(6) :1369–1385, 1990.

[63] Michael Renardy. An existence theorem for model equations resulting from kinetic theories of polymer solutions. *SIAM J. Math. Anal.*, 22(2) :313–327, 1991.

[64] David P. Rice, editor. *Craniofacial Sutures*, volume 12 of *Frontiers of Oral Biology*. Karger, 2008.

[65] David P. Rice. Developmental anatomy of craniofacial sutures. In David P. Rice, editor, *Craniofacial Sutures*, volume 12 of *Frontiers of Oral Biology*, pages 1–21. Karger, 2008.

[66] David P. Rice and Ritva Rice. Locate, condense, differentiate, grow and confront : developmental mechanisms controlling intramembranous bone and suture formation and function. In David P. Rice, editor, *Craniofacial Sutures*, volume 12 of *Frontiers of Oral Biology*, pages 22–40. Karger, 2008.

[67] Jean-Claude Saut. Notes de cours de l'école dété franco-chinoise sur "Stress Tensor Effect on Fluid Mechanics". A paraître dans *Science China Mathematics*.

[68] Peter Sollich, François Lequeux, Pascal Hébraud, and Michael E. Cates. Rheology of soft glassy materials. *Phys. Rev. Lett.*, 78(10) :2020–2023, Mar 1997.

[69] Zonngyang Sun, Eugenia Lee, and Susan W. Herring. Cranial sutures and bones : growth and fusion in relation to masticatory strain. *Anat. Rec.*, 276(2) :150–161, 2004.

[70] Athanassios E. Tzavaras. Nonlinear analysis techniques for shear band formation at high strain-rates. *AMR*, 45(3, part 2) :S82–S94, 1992. Material instabilities (Rolla, MO, 1991).

[71] Stephen M. Warren, Benjamin Walder, Wojciech Dec, Michael T. Longaker, and Kang Ting. Confocal laser scanning microscopic analysis of collagen scaffolding patterns in cranial sutures. *J. Craniofac. Surg.*, 19(1) :198, 2008.

Résumé

On s'attache à étudier des modèles mathématiques multi-échelles pour des domaines variés : la rhéologie des matériaux vitreux, la biochimie dans la balnéothérapie et la biomécanique des sutures craniofaciales. Pour les matériaux vitreux, nous étudions un modèle de type cinétique et justifions mathématiquement des propriétés macroscopiques (transition vitreuse à faible cisaillement et comportement de type fluide newtonien à fort taux de cisaillement) après avoir remarqué une certaine analogie avec la pénalisation d'obstacles en mécanique des fluides. Nous proposons également une généralisation multi-dimensionnelle de ce modèle afin de prendre en compte des types d'écoulements généraux. En biochimie nous présentons un premier modèle très simplifié de réaction-diffusion et montrons comment concevoir un schéma numérique adapté en utilisant les hypothèses de modélisation. Enfin nous proposons un modèle de couplage biomécanique pour le développement des sutures qui rend compte du phénomène d'interdigitation que l'on observe en pratique.

Abstract

We study multiscale mathematical models for various scientific fields: soft glassy rheology, biochemistry for balneotherapy and the biomechanics of craniofacial suture development. In soft glassy rheology, we study a kinetic-type of model and justify mathematically some macroscopic properties of the model (especially the glass transition at low shear rate and the Newtonian behaviour at large shear rate) by noticing an analogy with the problem of obstacle penalization in fluid mechanics. Moreover, we propose a multidimensional generalization of this model in order to handle more general flow types. In biochemistry, we introduce a first, very simplified, model and show how we can design a numerical scheme based on the modelling hypotheses. Finally, we present a model for suture growth coupling biology and mechanics which accounts for the interdigitation pattern observed in practice.